YEAST CELL IMMOBILISATION ON CARBON NANOTUBES FOR FERMENTATION PROCESSES

Tirivaviri Augustine Mamvura

A dissertation submitted to the Faculty of Engineering and the Built Environment, University of Witwatersrand, in fulfilment of the requirements for the degree of Master of Science in Engineering

Johannesburg, 2010

DECLARATION

I declare that this dissertation is my own unaided work. It is being submitted to the Degree of Master of Science in Engineering to the University of the Witwatersrand, Johannesburg. It has not been submitted before for any degree or examination to any other University.

.....

(Signature of Candidate)

.....day of.....year.....

day *month* *year*

ABSTRACT

Fermentation and maturation are the most time consuming steps in the production of beer, the duration of which is typically between 5–7 and 7–30 days, respectively. The continuous fermentation process based on immobilised yeast cell technology allows producing an acceptable end product within as little as 2–3 days. In spite of the economic advantages that continuous beer fermentation offers, difficulties of technical and economic origin have retarded the implementation of the process at industrial scale so far. For example, the total investment costs depend significantly on carrier costs and applied technology. Thus the use of cheap carrier materials in a suitably designed bioreactor could favour the economics of the immobilised process, inspire researchers and encourage brewing engineers. Among the available yeast cell immobilisation techniques, flocculation of micro-organisms, due to its simplicity and low cost, is very attractive because there are no complex mechanical devices needed as well as any supporting material in this technique. This can be an advantage over other immobilisation techniques since it is well known that a support represents a major cost in immobilisation procedures.

Flocculation of yeast cells usually observed at the end of fermentation and is of great importance in beer brewing. It can occur naturally or it can be artificially induced by different agents. The focus of the study was to investigate the immobilisation of yeast cells onto Carbon Nanotubes (CNTs) using flocculation method. CNTs; long, thin cylinders of carbon; can be used as artificial agents to induce flocculation of yeast cells because they are increasingly being recognised as promising materials for catalysis, either as catalysts themselves, as catalyst additives or as a catalyst support. CNTs are inert and positively charged which enable them to attract negatively charged yeast cells to form flocs. The use of CNTs to improve yeast flocculation for fermentation processes has not been reported yet in literature.

CNTs were synthesised by Swirled Floating Catalyst Chemical Vapour Deposition (SFCCVD) method. The optimum conditions required to synthesise the best samples of CNTs were temperature of 800 ^{o}C, acetylene flowrate of 844 ml/min for a reaction time of 20 minutes. The synthesised CNTs were characterised by Transmission Electron Microscopy (TEM) and Raman Spectroscopy to obtain the type of nanotubes, morphology and their purity.

The yeast cells (*Saccharomyces cerevisiae* strain NRRL Y2084, a dry brewer's yeast obtained from National Food Products, Emmarentia, Johannesburg) were immobilised onto CNTs by flocculation method to produce a immobilised cells. The flocculation process was measured by two methods: a qualitative process of using the naked eye to rank the flocs as either -, +, ++ or +++ and a quantitative method of measuring the floc weight recovered using a centrifuge and dried in an oven at 40 ^{o}C for 24 hours. The flocculation of the immobilised cells was compared with a control experiment which had free cells. The immobilised cells and free cells were both recovered and dried using a freeze dryer for analysis and use in fermentation. Conditions required for the flocculation process were an agitation speed of 110 rpm, pH 5.60, a temperature of 30 ^{o}C and concentration of 53.57 μg/ml of CNTs. Addition of calcium ions at 5.49 mM resulted in good flocculation but the presence of glucose delayed onset of flocculation by 4 – 5 days. The flocculated cells were characterised by Scanning Electron Microscopy (SEM) and Optical Microscopy. The flocculation conditions used in the study were comparable with those in literature.

The immobilised cells and the free cells were introduced into malt extract for fermentation at 15 and 30 ^{o}C. The fermentation rates observed were compared with those found in literature by comparing the final ethanol concentration observed. Free cells produced more ethanol, 2.49 % (v/v) than the immobilised

cells, 1.56 % (v/v) at 15 ^{o}C but these values were not comparable to literature with 5.50 % (v/v) for free cells and 5.20 % (v/v) using the immobilised cells. Free cells produced higher alcohol content (0.52 % v/v) than the biocatalyst (0.39% v/v) at 30 ^{o}C but these values were not comparable to the reported literature values of 6.20 % (v/v).

DEDICATION

In memory of my mother and father

Getrude and Cephas Mamvura

To my love Leniency Matsekeza

ACKNOWLEDGEMENTS

Firstly, I would like to thank God as I am still alive and all the wonderful things that happened and will happen in my life.

Secondly, I wish to express my greatest appreciation to my supervisor, Professor S. E. Iyuke and my co-supervisors Dr V. Sibanda and Dr S. C. Yah for their guidance and invaluable support throughout the study.

Sincere thanks also to Professor M. Witcomb, Caroline and Abe from Biology Electron Microscope Unit of the University of Witwatersrand for all their help during this study.

To all my family members, I say thanks guys for your understanding all the time.

Lastly, I gratefully acknowledge the financial support from the National Research Foundation, NRF Nanotechnology flagship programme and FoodBev SETA.

TABLE OF CONTENTS

DECLARATION ii

ABSTRACT iii

DEDICATION vi

ACKNOWLEDGEMENTS vii

TABLE OF CONTENTS viii

LIST OF FIGURES xiii

LIST OF TABLES xix

CHAPTER 1: INTRODUCTION 1

1.1 Immobilisation of Yeast Cells on Carbon Nanotubes 1

1.2 Research Problem 2

1.3 Research Aim 3

CHAPTER 2: LITERATURE REVIEW 5

2.1 Carbon Nanotubes 5

2.2 Synthesis of Carbon Nanotubes 5

2.2.1 Arc Discharge Method 7

2.2.2 Pulsed Laser Ablation (PLA) Method 7

2.2.3 Catalytic Decomposition and Chemical Vapour Deposition 8

2.2.4 Growth Models for CNTs 9

2.2.5 Characterisation of CNTs 10

2.2.6 Applications of Carbon Nanotubes 11

2.3 Immobilisation of Brewers' Yeast 12

2.3.1 Yeast Cells 12

2.3.2 Immobilisation of Microorganisms on Carbon Nanotubes 13

2.3.3 Yeast Growth Phases 15

2.3.4 Immobilisation Methods 17

2.3.5 Yeast Autolysis 31

2.3.6 Immobilisation in Brewing 35

2.3.7 Zeta Potential 36

2.4 Preservation of the Immobilised Cells 42

2.5 Brewing 43

2.5.1 Malts 43

2.5.2 Mash Tun Adjuncts 44

2.5.3 Brewing Liquor 44

2.5.4 Milling and Mashing 44

2.5.5 Wort Separation 45

2.5.6 Wort Boiling 45

2.5.7 Wort Clarification, Cooling and Aeration 46

2.5.8 Fermentation 46

2.5.9 Yeast Removal and Processing of Beer 52

2.6 Summary 52

CHAPTER 3: SCIENTIFIC METHODY 54

3.1 Operating Conditions 54

3.1.1 Reaction Gases 56

3.1.2 Catalyst 57

3.1.3 Consumables 57

3.1.4 Reactor Tube 57

3.1.5 Reactor Tube Heater 57

3.1.6 Cole Parmer Flowmeter 58

3.1.7 Transmission Electron Microscopy (TEM) 58

3.1.8 Experimental Design 58

3.2 Strain and Culture Conditions 60

3.2.1 Yeast Strain and Medium 61

3.2.2 Yeast Viability 62

3.2.3 Carbon Nanotubes 63

3.2.4 Shaking Incubator 63

3.2.5 Autoclave 63

3.2.6 pH meter 63

3.2.7 Zetasizer 63

3.2.8 Preservation of the Immobilised Cells 63

3.2.9 Centrifuge 64

3.2.10 Analytical Methods 64

3.2.11 Experimental Design 64

3.2.12 Flocculation Measurements 68

3.3 Fermentation Studies 69

CHAPTER 4: RESULTS AND DISCUSSION 71

4.1 Synthesis of Carbon Nanotubes 71

4.1.1 Growth Temperature 75

4.1.2 Acetylene Flowrate 84

4.1.3 Reaction Time 89

4.2 Yeast Cell Immobilisation 101

4.2.1 Agitation Speed 106

4.2.2 pH 120

4.4.3 Immobilisation Temperature 134

4.2.4 Effect of Concentration of Carbon Nanotubes on Flocculation 140

4.2.5 Calcium Ion Concentration 145

4.2.6 Presence of Glucose 148

4.3 Theory of Yeast Cell Flocculation and Immobilisation on Carbon Nanotubes 151

4.4 Fermentation Studies 152

4.4.1 Reversible Nature of Flocculation 155

4.4.2 pH 155

4.4.3 Sugar concentration 158

4.4.4 Alcohol Content 165

CHAPTER 5: CONCLUSIONS AND RECOMMENDATIONS 171

5.1 Conclusions 171

5.2 Recommendations 175

CHAPTER 6: REFERENCES 177

APPENDICES 197

Appendix I: Publications 197

Appendix II: Procedure for using TEM 198

Appendix III: VirTis Freeze Dryer Cooling Rate Calculation 202

Appendix IV: Procedure for using SEM 203

Appendix V: Cole Parmer flowmeters calibration chart 207

Appendix VI: Statistical Results for CNTs Production 208

Appendix VII: Statistical Results for Yeast Immobilisation 210

Appendix VIII: Statistical Results for Fermentation Studies 218

LIST OF FIGURES

Figure 1.1: Schematic representation of the immobilisation process. 2

Figure 2.1: Methods for CNTs synthesis where 6

Figure 2.2: Schematics of growth mechanisms 10

Figure 2.3: The growth curve showing the phases of yeast cell population 15

Figure 2.4: Basic methods of cell immobilisation 18

Figure 2.5: Factors affecting flocculation 30

Figure 2.6: The lectin model for flocculation 31

Figure 2.7: Effect of different pH values on accumulation of glycogen in *Saccharomyces cerevisiae* 33

Figure 2.8: Effect of cellular glycogen content on the longevity of *Saccharomyces cerevisiae* 33

Figure 2.9: Changes in cell viability during autolysis of Saccharomyces cerevisiae at different temperatures and pH 7.0 34

Figure 2.10: Schematic drawing of the electrochemical double layer and zeta potential of a charged particle 36

Figure 2.11: Typical plot of zeta potential versus pH showing the position of the iso-electric point and the pH values where the dispersion would be expected to be stable 38

Figure 2.12: Schematic illustration of (a) bridging flocculation and (b) restabilisation by adsorbed polymers 41

Figure 2.13: Effect of temperature on fermentation rate 48

Figure 2.14: Effect of oxygen on fermentation rate 50

Figure 2.15: Effect of pitching rate on fermentation rate 51

Figure 2.16: The relationship between fermentation time and increasing the OG of wort 51

Figure 3.1: Flowsheet for SFCCVD method for synthesising CNTs 55

Figure 3.2: Part of SFCCVD equipment showing the arrangement in the reactor tube. 55

Figure 3.3: Labcon Shaking incubator. 66

Figure 3.4: Zetasizer Nanoseries Nano ZS (Malvern Instruments). 66

Figure 3.5: VirTis freeze dryer (SP Industries). 67

Figure 3.6: Hermle Z365 BHG Centrifuge. 67

Figure 4.1 Electron micrographs showing carbon nanoparticles synthesised using the SFCCVD method. 72

Figure 4.2: Raman spectroscopy to confirm presence of CNTs. 74

Figure 4.3: Electron micrographs obtained at 750 ^{o}C 77

Figure 4.4: Electron micrographs obtained at 800 ^{o}C 78

Figure 4.5: Electron micrographs obtained at 850 ^{o}C 79

Figure 4.6: Electron micrographs obtained at 900 ^{o}C 81

Figure 4.7: Electron micrographs obtained at 950 ^{o}C 82

Figure 4.8: Electron micrographs obtained at 1000 ^{o}C 83

Figure 4.9: Electron micrographs obtained at 308 ml/min 85

Figure 4.10: Electron micrographs obtained at 594 ml/min 86

Figure 4.11: Electron micrographs obtained at 844 ml/min 87

Figure 4.12: Effect of acetylene flowrate on production rate and yield. 88

Figure 4.13: Electron micrographs obtained at 5 minutes 90

Figure 4.14: Electron micrographs obtained at 10 minutes 91

Figure 4.15: Electron micrographs obtained at 15 minutes 92

Figure 4.16: Electron micrographs obtained at 20 minutes 93

Figure 4.17: Electron micrographs obtained at 25 minutes 94

Figure 4.18: Effect of reaction time on production rate and yield. 95

Figure 4.19: Electron micrographs obtained at 2 grams 97

Figure 4.20: Electron micrographs obtained at 3 grams 98

Figure 4.21: Electron micrographs obtained at 5 grams 99

Figure 4.22: Electron micrograph obtained at 10 grams 100

Figure 4.23: Effect of catalyst quantity on production rate and yield. 101

Figure 4.24: Electron micrographs showing the immobilised yeast cells on CNTs. 102

Figure 4.25: Stereo Microscopy photographs showing the immobilised yeast cells on CNTs. 104

Figure 4.26: Electron micrographs showing yeast cells that flocculated without CNTs. 105

Figure 4.27: Digital photographs of yeast flocculation after 4 days at 0 rpm. 108

Figure 4.28: Change in zeta potential over time at 0 rpm, 109

Figure 4.29: Digital photographs of yeast flocculation after 3 days at 50 rpm. 110

Figure 4.30: Change in zeta potential over time at 50 rpm, 111

Figure 4.31: Digital photographs of yeast flocculation after 4 days at 110 rpm. 112

Figure 4.32: Change in zeta potential over time at 110 rpm 114

Figure 4.33: Digital photographs of yeast flocculation after 3 days at 150 rpm. 115

Figure 4.34: Change in zeta potential over time at 150 rpm 116

Figure 4.35: Digital photographs of yeast flocculation after 3 days at 200 rpm. 117

Figure 4.36: Change in zeta potential over time at 200 rpm 118

Figure 4.37: Effect of agitation speed on initial rate of flocculation of *Saccharomyces cerevisiae* S646-1B 120

Figure 4.38: Digital photographs of yeast flocculation after 4 days at pH 4.60. 123

Figure 4.39: Change in zeta potential over time at pH 4.60 124

Figure 4.40: Digital photographs of yeast flocculation after 4 days at pH 5.60. 125

Figure 4.41: Change in zeta potential over time at pH 5.60 126

Figure 4.42: Digital photographs of yeast flocculation after 4 days at pH 6.00. 127

Figure 4.43: Change in zeta potential over time at pH 6.00 129

Figure 4.44: Digital photographs of yeast flocculation after 4 days at pH 6.50. 130

Figure 4.45: Change in zeta potential over time at pH 6.50 131

Figure 4.46: Effect of changing pH on flocculation 132

Figure 4.47: Digital photographs of yeast flocculation after 4 days at 25 ^{o}C. 135

Figure 4.48: Change in zeta potential over time at 25 ^{o}C 136

Figure 4.49: Digital photographs of yeast flocculation after 4 days at 30 ^{o}C. 137

Figure 4.50: Change in zeta potential over time at 30 ^{o}C 138

Figure 4.51: Effect of temperature on immobilisation 140

Figure 4.52: Digital photographs of yeast flocculation after 4 days at different CNT concentrations. 141

Figure 4.53: Effect of CNTs concentration on brewers' yeast flocculation (quantitative) 143

Figure 4.54: Change in zeta potential over time as a function of CNT concentrations 144

Figure 4.55: Digital photographs of yeast flocculation after 4 days using sheet-like CNTs. 145

Figure 4.56: Effect of Ca^{2+} ions on brewers' yeast flocculation 146

Figure 4.57: Change in zeta potential over time as a function of calcium ion concentration 147

Figure 4.58: Effect of the presence of glucose on pH and zeta potential 149

Figure 4.59: Effect of the presence of glucose and calcium ions on pH and zeta potential 150

Figure 4.60: Theory of yeast cell immobilisation onto CNTs. 152

Figure 4.61: Time course of fermentation for lager beers 156

Figure 4.62: Change in pH over time during fermentation at 15 ^{o}C. 156

Figure 4.63: Change in pH over time during fermentation at 30 ^{o}C. 157

Figure 4.64: Change in maltose over time during fermentation at 15 ^{o}C. 158

Figure 4.65: Change in maltose over time during fermentation at 30 ^{o}C. 159

Figure 4.66: Change in glucose over time during fermentation at 15 ^{o}C. 161

Figure 4.67: Change in glucose over time during fermentation at 30 ^{o}C. 161

Figure 4.68: Carbohydrate assimilation profiles (from Priest and Stewart, 2006). 164

Figure 4.69: Carbohydrate assimilation profiles 164

Figure 4.70: Change in ethanol content over time during fermentation at 15 ^{o}C. 166

Figure 4.71: Change in ethanol content over time during fermentation at 30 ^{o}C. 167

LIST OF TABLES

Table 2.1: Different methods for characterisation of CNTs 11

Table 2.2: Stability of solution through zeta potential 39

Table 2.3: Composition of sugars in malt wort 46

Table 3.1: Physical properties of acetylene 56

Table 3.2: Physical properties of argon 56

Table 3.3: Physical properties of ferrocene 57

Table 3.4: Data recorded and rates calculated during analysis of CNTs 60

Table 3.5: Composition of yeast extract powder 62

Table 4.1: Conditions used to investigate the effect of temperature on the synthesis of CNTs. 76

Table 4.2: Conditions used to investigate the effect of acetylene flowrate on the synthesis of CNTs. 84

Table 4.3: Conditions used to investigate the effect of reaction time on the synthesis of CNTs. 89

Table 4.4: Conditions used to investigate the effect of catalyst quantity on the synthesis of CNTs. 96

Table 4.5: Conditions used to investigate the effect of agitation on the flocculation of brewers' yeast. 107

Table 4.6: Analysis of flocculation at 0 rpm 108

Table 4.7: Analysis of flocculation at 50 rpm 111

Table 4.8: Analysis of flocculation at 110 rpm 113

Table 4.9: Analysis of flocculation at 150 rpm 116

Table 4.10: Analysis of flocculation at 200 rpm 117

Table 4.11: Conditions used to investigate the effect of pH on the flocculation of brewers' yeast. 121

Table 4.12: Analysis of flocculation at pH 1.00 to 3.00 121

Table 4.13: Analysis of flocculation at pH 3.00 to 4.00 122

Table 4.14: Analysis of flocculation at pH 4.60 123

Table 4.15: Analysis of flocculation at pH 5.60 125

Table 4.16: Analysis of flocculation at pH 6.00 128

Table 4.17: Analysis of flocculation at pH 6.50 130

Table 4.18: Conditions used to investigate the effect of temperature on the flocculation of brewers' yeast. 134

Table 4.19: Analysis of flocculation at 25 ^{o}C 135

Table 4.20: Analysis of flocculation at 30 ^{o}C 137

Table 4.21: Analysis of flocculation at 25 and 30 ^{o}C. 139

Table 4.22: Conditions used to investigate the effect of concentration of CNTs on the flocculation of brewers' yeast. 141

Table 4.23: Qualitative analysis of flocculation at different concentrations of CNTs 142

Table 4.24: Analysis of flocculation at 62.50 and 71.43 µg/ml 142

Table 4.25: Conditions used to investigate the effect of concentration of calcium ions on the flocculation of brewers' yeast. 145

Table 4.26: Effect of calcium ion concentration on flocculation 146

Table 4.27: Conditions used to investigate the effect of glucose on the flocculation of brewers' yeast cells. 149

Table 4.28: Final concentration of maltose during fermentation studies 160

Table 4.29: Maltose consumption during fermentation studies. 160

Table 4.30: Final concentration of glucose during fermentation studies 162

Table 4.31: Glucose consumption during fermentation studies. 163

Table 4.32: Sugar consumption during fermentation studies. 165

Table 4.33: Gravities during fermentation studies at 15 and 30 ^{o}C 166

Table 4.34: Comparison of fermentation rates with literature for freeze-dried cells at 15 ^{o}C. 168

Table 4.35: Comparison of fermentation rates with literature for freeze-dried cells. 169

CHAPTER 1: INTRODUCTION

1.1 Immobilisation of Yeast Cells on Carbon Nanotubes

Fermentation and maturation are the most time consuming steps in the production of beer, the duration of which is typically between 5 – 7 and 7 – 30 days, respectively. The continuous fermentation process based on immobilised yeast cell technology allows producing an acceptable end product within as little as 2 – 3 days (Brányik *et al*., 2002; Dömény *et al*., 1998; Tata *et al*., 1998). In spite of the economic advantages that continuous beer fermentation offers, difficulties of technical and economic origin have retarded the implementation of the process at industrial scale so far (Linko *et al*., 1998; Pilkington *et al*., 1998; Shen *et al*., 2003). For example, the total investment costs depend significantly on carrier costs and applied technology. Thus the use of cheap carrier materials in a suitably designed bioreactor could favour the economics of the immobilised process, inspire researchers and encourage brewing engineers (Brányik *et al*., 2006).

Among the available immobilisation techniques, flocculation of micro-organisms, due to its simplicity and low cost, is very attractive because there are no complex mechanical devices needed as well as any supporting material in this technique. This can be an advantage over other immobilisation techniques since it is well known that a support represents a major cost in immobilisation procedures (Domingues *et al*., 1995).

Carbon nanotubes (CNTs), which are increasingly recognised as promising materials for catalysis, either as catalysts themselves, as catalyst additives or as a

catalyst support (Berger, 2007), were investigated to see their possible use in immobilisation of brewers' yeast using flocculation method for fermentation studies. Multiwalled carbon nanotubes (MWCNTs) are relatively affordable materials ($150 per kg in June 2010, which converts to R1.16/gram using US$1=ZAR7.75) making them attractive option as artificial flocculation agents as the cost will be negligible (O'Connor, 2009).

Flocculation of yeast cells is usually observed at the end of beer fermentation and is of great importance in brewing. It is defined as the reversible phenomenon wherein yeast cells adhere in clumps and either sediment rapidly from the medium in which they are suspended or rise to the medium's surface (Stewart and Russell, 1981).

However, the focus of this study was immobilisation of yeast cells onto CNTs by flocculation method to produce immobilised cells for application in fermentation studies. The process is presented schematically as shown in Figure 1.1.

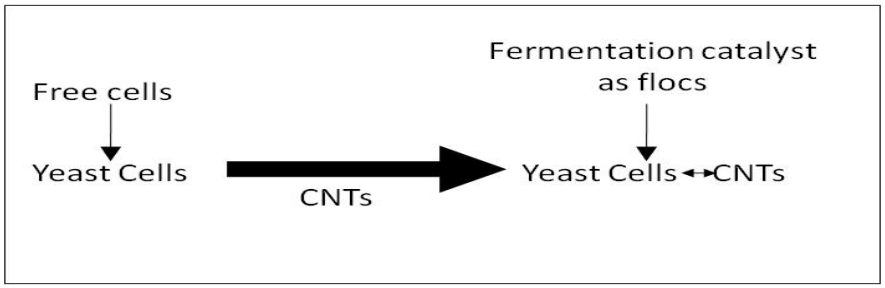

Figure 1.1: Schematic representation of the immobilisation process.

1.2 Research Problem

As mentioned before in Section 1.1, CNTs are increasingly recognised as promising materials for catalysis, and the nanotubes were investigated to assess

their possible use in promoting flocculation of brewers' yeast. Flocculation is attractive because it is a low cost option. The use of CNTs to promote yeast flocculation for fermentation studies has not yet been reported in literature.

According to Berger (2007) CNTs may act as catalysts and/or reaction vessels thereby increasing the reaction rates of ethanol production. CNTs distinguish themselves from other carbon materials, e.g. activated carbon and Carbon Nanofibres (CNFs), in that they have well graphitised graphene with semiconducting or metallic characteristics and a tubular morphology with well defined dimensions. Earlier theoretical studies have shown that the electron density is shifted from the inside to the outside of CNT channels, and that inside gas molecules exhibit a binding energy different from those outside of the nanotubes.

This work was divided into three areas:

1. The synthesis of CNTs by Swirled Floating Catalyst Chemical Vapour Deposition (SFCCVD) method (Iyuke, 2005),
2. The immobilisation of brewers' yeast cells onto CNTs by flocculation method to produce immobilised cells, and
3. Fermentation studies to assess the performance of the immobilised cells against free cells.

1.3 Research Aim

The aim of this study was immobilisation of yeast cells onto CNTs by flocculation method to produce immobilised cells for application in fermentation studies.

The specific objectives of the study work were:

A. To find the optimum conditions for the production of CNTs by SFCCVD method. This entailed looking at all parameters which affect the production process, which are:
    a. Temperature
    b. Acetylene flow rate, and
    c. Reaction time
B. To immobilise yeast cells onto CNTs. For immobilisation of yeast cells the following parameters were investigated:
    a. Incubator shaker speed or agitation
    b. pH of medium
    c. Incubation temperature
    d. Concentration of CNTs
    e. Concentration of calcium ions
    f. Presence of glucose
C. To find if there is a relationship between zeta potential and the flocculation process in the presence of CNTs and attempt to use the potential to predict flocculation
D. To assess the performance of the immobilised cells in fermenting malt extract:
    a. The fermentation studies were conducted at 15 and 30 ^{o}C for 9 days.
    b. The results of the studies were compared with previous studies in literature.

CHAPTER 2: LITERATURE REVIEW

2.1 Carbon Nanotubes

Carbon nanotubes (CNTs) are hollow tubules of graphite sheets. They can be observed as two forms namely; Single-Walled Carbon Nanotubes (SWCNTs) and Multi-Walled Carbon Nanotubes (MWCNTs). SWCNTs consist of a single graphite cylinder, while MWCNTs are made of concentric graphitic layers surrounding the central tubule. The diameter of the CNTs is usually between 2 and 90 nm and the length varies from μm to mm (Di Ventra *et al*., 2004).

Synthesis of CNTs and their possible use in immobilising brewers' yeast is a challenging idea particularly on immobilisation due to the fact that CNTs have smaller diameters i.e. they are in the nanometre range as compared to yeast cells with diameters which are in the micrometre range. There are different methods that can be used to produce CNTs. These methods were discussed and the most suitable method to be used was selected.

2.2 Synthesis of Carbon Nanotubes

There are several methods used for the synthesis of CNTs but the well known techniques are arc discharge technique, laser-ablation and chemical vapour deposition (Figure 2.1).

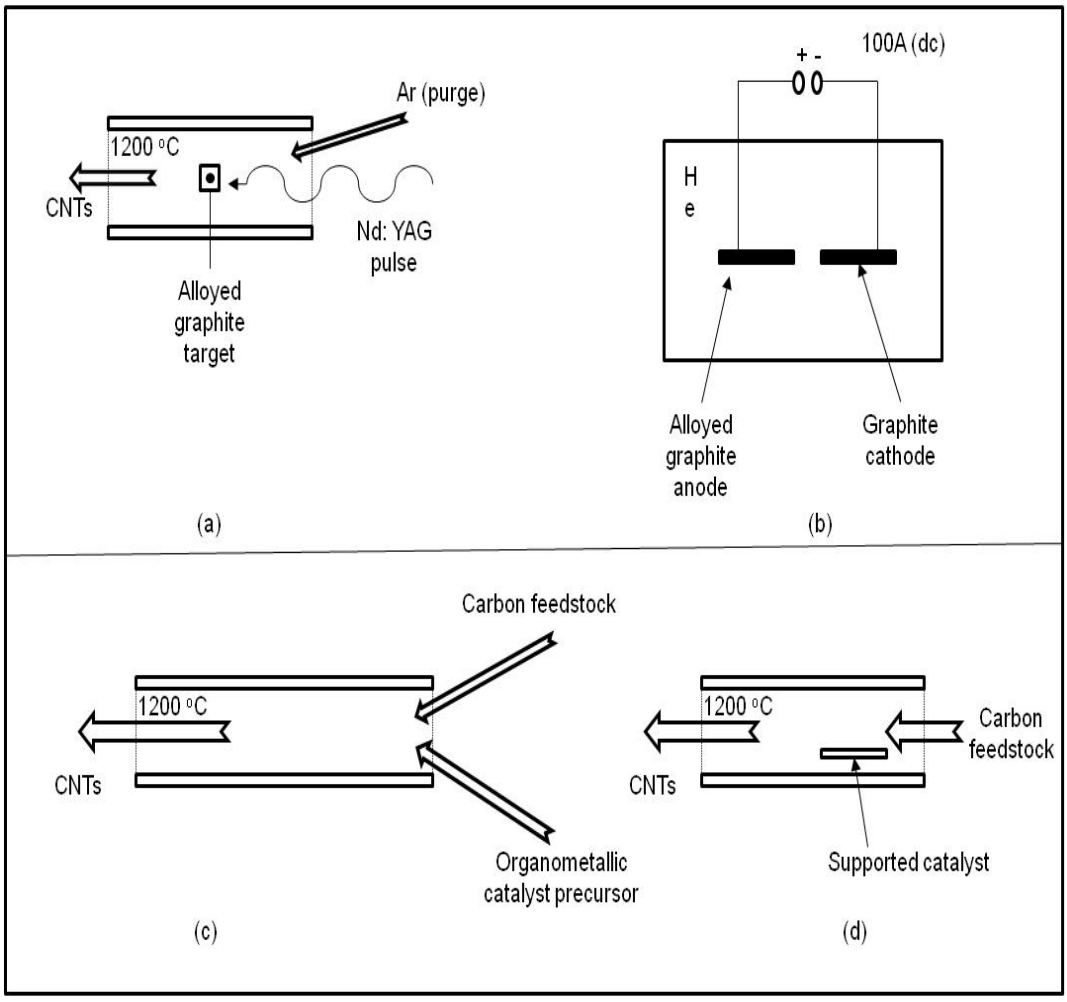

Figure 2.1: Methods for CNTs synthesis where Nd:YAG is a Neodymium:Yttrium-Aluminum-Garnet continuous wave laser (a) Pulse laser ablation, (b) Arc discharge, (c) Catalytic decomposition, (d) Chemical Vapour Deposition (from Di Ventra *et al*., 2004).

Considering the above mentioned methods, Chemical Vapour Deposition (CVD) technique offers the advantage of simplicity and scalability (Di Ventra *et al*., 2004). In general, supported transition metal nanoparticles such as Fe, Co and Ni are used as active catalysts to grow CNTs through hydrocarbon decomposition. During hydrocarbon decomposition over these transition metal nanoparticle

catalysts, carbon atoms are deposited on the surfaces of metal nanoparticles. These carbon atoms diffuse on the surfaces and/or within the structure of the transition metal nanoparticles resulting in growth of CNTs. These transition metals grow CNTs through hydrocarbon decomposition because the transition metals can exist as metastable metal carbides. In contrast, precious metals such as Pt and Au do not form metal carbides (Takenaka *et al*., 2009).

2.2.1 Arc Discharge Method

Arc-discharge is the easiest and most common method of producing CNTs. This technique involves the growth of CNTs on carbon (graphite) electrodes during the direct current (dc) arc-discharge evaporation of carbon in the presence of an inert gas such as helium or argon. The anode is moved towards the cathode until they are less than 1 mm apart and a current of 100 A passes through the electrodes, creating a plasma between them. The temperature of this plasma typically reaches temperatures of 4000 K. At this temperature, the carbon on the anode is vaporised and deposits onto the cathode. It should be noted that the diameter of the anode is usually smaller than the diameter of the cathode and both electrodes are water-cooled. Also, the anode must be continuously moved to ensure a constant distance between the electrodes. Two kinds of synthesis can be achieved by the arc-discharge method: with or without catalyst to produce MWCNTs and SWCNTs, respectively (Baddour and Briens, 2005).

2.2.2 Pulsed Laser Ablation (PLA) Method

The apparatus consists of a tube furnace maintained at about 1200 ^{o}C under flowing argon and a high power pulsed laser (typically Nd:YAG operated at 532nm, 30 Hz and about 500 mJ per pulse) directed down the furnace tube. Nd:YAG acronym for Neodymium:Yttrium-Aluminum-Garnet is a type of continuous wave laser used for ablation of specific structures, Nd is a rare earth

metal with atomic number of 60. A graphite target impregnated with transition metal catalyst is ablated inside the furnace, forming SWCNTs that are then collected downstream. This method produces a high percentage of SWCNTs (about 70%) with the rest being catalyst particles and soot (Di Ventra *et al*., 2004).

The PLA and arc discharge methods have common reaction products with impressively narrow diameter distributions averaging about 1.4 nm. Unfortunately, both methods also generate large quantities of unwanted by-products and require high temperatures (3000 – 4000 ^{o}C) to evaporate solid carbon sources, although the nanotubes form at a much lower temperature within the chamber (Di Ventra *et al*., 2004).

2.2.3 Catalytic Decomposition and Chemical Vapour Deposition

The difference between CVD and catalysed decomposition is largely semantical. The two terms are commonly used interchangeably although a distinction is made to reflect the fact that CVD often refers to growth on a surface (Di Ventra *et al*., 2004). The CVD method involves the decomposition of a gaseous or volatile compound of carbon, catalysed by metallic nanoparticles, which also serve as nucleation sites for the initiation of CNT growth. This method, which can be easily scaled up to industrial production levels, has become the most important commercial method for SWCNT production. Chemical vapour deposition is the term used to describe heterogeneous reactions in which both solid and volatile products are formed from a volatile precursor through chemical reactions, and the solid products are deposited on a substrate. Both MWCNT and SWCNT synthesis have been well developed using CVD. Another advantage of CVD methods is that they allow more control over the morphology and structure of the produced nanotubes. With the CVD methods, one can produce well-separated individual

nanotubes either supported on flat substrates or suspended across trenches. These nanotubes can be directly used to fabricate nanoscale electronics (Jorio *et al*., 2008).

2.2.4 Growth Models for CNTs

Understanding the mechanism of growth is critical in the yield and quality of CNTs in various applications. However, the growth mechanisms of CNTs are very complex and remain controversial. They depend on the method of deposition, the catalyst used and the process parameters. Figure 2.2 schematically depicts the growth models of CNTs. The first stage is the formation of a ‘‘large’’ catalytic particle, originating from the catalytic decomposition of catalyst particle. Under such conditions, the system energy and surface energy for forming new particles favour the formation of large particles. At the growth temperature, the liquid state of the catalytic particles enables carbon atoms to dissolve in the droplets, reaching supersaturation conditions. The introduction of more carbon atoms into nanoparticles, which are in the liquid state, may cause surface instabilities. These surface instabilities lead to the formation of small protrusions, which act as nucleation sites for the subsequent growth of MWCNTs. Notably; CNTs grow perpendicular to the sample surface, underneath, or above the catalytic film, suggesting that growth involves bulk and surface diffusion of carbon atoms through the catalytic liquid particles. When the carbon atoms are segregated from the catalytic particles and diffuse on their surface, the CNTs grow randomly rather than perpendicularly to the catalytic film and surface of the substrate. The growth of CNTs proceeds via the further incorporation of carbon atoms into the root particles. During the synthesis, part of liquefied nanoparticles split off from root particles due to capillary suction, as a results of the fuse state of the particles and surface instabilities (Hsu *et al*., 2005).

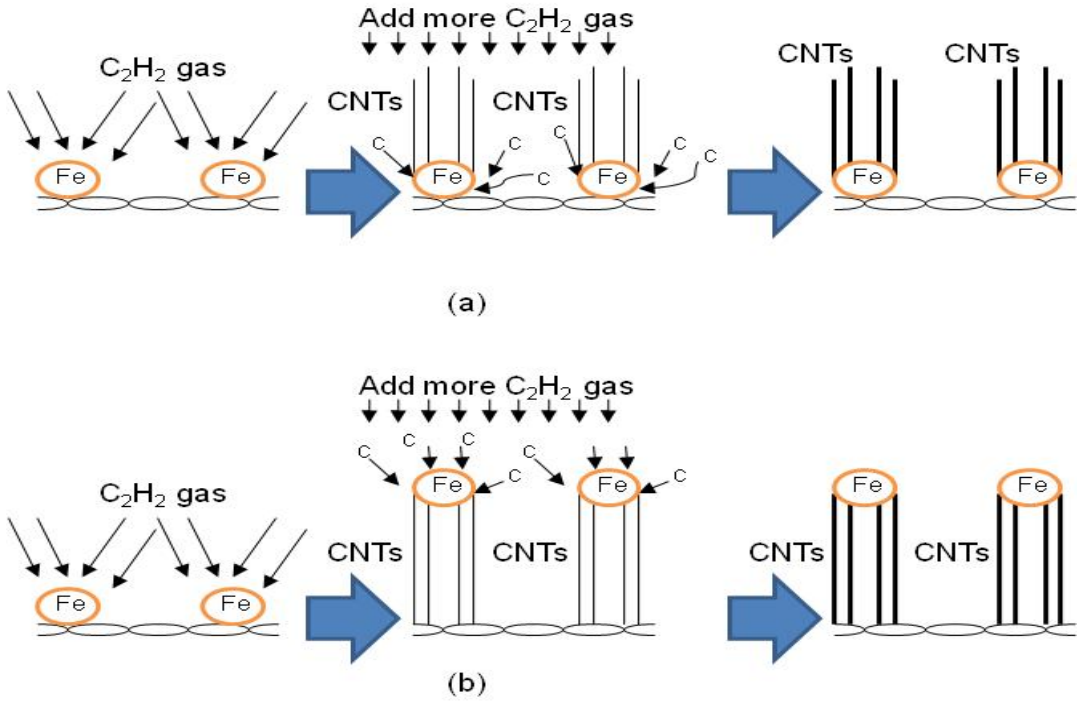

Figure 2.2: Schematics of growth mechanisms of tip- (a) and base-root (b) growth of MWCNTs (from Hsu *et al*., 2005).

2.2.5 Characterisation of CNTs

The different methods that can be used to characterise CNTs are highlighted in Table 2.1.

Table 2.1: Different methods for characterisation of CNTs (from Di Ventra *et al*., 2004).

Technique	**Information typically obtained**
Transmission Electron Microscopy	Atomic and supramolecular structure
Scanning Electron Microscopy	Macro structural information
X-ray diffraction (XRD)	Supramolecular structure
Raman spectroscopy	Diameter distributions; to check the presence of CNTs and to verify the presence of SWCNTs or MWCNTs

2.2.6 Applications of Carbon Nanotubes

Carbon Nanotubes in Electronics

It should be pointed out that the integration of nanotubes into electronic devices is still a long-term application. However, nanotubes (in particular, SWCNTs) have emerged as a promising class of electronic materials due to their nanoscale dimensions and outstanding properties, such as ballistic electronic conduction and sensitivity to electro-migration. Both metallic and semiconducting SWCNTs are found to possess electrical characteristics that compare favourably with the best electronic materials presently available. The recent advances in the separation of SWCNTs with different electronic properties have enabled the nanotube community to develop the field-effect transistors (FET) and interconnect on a large scale (Jorio *et al*., 2008).

Carbon Nanotubes for Mechanical Properties

Carbon nanotubes display unique mechanical and electrical properties that have triggered the search for applications in composite materials. Enforcement of materials as well as enhancement of electrical conductivity is actively considered. In order to enhance polymer conductivity, one can add well-known conventional carbon nanotubes with micrometre thickness. Using nanotubes enables one to achieve enhanced conductivity at a much reduced loading of carbon (De Jong and Geus, 2000).

Carbon Nanotubes in Energy Applications

Conventional carbon materials have been utilised either as the electrode materials themselves or the conductive filler for the active materials in various electrochemical energy-storage systems due to their good chemical stability and high electrical conductivity. Therefore, it is natural that CNTs have been adopted as the preferred alternative electrode material because they have unique electrical and electronic properties, a wide electrochemical-stability window, and a highly accessible surface area. With regard to energy generation and storage, nanotubes show great promise in super-capacitors, Li-ion batteries, solar cells and fuel cells (Jorio *et al*., 2008).

2.3 Immobilisation of Brewers' Yeast

2.3.1 Yeast Cells

Yeast cells are used to ferment sugars to produce alcohol during beer production. Kunze (1999) describes yeast as oval to round with a length between 8 – 10 μm and a width between 5 – 7 μm. The costs of removing the yeast cells from beer in the clarification stage are high due to equipment costs and there is need to find

cheaper and/or more efficient alternative ways to do this process once the required alcohol content has been achieved.

There are thousands of unique strains of *S. cerevisiae* with interest in brewing centres around the world. These strains encompass brewing, baking, wine-distilling, and laboratory cultures (Batistote *et al*., 2006). *Saccharomyces*, Latin for sugar fungus, is the name first used for yeast in 1838 by Meyen. The species name *cerevisiae* derives from the Latin for beer as in *ceres* (= grain) and *vise* (= strength) (Briggs *et al*., 2004). Traditionally, lager is produced by bottom-fermenting yeasts at fermentation temperatures between 7 and 15 ^{o}C and, at the end of fermentation; these yeasts flocculate and collect at the bottom of the fermenter. Top-fermenting yeasts, used for the production of ale at fermentation temperatures between 18 and 22 ^{o}C, tend to be somewhat less flocculent, and loose clumps of cells adsorbed to carbon dioxide bubbles are carried to the surface of the fermenting wort. Consequently, top yeasts are collected by skimming from the surface of the fermenting wort, whereas bottom yeasts are collected, or cropped, from the fermenter bottom (Priest and Stewart, 2006).

2.3.2 Immobilisation of Microorganisms on Carbon Nanotubes

The interactions of nanomaterials with biomolecules and the formation of nano-bio hybrid complexes have only recently been studied and are still not well understood (Bhattacharyya *et al*., 2007). The biocompatibility and bioelectrochemical applications of CNTs are also attracting much attention. Thus, proteins and enzymes immobilised on CNTs have been used as electrochemical biosensors (Azamian *et al*., 2002) and recently direct methanol fuel cells (DMFC) with CNT based electrodes was reported (Gutiérrez *et al*., 2007; Prabhuram *et al*., 2006). Given that CNTs are also suitable supports for cell growth (Correa-Duarte *et al*., 2004; Gheith *et al*., 2005) they can find use as CNT based electrodes in

microbial fuel cells (MFCs). Huang *et al*., (2004) reported the immobilisation of antibodies and bacterial binding on nanodiamond and CNTs for biosensor applications.

CNTs have high bacterial adsorption capacity (Upadhyayula *et al*., 2008) and are able to concentrate different types of pathogens (Srivastava *et al*., 2004). This exceptionally high adsorption capacity of nanotubes is due to its large surface to volume ratio and high aspect ratio that imparts high antimicrobial nature to the material (Upadhyayula *et al*., 2008). CNTs produced by the previously mentioned methods (Section 2.2) are hydrophobic in nature i.e. more attractive to non-polar groups than polar substance. The CNTs can be functionalised to become hydrophilic, since the bacterial binding capacity of hydrophilic nanotubes is higher than hydrophobic nanotubes (Elkin *et al*., 2005; Huang *et al*., 2004). This is true but when it is desired to use CNT adsorbent media to simultaneously concentrate and detect pathogens from the flowing stream of water, it is desirable to have hydrophobic nanotubes from a practical standpoint (Upadhyayula *et al*., 2008).

Tzeng *et al*., (2004) found out that there was good bacterial binding on the surface of hydrophilic CNTs and no bacterial binding on hydrophobic CNTs. They investigated the hydration properties of CNTs and their effects on electrical and biosensor applications. The CNTs were synthesised by CVD method, functionalised by subjecting them to oxidising environments and immobilised antibodies on functionalised the nanotubes.

2.3.3 Yeast Growth Phases

When a culture of yeast cells is inoculated in a fresh growth medium, they enter a brief lag phase where they are biochemically active but not dividing. After this lag phase, cells enter their cell cycle and start dividing. The cells grow exponentially in number and the population is said to be in an exponential phase of growth. They multiply until the nutrients are exhausted or some metabolite accumulates to toxic concentrations. Subsequently, the cells stop dividing and enter a stationary phase followed by a decreasing phase when cells start dying as depicted in Figure 2.3 (Singh *et al*, 2006).

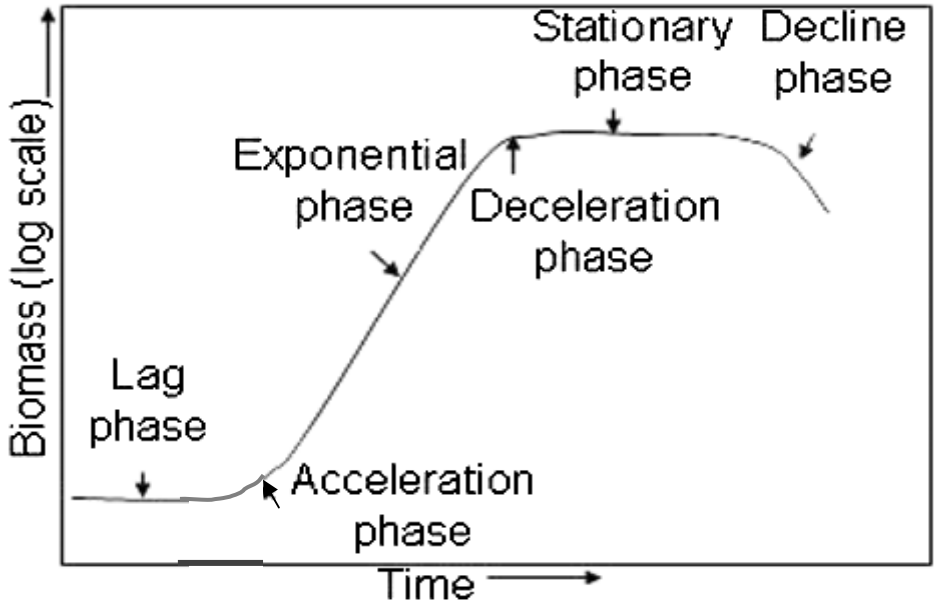

Figure 2.3: The growth curve showing the phases of yeast cell population (from Singh *et al*, 2006).

Lag Phase

The lag phase is the time lag (usually 12–24 h) between inoculation of the wort and the appearance of fermentative activity. During the lag phase the yeast readjusts to a new environment rich in nutrients. The cells synthesise enzymes

needed to utilise nutrients and support growth. Because wort sugars are not assimilated early in the lag phase, glycogen is essential as an energy source for cell activity. After the lag phase, there is a short transition into the logarithmic or exponential growth phase (Priest and Stewart, 2006).

Growth Phase

After this lag phase cells enter their cell cycle and start dividing. The cells grow exponentially in number and the population is said to be in an exponential phase of growth. They multiply until some nutrient is exhausted or some metabolite accumulates to toxic concentrations. Subsequently, the cells stop dividing and enter a stationary phase. During this period, the yeast cells use the oxygen in the wort to oxidise a variety of acid compounds, resulting in a significant drop in pH. In this connection, some yeast strains will result in a much greater fall in pH than others within the same fermenting wort (Singh *et al*, 2006).

Fermentation Phase

This is also the stationary phase. The fermentation phase quickly follows the growth phase when the oxygen supply has been depleted because fermentation is an anaerobic process. In fact, any remaining oxygen in the wort is “scrubbed off”, that is, stripped out of solution by the carbon dioxide bubbles produced by the yeast. As the cell population increases and the pools of unsaturated fatty acids and sterols are distributed among the increasing cell population, the growth rate slows. This is the stationary phase and cells begin to assimilate maltose (Priest and Stewart, 2006).

Sedimentation Phase

The sedimentation phase is the process through which yeast flocculates and settles to the bottom or floc on the top of the fermenter solutions or fermentables medium. The yeast begins to undergo a process that will preserve its life as it readies itself for dormancy, by producing a substance called glycogen. Glycogen

is necessary for cell maintenance during dormancy and, as mentioned, is an energy source during the lag phase of fermentation (Singh *et al*, 2006).

Decline Phase

This is a decreasing phase when the cells start to die.

2.3.4 Immobilisation Methods

Various supports and immobilisation techniques have been proposed and tested for application in winemaking, cider-making, brewing, distillates, potable alcohol and novel beverages production. Several techniques and support materials have been proposed and these techniques can be divided into four major categories based on the physical mechanism employed (Figure 2.4).

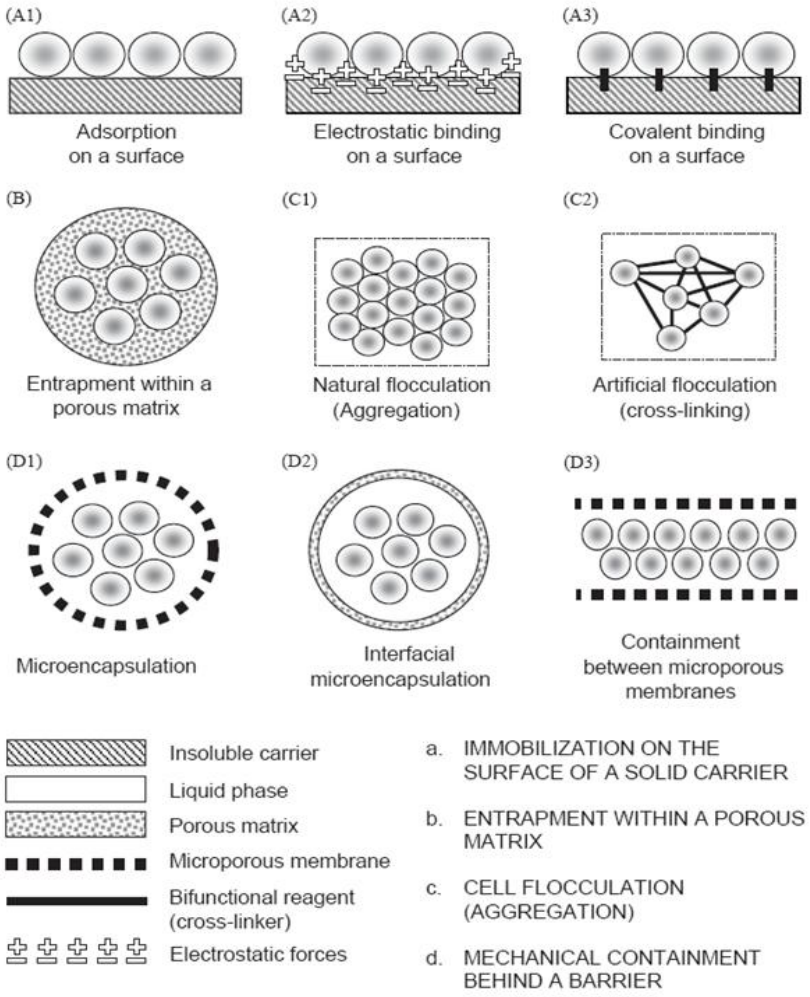

Figure 2.4: Basic methods of cell immobilisation (from Kourkoutas *et al*., 2004).

The four basic methods for cell immobilisation are (a) attachment or adsorption on solid carrier surfaces (b) entrapment within a porous matrix (c) self aggregation by flocculation (natural) or with crosslinking agents (artificially induced), and (d) cell containment behind barrier.

Immobilisation on Solid Carrier Surfaces

In this type of immobilisation, yeast cells are allowed to attach to a solid support. Cellular attachment to the carrier can be induced using linking agents (such as

metal oxides, glutaraldehyde or aminosilanes). However, for the production of beverages and ethanol, natural adhesion is often preferred over the use of (potentially harmful or unstable) inducers. Natural immobilisation is very simple and the conditions are mild, but cell loadings are usually not as high as those obtained in systems in which the cells are entrapped. Moreover, as there are no barriers between the cells and the solution, cell detachment and relocation is possible (Verbelen *et al*., 2006).

Entrapment within a Porous Matrix

In this type of immobilisation, the cells are either allowed to penetrate into the porous matrix until their mobility is obstructed by the presence of other cells, or the porous material is formed in-situ into a culture of cells. Both entrapment methods are based on the inclusion of cells within a rigid network to prevent the cells from diffusing into the surrounding medium, while still allowing mass transfer of nutrients and metabolites. Characteristic examples of this type of immobilisation are the entrapment into polysaccharide gels like alginates, k-carrageenan, agar, chitosan and polygalacturonic acid or other polymeric matrixes like gelatin, collagen and polyvinyl alcohol. Cell growth in the porous matrix depends on diffusion limitations imposed by the porousity of the material and later by the impact of accumulating biomass. One of the problems of cell entrapment within a porous matrix such as polysaccharide gel is the ability of cells located on the outer surface of the beads to multiply and be released from the inclusion bead. This leads to a system comprising of immobilised and free cells. The enumeration of biomass entrapped in a gel matrix is critical for application of biotechnological processes using viable immobilised cells (Kourkoutas *et al*., 2004).

Cell Flocculation (Aggregation)

Cell flocculation or aggregation is defined as the reversible phenomenon wherein yeast cells adhere in clumps and either sediment rapidly from the medium in which they are suspended or rise to the medium's surface (Stewart and Russell, 1981). Therefore, the aggregation may include agglutination (mating) and flocculation but not chain formation. However, the European Brewery Convention (EBC) suggested that `the aggregation of yeast cells into flocs which may be due to either non-separation of cells after budding or coalescence of single cells into clumps late in fermentation' (EBC Microbiologica, 1981). Chain formation has been generally held as a unique type of cell aggregation. Chain formation is caused by failure of daughter cells to separate from mother cells during cell division. The cells grow into chains of up to 100 cells by further budding of mother and daughter cells. Such chains can be dispersed irreversibly by mechanical shear rather than ethylenediaminetetraacetic acid (EDTA) since the chain structure is calcium-independent (Jin and Speers, 1998).

Flocculation, a property of the yeast cell wall, is also the characteristic of brewing yeast that allows the separation of yeast from beer, and is strongly correlated to the physical surface properties of the cell. Individual strains of yeast differ considerably in their flocculating power. At one extreme are the very flocculent strains referred to as "gravelly" and at the other extreme are totally non-flocculent strains sometimes referred to as "powdery." This means that the strongly flocculating yeasts can sediment out of the fermentation broth prematurely, giving rise to sweeter and less fermented beers, whereas the weakly flocculating strains can remain in the beer during aging and cause yeasty flavor and filtration difficulties (Priest and Stewart, 2006).

Yeast cell wall surface possesses a net negative charge and exhibits hydrophobicity. The negative charge is attributable to phosphate chains located in the mannoprotein outer wall and can be demonstrated by alcian blue staining. The extent of the charge can be measured by ion-exchange chromatographic or electrophoretic (zeta-potential) methods. The charge is particularly important during the fining of cask beer, when the positively-charged sites on the collagen molecules in isinglass (a material used for fining) attract individual yeast cells and promote sedimentation. The strength of the charge varies with environmental conditions (such as starvation) and during fermentation there is a reduction in the charge at the onset of flocculation. Hydrophobicity increases immediately prior to flocculation and is thought to be very important in this process (Hornsey, 1999). Flocculation of *S. cerevisiae* is thought to be caused by nutrient limitation. All in all, it seems that flocculation may be a defence mechanism adopted by some yeast strains in response to adverse factors to the cells. The formation of flocs may generate nutritionally rich microenvironments by selective lysis (Domingues *et al.,* 2000).

Factors Affecting Flocculation

There are several factors that affect flocculation of brewers' yeast, which are (a) mechanical agitation, (b) medium salt content, (c) presence of sugar, (d) pH of solution, (e) incubation temperature, (f) aeration, (g) ethanol, (h) cell age, (i) cell surface properties, (j) genetics of yeast flocculation and (k) flocculins (Domingues *et al*., 2000; Jin and Speers, 1999; Verstrepen *et al*., 2003).

(a) Mechanical Agitation

Cells must come into contact with each other for flocculation to occur, hence the surprising observation that flocculation and the vigour of mechanical agitation are positively correlated. Thus in well stirred systems there is a high probability that cells will contact each other and once formed, flocs are relatively stable structures (Briggs *et al*., 2004). Mechanical agitation may affect particle interactions either by increasing interparticle collision frequency, or by increasing the force of those

collisions. Mechanical agitation becomes more important than Brownian motion (irregular motion of microscopic suspended particles, which are in kinetic equilibrium with the molecules of the medium) when the diameter of at least one of the colliding particles is greater than 1 μm. Based solely on collision frequency, yeast (~8 μm) interactions are expected to be strongly influenced by mechanical agitation to a certain extend (Stratford and Wilson, 1990).

Agitation has two antagonistic effects: enhanced particle collision rate which induces flocculation on the one hand, and on the other higher shear forces which causes particle breakage. An increase in agitation intensity leads to a decrease in floc size. Gentle agitation gives large flocs while vigorous agitation gives smaller denser flocs that settle more slowly but giving a more compact sediment (Domingues *et al*., 2000).

Classical colloid theory involves attractive, van der Waals, and repulsive electrostatic forces between particles. The electrostatic charge of particles attracts an ion atmosphere of oppositely charged ions and thus forms an electric double-layer. If the ionic concentration is raised, the electric double-layer is compressed and repulsion between particles becomes negligible. Rapid coagulation then occurs, due to attractive van der Waals forces, the rate being limited only by particle collision frequency. Biological particles, however, differ in several respects from ideal sphaerocolloidal particles. In addition to electrostatic repulsion due to negative surface charge, cells exhibit steric repulsion by surface glycoproteins partly due to their hydrophilic nature. Cell-cell contact also causes physical displacement of the electric double-layers and attracted water-shells. While overall electrostatic repulsion may be neglected, energy is required to push aside attracted ions and water molecules and permit cell-cell interaction (Stratford and Wilson, 1990).

(b) Medium Salt Content

Although some controversial data is found in literature concerning other cations, it is widely accepted that the "activation" of flocculation is achieved by calcium ions. The presence of calcium ions is required at a very low concentration in order to induce flocculation (Taylor and Orton, 1973). The controversial data involving other cations is due to the use of different cation concentrations, different flocculation measurement techniques, different pH values and strains with different genetic background. For low salt concentrations (cations other than Ca^{2+} ions e.g. Mg^{2+}, Mn^{2+}), there is an observed flocculation enhancement, while at high concentrations inhibition of flocculation by the salt is observed (Domingues *et al*., 2000).

(c) Presence of Sugar

Different sugars cause different effects on flocculation. Generally it was found that maltose and mannose were the most effective inhibitors of flocculation whereas sucrose and glucose were less effective. Sugars like galactose and fructose were ineffective (Jin and Speers, 1999). The sugar inhibition of flocculation is therefore strain-dependent, having a direct effect rather than acting metabolically (Domingues *et al*., 2000).

(d) pH of Medium

Flocculation occurs towards the end of primary fermentation where the pH value of wort has fallen from 5.2 to around 4.5 to 4.0 (Jin and Speers, 1998). The hydrogen-ion concentration was considered as an important factor promoting flocculation by early researchers (Calleja, 1987; Stratford, 1992). Lower surface charge caused by increased hydrogen-ion concentration may have a role to play for the colloidal theory of flocculation. One would expect that lowered surface charge may make cell-cell contact easier and increase the rate of flocculation (Stratford, 1992).

pH was first considered not to be a determinant factor of flocculation, but that it alters the cell surface charge (Stratford, 1992). Many brewing strains do not flocculate in laboratory culture medium, because their initial pH and buffering capacity do not allow for the pH range within which these yeasts flocculate. Once the pH was corrected the brewing yeast strains were able to flocculate in laboratory culture medium. With these strains, a simple change of pH at any desired time during fermentation, allows for cell separation from the medium (Stratford, 1996).

In aqueous suspensions at the pH values of worts and beers (3.80–5.60), brewers' yeasts migrate to the anode in electrophoresis experiments, thus behaving as negatively charged colloids. At more acid pH values (2.30), reversal of the charge may take place (Ross and Harrison, 1970). This property can allow the use of a positively charged flocculating agent to induce flocculation within the mentioned pH range.

It has been shown that yeast flocculation is optimal in slightly acidic conditions, with pH values ranging from 3.5 to 5.8 (Jin and Speers, 2000; Jin *et al*., 2001; Soares *et al*., 1994; Stratford, 1992). Recent studies showed that flocculation can occur between pH 1.5 and 9.0, clearly indicating that pH is not the dominant factor causing flocculation but this does not mean that pH is not important (Verstrepen *et al*., 2003). However, the optimum pH for flocculation seems to be highly strain-dependent, so that no general conclusions can be drawn (Verstrepen *et al*., 2003).

(e) Immobilisation Temperature

There is an apparent contradiction in the literature about the effect of temperature, some authors noted deflocculation with increasing temperature while others noted an increase in flocculation with increasing temperature. This discrepancy maybe

attributed to differences in the response of ale and lager strains (Speers *et al*., 1992). Nevertheless, it was shown that temperature does not inhibit cell-cell interactions, but it induces or represses the formation of a certain cell wall component involved in flocculation (Verstrepen *et al*., 2003).

Mill (1964) observed that flocculation was the same at 23 and 45 ^{o}C and it steadily decreased as temperature was increased (47, 50, 51, 54, 58 and 62 ^{o}C). This was interpreted as dispersion of flocs due to heating (50 – 60 ^{o}C) and such a 'melting' of flocs was readily reversible on cooling. Kamada and Murata (1984) investigated the effect of temperature on yeast immobilisation and concluded that yeast flocculation rate increases as the temperature rises. Also they concluded that hydrophobic interactions increased at higher temperature supporting the assumption that hydrophobic bonds participate in yeast flocculation.

The capture coefficient of yeast cells in suspension was shown to be directly proportional to the product of the cell wall mannose and zymolectin densities, the reciprocal of shear rate, and exhibited an increase as the temperature was increased from 5°C to 45°C (Hsu *et al*., 2001). Their studies were based on 2 *S. cerevisiae* ale yeast strains 125 and 1209 incubated at 30 ^{o}C and 100 rpm and the increase showed an increase in flocculation as temperature increased. Jin *et al*. (Jin and Speers, 2000; Jin *et al*., 2001) found that flocculation of a lager yeast strain varied between 24.1 % at 5 ^{o}C to 66.8% at 25 ^{o}C. Generally however, there is little influence of temperature on flocculation of brewing yeast at physiological temperatures of 15 – 32 ^{o}C (Jin and Speers, 1999).

Peinado *et al.* (2005) conducted their studies at 28 ^{o}C and 150 rpm for 7 days and had successful immobilisation to produce yeast biocapsules while Sakurai *et al.*

(2000) used 30 ^{o}C and 160 rpm during their immobilisation studies of yeast cells on porous cellulose carriers. Öztop *et al*. (2003) immobilised *S. cerevisiae* onto acrylamide-sodium acrylate hydrogels at 30 ^{o}C for 72 hours.

Tosch *et al*. (2005) conducted their studies on polar lips of brewer's yeasts on 6 strains of *S. cerevisiae* at 25 ^{o}C for 10 days with occasional stirring every second day after growing the cultures on wort at 25 ^{o}C for 4 days. They were able to differentiate 2 strains from the other 6 on the basis of lipid chemistry.

(f) Aeration

No flocculation can be monitored during the exponential growth phase, but as soon as the cells stop dividing, flocculence gradually reappears (Soares and Mota, 1996; Straver *et al*., 1993). Oxygen consumption occurs during the very early stages of beer fermentation and it is used for the production of unsaturated fatty acids and sterols, which are essential constituents of yeast cell membrane. When oxygen is insufficient for membrane synthesis, yeast cells would fail to grow (Jin and Speers, 1999). Starver *et al*. (1993) found that poor wort aeration resulted in early and incomplete flocculation, while normal saturation with oxygen both delayed and intensified flocculation. Remarkably, the poor growth and flocculation characteristics of yeast grown in de-aerated medium could be restored by addition of ergosterol and oleic acid to the medium. This indicates that oxygen probably does not act directly on flocculation, but rather indirectly through its importance for the synthesis of unsaturated fatty acids and sterols.

(g) Ethanol

Addition of ethanol does not influence flocculation of stationary cells for bottom yeast but induced flocculation of stationary ale yeast (Dengis *et al*., 1995). A relationship was found between flocculation behaviour and the dielectric constant of suspensions containing organic solvents at high concentrations and was explained by a decrease in ionisation of salt bonds and an increase in the strength

of hydrogen bonds (Mill, 1964) which implies an increase of hydrophobicity. Considering the yeast cell as a hydrophobic colloid, the effect of ethanol may be a result of its adsorption at the cell surface. It may cause a reduced local dielectric constant and a decreased cell-cell electrostatic repulsion, or a decreased steric stabilisation by allowing the protrusion of mannoproteins for specific or non-specific binding. Organic solvents would then promote the cell-cell interactions (Dengis *et al*., 1995).

(h) Cell Age

Genealogically older yeast cells (cells that have produced a number of daughter cells) tend to flocculate earlier and more intensely than their younger counterparts. There are several reasons for this difference. Firstly, young "virgin" daughter cells do not have flocculins in their cell walls (Soares and Mota, 1996). Secondly, and more importantly, genealogically older cells tend to be larger than younger cells, and their cell walls are more hydrophobic and "wrinkled" than those of young cells (Barker and Smart, 1996; Jin *et al*., 2001). The wrinkled surfaces may facilitate cell-to-cell adhesion and thus favour flocculation (Barker and Smart, 1996). Additionally, older cells seem to display an increased resistance to mechanical separation of mother and daughter cells, so that mother and daughter often stay attached to each other for a longer time. These linked cells possibly provide nuclei for floc formation, explaining why older yeast populations show increased flocculation (Barker and Smart, 1996).

Cell death may occur via one of two distinct pathways: necrosis and senescence. Necrosis may be defined as the accumulation of irreparable damage to intracellular components compromising cell integrity, leading to death and autolysis. In contrast, senescence is the predetermined cessation of life as a result of the genetically controlled progression from youth to old age (Powell *et al*., 2000).

In the brewing industry, yeast age is measured chronologically in terms of the number of times a yeast population is serially repitched. In addition, yeast which has been stored (in the form of a highly concentrated cell suspension), or maintained in extended stationary phase is often referred to by brewers as aged. Such populations exhibit impaired physiological states, although their phenotypic characteristics more closely resemble those associated with necrosis than senescence (Powell *et al*., 2000).

(i) Cell Surface Properties

There is evidence of an increase of the water contact angle at the beginning of flocculation. It was demonstrated that a relation existed between cell division arrest, the increase of Cell Surface Hydrophobicity (CSH) and initiation of flocculence during fermentation (Straver *et al*., 1993). A high level of CSH may facilitate cell-cell contact in an aqueous medium resulting in more specific lectin-carbohydrate interactions (Straver and Kijne, 1996). To date, there is no significant correlation between cell surface charge and flocculation of yeast. However, it has been suggested that surface charge and the non-separation of progeny from mother cells rather than surface hydrophobicity influences the chain-formation of brewing yeast (Jin and Speers, 1999).

Speers *et al*. (2006) conducted their fermentation studies using an ale brewing yeast strain (LCC125) at 30 ^{o}C between 72 and 120 hours observed that the CSH increased rapidly in the exponential phase of fermentation but readily reached high and stable levels in stationary phase. The reduced CSH of yeast cells in the exponential phase was explained by the occurrence of large numbers of daughter cells or virgin cells that are reported to be significantly less hydrophobic than their older counterparts. The variation of CSH partially explained the change in flocculation ability of yeast cells during fermentation. This result supported the

previous reports on relationships of CSH and flocculent strains (Kock *et al*., 2000).

(j) Genetics of Yeast Flocculation

Like any other protein, flocculins are encoded by specific genes, the so-called *FLO* genes. The best-known flocculation gene is *FLO1*, a dominant gene situated at the right arm of chromosome 1 (Verstrepen *et al*., 2003). Expression of *FLO1* and its homologues causes flocculation of the Flo1 phenotype. When these *FLO* genes become active, flocculins are formed and flocculation can take place (Stratford, 1992). Unfortunately, the situation is more complex than this. Firstly, the *FLO* family consists of several different *FLO* genes, each of which may be regulated through different complex mechanisms and therefore may be induced (or repressed) by different factors (Verstrepen *et al*., 2003). Secondly, the *FLO* gene family is very unstable, causing great differences in the flocculation profile and response between different yeast strains and even between different generations of a specific yeast strain (Verstrepen *et al*., 2003). Thirdly, flocculation is not only a biochemical process, but also implies physical interaction: cells need to collide in order to bind to each other. Therefore, factors that influence these cell-cell interactions also play an important role, even if they do not influence the activity of the *FLO* genes (Verstrepen *et al*., 2003).

More specifically, factors that raise the collision frequency between cells, e.g. agitation of the growth medium, may promote flocculation. Factors that increase the hydrophobic character of the yeast cell walls (CSH) or factors that decrease the repulsive negative electrostatic charges in cell walls (cell surface charge) are also known to cause stronger flocculation, presumably because they facilitate cell-cell contact (Stratford, 1992; Straver *et al*., 1993). Factors influencing flocculation can therefore be divided into three groups: the genetic background of the strain; environmental factors that influence *FLO* gene expression e.g. nutrition, ethanol and temperature, and *Flo* protein activation, and factors that act upon the physical

interactions between yeast cells e.g. agitation, ionic strength, Ca^{2+} concentration (Figure 2.5) (Verstrepen *et al*., 2003).

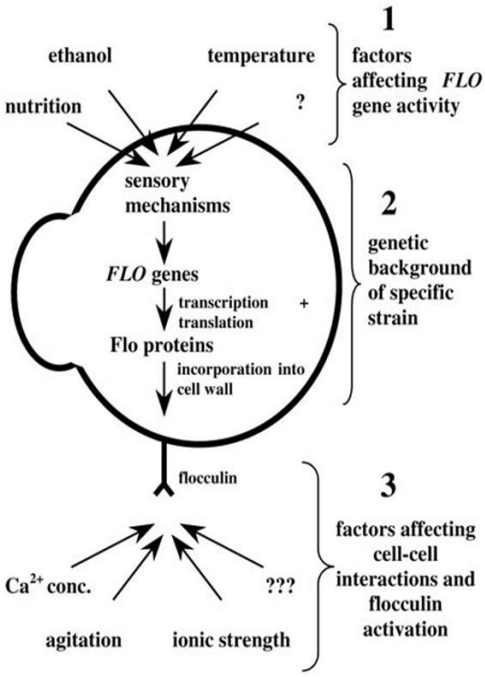

Figure 2.5: Factors affecting flocculation (from Verstrepen *et al*., 2003).

(k) Flocculins

Flocculation of yeast cells involves lectin-like proteins, the so-called flocculins – that stick out of the cell walls of flocculent cells and selectively bind mannose residues present in the cell walls of adjacent yeast cells. Calcium ions in the medium are needed in order to activate the flocculins (Stratford, 1992; Verstrepen *et al*., 2003) (Figure 2.6). In addition, the work of Straver *et al*., suggests that, in some cases, flocculation is not only solely dependent on the presence of flocculins, but also requires agglutinins and/or fimbriae-like structures (Straver *et al*., 1993; Straver and Kijne, 1996).

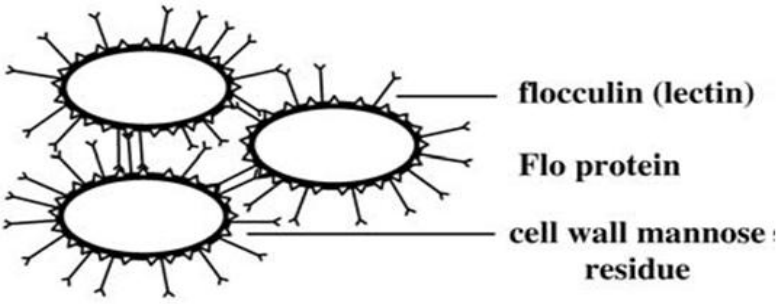

Figure 2.6: The lectin model for flocculation (from Verstrepen *et al*., 2003).

Summary

The environmental properties mentioned above may be controlled allowing not only for a better understanding of the phenomenon but also for its control. Nevertheless, the strain variability must be taken into account, as this is one of the reasons for most of the controversy found in literature data concerning flocculation (Domingues *et al*., 2000).

Mechanical Containment behind a Barrier

Containment of cells behind a barrier can be attained either by use of a microporous membrane filter or by entrapment of cells in a microcapsule or by cell immobilisation onto an interaction surface of two immiscible liquids. Selected yeasts confined by microfiltration membranes have been developed and are available for winemaking in the market. The major disadvantages of cells immobilisation between microporous membranes are mass transfer limitations and possible membrane biofouling caused by cell growth (Kourkoutas *et al*., 2004).

2.3.5 Yeast Autolysis

Autolysis of yeast cells occurs after they have completed their life cycle and entered the decline or death phase. It is characterised by a loss of cell membrane permeability, alteration of cell wall porosity, hydrolysis of cellular

macromolecules by endogenous enzymes, and subsequent leakage of the breakdown products into the extracellular environment (Zhao and Fleet, 2003). Although a naturally occurring event, autolysis can be initiated by exposing yeasts to elevated temperatures (40–60 ^{o}C), organic solvents, salts or detergents (Arnold, 1981; Hernawan and Fleet, 1995; Zhao and Fleet, 2003; Alexandre and Guilloux-Benatier, 2006). Yeast autolysis can be natural autolysis or induced autolysis. Induced autolysis is widely used in industrial applications, such as for the production of a yeast extract used as a flavour enhancer or for production of intracellular enzymes. The autolysis process can be very fast, from 48 h to 72 h, depending on the inducer. Natural autolysis, however, takes much longer. The principal factors that may affect autolysis are physical inductors (rise in temperature, alternate freezing and thawing, and osmotic pressure), chemical inductors (pH, detergents, and antibiotics), or biological inductors (aeration and starvation) (Alexandre and Guilloux-Benatier, 2006).

Abdel-Azeem (2009) noted that using yeast extract or peptone as the sole source of nitrogen in carbon limited medium for *S. cerevisiae* is sufficient for glycogen synthesis and this enables the cells to survive long starvation periods thereby preventing autolysis. His experiments were carried out at 30 ^{o}C on a rotary shaker at 170 rpm for 5 days. Using yeast extract, the glycogen accumulated was 20.19% for a final pH of 4.90 and 20.96% when using peptone for a final pH of 4.85. Also Abdel-Azeem investigated the effect of initial pH on accumulation of glycogen and he found that a pH of 6.0 was the most favourable for *S. cerevisiae* strain with the final pH between 4.85 and 5.00. This information showed the decrease in pH as the yeast cells grows. The maximum glycogen reached with an initial pH of 6.0 was 33.78% after 3 days incubation (Figure 2.7). Lastly, he tested the effect of yeast glycogen on the longevity of the cells for 3 days and the results are shown in Figure 2.8.

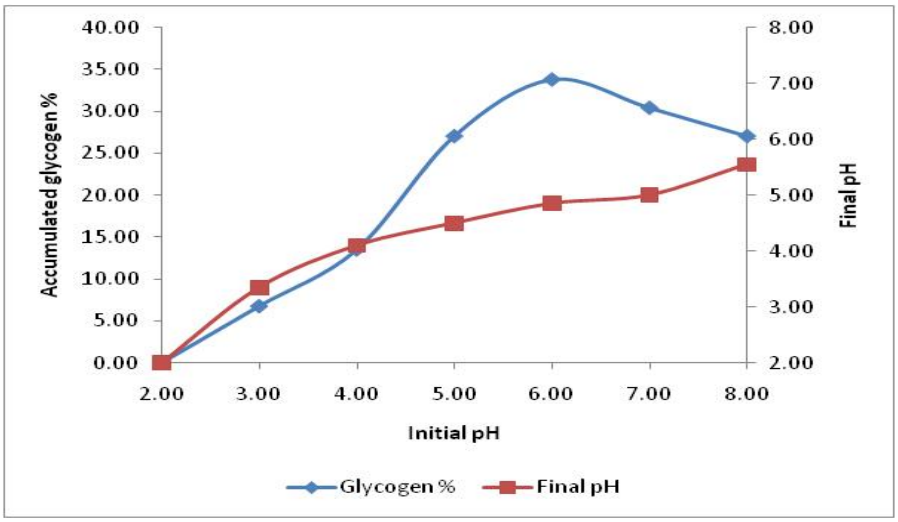

Figure 2.7: Effect of different pH values on accumulation of glycogen in *Saccharomyces cerevisiae* (from Abdel-Azeem, 2009).

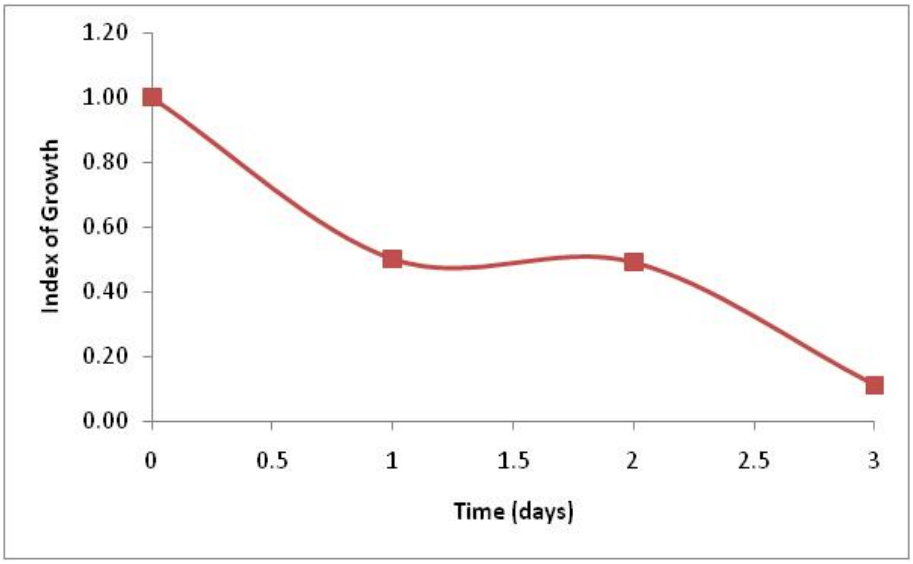

Figure 2.8: Effect of cellular glycogen content on the longevity of *Saccharomyces cerevisiae* (from Abdel-Azeem, 2009).

From Figure 2.8, it can be seen that the viability loss after 1, 2 and 3 days was 50%, 51% and 89% respectively. Hernawan and Fleet (1995) found a viability loss of 15%, 26%, 29%, 33% and 36% after 1, 2, 3, 4 and 5 days respectively for

S. cerevisiae using 45 °C and a pH of 4.5 with orbital shaking at 100 rpm. The cell dry weight decreased by 10.9%, 25% and 26.6% after 1, 5 and 10 days respectively.

Zhao and Fleet (2003) investigated viability of *S. cerevisiae* at a pH of 7.0, orbital shaking of 200 rpm and different temperatures of 30, 40, 50 and 60 °C. The reactions occurred rapidly at 50 and 60 °C leading to 100% loss in viability after 1 day but more gradually at 30 and 40 °C (Figure 2.9). Viability of losses at 30 °C was 2%, 13% and 24% after 1, 5 and 10 days respectively while at 40 °C, the viability losses were 29%, 39% and 100% after 1, 5 and 10 days respectively. At 40 °C there was little difference in viability losses at different pH of 4.0, 5.0, 6.0 or 7.0.

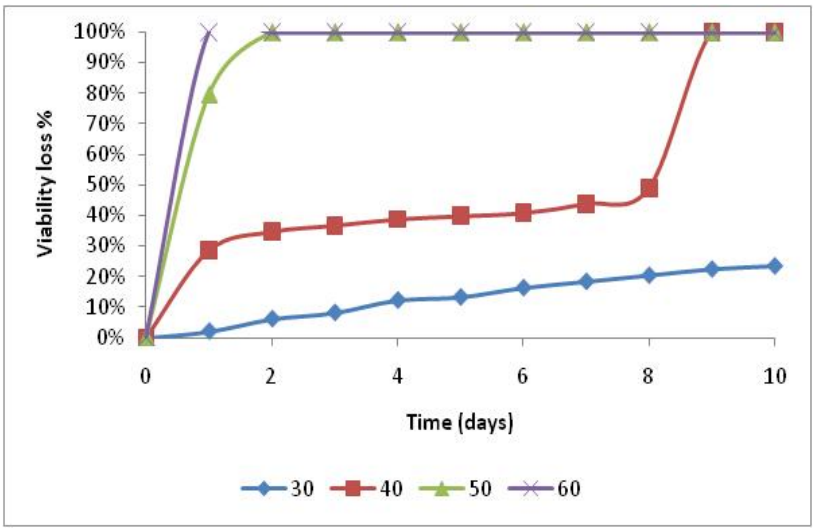

Figure 2.9: Changes in cell viability during autolysis of Saccharomyces cerevisiae at different temperatures and pH 7.0 (from Zhao and Fleet, 2003).

2.3.6 Immobilisation in Brewing

Beer production is traditionally a batch process. In the 1960s, the interest in continuous beer fermentation rose intensively, giving birth to a series of systems (Boulton and Quain, 2001). However, these continuous beer fermentation processes never became commercially successful due to many practical problems, such as increased risk of contamination (mainly because of the necessity to store wort in supplementary holding tanks), variations in beer flavour, complex system design and a lack of flexibility (Verbelen *et al*., 2006). In the 1970s there was a revival in the development of new continuous beer fermentation systems, owing to the development of immobilised cell technology.

At present, only beer maturation and alcohol-free beer production are obtained by means of commercial-scale immobilised yeast reactors (Mensour *et al*., 1997). In these processes, no real yeast growth and flavour formation is required. To date, only the continuous beer production process of Dominion Breweries in New Zealand by Morton Coutts has been successfully implemented (Coutts, 1966; Dunbar *et al*., 1988) and two continuous maturation systems have been implemented industrially so far: one at Sinebrychoff Brewery (Finland, capacity: 1 million hl per year) and another system, developed by Alfa Laval and Schott Engineering (Mensour *et al*., 1997).

The main objective during fermentation of alcohol-free beer is the reduction of wort carbonyl flavours by yeast, without the formation of alcohol, and therefore it resembles the secondary fermentation. Bavaria (the Netherlands) is using a packed bed immobilised yeast bioreactor to produce alcohol-free beer (Verbelen *et al*., 2006).

2.3.7 Zeta Potential

The concept of the zeta potential has been applied very successfully in the field of colloid sciences to understand colloid interactions and has been used frequently to describe, predict and control the stability of a colloid system. Zeta potential is defined as the potential at the boundary of the hydrodynamic shear plane of a charged particle (Figure 2.10) (Lin *et al*., 2003). Measurement of the zeta potential also helps to understand flocculation processes. The zeta potential depends on both the surface charge of the particle as well as on the thickness of the electric double layer i.e. it describes not only the electrochemical property of a particle surface but also the environmental conditions (e.g. pH and ion concentration) (Hunter, 1981). Therefore the zeta potential should always be stated with medium conditions (e.g. pH, conductivity, temperature and additives). Furthermore, influencing the zeta potential by changing pH and conductivity in the suspension affects flocculation of the suspension (Lin *et al*., 2003). In general, zeta potential can be regarded as the controlling parameter for charged particle interactions.

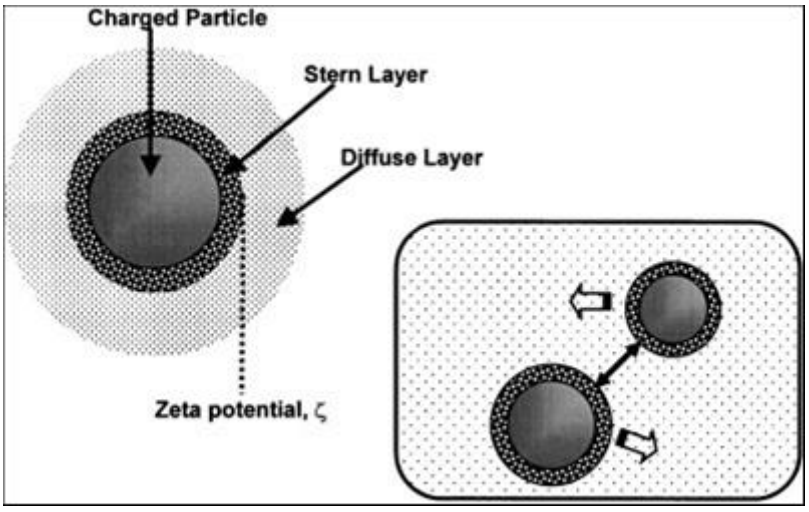

Figure 2.10: Schematic drawing of the electrochemical double layer and zeta potential of a charged particle (from Lin, *et al*., 2003).

The greater the zeta potential, the more likely the suspension will remain in stable form. Zeta potential is very much dependent on pH of the suspension. A plot of zeta potential vs. pH is called an iso-electric curve. The pH for which the zeta potential is zero is called the iso-electric point or point of zero charge (PZC). Yeast cells with small diameters (8 – 10 μm, see Section 2.3.1) can be considered as colloid particles (1 μm – 10 Angstroms) (Tripathy and De Ranjan, 2006).

Zeta potential or electrokinetic potential is the electrical potential that exists across the interface of all solids and liquids. There are four interaction forces relevant to microbial cells: (a) hydrodynamic forces which act repulsively, (b) long range interactions such as van der Waals forces and the electric double layer forces which are attractive or repulsive, (c) biopolymer bridging forces, and (d) short range forces which may either be attractive or repulsive (positive or negative) (Tripathy and De Ranjan, 2006). Among these forces, the electric double layer forces characterised by zeta potential are the most important and are usually repulsive as particles that are composed of the same material will have similar charge. When the zeta potential is negative, the particles will be attracted to each other and flocculation will occur (Narong and James, 2006).

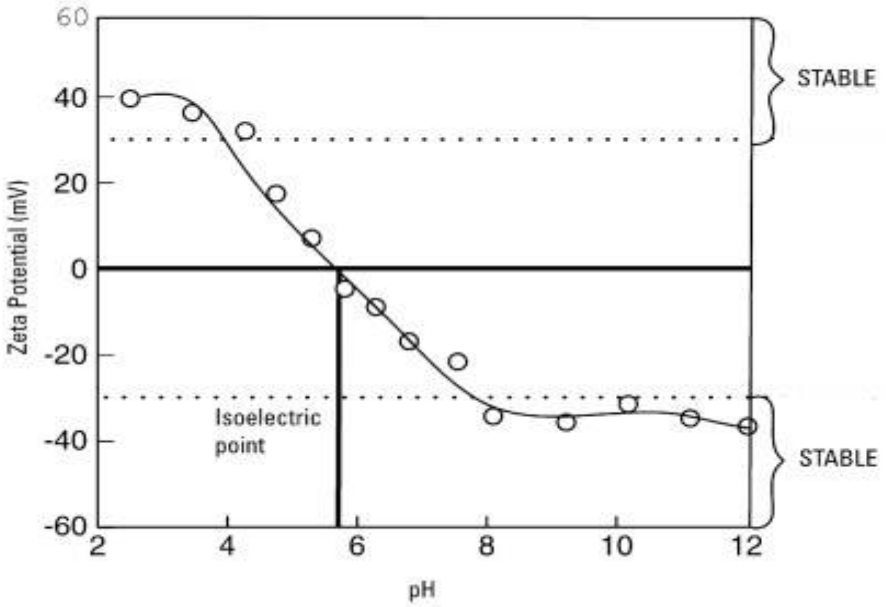

Figure 2.11: Typical plot of zeta potential versus pH showing the position of the iso-electric point and the pH values where the dispersion would be expected to be stable (from Tripathy and De Ranjan, 2006).

A typical plot of zeta potential versus pH is shown in Figure 2.11. In this example, the iso-electric point of the sample is approximately at pH 5.5. In addition, the plot can be used to predict that the sample should be stable at pH values less than 4 (sufficient positive charge is present) and greater than pH 7.5 (sufficient negative charge is present). Problems with dispersion stability would be expected at pH values between 4.0 and 7.5 as the zeta potential values are between +30 and -30mV (Zetasizer Technical Notes MKR654-01).

As they flocculate, the flocs will have the same charge as that of the particles, a mutual repulsion exists between the floc particles and the colloids, and these

repelling forces prevent the colloid from making permanent contact with the floc, regardless of agitation. Such colloids can effectively be removed by lowering the zeta potential of both the floc and colloid to a value approximately 0 ± 5 mV as shown in Table 2.2 (Tripathy and De Ranjan, 2006).

Table 2.2: Stability of solution through zeta potential (from Riddick, 1968).

Stability	**Average Zeta Potential (mV)**
Extreme to very good stability	–100 to –60
Reasonable stability	–60 to –40
Moderate stability	–40 to –30
Threshold of light dispersion	–30 to –15
Threshold of flocculation	–15 to –10
Strong flocculation	–5 to +5

The charge presented to the solution at the stern layer (Figure 2.10) naturally attracts a diffuse layer of free ions with a net different opposite charge, i.e., the diffuse layer. For particles to make contact and flocculate, the potential at the stern layer must be overcomed. In order to cause the particles of a stable dispersion to flocculate, it is necessary to provide enough kinetic energy to particles to overcome the potential energy barrier (Narong and James, 2006). Alternatively, the barrier can be eliminated by surface charge neutralisation. This may be accomplished either by double layer compression (charge neutralisation mechanism) or adsorption of flocculant onto the particle surface (bridging mechanism) as reported by Tripathy and De Ranjan (2006).

Bridging Mechanism

Long chain particles when added in small dosage to a suspension of colloidal cells, adsorb onto them in such a manner that an individual chain can become attached to 2 or more cells thus "bridging" them together (Figure 2.12a). But interestingly this phenomenon is observed up to a particular optimum particle dosage beyond which flocculation diminishes, a process known as steric stabilisation (Figure 2.12b). The essential requirements for cell bridging are:

- There should be sufficient unoccupied cell surface for attachment of particle segments from chains attached to other cells.
- The particle bridges should be of such an extent that they span the distance over which inter-cell repulsion prevails.

Thus at lower dosages there is insufficient particle to form adequate bridging links between cells. With excess particle, there is no longer enough bare cell surface available for attachment of segments and the cells become destabilised, which may involve some steric repulsion. On the average, bridging flocculation gives flocs which are much stronger than those produced by addition of salts (i.e., by reduction in electrical repulsion). However, such stronger flocs produced by the bridging mechanism may not reform once broken at high shear rates.

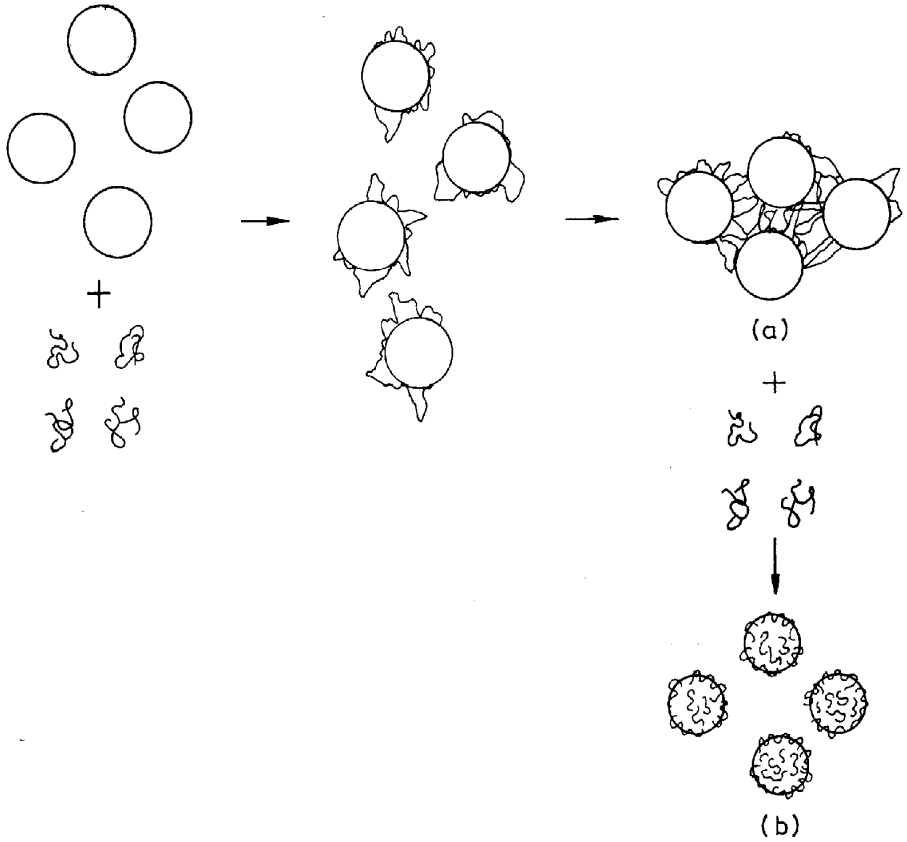

Figure 2.12: Schematic illustration of (a) bridging flocculation and (b) restabilisation by adsorbed polymers (from Tripathy and De Ranjan, 2006).

Zeta potential becomes more negative as pH becomes basic i.e. increases and it becomes less negative as yeast cells age. The surface charge can be reduced to zero by suppressing the surface ionisation using either of:

- Decreasing pH in case of negatively charged particles
- Increasing pH in case of positively charged particles (Zetasizer Technical Notes MKR654-01).

2.4 Preservation of the Immobilised Cells

Freeze-drying is a most convenient and successful method of preserving yeasts and sporulating fungi as well as bacteria. The advantages of freeze-drying are the protection from contamination or infestation during storage, long viability, and facility for strain distribution (Berny and Hennebert, 1991). The cooling rate of the cells during the process and the presence of protective agents are two critical factors for the viability and stability of microorganisms (Bekatorou *et al*., 2001a; Tsinontides *et al*., 2004). Freeze-drying has undesirable effects, such as denaturation of sensitive proteins and decreased viability for many cell types. To prevent or reduce these adverse effects, protective substances as skimmed milk, sucrose, glycerol, polymeric carbohydrate, and dimethyl sulfoxide are commonly added to samples before freezing and freeze drying. (Diniz-Mendes *et al*., 1999).

An example of the importance of freeze drying is shown in the increasing demand for frozen doughs containing baker's yeast with conserved desirable metabolical features. Yeast cells, when exposed to a mild temperature shift, 5 – 10°C above their normal growth temperature, may become tolerant to several additional stresses. This cellular response seems to be the result of two different mechanisms: the induced synthesis of Heat Shock Proteins (HPS) and accumulation of trehalose (Diniz-Mendes *et al*., 1999).

The cooling rate of the cells during the cooling phase is a critical factor in the freeze-drying process and the optimum cooling rate results from two opposite effects: concentration of intra- and extracellular solutes, responsible for cell injury when the cooling rate is lower than optimum and intracellular freezing, responsible for cell injury when the cooling rate is faster than optimum. At very slow cooling rates, extracellular and intracellular osmolalities can remain in equilibrium. As water is frozen out of solution, there is a progressive

concentration of intra- and extracellular solutes, leading to cell damage. As the cooling rate becomes more rapid, the concentration of extracellular solutes increases more rapidly (Berny and Hennebert, 1991). At fast cooling rates, the cell is not able to lose water fast enough to maintain the osmotic potential of intracellular water in equilibrium with that of extracellular water. The intracellular solution becomes more and more supercooled resulting finally in intracellular ice nucleation. The optimum cooling rate for yeast cells was shown to be between 1 and 10^{o}C/min (Berny and Hennebert, 1991).

2.5 Brewing

"Brewing" is defined in dictionaries as the making of beer or related beverages by infusion, boiling, and fermentation. Brewing is not unique to beer production: it is also the essential first part of the process of whisky production. We are also familiar with the term applied to the making of tea and herbal infusions (Priest and Stewart, 2006). Beers and beer-like beverages maybe prepared from raw cereal grains, malted cereal grains and (historically) bread. The simplest preparation of beers involves (a) incubating and extracting malted, ground up cereal grains (usually barley) with warm water. Sometimes the grounded malt is mixed with other starchy materials and/or enzymes (b) the solution obtained is boiled with hops or hop preparations (c) the boiled solution is clarified and cooled (d) the cooled liquid is fermented by added yeast. Usually the beer is clarified, packaged ad served while effervescent with escaping CO_2 (Briggs *et al*., 2004). The following is a brief description of the malting and brewing processes.

2.5.1 Malts

Malts are made from selected cereal grain, usually barley, (but sometimes wheat, rye, oats, sorghum or millet), that have been cleaned and stored until dormancy has declined and it is needed (Briggs *et al*., 2004). The malting process converts the raw barley by controlled steeping, germination, and kilning into a product that

is much more friable, with increased enzyme levels and with altered chemical and physical properties (Priest and Stewart, 2006). The moisture content of the grains should be no higher than 20% (15% is preferable). If prolonged storage is required then they should be further dried to 12% (Hornsey, 1999).

2.5.2 Mash Tun Adjuncts

These are preparations of cereals (e.g. flaked maize or rice flakes, wheat flour, micronized wheat grains, or rice or maize grits which have to be cooked separately in the brewery) which may be mixed with ground malt (provided local legislation permits their use) in the mashing process. An adjunct's starch is hydrolysed during mashing by enzymes from the malt, so providing a (sometimes) less expensive source of sugars as well as changing the character of the wort. Sometimes microbial enzymes are added to the mash (Briggs *et al*., 2004). An adjunct is added for any of the following reasons; (a) to produce a more stable beer, as they contain less protein (b) to produce a different flavour – maize, for example, is said to give a fuller flavour (c) to produce a better beer foam due to lower fat (lipid) levels and different proteins (d) to improve the ease of processing in the brew house, and (e) to produce beer at lower cost (Priest and Stewart, 2006).

2.5.3 Brewing Liquor

In brewing, water is commonly known as liquor. It is used for many purposes besides mashing, cleaning and in raising steam, and in beer dilution at the end of high-gravity brewing (Briggs *et al*., 2004).

2.5.4 Milling and Mashing

Mashing is the process of mixing the crushed malt, and cereal adjuncts if used, with hot water and letting the mixture stand while the enzymes degrade the proteins and starch to yield the soluble malt extract, wort (Priest and Stewart, 2006). The malt is broken up to a controlled extent by milling to create the "grist". The type of mill used and the extent to which the malt (and adjunct) is

broken down is chosen to suit the types of mashing and wort separation systems being used. If dry milling is used the grist, possibly mixed with adjuncts, is collected in a container (Briggs *et al*., 2004).

2.5.5 Wort Separation

Regardless of the mode of mashing, mash separation is important for three main reasons (1) to get maximum extraction of soluble fermentable sugars; (2) to obtain bright worts with minimum suspended solids; and (3) to minimise dissolved oxygen concentration ($d0_2$) in the wort. Secondary considerations must be: (a) to turn around the brew house as quickly as possible; (b) to minimise moisture content of spent grains; and (c) to minimise effluent production (Hornsey, 1999). These solids are sold as animal feed, draff, or spent grains for milk and beef cattle herds (Priest and Stewart, 2006).

2.5.6 Wort Boiling

The sweet wort is transferred to a vessel in which it is boiled with hops or hop preparations, usually for 1 – 2 hours. Hops are the female cones of hop plants. They may be used as whole or grounded up or as pellets or as extracts. Pelleted powders are often preferred (Briggs *et al*., 2004). Wort boiling is the process unique to beer production, as it is not required in the distilling or vinegar production processes. Wort boiling satisfies a number of important objectives; (a) sterilisation of the wort to eliminate all bacteria, yeasts, and moulds that could compete with the brewing yeast and possibly cause off-flavours (b) extraction of the bittering compounds from hops added early to the boil and oils and aroma compounds from late additions (c) coagulation of excess proteins and tannins to form solid particles (trub) that can be removed later. This is important for beer stability and foam (d) colour and flavour formation (e) removal of undesirable volatiles, such as dimethyl sulphide, by evaporation (f) concentration of the sugars by evaporation of water (Priest and Stewart, 2006).

2.5.7 Wort Clarification, Cooling and Aeration

At the end of the boil the transparent or 'bright' wort contains flocs of trub and suspended fragments of hops. These are separated from the wort by straining, centrifuging, sedimentation/flocculation, filtration or whirlpool (Priest and Stewart, 2006). The clear 'hopped wort' is cooled to fermentation temperatures to check continuing darkening and flavour changes and so it is inoculated ('pitched') with yeast, and can be aerated or oxygenated without a risk of oxidative deterioration. The temperature for fermentation is typically 10 – 15 ^{o}C for lager and 15 – 20 ^{o}C for ale for 2 – 3 days (Briggs *et al*., 2004).

2.5.8 Fermentation

For both ale and lager, the basic process of fermentation is similar; yeast uses sugars and proteins to produce alcohol, CO_2, new yeast cells, and flavour compounds (Priest and Stewart, 2006). As wort is converted into beer the removal of materials (especially sugars) from solution and the appearance of ethanol both contribute to the decline in specific gravity. The initial or original gravity (OG), the final or present gravity (FG or PG) at the end of the fermentation, and the final alcohol content are important characteristics of beers (Briggs *et al*., 2004).

Carbon Metabolism

The major sugars in an all-malt wort are expected to exhibit the following profile, in terms of percentage composition (Table 2.3).

Table 2.3: Composition of sugars in malt wort (from Hornsey, 1999).

Sugar	Maltose	Dextrins	Maltotriose	Glucose	Fructose	Sucrose
% Composition	50 – 60	20 – 30	15 – 20	10 – 15	1 – 2	1 – 2

Some are taken up passively by the cell in an intact form (e.g. glucose and fructose), some are hydrolysed outside the cell and the breakdown products are absorbed (sucrose), whilst others are actively transported across the cell membrane and hydrolysed in the cytosol of the cell (maltose and maltotriose). Dextrins, comprising maltotetraose and larger starch breakdown products, are not metabolised. Any minor amounts of pentose sugars are also left unfermented (Hornsey, 1999). The general pattern of disappearance of fermentable sugars from wort during fermentation is sucrose→glucose→fructose→maltose→maltotriose, although there are differences between yeast strains (Batistote *et al*., 2006).

Fermentability of Wort

The main objective is to ferment wort to the desired gravity; this is often called the required degree of attenuation. The proportion of the wort dissolved solids (extract) which can be fermented is called the percentage fermentability of the wort (Briggs *et al*., 2004):

$$\text{Fermentability (\%)} \qquad \frac{Original\ gravity - Final\ Gravity}{Original\ gravity} \times 100$$

The original gravity can be expressed in ^{o}Sacch, which relates the specific gravity of the wort to that of water taken as 1,000. Final gravity means the gravity of the wort when it is fully fermented such that adding more yeast or leaving it longer will lead to no further fall in gravity (Briggs *et al*., 2004).

Horney (1999) states that for an approximate calculation of ABV it is more appropriate to use the expression,

$$ABV(\%) = 0.129 \times (OG - FG)$$

which, for beer with OG of 1040^{o} and is fermented down to 1009^{o}, as above, gives

ABV = 31 x 0.129 = 3.99% ABV

Effect of Process Variables on Fermentation Performance

The batch growth curve is influenced by a number of physical parameters. These are temperature, dissolved oxygen concentration, pitching rate, wort concentration and pressure. Adequate control of these parameters is essential to ensure consistent fermentation performance and beer quality (Briggs *et al*., 2004).

Fermentation Temperature

An increase in fermentation temperature reduces the time taken to attenuate the wort (Figure 2.13). To minimise the consequences early in fermentation from process variations, fermentation temperature control is necessary for consistent yeast growth. Fermentation rates will increase with temperature by increasing the rate of yeast metabolism giving higher specific fermentation rates. Higher temperatures will give a faster conversion of Vicinal Diketones (VDK) precursors and shorten the time required to reduce potential VDK off-flavours. Faster fermentation rates raise the peak demand for cooling (Priest and Stewart, 2006).

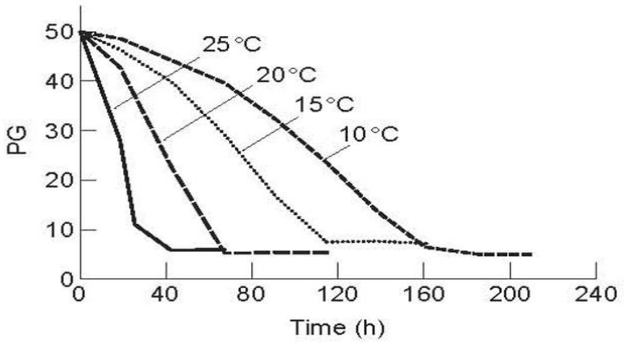

Figure 2.13: Effect of temperature on fermentation rate (from Briggs *et al*., 2004).

Most brewing strains have an optimum temperature for growth between 30 and 34 ^{o}C but fermentations are maintained at lower temperatures. Superficially, the use of elevated temperatures for minimising vessel turn-round times appears to be an attractive strategy but there are several disadvantages. At high temperatures,

especially in cylindroconical vessels, fermentation is very vigorous. Rates of CO_2 evolution are very rapid and losses of volatiles, via gas stripping, may become unacceptable. Indeed, beer losses due to uncontrollable fobbing may occur. To avoid this it may be necessary to operate fermenters with a large freeboard. The consequent reduction in vessel productive capacity offsets some of the gains made by shorter vessel residence times. At the end of fermentation, the time taken to chill is directly proportional to the fermentation temperature. Deviating from the normal temperature ranges (10 – 15 ^{o}C for lager and 15 – 20 ^{o}C for ale) may produce totally unacceptable shifts in beer flavour. Increasing the fermentation temperature leads to increases in the concentrations of higher alcohols and esters during fermentation. These flavour changes are particularly undesirable in the case of pale lager beers (Briggs *et al*., 2004).

Dissolved Oxygen Concentration

Overall, oxygen is regarded as being one of the worst enemies of beer; something to be avoided. There is, however, a precise requirement for oxygen by the yeast at the pitching stage. The brewing yeast is unable to synthesise sterols and unsaturated fatty acids in its absence. These two entities are present in wort (malt-derived), but in sub-optimal amounts and so there must be a sufficient level of molecular oxygen in the wort during the early stages of fermentation to facilitate the vast amount membrane synthesis necessary for cell multiplication (Hornsey, 1999). High oxygen concentrations produce rapid primary fermentations but this may be at the expense of ethanol yield. The increased availability of oxygen promotes high rates of yeast growth at the expense of sugar, which would otherwise be available for ethanol formation as shown in Figure 2.14 (Briggs *et al*., 2004).

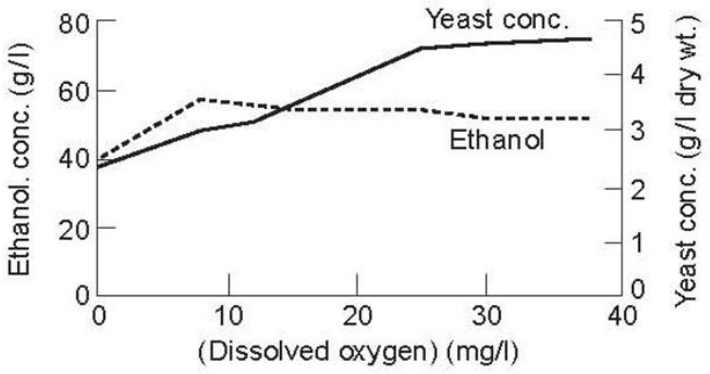

Figure 2.14: Effect of oxygen on fermentation rate (from Briggs *et al*., 2004).

Pitching Rate

Higher pitching rates give shorter lag phases, higher maximum fermentation rates, and shorter times to complete carbohydrate fermentation. A pitching rate of about $10 – 15 \times 10^6$ cells per millilitre for a normal gravity lager wort is typical. Because growth of new cells is limited by the oxygen supply in the wort, the increase in cell population (net cell growth) is nearly independent of initial yeast concentration under fixed, dissolved oxygen conditions. Compared to low pitching rates, higher pitching rates will lead to a lower number of cell doublings. As the pitching rate becomes too low, the amount of oxygen utilised to make sterols for new cells is lower and overall growth is lowered. Insufficient growth will lead to slower and perhaps stuck fermentations. Poor yeast growth can also lead to high SO_2 concentrations (Priest and Stewart, 2006). At higher pitching rates an inflection point is reached beyond which yeast growth decreases and there is no further increase in primary fermentation rate as shown in Figure 2.15 (Briggs *et al*., 2004).

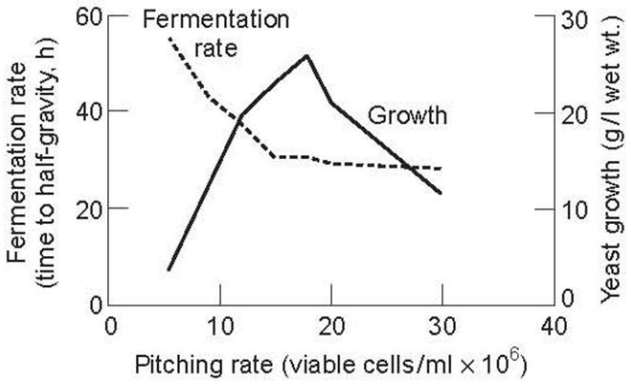

Figure 2.15: Effect of pitching rate on fermentation rate (from Briggs *et al*., 2004).

Wort Concentration

Increasing the wort concentration, without changing any other parameters, results in an increase in fermentation time. However, providing the pitching rate and wort dissolved oxygen concentration are increased *pro rata*, there is only a small increase in fermentation times (Figure 2.16). This forms the basis of high-gravity brewing in which concentrated worts are fermented and subsequently diluted to sales gravity.

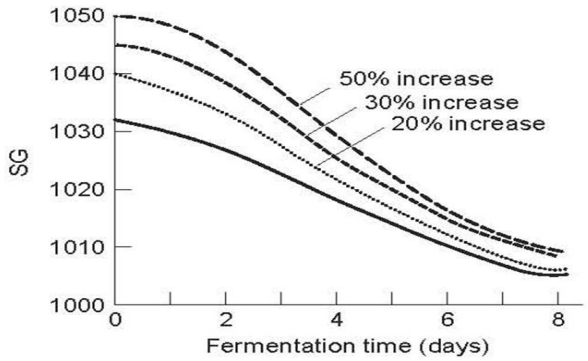

Figure 2.16: The relationship between fermentation time and increasing the OG of wort (from Briggs *et al*., 2004).

Pressure

In fermenters yeast is subjected to a hydrostatic pressure that is a function of the height of the vessel. In addition, if the exit of CO_2 produced during fermentation is restricted, the vessel will become pressurised. Very high pressures are deleterious to yeast. Very high-pressure treatments (>10^8 Pa; 100 Bar) have been used to sterilise some foods where heat treatments cause deleterious flavour changes. In similar fashion to the dual effects of osmotic pressure and water activity, pressurisation of fermenters leads to a concomitant increase in the concentration of dissolved CO_2. The latter may have a greater effect on yeast than pressure alone (Briggs *et al*., 2004).

2.5.9 Yeast Removal and Processing of Beer

It is important to remove the bulk of the excess yeast before maturation, generally by removing the beer from the sedimented yeast. The maturation of the 'green' or immature beer (it is not green in colour but has an unacceptable or immature flavour) to produce a stable, quality product suitable for filtration and packaging is called aging or, alternatively, cold conditioning or cold storage. The objectives of beer aging are: (a) chill haze formation (b) clarification (c) carbonation (to a limited extent) (d) flavour maturation (again to a limited extent), and (e) stored capacity for demand smoothing (Priest and Stewart, 2006). Sometimes priming sugar or a small amount of wort is added to boost yeast metabolism and the maturation or aging process (Briggs *et al*., 2004).

2.6 Summary

In this study therefore, CVD method was chosen for synthesising CNTs. The actual method employed was swirled fluidised catalytic chemical vapour deposition (SFCCVD) method (Iyuke, 2005) and this enable synthesis of long

CNTs. The yeast cells were immobilised on CNTs to form biocatalysts using flocculation method and the flocs were recovered by freeze drying them using VirTis freeze dryer. This enabled the preservation of the flocs for analysis using SEM and future use in beer brewing. The growth model for CNTs was predicted to be base-root growth model. Zeta potential data was used to explain the formation and stability of the flocs produced during the study.

CHAPTER 3: SCIENTIFIC METHODY

Several methods have been used to synthesise CNTs but the SFCCVD method was the chosen method in this study. CNTs synthesised by SFCCVD method usually contain other carbon products. The synthesised CNTs were used as produced in order to keep the cylindrical structure and length intact.

Yeast cell immobilisation can be achieved using several methods mentioned in Literature Review (Section 2.3.5). Flocculation method was the technique of choice because it is a low cost option.

3.1 Operating Conditions

The different equipment used in the synthesis of CNTs is shown in Figures 3.1 and 3.2. Quartz wool was inserted inside the reactor tube (Figure 3.2) as a modification to the existing equipment in Figure 3.1.

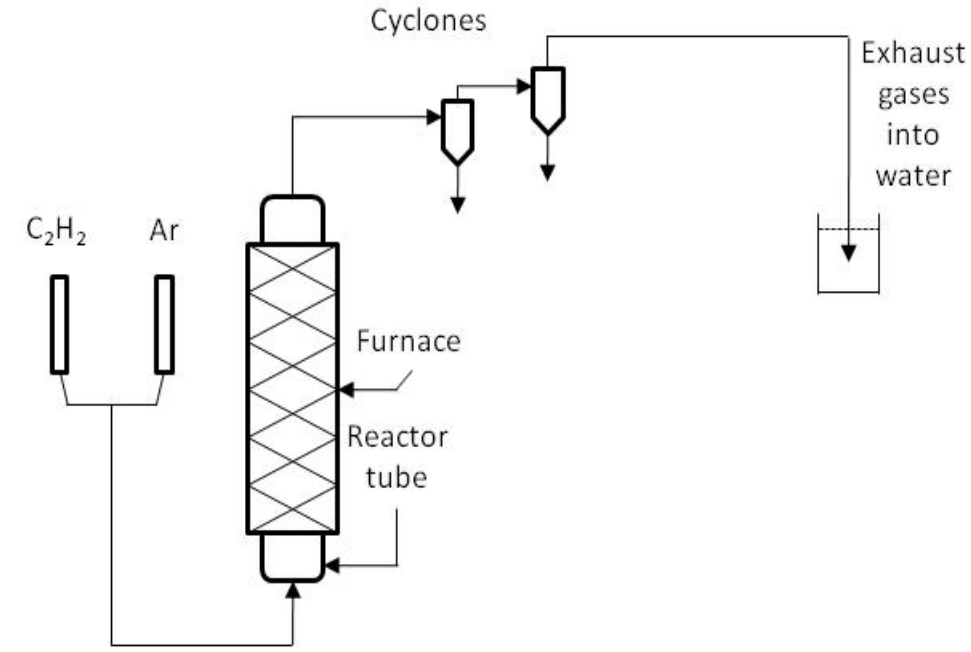

Figure 3.1: Flowsheet for SFCCVD method for synthesising CNTs (Iyuke, 2005).

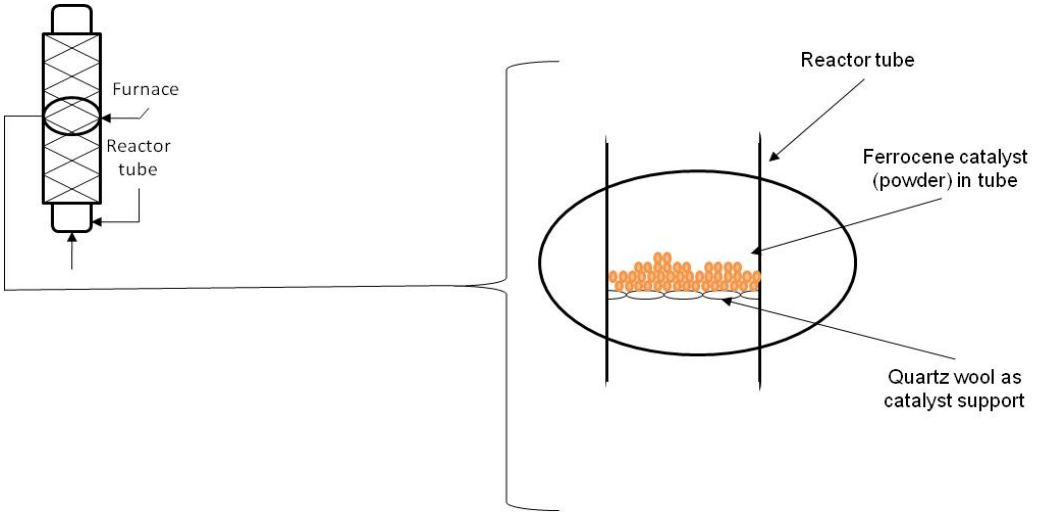

Figure 3.2: Part of SFCCVD equipment showing the arrangement in the reactor tube.

Several materials were required to synthesise CNTs using the SFCCVD process. These materials include: (a) reactants, acetylene gas (C_2H_2) and argon gas (Ar); (b) organometallic catalyst, ferrocene ($Fe(C_5H_5)_{2(s)}$), and (c) consumables.

3.1.1 Reaction Gases

The two gases used were; acetylene (Ultra High Purity, UHP, 99.997% pure) which acted as the carbon source while the argon (Ultra High Purity, UHP, 99.997% pure) was used to purge the system at the beginning of the experiment. The purging process helped to remove oxygen that could react with the catalyst. These two gases were supplied by Afrox, South Africa. Physical properties of the gases used were as follows:

Acetylene

Table 3.1: Physical properties of acetylene

Property	Molecular weight	Boiling point	Melting point	Specific gravity	Description
Value	26.04 g/mol	-120.6 ^oC	-113.0 ^oC	0.92 at 21 ^oC	It is a colourless and flammable gas

Argon

Table 3.2: Physical properties of argon

Property	Molecular weight	Boiling point	Melting point	Density	Description
Value	39.95 g/mol	-185.7 ^oC	-189.0 ^oC	1.78 mg/cm^3 at 21 ^oC	It is an inert gas and forms no known chemical compounds

3.1.2 Catalyst

An iron based organometallic catalyst ferrocene ($Fe(C_5H_5)_2$), with Fe>98%, was used in the study and it was supplied by Sigma-Aldrich, South Africa. Physical properties of ferrocene were (Li *et al*., 2006):

Table 3.3: Physical properties of ferrocene

Property	Boiling point	Melting point	Thermal stability
Value	249 ^{o}C	172 – 174 ^{o}C	~ 400 ^{o}C

3.1.3 Consumables

Quartz wool which can withstand high temperatures (maximum temperature used in this study was 1000 ^{o}C) was used as a catalyst support. The quartz wool was inserted inside the reactor tube in the heating zone (Figure 3.2). CNTs produced during the reaction were deposited on the wool and collected when the reactor had cooled to normal temperatures. The vacuum grease (Dow Corning high vacuum grease) was also used to aid in preventing gas leaks. It was applied at the joints on top and at the bottom of the reactor. The grease was chosen because it was stable at the operating conditions.

3.1.4 Reactor Tube

The reactor tube was made from mullite which can withstand temperatures up to 1200 ^{o}C. The internal diameter is 47 mm and a height of 1050 mm. The height within the heating zone was 800 mm.

3.1.5 Reactor Tube Heater

The heater was supplied by Elite Thermal Systems Ltd and it was a 1200°C Single Zone, Vertical Tube Furnace with a rate of temperature increase of 5 ^{o}C per minute.

3.1.6 Cole Parmer Flowmeter

These were used to measure the flowrate of the gases. The flowmeter has an accuracy of ±2% full scale; flowrate 374 ml/min; maximum pressure of 100 psi and operating temperature from -26 to 65 ^{o}C.

3.1.7 Transmission Electron Microscopy (TEM)

The model of TEM used was JEOL JEM 100S Transmission Electron Microscopy operating at 80kV. The procedure on how to view a sample of CNTs as described in Appendix II.

3.1.8 Experimental Design

To synthesise CNTs the following experimental procedure was followed:

1. The reactor tube was removed and cleaned to remove any residual CNTs and foreign materials that could interfere with the results. The cleaning process involved inserting quartz wool from the bottom of the reactor and pushing all the contents to come out at the top. This procedure was repeated for 4 – 5 times until whereby there where very little carbon materials coming out. Nitric acid was used to remove the remaining CNTs.
2. Quartz wool was weighed and inserted from the bottom of the tube at approximately 30cm from the bottom.
3. The required amount of ferrocene catalyst was added onto the catalyst support from the top (quartz wool).
4. The reactor tube was fitted and checked for gas leaks. Grease was applied on the joints at the top and bottom of the reactor to aid in reducing gas leakage.
5. The argon gas valve was then opened at a scale reading of 50 (308ml/min) for 8 – 10 minutes to purge oxygen from the system. To ensure there are no gas leakages, argon should bubble out in a flask or beaker full of water.
6. The temperature controller was switched on and set to the desired temperature. It took about 195mins (3hrs 15mins) to heat the reactor from 25^{o}C to 1000^{o}C.
7. Once the desired temperature was reached, the acetylene gas valve was opened to the desired flowrate for the required time period (reaction time).

8. The experiment was monitored to ensure that it proceeded safely. Acetylene gas is highly flammable and if there is any leakage it may cause a major accident.

9. After the reaction time was up, close the acetylene gas valve followed by switching off the furnace heater. The contents are left to cool down to room temperature. It took about 16 hours for the equipment to reach the ambient conditions.

10. Safe working practises are observed at all times such as the use of dust masks, use of gloves, laboratory coats and reporting all accidents.

11. When the equipment was at ambient temperatures, unscrew and collect samples for analysis and record the weight of the collected sample of carbon nanoparticles. The quartz wool was removed from the reactor tube and the weight recorded.

12. Check for residual catalyst in the catalyst chamber, measure it and record its weight.

13. The equipment is cleaned in preparation for the next experiment.

Process efficiency was characterised by different parameters calculated from data recorded during the experiment according to Morancais *et al.*, (2007) and is shown in Table 3.4.

Table 3.4: Data recorded and rates calculated during analysis of Carbon Nanotubes synthesised by Swirled Floating Catalytic Chemical Vapour method (from Morancais *et al.*, 2007.

ITEM	WEIGHT (grams)
Mass of fresh catalyst at start of the study	M
Mass of quartz wool at start of the study	a
Mass of quartz wool and CNTs at the end	b
Mass of CNTs lost (CNTs that cannot be recovered from the wool)	b-a=c
Mass of residual catalyst collected	d
Mass of CNTs recovered	e
Time taken of the study	t (minutes)
Carbon Yield (per catalyst mass)	$\frac{c+e}{M} \times 100\%$
Production Rate*1000 (g_{CNTs}/g_{Fe}/min)	$\frac{c+e}{M \times t} \times 1000$

3.2 Strain and Culture Conditions

Several materials and equipment were required for this part of the study. The materials required were: (a) Yeast strain and medium and (b) CNTs, produced in Section 3.1. The equipment required were: (a) Shaking incubator, (b) Autoclave, (c) pH meter, (d) Zetasizer, (e) Centrifuge, (f) Scanning Electron Microscopy and (g) Stereo Microscopy.

3.2.1 Yeast Strain and Medium

The cultured *S. cerevisiae* strain NRRL Y2084 (a dry brewer's yeast which was obtained from National Food Products, Emmarentia, Johannesburg) used in this study was maintained on Malt Extract Agar (MEA, Merck). It was supplied on plates (petri dishes), stored at 4 ^{o}C and used within 3 months. The cells were grown without adding oxygen (rubber cork was used to cover the mouth of the flask throughout the experiment) at 30±0.5 ^{o}C in a 500 mL flask held on a rotary shaking incubator working at 110±2 revolutions per minute (rpm) and used during immobilisation stages. The cells were transferred from the flask used for growth to the flasks used for immobilisation studies according to section 3.2.11 (Yeast Immobilisation). Peinado *et al.* (2005) conducted their studies at 28 ^{o}C and 150 rpm for 7 days and had successful immobilisation to produce yeast biocapsules while Sakurai *et al.* (2000) used 30 ^{o}C and 160 rpm during their immobilisation studies of yeast cells on porous cellulose carriers. Öztop *et al.* (2003) immobilised *S. cerevisiae* onto acrylamide-sodium acrylate hydrogels at 30 ^{o}C for 72 hours. Growth curves were investigated for stationary phase and showed that the yeast cells concentrations were on average 65.75x10^{6} CFU/ml after growth and 62.63x10^{6} CFU/ml on average before flocculation studies.

Yeast extract (Merck, South Africa), was used for cell growth during the study. Physical properties are summarised in Table 3.5. Five grams of the yeast extract powder was added into one litre of distilled water and then sterilised in an autoclave at 121 ^{o}C, 1.1kg/cm^{2} gauge (1.079 bar gauge) and for 20 minutes. Once the medium had been prepared it was stored at room temperature before use. An aluminium foil was used to cover the flask to prevent contamination.

Table 3.5: Composition of yeast extract powder (Merck, SA)

Item	Colour	Total N_2, %	Amino N_2, %	Solids	NaCl	Ignition residue	pH	Description
Composition	Light yellow powder	≥ 9.0 %	≥ 3,5 %	≥ 94 %	≤ 4 %	≤ 10 %	5–6.5	store away from heat and moisture

3.2.2 Yeast Viability

Yeast viability was determined, post-culturing, by dilution series and plate counts. The dilution series was carried out using Buffered Peptone Water (BPW, Merck), as the diluent. Plate counts were determined using Dried Malt Extract (DME) for *S. cerevisiae*. Tenfold serial dilutions (10^{-1} – 10^{-6}) were carried out in triplicate using the 1.5L medium culture. From each appropriate dilution, 0.1mL of the diluted suspension was spread on plates with MEA. Lyphosised samples were rehydrated at 30 ^{o}C for 1 hour before plating. Plates were incubated at 30 °C for 48 hours. The pitching rate was determined according to the following equation:

$$Colony\ Forming\ Units/ml = \frac{Number\ of\ Colonies \times Dilution\ Factor}{Volume}$$

The yeast cells concentrations were on average 65.75x10^6 CFU/ml after growth and 62.63x10^6 CFU/ml on average before flocculation studies. The cells were freeze dried for analysis and fermentation studies, and viability tests showed that there were; on average 5.22x10^3 CFU/ml for free cells and 4.51x10^3 CFU/ml for immobilised cells. This showed a decrease in magnitude of 10^4.

3.2.3 Carbon Nanotubes

The CNTs were synthesised in the Nanotechnology Laboratory (Section 3.1) and used to immobilise the yeast cells.

3.2.4 Shaking Incubator

The shaking incubator (Labcon, SA) provided the optimal control temperature and agitation speed needed during the immobilisation process.

3.2.5 Autoclave

The autoclave (HL-340 Vertical Type Steam Steriliser, Already Enterprise Inc., SA) was used to sterilise the prepared medium and all glassware to be used during the experiments. The operating conditions were at 121 ^{o}C, 1.1kg/cm^{2} gauge (1.079 bar gauge) and for 20 minutes.

3.2.6 pH meter

The pH of the medium was analysed by a pH meter (Eutech Instruments, SA) before flocculation studies and adjusted using 10 % (v/v) acetic acid to the desired value. The pH was measured at the beginning of immobilisation studies.

3.2.7 Zetasizer

The Zetasizer (Malvern Instruments Zetasizer Nano series Nano ZS) was used to measure the zeta potential of the broth (medium, yeast cells and CNTs). Zeta potential measurements were done in triplicate for one sample with a calculated standard deviation. The mean zeta potential was calculated based on the three measurements and its standard deviation calculated accordingly.

3.2.8 Preservation of the Immobilised Cells

The freeze dryer (VirTis, SP Industries) was used to recover the flocs and preserve them for analysis and for future use. The cooling rate for the freeze dryer was 2.6 ^{o}C/min (Appendix III). The samples recovered were analysed within 2 days. For fermentation studies the samples were used within 3 – 4 days.

3.2.9 Centrifuge

The centrifuge (Hermle Z365 BHG Centrifuge) was used to recover the flocs from the solution and measure the weight so as to compare flocculation rates. The centrifuge was operated as 9000 rpm at 30 ^{o}C for 5 minutes.

3.2.10 Analytical Methods

The immobilised cells were characterised by Scanning Electron Microscopy (SEM) and Stereo Microscopy. The model for SEM was JEOL JSM 840A Scanning Electron Microscopy and the procedure on how to view a sample was described in Appendix IV. The model for the Stereo Microscopy was Carl Zeiss DiscoveryV12 AxioCam MRC Stereo Microscopy. Maximum magnification was x150 and it was used to aid in understanding the immobilised cells.

3.2.11 Experimental Design

Yeast extract medium was used in all the experiments for flocculation. The procedure was divided into two parts (i) growing yeast cells and (ii) immobilising the grown cells using CNTs. Two experiments were run in parallel, one as the control without CNTs and the other the main experiment with CNTs. This made it easier to compare the effect of CNTs on flocculation at different conditions.

Yeast Growth

The yeast available was from slants and as a result inoculation was the first step. The procedure for growing yeast cells is discussed below:

1. Yeast extract medium and all the glassware to be used in the experiment were sterilised in the autoclave.

2. The medium was allowed to cool to room temperature and stored.

3. A loopful of inoculum was added to an Erlenmeyer flask containing 100 ml of sterile yeast extract medium and incubated in a shaker at 110 rpm, 30 ^{o}C for

24 hours under anaerobic conditions (rubber cork used to seal the flask to prevent air uptake during the study).

4. After 24 hours the yeast cells were used for immobilisation studies according to the procedure in section 3.2.11.2 (30 ml (7.04x106) of grown cells were added into the flask to make total volume 280 ml – see Yeast Immobilisation). Refer to Section 3.2.2 for cell count viability.

Yeast Immobilisation

Two experiments were run in parallel, the main experiment with CNTs and a control experiment without CNTs. This was done to observe and compare the effect of CNTs on the flocculation. The procedure is discussed below.

1. 250 ml of yeast extract medium was transferred to a sterilised 500 ml Erlenmeyer flask.

2. 30 ml ($7.04x10^6$) of grown cells were added into the flask to make total volume 280 ml.

3. pH of the broth (grown cells and yeast extract) was measured before adjustment and adjusted to the required pH value. The final pH was recorded and it was regarded as the reference pH.

4. Carbon nanotubes were weighed and added into the Erlenmeyer flask. The weight was recorded.

5. Any other substances such as calcium chloride or glucose were weighed and added at this stage.

6. The flasks were then incubated in a rotary shaking incubator at the desired conditions (temperature and agitation speed) under anaerobic conditions.

7. Samples were taken every 24 hours to measure change in pH and zeta potential. Zeta potential was measured 3 times per sample and an average zeta potential value was used with a calculated standard deviation.

8. When the experiment had reached the end, the flocs were recovered for analysis by a freeze dryer.

Some of the apparatus used for yeast immobilising experiment are shown below:

Figure 3.3: Labcon Shaking incubator.

Figure 3.4: Zetasizer Nanoseries Nano ZS (Malvern Instruments).

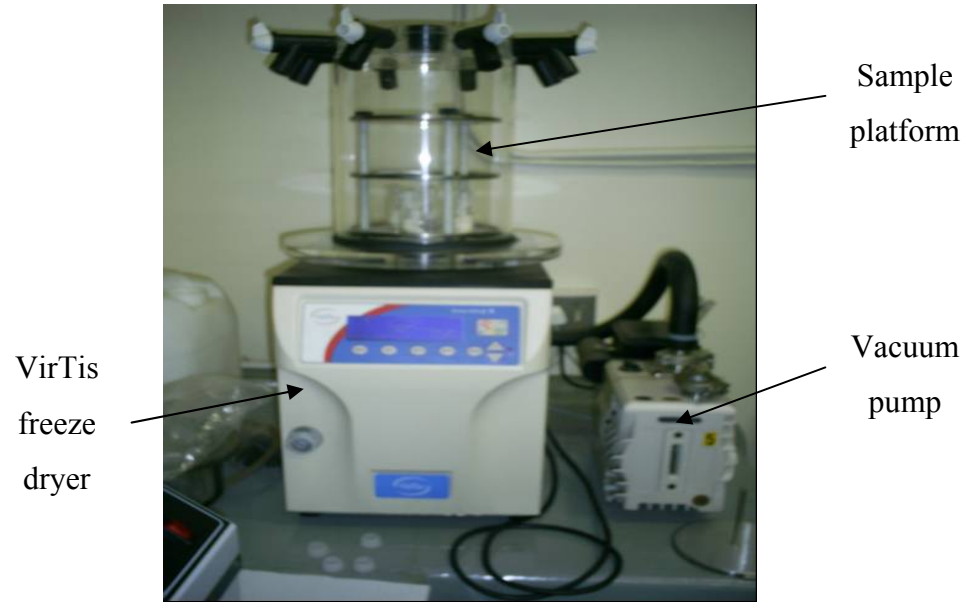

Figure 3.5: VirTis freeze dryer (SP Industries).

Figure 3.6: Hermle Z365 BHG Centrifuge.

The flocculation for the main experiment and the control experiment were analysed using two methods: a qualitative process to determine the quality of the flocs produced and a quantitative process to measure the flocculation weight. These two methods enabled the optimisation of the parameters that affect flocculation during the process.

3.2.12 Flocculation Measurements

The first procedure which was qualitative in nature involved estimating flocculation with the naked eye. This process was used to measure the quality of the flocs produced. This involved looking at the sides and at the bottom of the Erlenmeyer flask and expressing flocculation qualitatively according to Ross and Harrison (1970).

No formation of flocs	-
Least flocculent (powdery yeast; *Staubhefe*)	+
Intermediate flocculent	++
Most flocculent (clumping yeast; *Bruchhefe*)	+++

A digital camera (EuroCyber X-688CCD) was used to take photographs at the bottom of the erlenmeyer flasks to capture the floc formation.

The second method involved using a centrifuge to concentrate the flocs and then drying them to determine their dry weight. The process was quantitative in nature and it was used to rank and compare the flocculation as shown below:

1. Measure the weight of the empty 50 ml container (g) = c
2. Fill the empty container with the broth
3. Use the centrifuge to recover the flocs at 9000 rpm for 5 minutes
4. Once done, decant the supernatant from the flocs
5. Measure the weight of the wet flocs and container (g) = d
6. Dry the flocs in an oven at 40 ^{o}C for 1 day.
7. Measure the weight of the dry flocs and container (g) = e
8. Therefore, dry weight of flocs recovered (g) = e – c

The floc weight was then plotted against the changing variable to determine the effect of the variable. These two methods together gave an indication of the

flocculation ability of the brewers' yeast in the presence of CNTs and glucose and calcium ions.

3.3 Fermentation Studies

The materials required for fermentation studies were as follows:

- 100 – 150 g/L of DME.
- Yeast cells (Immobilised and free yeast cells, which were all recovered by a freeze dryer and the viability analysed before fermentation studies were conducted).
- Two fermenters (2 L capacity) – 2L erlenmeyer flasks modified to have a sampling valve located at the bottom of the flask and a rubber cork at the top of the fermenter with a tube immersed in water to release any CO_2 produced during the studies.
- Temperature control water bath.

The procedure used was as follows:

1. The fermentation conditions were: 15 ^{o}C (Bekatorou *et al*., 2001b; Inconomopoulou *et al.,* 2000; Kopsahelis *et al*., 2006; Plessas *et al.*, 2005) or 30 ^{o}C (Batistote *et al*., 2006; Bekatorou *et al*., 2002; Bekers *et al*., 1999; Inconomopoulou *et al.,* 2000; Plessas *et al.*, 2005; Speers *et al*., 2006), no shaking, anaerobic single-stage fermentation for 9 days and 3.5 days respectively.
2. The equipment and media were sterilised with an autoclave in preparation for the experiment.
3. The original gravity of the medium was measured.

4. 0.030 g (5.22×10^3 CFU/ml of free cells and 4.51×10^3 CFU/ml of immobilised cells) of the dried yeast cells were pitched in 1L of the medium in each fermenter. The contents were tightly closed by rubber cork to prevent contamination with a tube immersed in water for CO_2 gas to escape.

5. Incubation was done at the required conditions.

6. A complete sterility test of the fermentation process was not carried out. However, the media and the glassware were autoclaved prior to the fermentation studies.

7. Samples were taken every 24 hours for analysis: alcohol content and sugar content (glucose and maltose) were tested using an HPLC (Agilent Technologies 1200 Series) while pH of the broth was monitored throughout the experiment.

8. After the required time period the final gravity was measured.

CHAPTER 4: RESULTS AND DISCUSSION

4.1 Synthesis of Carbon Nanotubes

The chemical equation for the catalytic decomposition of acetylene gas reaction is shown as:

$$C_2H_{2\,(g)} \xrightarrow{Fe\ catalyst} 2C_{(s)} + H_{2\,(g)} \qquad \Delta H_{reaction} = -226.9 MJ/kmol$$

(Babushok and Miziolek, 2004).

The enthalpy of reaction is negative indicating that acetylene decomposition is an exothermic reaction with the main products being solid carbon materials e.g. CNTs and hydrogen gas.

The SFCCVD method produced carbon nanoparticles like MWCNTs, Carbon Nanofibres (CNFs), Carbon Nanoballs (CNBs), Helical Carbon Nanotubes (HCNTs) and Helical Carbon Nanofibres (HCNFs) mixed together. The synthesised carbon nanoparticles were confirmed by TEM analysis (Figure 4.1) which was used to analyse the quality of the nanoparticles, i.e. the purity of the sample. This process is mainly qualitative in nature but diameters of the nanoparticles can be measured directly from the micrographs with the help of the magnification.

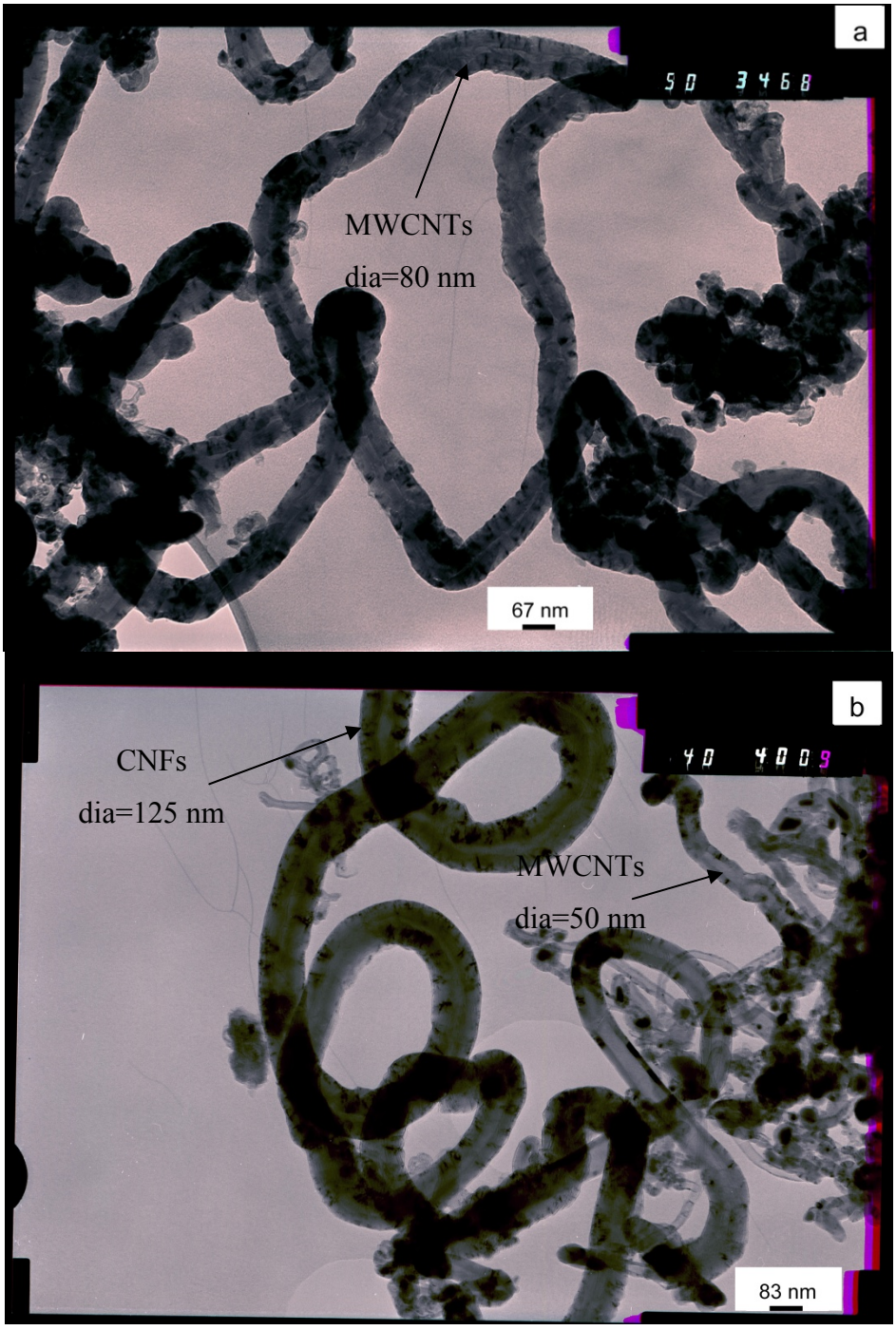

Figure 4.1 Electron micrographs showing carbon nanoparticles synthesised using the SFCCVD method. (a) and (b) consists of MWCNTs.

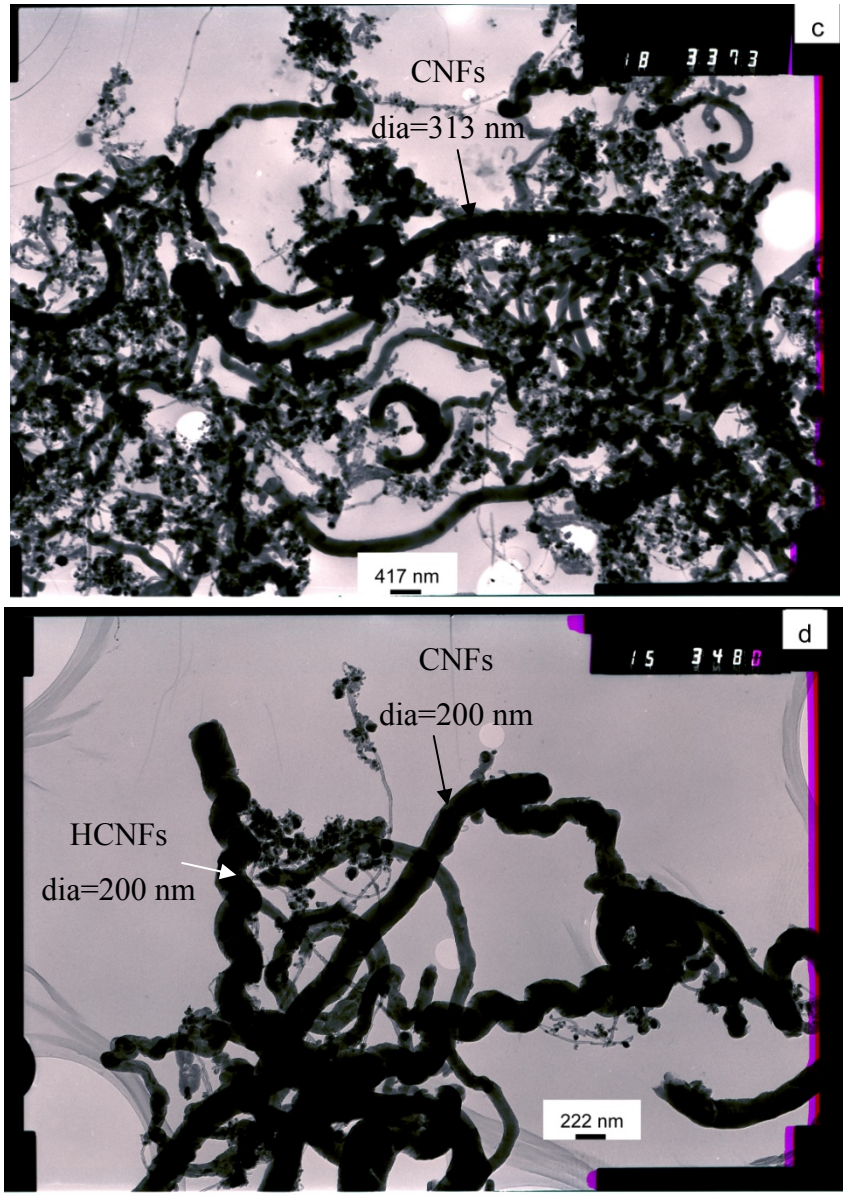

Figure 4.1 continued..: Electron micrographs showing carbon nanoparticles synthesised using the SFCCVD method. (c) consists of CNFs and (d) consists of HCNFs and CNFs.

The synthesised carbon nanoparticles had an average diameter of 161 nm. The main types of nanoparticles observed in the studies were MWCNTs but some

HCNTs, HCNFs and CNFs were also observed. The synthesised CNTs were not purified and as a result impurities can be observed in the micrographs.

Raman spectroscopy was used to check for the presence of CNTs in the samples and the results are presented in Figure 4.2. The spectroscopy was conducted by a 514.5 nm line of an argon ion laser and the first order bands arising from Csp^2 vibrational modes (1200 – 1700 cm^{-1}) were analysed.

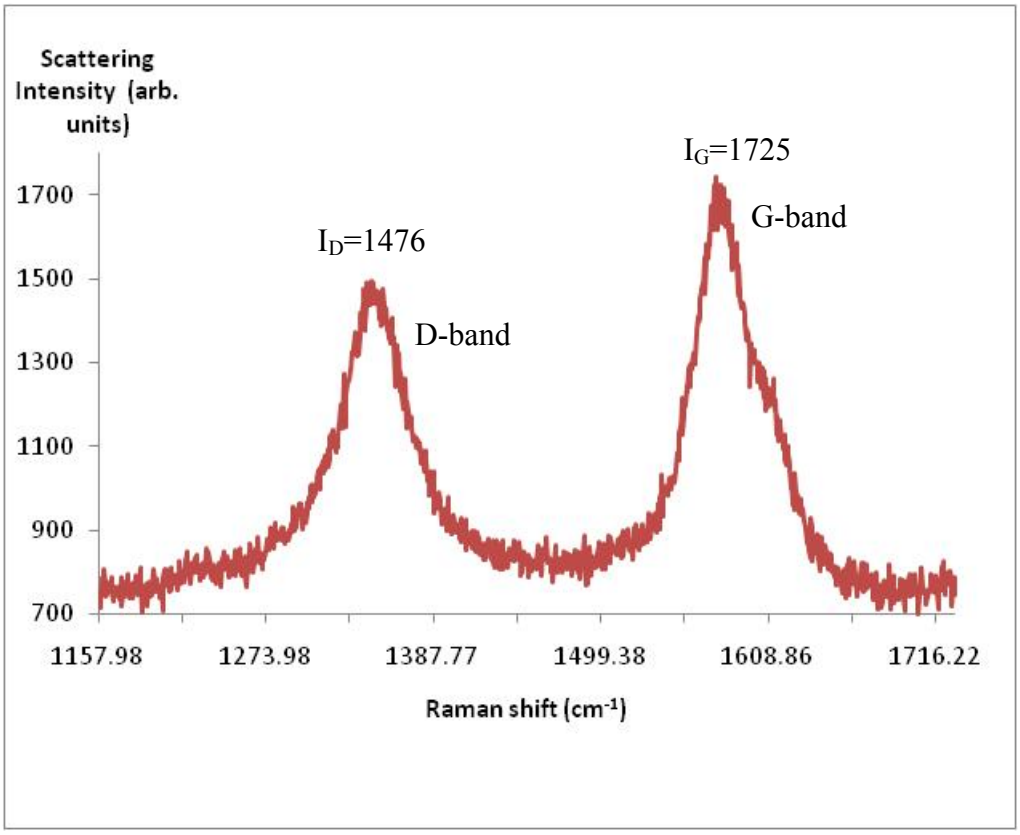

Figure 4.2: Raman spectroscopy to confirm presence of CNTs.

From Figure 4.2 there are two peaks at 1355 and 1585 cm^{-1}, which were designated as the 'D-band' and 'G-band', respectively indicating that CNTs are

present in the analysed sample. The ratio of their intensities I_D/I_G=0.856 were close to 0.80 indicates the presence of MWCNTs (Ouyang *et al*, 2008).

Parameters that were investigated during the synthesis of carbon nanoparticles were:

- Growth temperature
- Acetylene (C_2H_2) flowrate
- Reaction Time

Studies were conducted to investigate the effect of changing any of these parameters. Experiments were done at least twice with the mean and standard deviation included in the results. The results for the efficiency parameters were presented as graphs showing the mean value of the two experiments with standard deviation bars.

4.1.1 Growth Temperature

Growth temperature affects the quality of the carbon nanoparticles synthesised. Studies were conducted to investigate the effect of change in temperature on the quality of nanoparticles and these were done at 6 different temperatures: 750, 800, 850, 900, 950 and 1000 ^oC. The conditions for the studies are presented below (Table 4.1).

Table 4.1: Conditions used to investigate the effect of temperature on the synthesis of CNTs.

Parameter	**Temperature (^{o}C)**	**Catalyst quantity (g)**	**C_2H_2 flowrate (ml/min)**	**Reaction time (min)**
Value	Variable	1.0	594	20

(A) 750 ^{o}C

At 750 ^{o}C carbon nanofibres (CNFs) and carbon nanoballs (CNBs) were the main products synthesised although MWCNTs were also observed. The CNFs had fibrous morphology as observed in the micrographs in Figure 4.3. The diameter distributions were in the range 60 – 140 nm.

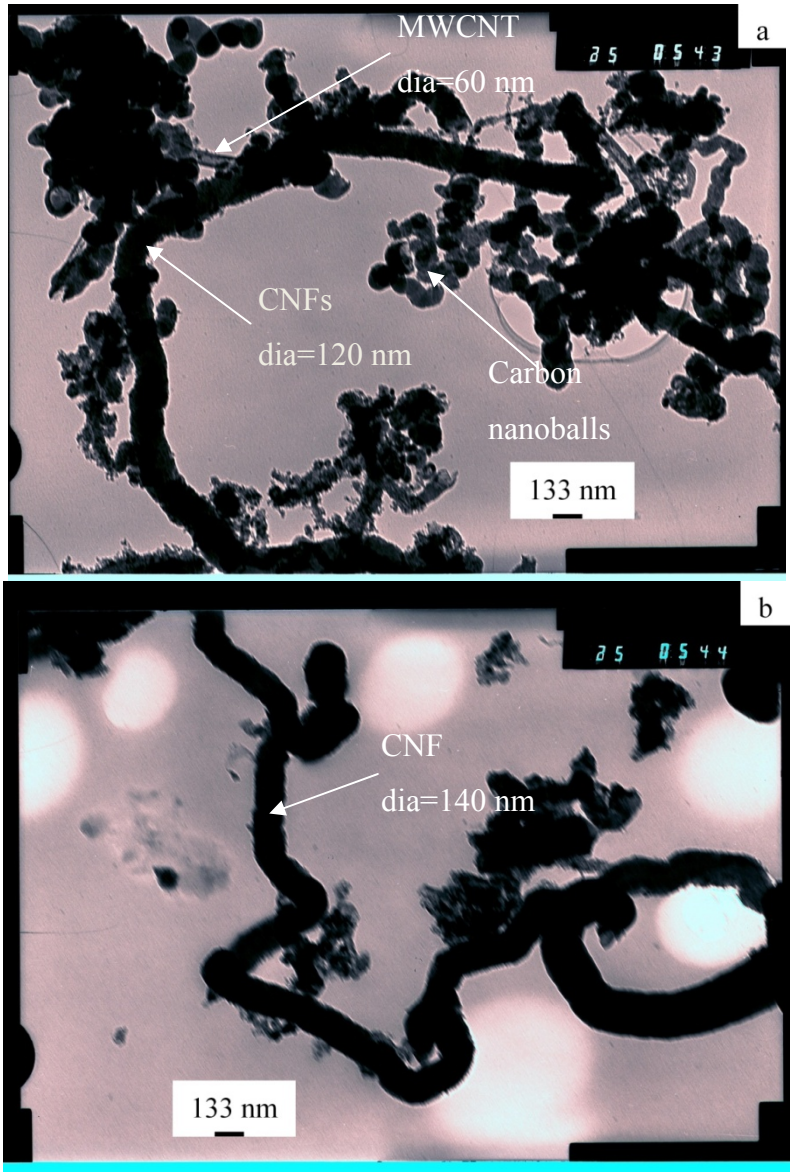

Figure 4.3: Electron micrographs obtained at 750 ^{o}C, 1 g catalyst, 594 ml/min C_2H_2 flowrate and 20 minutes. (a) consists of MWCNTs and CNFs while (b) consists of a CNF and MWCNTs.

(B) 800 ^{o}C

At 800 ^{o}C MWCNTs and helical carbon nanotubes (HCNTs) were the main products synthesised. Diameter distributions were in the range 77 – 100 nm.

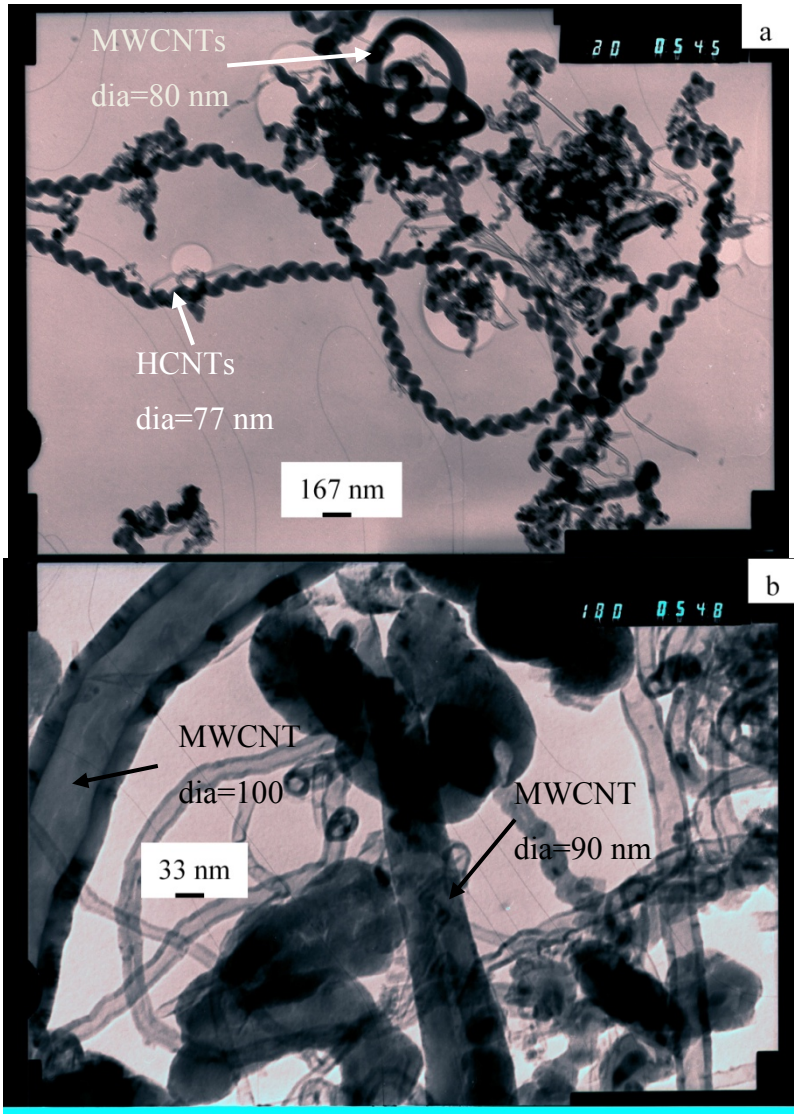

Figure 4.4: Electron micrographs obtained at 800 ^{o}C, 1 g catalyst, 594 ml/min C_2H_2 flowrate and 20 minutes.](a) and (b) consists of MWCNTs and HCNTs.

(C) 850 ^{o}C

The temperature was increased to 850 ^{o}C and only CNFs were synthesised with diameter distributions in the range 120 – 200 nm.

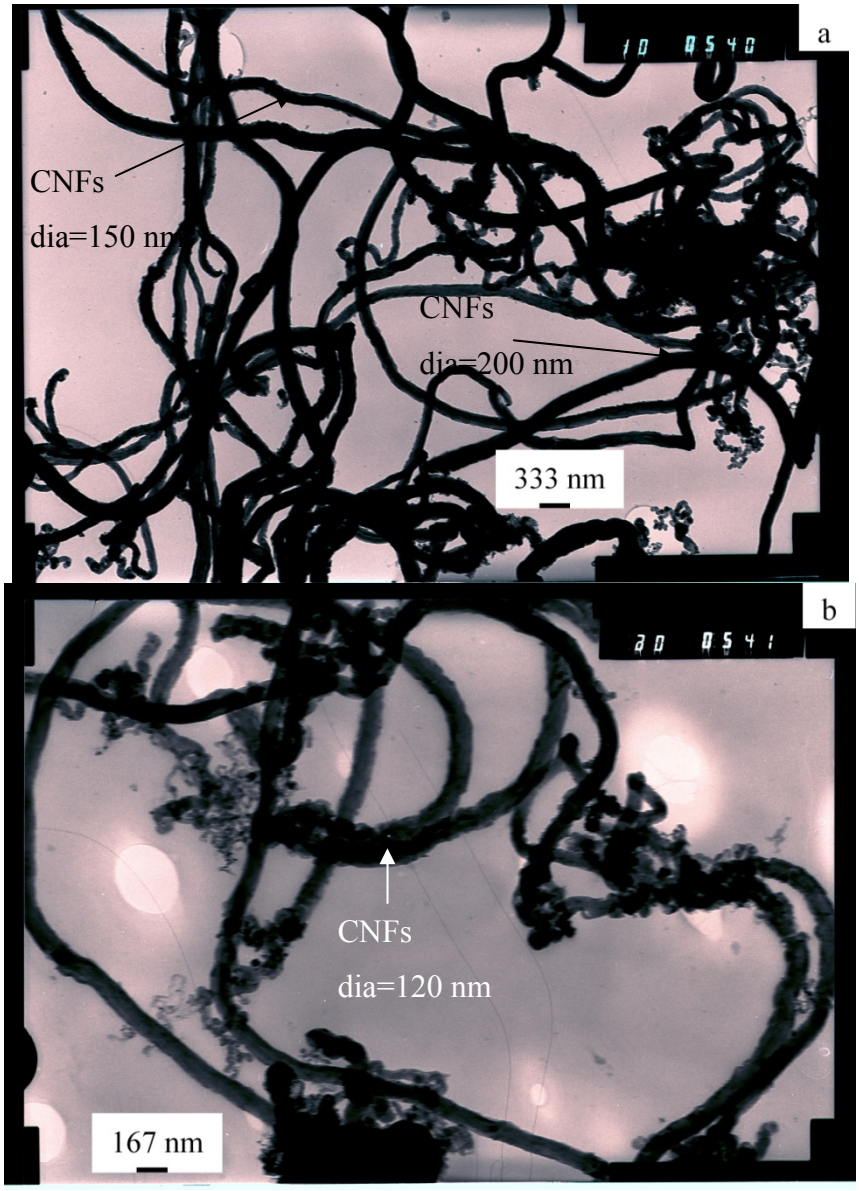

Figure 4.5: Electron micrographs obtained at 850 ^{o}C, 1 g catalyst, 594 ml/min C_2H_2 flowrate and 20 minutes. (a) and (b) consists of CNFs.

(D) 900 ^{o}C

Increasing the temperature to 900 ^{o}C resulted in MWCNTs and HCNTs as the main products synthesised although some CNFs were observed. The MWCNT observed (Figure 4.6a) was cyclical showing the tendency of becoming helical in

nature as temperature increases. A strand of bamboo-like HCNT could be observed in Figure 4.6b. The diameter range was 60 – 133 nm. The micrographs are presented below (Figure 4.6).

(E) 950 ^{o}C

At 950 ^{o}C only CNFs were synthesised and these fibres were very long and appeared as single strands. The diameter was ranging between 200 and 267 nm with the micrographs presented in Figure 4.7.

(F) 1000 ^{o}C

A temperature of 1000 ^{o}C gave MWCNTs and HCNTs as the main products observed. Some CNFs were observed within the sample. The diameter was ranging between 90 and 154 nm with the micrographs shown in Figure 4.8.

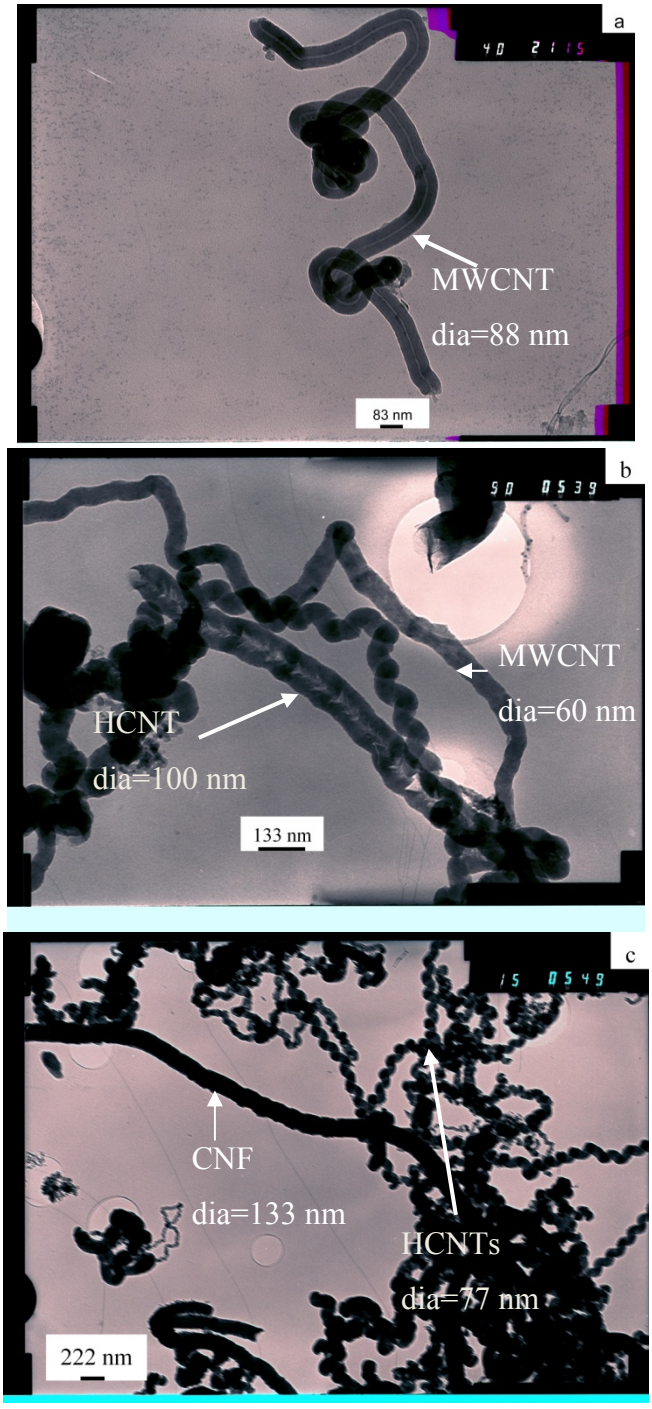

Figure 4.6: Electron micrographs obtained at 900 ^{o}C, 1 g catalyst, 594 ml/min C_2H_2 flowrate and 20 minutes. (a) and (b) consists of MWCNTs and HCNTs while (c) consist of HCNTs and CNFs.

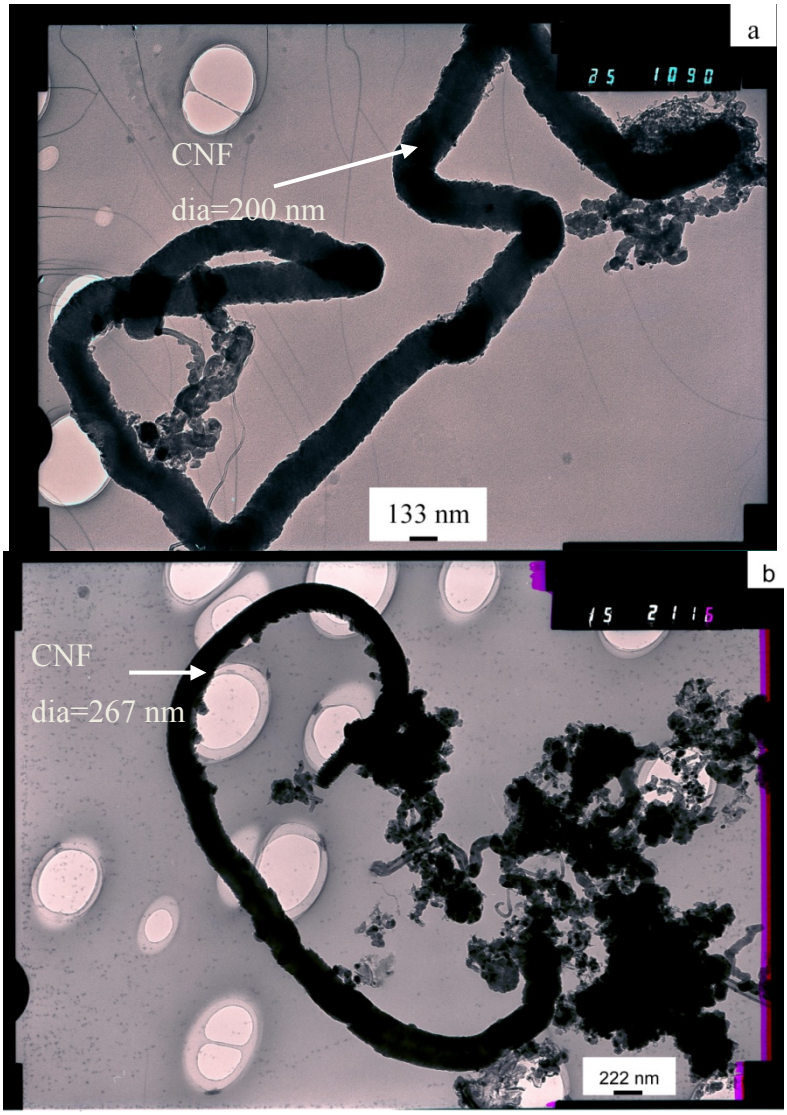

Figure 4.7: Electron micrographs obtained at 950 ^{o}C, 1 g catalyst, 594 ml/min C_2H_2 flowrate and 20 minutes. (a) and (b) consists of CNFs.

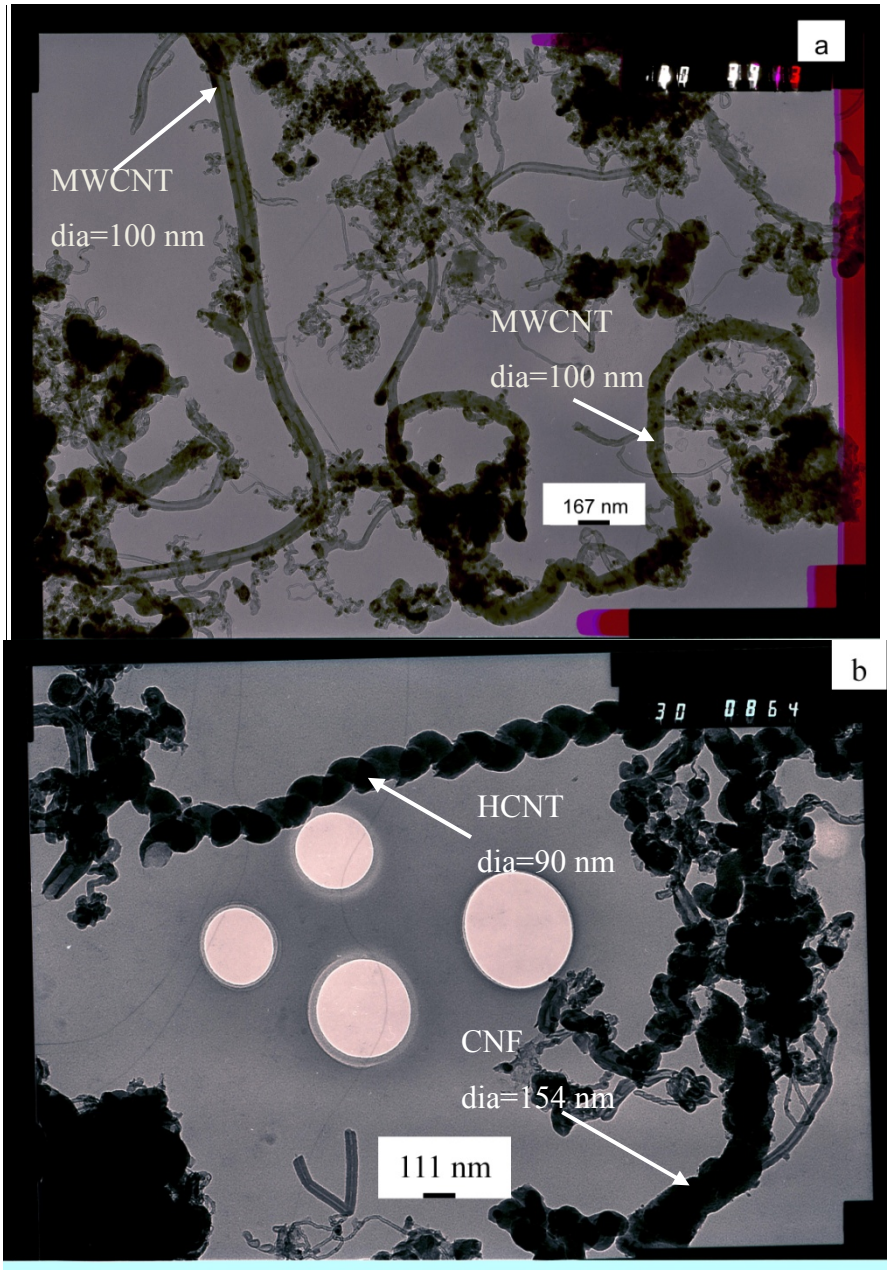

Figure 4.8: Electron micrographs obtained at 1000 ^{o}C, 1 g catalyst, 594 ml/min C_2H_2 flowrate and 20 minutes. (a) consists of MWCNTs while (b) consists of HCNTs and CNFs.

4.1.2 Acetylene Flowrate

A change in acetylene flowrate (the carbon source) affects the quality and quantity of CNTs synthesised. Studies were conducted at 3 different acetylene flowrates 308, 594 and 844 ml/min corresponding to scale readings of 50, 100 and 150 respectively (Appendix IV). The conditions used during the studies are presented below (Table 4.2).

Table 4.2: Conditions used to investigate the effect of acetylene flowrate on the synthesis of CNTs.

Parameter	**Temperature (^oC)**	**Catalyst quantity (g)**	**C_2H_2 flowrate (ml/min)**	**Reaction time (min)**
Value	850	2.0	Variable	20

(A) 308 ml/min

The lowest flowrate investigated was 308 ml/min. At acetylene flowrate of 308 ml/min, MWCNTs with a lot of impurities were synthesised. The MWCNTs had ends helical in nature and they were poorly formed. The diameter ranged between 100 and 150 nm.

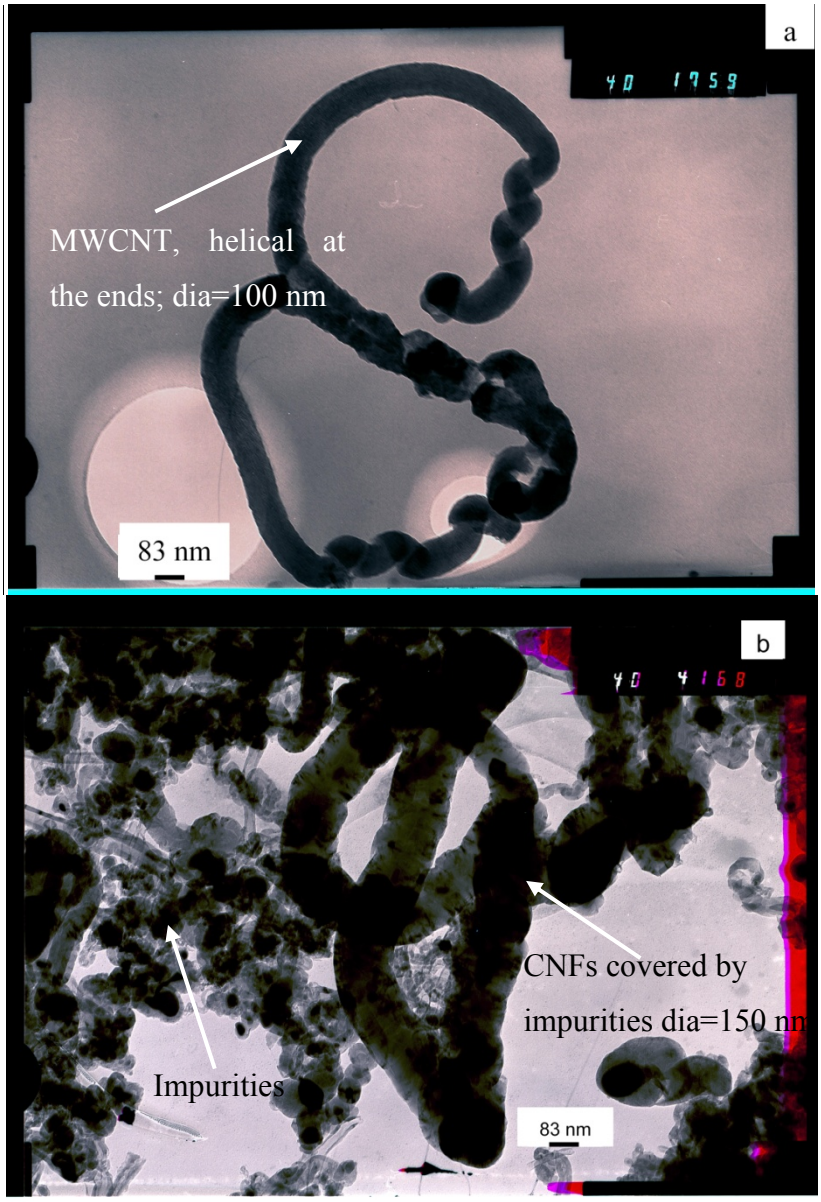

Figure 4.9: Electron micrographs obtained at 308 ml/min, 850 ^{o}C temperature, 2 g catalyst and 20 minutes. (a) consists of a MWCNT and (b) consists of CNFs

(B) 594 ml/min

At acetylene flowrate of 594 ml/min, MWCNTs were the main products synthesised. Long MWCNTs were observed in Figure 4.10b with diameter ranging between 50 and 100 nm.

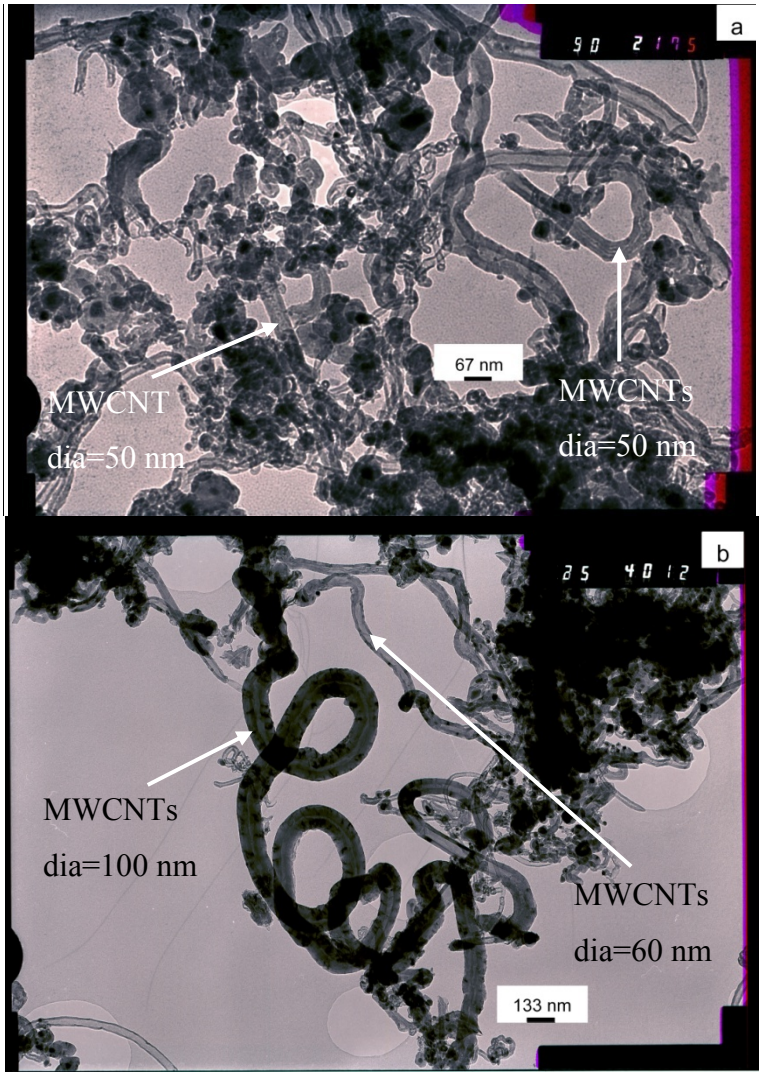

Figure 4.10: Electron micrographs obtained at 594 ml/min, 850 ^{o}C temperature, 2 g catalyst and 20 minutes. (a) and (b) consist of MWCNTs.

(C) 844 ml/min

Increasing the acetylene flowrate to 844 ml/min, CNBs of the same diameter were the main products synthesised. In Figure 4.11b, a CNF and a MWCNT were observed but poorly formed as seen in Figure 4.11b.

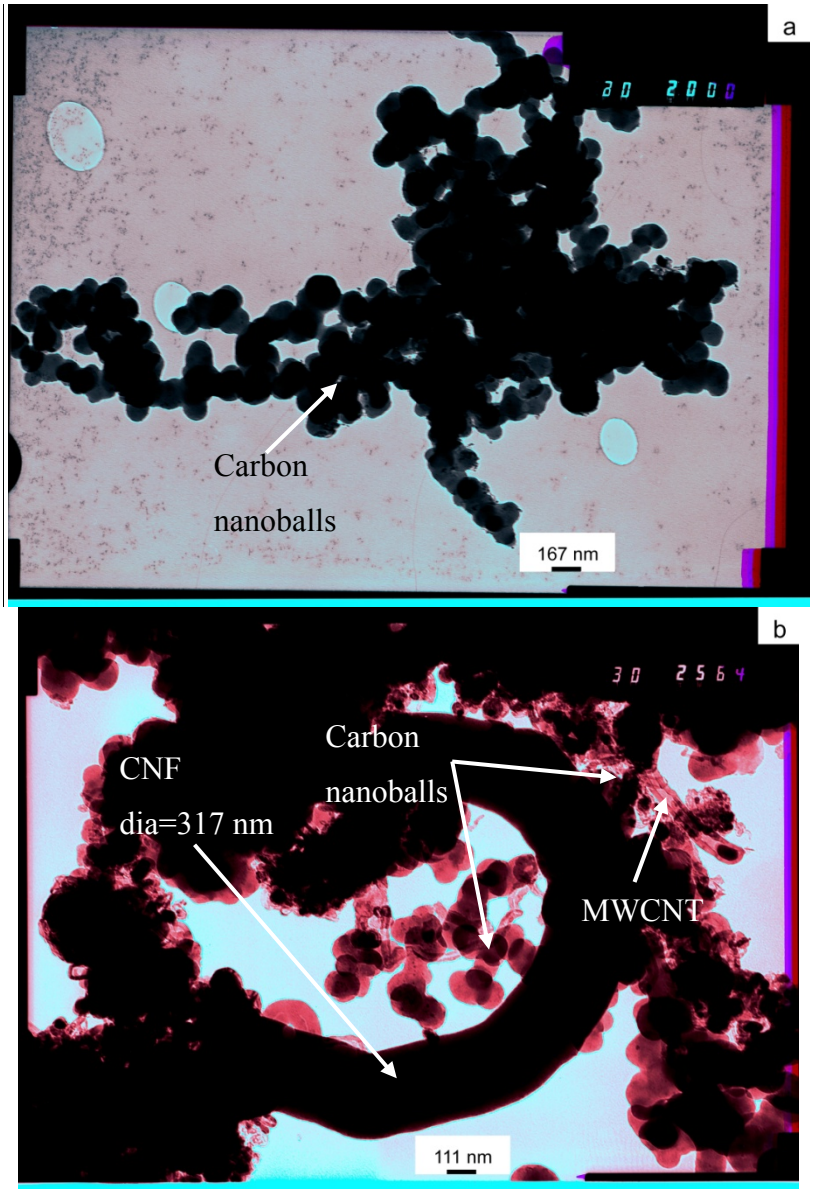

Figure 4.11: Electron micrographs obtained at 844 ml/min, 850 ^{o}C temperature, 2 g catalyst and 20 minutes. (a) and (b) consists of CNBs and CNFs.

(D) Summary

Process efficiency parameters were calculated for the 3 different flowrates to recommend the optimum flowrate. The procedure outlined in Section 3.1.8 was used to determine the production rate and carbon yield and the data was plotted in Figure 4.12 (see Appendix VI, Table 1 for the average data with standard deviation).

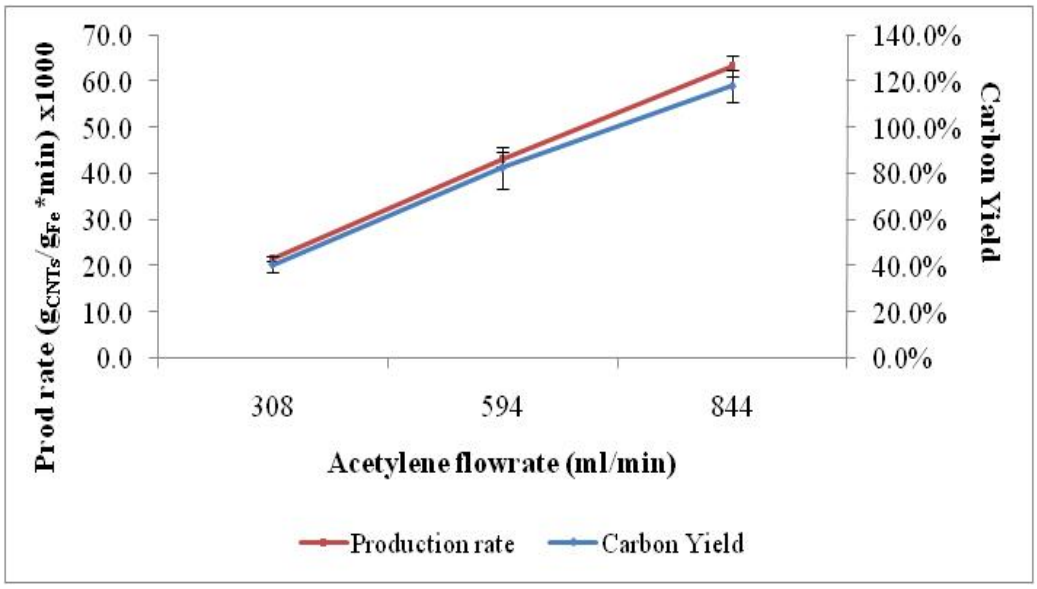

Figure 4.12: Effect of acetylene flowrate on production rate and yield. The standard deviations for the graphs were 18.7 for production rate and 35.1% for carbon yield.

From Figure 4.12 it can also be interpreted that there was an increase in carbon yield and production rate as acetylene flowrate was increased. This trend was expected and the choice of the optimum flowrate rests more on the quality of the CNTs synthesised.

4.1.3 Reaction Time

The study was carried to find out the effect of reaction time on the quality and quantity (production rate and carbon yield) of carbon nanoparticles synthesised at 5, 10, 15, 20 and 25 minutes. The conditions used in the study are presented in Table 4.3.

Table 4.3: Conditions used to investigate the effect of reaction time on the synthesis of CNTs.

Parameter	**Temperature (^oC)**	**Catalyst quantity (g)**	**C_2H_2 flowrate (ml/min)**	**Reaction time (min)**
Value	850	2.0	594	Variable

(A) 5 minutes

At 5 minutes, poorly formed CNFs and HCNFs were synthesised with a lot of impurities. The diameter ranges between 133 – 160 nm.

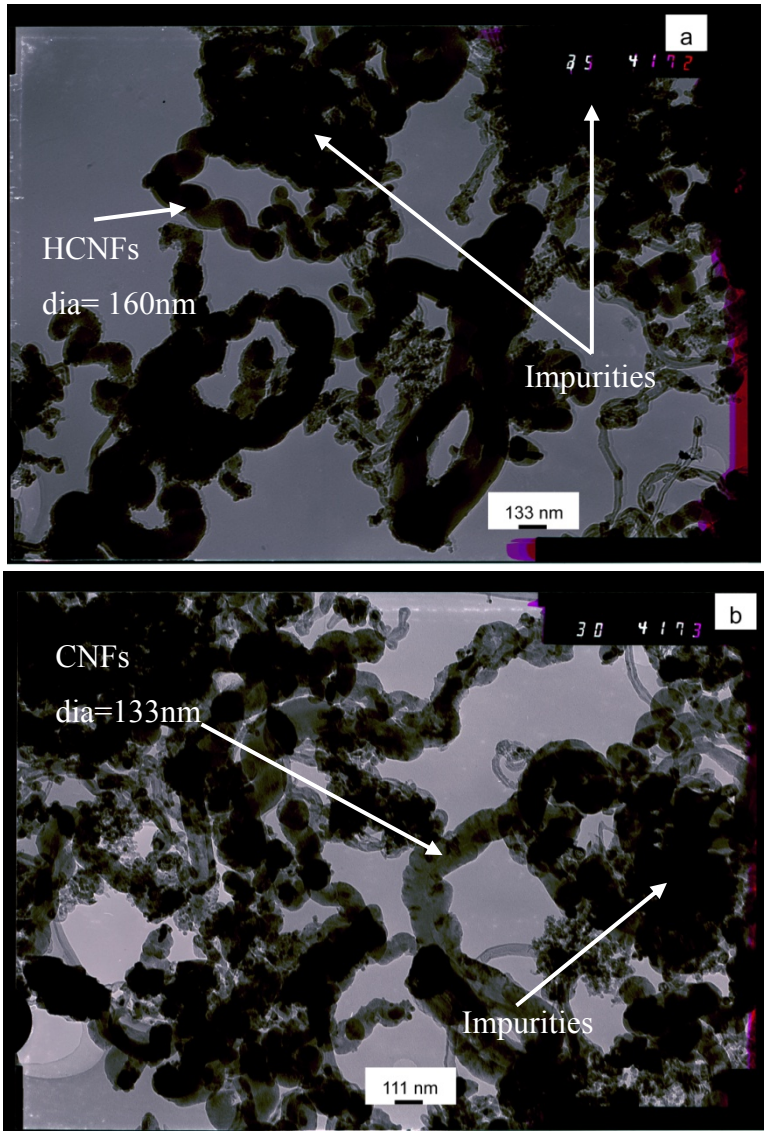

Figure 4.13: Electron micrographs obtained at 5 minutes, 850 ^{o}C temperature, 594 ml/min C_2H_2 flowrate and 2 g catalyst. (a) consists of HCNFs while (b) consists of CNFs.

(B) 10 minutes

At a reaction time of 10 minutes, poorly formed MWCNTs, CNFs and CNBs were observed together with impurities. The diameter ranges between 49 – 119 nm.

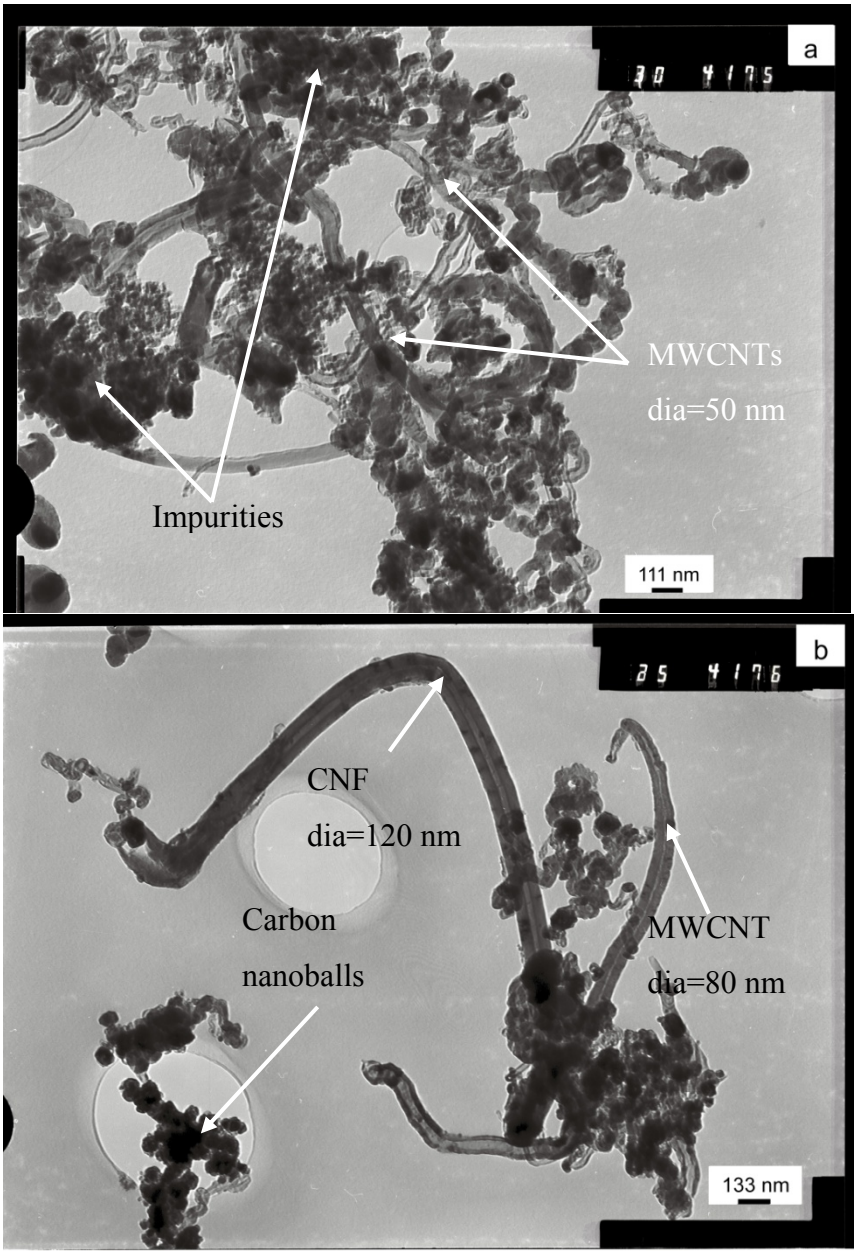

Figure 4.14: Electron micrographs obtained at 10 minutes, 850 ^{o}C temperature, 594 ml/min C_2H_2 flowrate and 2 g catalyst. (a) consists of MWCNTs while (b) consists of MWCNTs, CNBs and CNFs.

(C) 15 minutes

At 15 minutes CNFs and HCNFs together with some MWCNTs were observed but the MWCNTs were poorly formed. There were impurities observed in all the samples. The diameter ranges between 225 – 238 nm.

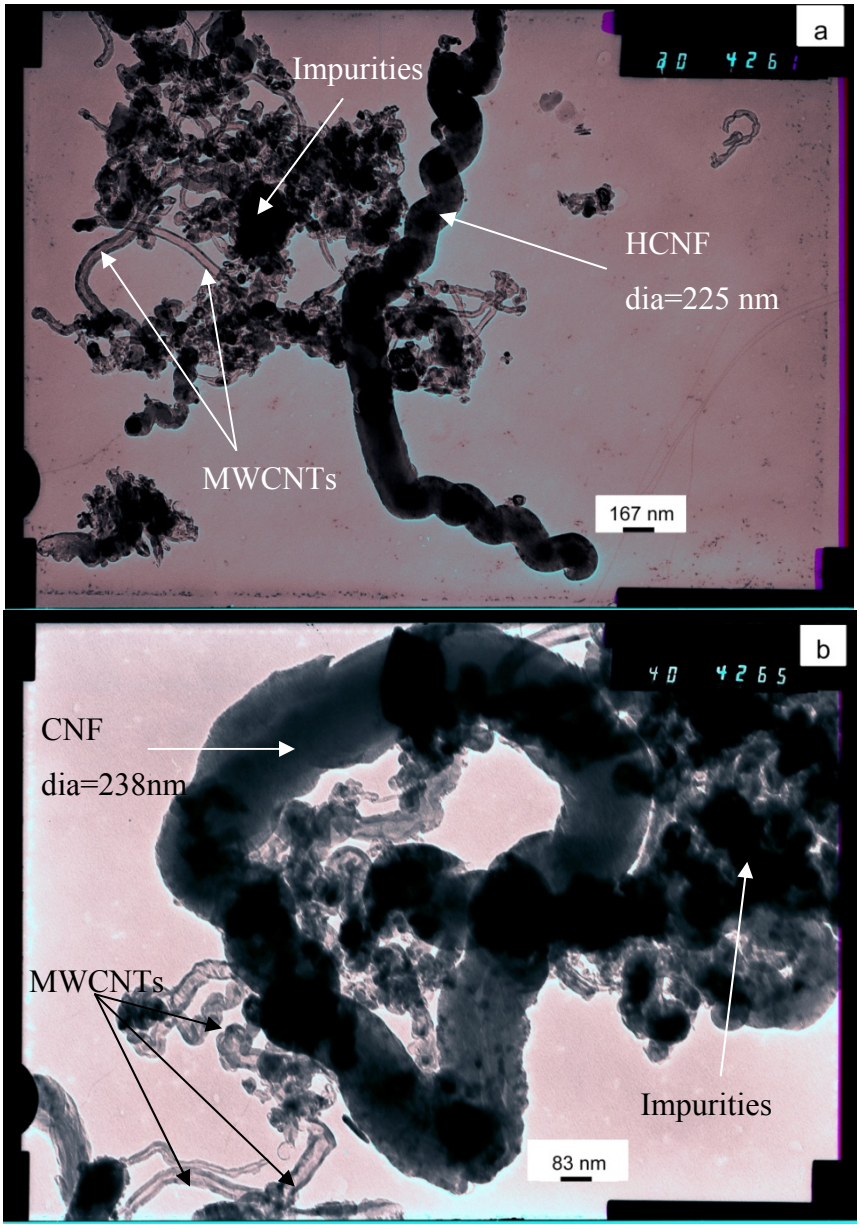

Figure 4.15: Electron micrographs obtained at 15 minutes, 850 ^{o}C temperature, 594 ml/min C_2H_2 flowrate and 2 g catalyst. (a) consists of HCNFs and MWCNTs while (b) consists of CNFs and MWCNTs.

(D) 20 minutes

At a reaction time of 20 minutes MWCNTs and some HCNTs were the main products synthesised. MWCNTs were long and were expanding out of the TEM focal length. The diameter ranges between 60 – 110 nm.

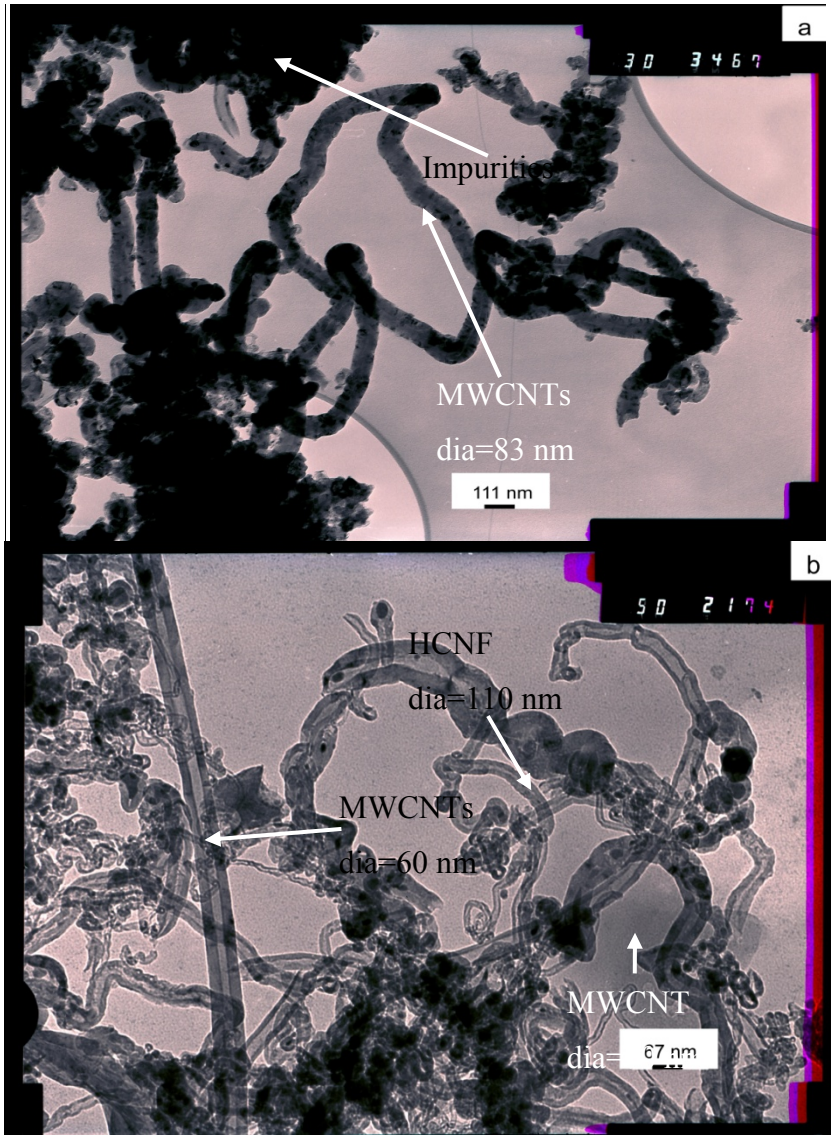

Figure 4.16: Electron micrographs obtained at 20 minutes, 850 ^{o}C temperature, 594 ml/min C_2H_2 flowrate and 2 g catalyst. (a) consists of MWCNTs while (b) consists of MWCNTs and HCNFs.

(E) 25 minutes

At a reaction time of 25 minutes, fibrous MWCNTs were the only product observed. In Figure 4.17c, a long MWCNT with good formation was observed and has a knot. The diameter ranges between 143 – 171 nm.

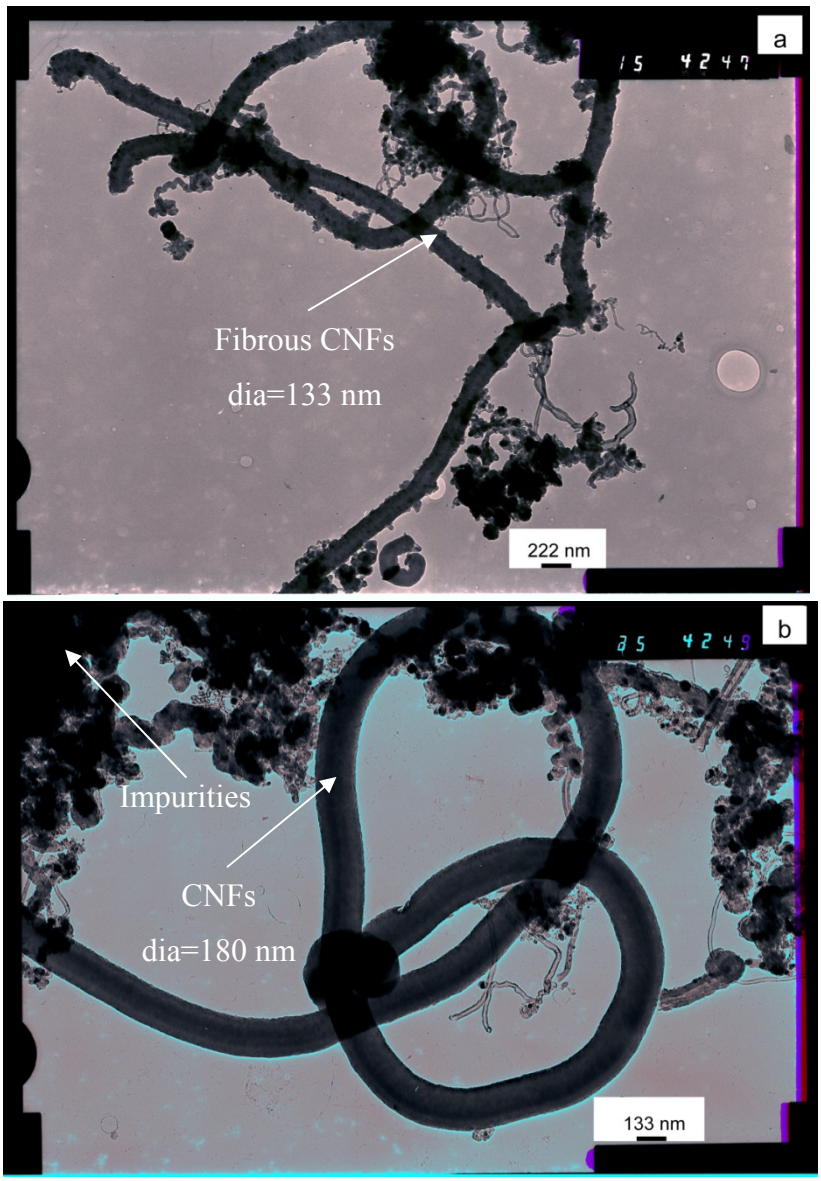

Figure 4.17: Electron micrographs obtained at 25 minutes, 850 ^{o}C temperature, 594 ml/min C_2H_2 flowrate and 2 g catalyst. (a) and (b) consists of CNFs.

(F) Summary

The process efficiency parameters were calculated for the different reaction times to investigate the optimum reaction time. The parameters calculated were carbon yield and production rate and the data is presented graphically (Figure 4.18) (see Appendix VI, Table 2 for the average data with standard deviation).

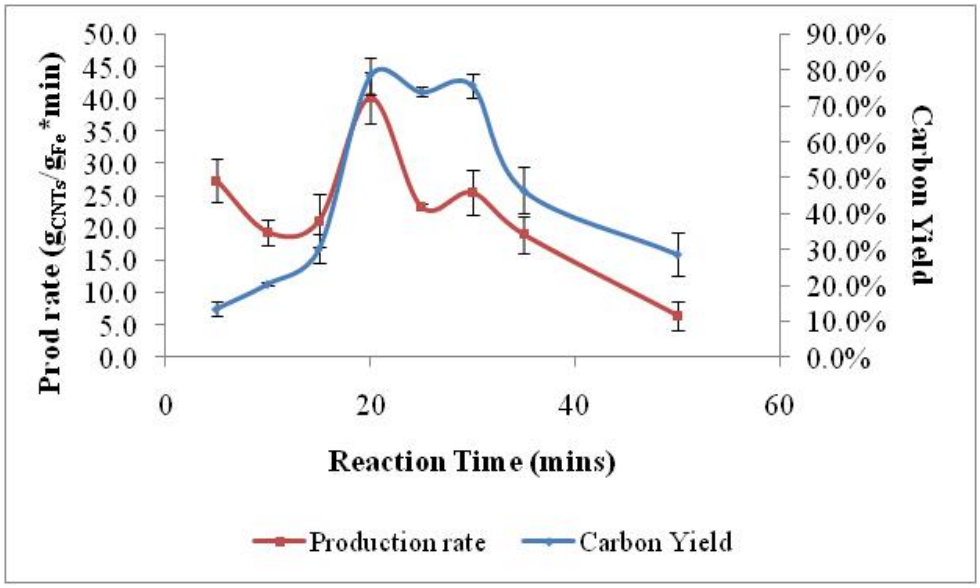

Figure 4.18: Effect of reaction time on production rate and yield. The standard deviations for the graphs were 9.40 for production rate and 26.0% for carbon yield.

Figure 4.18 showed a decrease in yield after 30 minutes and production rate after 20 minutes. This graph made it easier to determine the optimum parameters. The quantity of the catalyst was investigated to see its effect on the carbon nanoparticles synthesised.

Catalyst Quantity

Changing the catalyst quantity has an effect on the quality and quantity of CNTs synthesised. The quality of carbon nanoparticles synthesised at catalyst quantities of 2, 3, 5 and 10 grams were compared. The conditions used during the study are given in Table 4.4.

Table 4.4: Conditions used to investigate the effect of catalyst quantity on the synthesis of CNTs.

Parameter	**Temperature (^oC)**	**Catalyst quantity (g)**	**C_2H_2 flowrate (ml/min)**	**Reaction time (min)**
Value	850	Variable	594	20

(A) 2 Grams

Use of 2 grams of ferrocene catalyst resulted in long MWCNTs and CNFs. The diameter ranged between 83 – 150 nm.

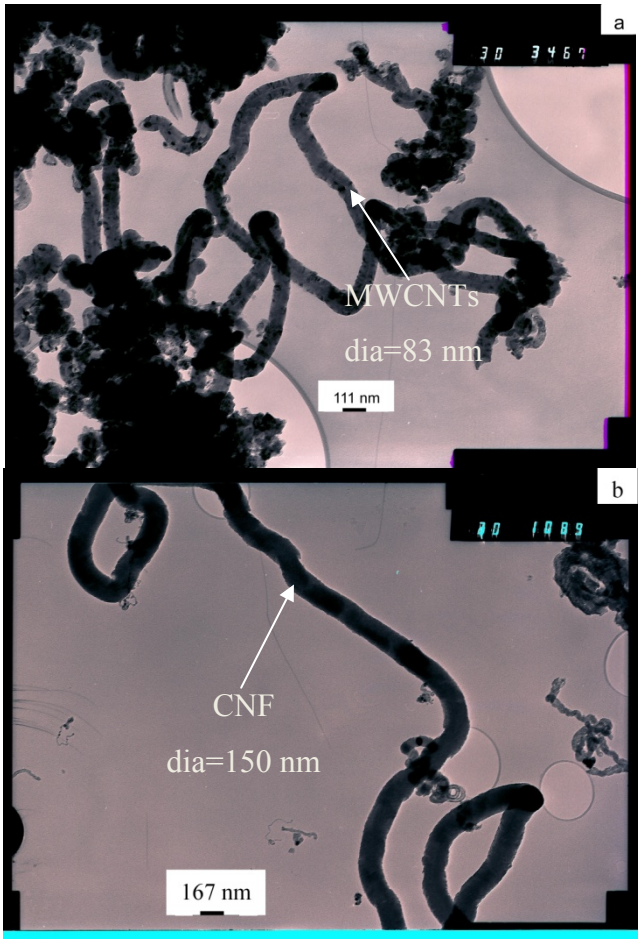

Figure 4.19: Electron micrographs obtained at 2 grams, 850 ^{o}C temperature, 594 ml/min C_2H_2 flowrate and 20 minutes. (a) consists of MWCNTs while (b) consists of CNFs.

(B) 3 Grams

Use of 3 grams resulted in poorly formed CNFs. A y-junction was observed in Figure 4.20a and Figure 4.20b had impurities. The diameter of products ranged between 160 – 185 nm.

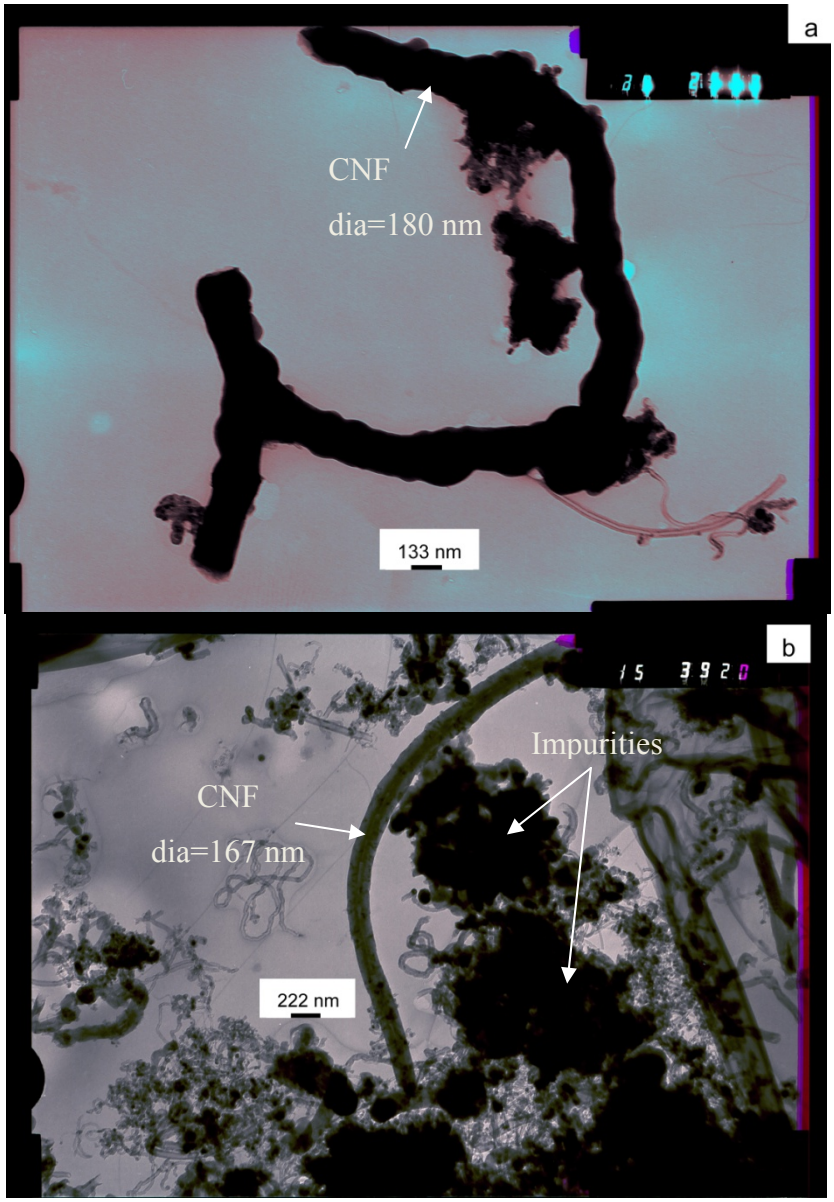

Figure 4.20: Electron micrographs obtained at 3 grams, 850 ^{o}C temperature, 594 ml/min C_2H_2 flowrate and 20 minutes. (a) and (b) consists of CNFs.

(C) 5 Grams

Use of 5 grams of catalyst resulted in poorly formed CNFs with MWCNTs were observed and they had a lot of impurities. The diameter ranges between 113 – 163 nm.

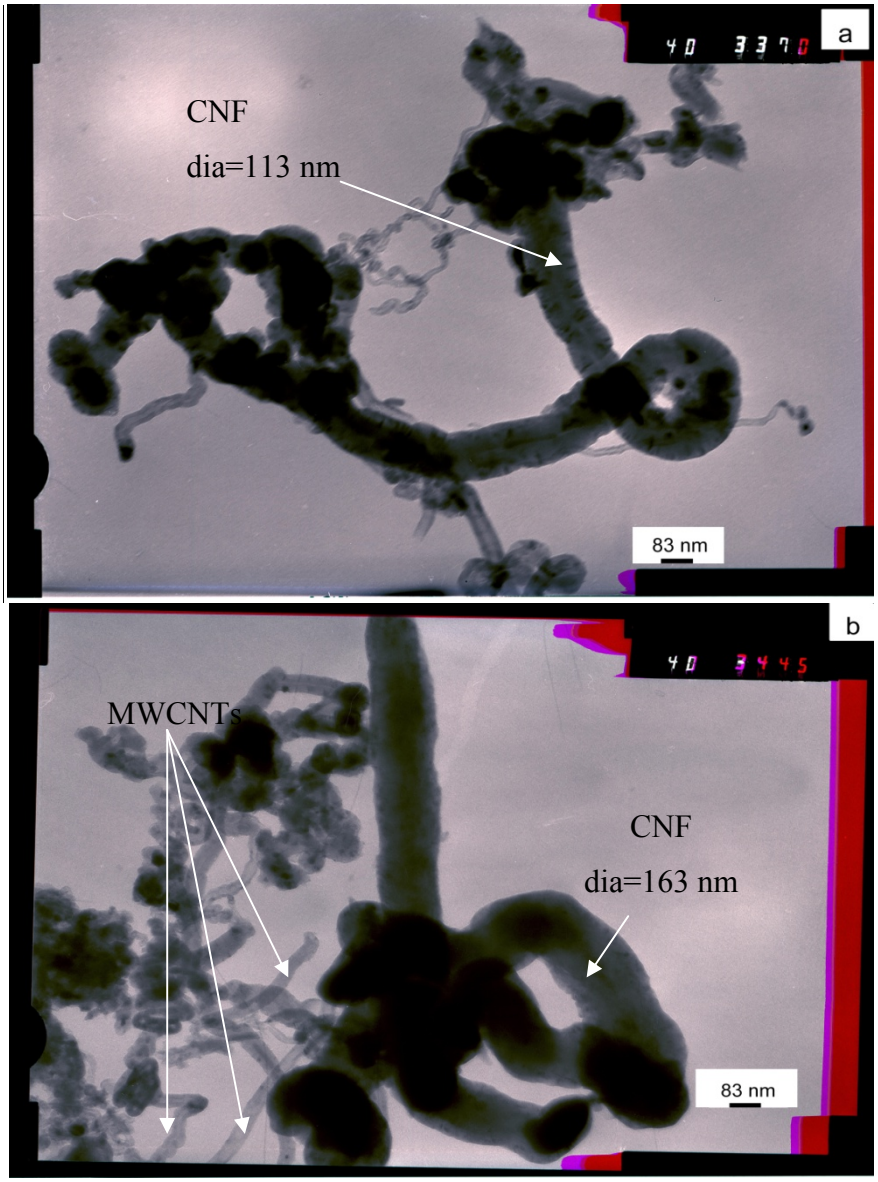

Figure 4.21: Electron micrographs obtained at 5 grams, 850 ^{o}C temperature, 594 ml/min C_2H_2 flowrate and 20 minutes. (a) and (b) consists of CNFs.

(D) 10 Grams

Use of 10 grams of ferrocene catalyst resulted in CNFs with fibrous morphologies were synthesised. Figure 4.22a has a CNF which is double in size while 4.22b has a CNF with a knot. The diameter ranges between 213 – 222 nm.

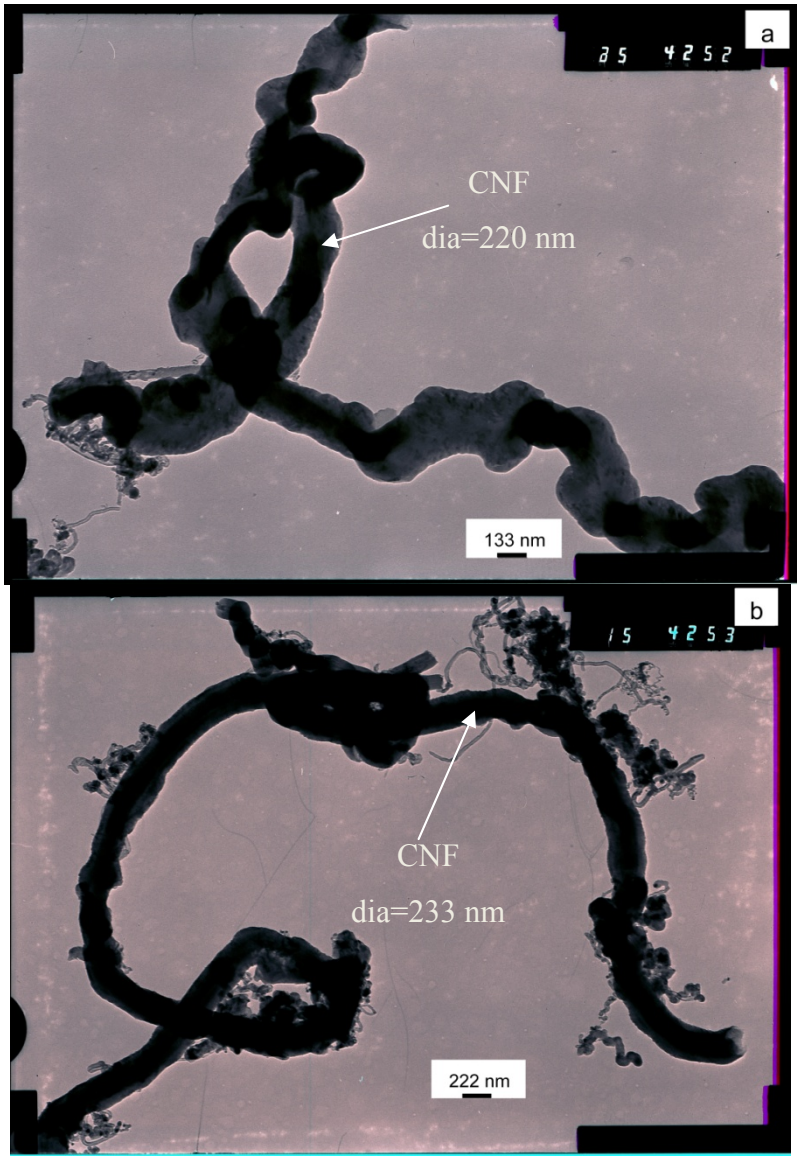

Figure 4.22: Electron micrograph obtained at 10 grams, 850 ^{o}C temperature, 594 ml/min C_2H_2 flowrate and 20 minutes. (a) and (b) consists of CNFs.

(E) Summary

The process efficiency parameters were calculated to determine the optimum catalyst quantity. The parameters calculated were carbon yield and production rate

and the data is presented below (Figure 4.23) (see Appendix VI, Table 3 for the average data with standard deviation).

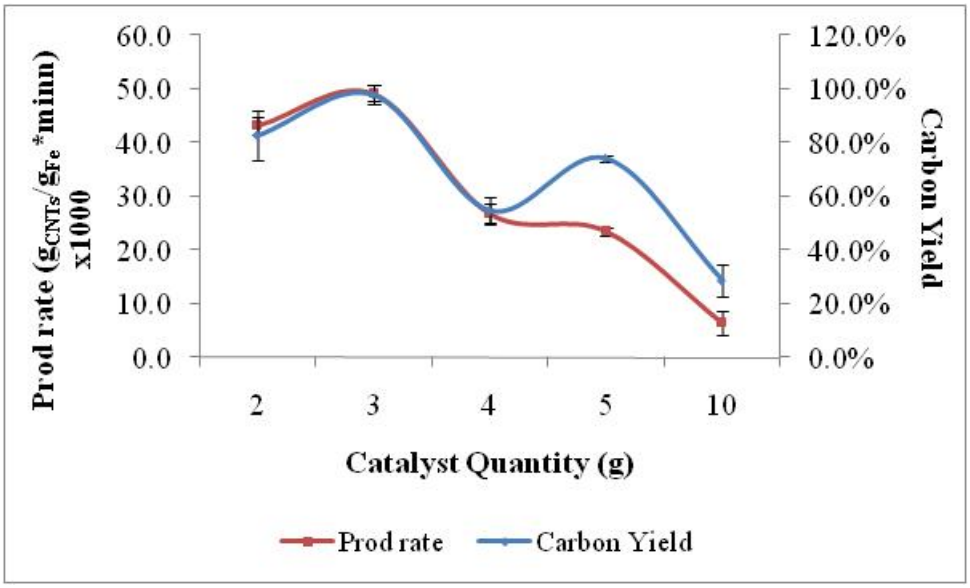

Figure 4.23: Effect of catalyst quantity on production rate and yield. The standard deviations for the graphs were 15.99 for production rate and 25.5% for carbon yield.

The graph shows that the carbon yield and production rates increased up to 3 grams and decreased from 3 grams to 10 grams. It was easier to determine the optimum catalyst quantity from the graph. However, the quality of the CNTs synthesised had to be taken into consideration.

4.2 Yeast Cell Immobilisation

The successful flocculation of brewers' yeast cells onto CNTs was confirmed by SEM (Figure 4.24) and Stereo Microscopy (Figure 4.25). All the immobilised cells were recovered by a freeze dryer to make it possible to analyse the immobilisation products using the SEM. The SEM required dry samples and the

freeze drying process was a necessary step to take although this was at the expense of the viability of the yeast cells for fermentation studies.

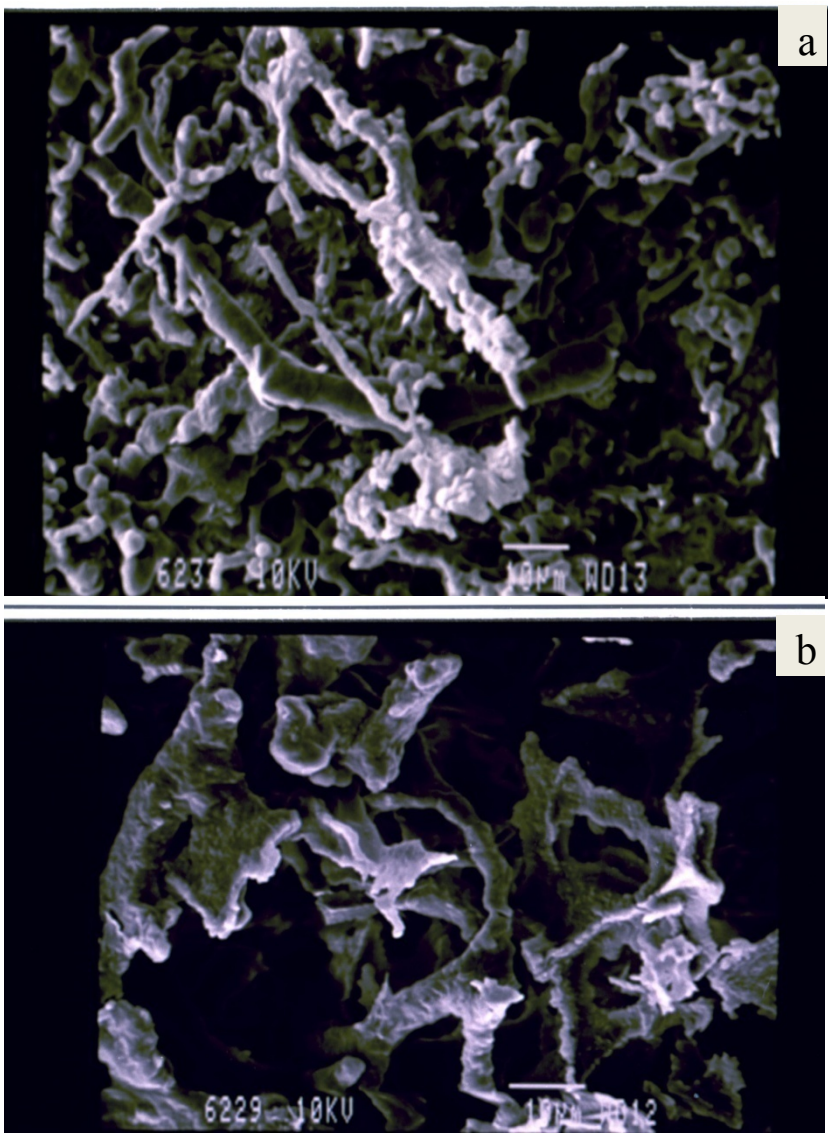

Figure 4.24: Electron micrographs showing the immobilised yeast cells on CNTs. (a) x1300 SEM magnification; (b) x1600 SEM magnification.

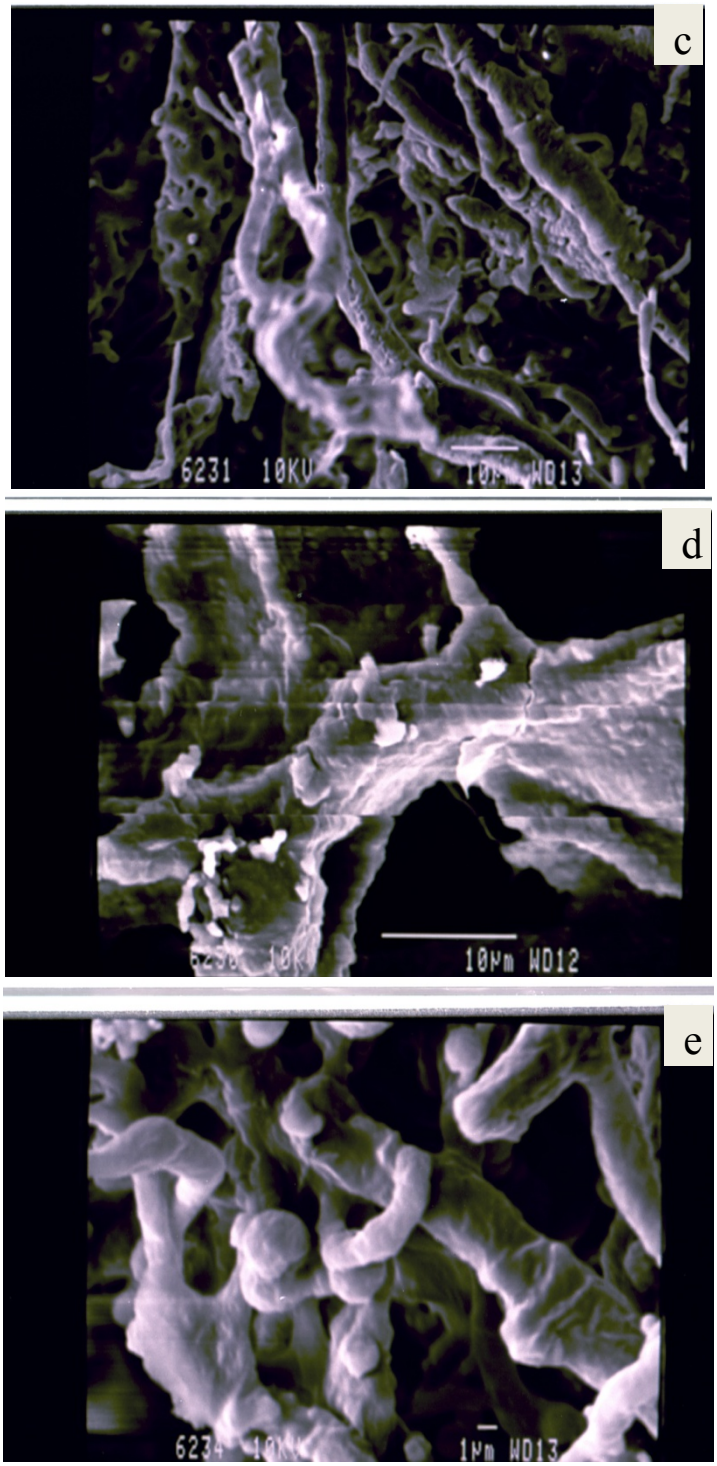

Figure 4.24 continued...: Electron micrographs showing the immobilised yeast cells on CNTs. (c) x1600 SEM magnification; (d) x3300 SEM magnification; (e) x5000 SEM magnification.

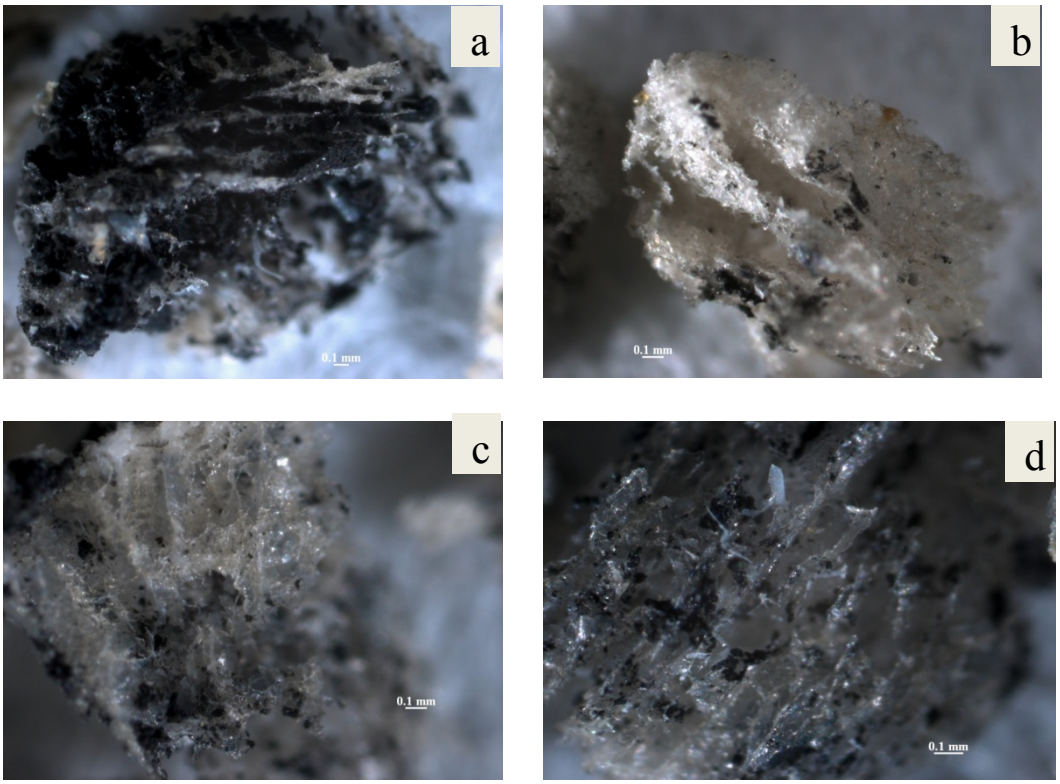

Figure 4.25: Stereo Microscopy photographs showing the immobilised yeast cells on CNTs. (a) x43.5 magnification; (b) x62 magnification; (c) x62 magnification; (d) x81 magnification.

The micrographs (Figure 4.24) showed that the flocculated yeast cells formed strands or rod-like shapes growing along the length of the CNTs. The flocs produced using the CNTs were more stable than flocs produced without CNTs and this was observed during the recovery stage using a freeze dryer (Figure 4.26). The results in Figure 4.25 showed that the flocs formed where crystalline in nature. The flocs were aligned in a rod-like shape as observed from the SEM micrographs.

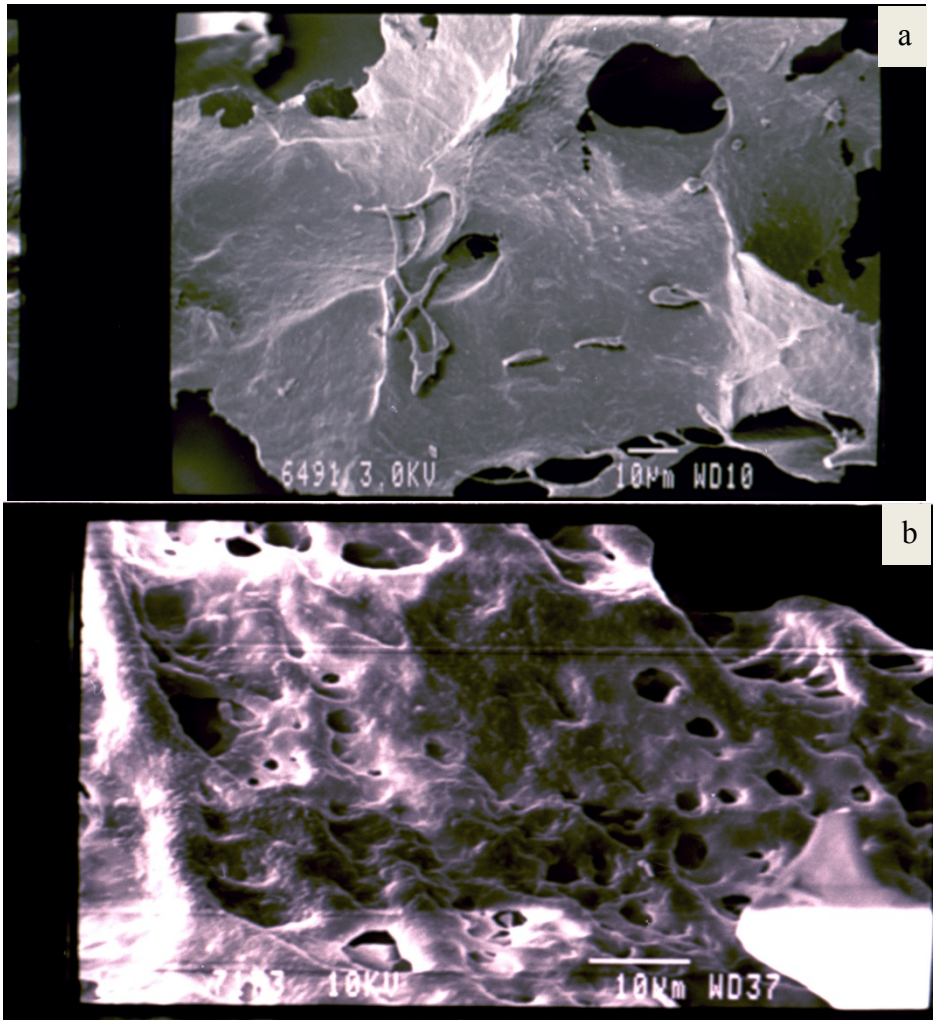

Figure 4.26: Electron micrographs showing yeast cells that flocculated without CNTs. (a) x1000 SEM magnification; (b) x1700 SEM magnification.

The results in Figure 4.26 showed that in the absence of CNTs the flocs formed were of a continuous sheet of cells or a planar-shape.

Parameters that affect yeast immobilisation were investigated during the study and these were as follows:

- Agitation speed (revolutions per minute, rpm)

- pH
- Concentration of CNTs abbreviated by [CNTs]
- Immobilisation temperature abbreviated by Temp
- Concentration of calcium (Ca^{2+}) ions abbreviated by [Ca^{2+}]
- Presence of glucose

The studies were conducted over a period of 3 or 4 days to assess the formation and stability of the flocs. Experiments were done at least twice with the mean and standard deviation included in the results. Results for the floc weight are presented in tabular form as mean±standard deviation or as a graph showing standard deviation bars. Zeta potential data were measured in triplicate and the mean value reported with a standard deviation. The data was presented graphically as the experiment progressed and the potential was negative for all the experiments showing the tendency for the colloids to flocculate. The measurements were done to help understand the flocculation process. The zeta potential should always be stated with medium conditions (e.g. pH, conductivity, temperature and additives).

4.2.1 Agitation Speed

Cells must come into contact with each other for flocculation to occur, hence the surprising observation that flocculation and the vigour of mechanical agitation are positively correlated. Thus in well stirred systems there is a high probability that cells will contact each other and once formed, flocs are relatively stable structures (Briggs *et al*., 2004). Agitation was varied from 0 to 250 rpm during the study to determine its effect on flocculation of brewers' yeast cells. The aim also was to determine the optimum agitation which resulted in most flocculation of brewers' yeast cells. The other conditions used during the study are in Table 4.5.

Table 4.5: Conditions used to investigate the effect of agitation on the flocculation of brewers' yeast.

Parameter	**Agitation speed**	**pH**	**Temp**	**[CNTs]**	**[Ca^{2+}]**	**Presence of glucose**
Value	Variable	4.60, 5.60	30 ^{o}C	54μg/ml	Nil	Nil

The pH, temperature and concentration of CNTs were chosen with reference from literature. It has been shown that yeast flocculation is optimal in slightly acidic conditions, with pH values ranging from 3.50 to 5.80 (Jin and Speers, 2000; Jin *et al*., 2001; Soares *et al*., 1994; Stratford, 1992) and the two different pH values (4.60 and 5.60) which were between the range 3.50 and 5.80 were chosen at the initial stage of this study. Most brewing strains have an optimum temperature for growth between 30 and 34 ^{o}C (Briggs *et al*., 2004; Jin and Speers, 1999) and a temperature of 30 ^{o}C was chosen. Peinado *et al.* (2005) conducted their studies at 28 ^{o}C and 150 rpm for 7 days and had successful immobilisation to produce yeast biocapsules while Sakurai *et al.* (2000) used 30 ^{o}C and 160 rpm during their immobilisation studies of yeast cells on porous cellulose carriers. Öztop *et al*. (2003) immobilised *S. cerevisiae* onto acrylamide-sodium acrylate hydrogels at 30 ^{o}C for 72 hours. Viability losses at 30 ^{o}C for 3 days during flocculation are negligible (Zhao and Fleet, 2003) with autolysis occurring at elevated temperatures of between 40 and 60 ^{o}C (Arnold, 1981; Hernawan and Fleet, 1995; Zhao and Fleet, 2003; Alexandre and Guilloux-Benatier, 2006). Ghafari, *et al* (2008) investigated bacteria ciliated protozoa between CNT concentrations of 0 – 17.2 μg/ml and for this study a concentration of 54μg/ml was chosen in the initial stages.

(A) 0 rpm

An agitation speed of 0 rpm was first investigated. The studies were stopped after 4 days because no flocculation was observed even after one day more. Due to this no flocs were recovered using a centrifuge to measure the weight and a digital camera was used to capture the bottom of the flasks (Figure 4.27).

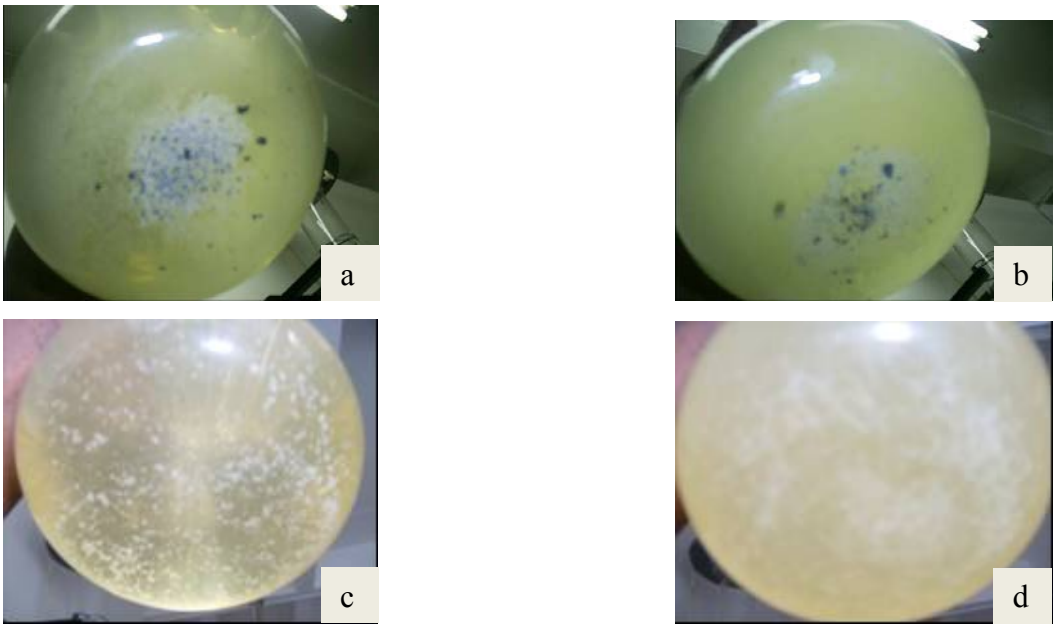

Figure 4.27: Digital photographs of yeast flocculation after 4 days at 0 rpm. (a) and (b) are main experiments while (c) and (d) are control experiments. (a) and (c) are at pH 4.60 while (b) and (d) are at pH 5.60.

Table 4.6: Analysis of flocculation at 0 rpm, 30^{o}C, pH 4.60 and 5.60, and [CNTs] of 54μg/ml.

Experiment	**a**	**b**	**c**	**d**
Floc quality	-	-	-	-

The flocculation was ranked (-) to show that there were flocs observed under these conditions. The zeta potential change was also monitored over the 4 day period

and the results are presented in Figure 4.28 (see Appendix VII, Table 1 for the average data with standard deviation).

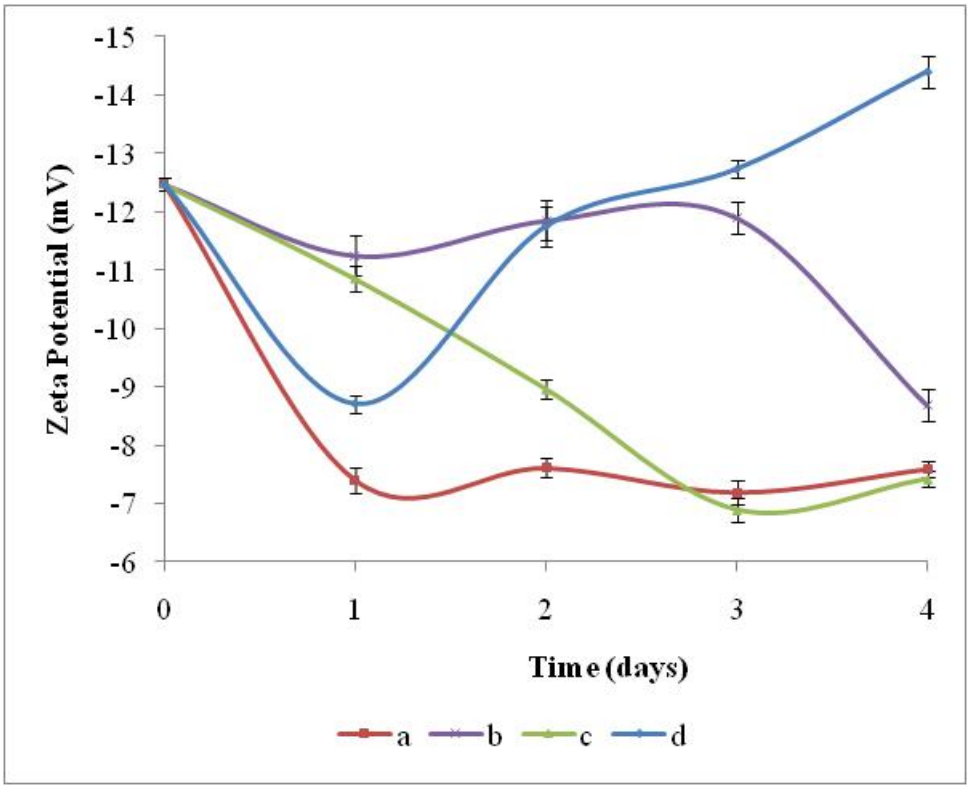

Figure 4.28: Change in zeta potential over time at 0 rpm, 30^{o}C, pH 4.60 and 5.60, and [CNTs] of 54μg/ml. The standard deviations for the graphs were 2.25 for a, 1.49 for b, 2.34 for c and 2.09 for d.

From Figure 4.28, it is observed that the final zeta potential for studies at pH 4.60 were more negative than those at pH 5.60. The zeta potential data were outside the ±5 mV range which is the flocculation range for the 4 days but was in the threshold of flocculation range (Table 2.2). This explained why no flocculation was observed under these conditions. The zeta potential for (b) and (d) at pH 5.60 showed an increase and decrease from -12.47±0.10 mV to -8.68±0.27 mV and -14.40±0.28 mV respectively while the zeta potential for (a) and (c) at pH 4.60 increased from -12.47±0.10 mV to -7.59±0.06 mV and -7.42±0.14 mV

respectively. The graph for (b) was steadily becoming negative moving towards the ±5 mV showing strong tendency towards flocculation. All the other graphs were moving away from the ±5 mV range and that may also help to explain the absence of flocculation. Statistical analysis was conducted to see if there was a significant difference between the zeta potential graphs for the study. The p value was 0.0405 which was considered significant as variation among the graphs was significantly greater than expected by chance.

(B) 50 rpm

The studies were repeated at an agitation speed of 50 rpm while maintaining all other conditions. The studies were conducted for 3 days and they were stopped because there was no flocculation observed. There were no flocs recovered using a centrifuge and the photographs are shown below.

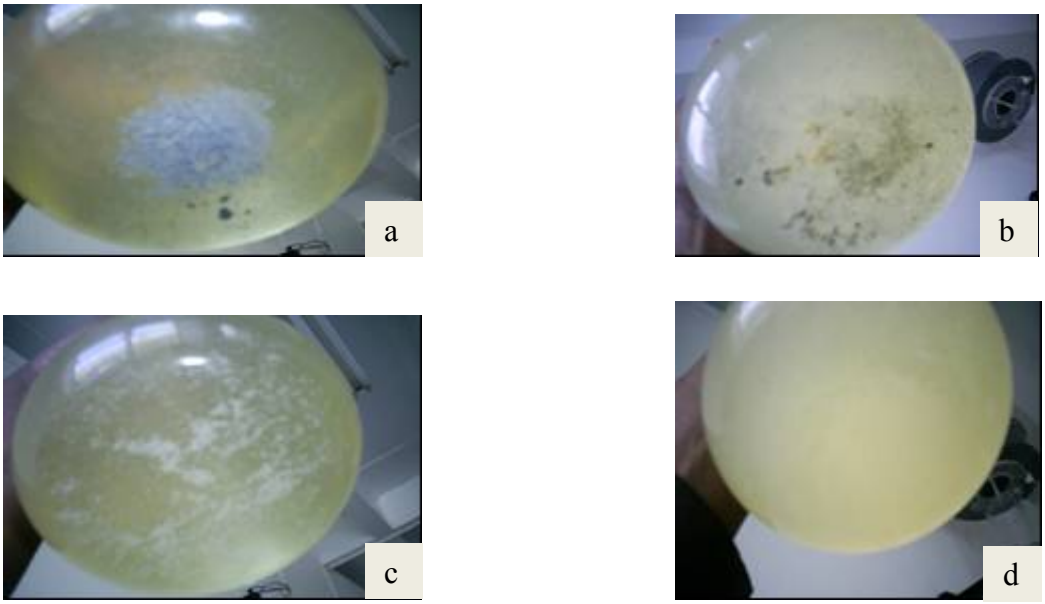

Figure 4.29: Digital photographs of yeast flocculation after 3 days at 50 rpm. (a) and (b) are main experiments while (c) and (d) are control experiments. (a) and (c) are at pH 4.60 while (b) and (d) are at pH 5.60.

Table 4.7: Analysis of flocculation at 50 rpm, 30°C, pH 4.60 and 5.60, and [CNTs] of 54µg/ml.

Experiment	a	b	c	d
Floc quality	-	-	-	-

The flocculation for all the studies was ranked (-) signifying the absence from the flocs over the period. The zeta potential change was also monitored and is presented in Figure 4.30 (see Appendix VII, Table 2 for the average data with standard deviation).

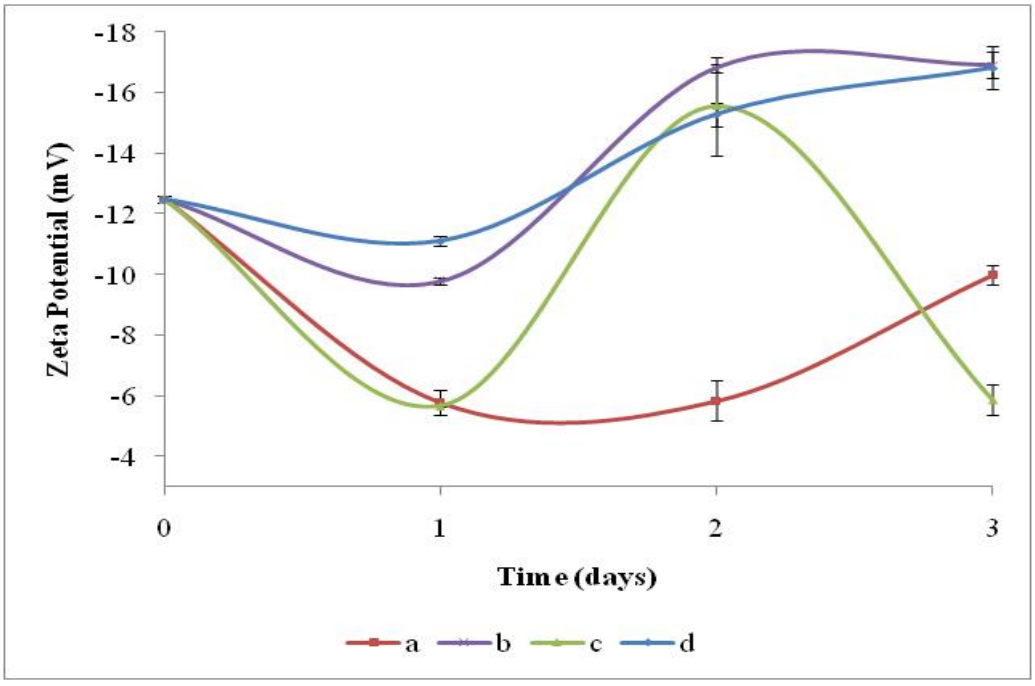

Figure 4.30: Change in zeta potential over time at 50 rpm, 30°C, pH 4.60 and 5.60, and [CNTs] of 54µg/ml. The standard deviations for the graphs were 3.29 for a, 3.48 for b, 4.92 for c and 2.59 for d.

The results in Figure 4.30 showed that the final zeta potential values were outside the ±5 mV range which helped to explain the absence of flocculation after the 3

days but however, they were in the threshold for flocculation (Table 2.2). The zeta potential values at pH 4.60 were more negative than those at pH 5.60. The zeta potential for (b) and (d) at pH 5.60 decrease from -12.47±0.10 mV to -16.90±0.42 mV and -16.80±0.71 mV respectively while the zeta potential for (a) and (c) at pH 4.60 increased from -12.47±0.10 mV to -9.97±0.33 mV and -5.87±0.52 mV respectively. The graph for (c) was steadily becoming negative moving towards the ±5 mV showing strong tendency towards flocculation. All the other graphs were moving away from the ±5 mV range and that may also help to explain the absence of flocculation. Statistical analysis was conducted to see if there was a significant difference between the zeta potential graphs for the study. The p value was 0.5076 which was considered not significant as variation among the graphs was not significantly greater than expected by chance.

(C) 110 rpm

The studies were repeated at an agitation speed of 110 rpm. The experiments were stopped after 4 days as flocculation was observed. The flocs were recovered and ranked according to the procedure 1 and 2 in Section 3.2.12.

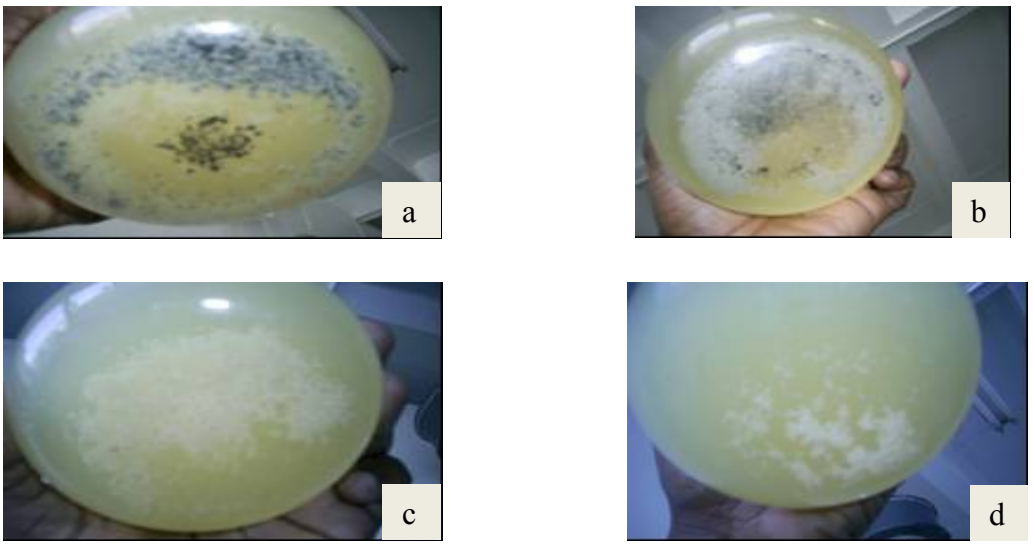

Figure 4.31: Digital photographs of yeast flocculation after 4 days at 110 rpm. (a) and (b) are main experiments while (c) and (d) are control experiments. (a) and (c) are at pH 4.60 while (b) and (d) are at pH 5.60.

Table 4.8: Analysis of flocculation at 110 rpm, 30^{o}C, pH 4.60 and 5.60, and [CNTs] of 54μg/ml.

Experiment	**a**	**b**	**c**	**d**
Floc quality	++	++	+	++
Dry floc weight (g)	0.124±0.003	0.143±0.007	0.132±0.005	0.123±0.005

Experiment (b) had the highest flocculation weight (0.143±0.007g) but the quality of the flocs was ranked as the same as (a) and (d). The CNTs increased the flocculation weight from 0.124±0.003 at pH 4.60 to 0.143±0.007 at pH 5.60, a difference of 0.019 g while for the control experiment the difference was -0.008 g. These results suggest that flocculation onto CNTs gave better results at pH 5.60 but flocculation in the absence of CNTs gave better results at pH 4.60. The change in zeta potential was monitored for the 4 days and is presented in Figure 4.32 (see Appendix VII, Table 3 for the average data with standard deviation).

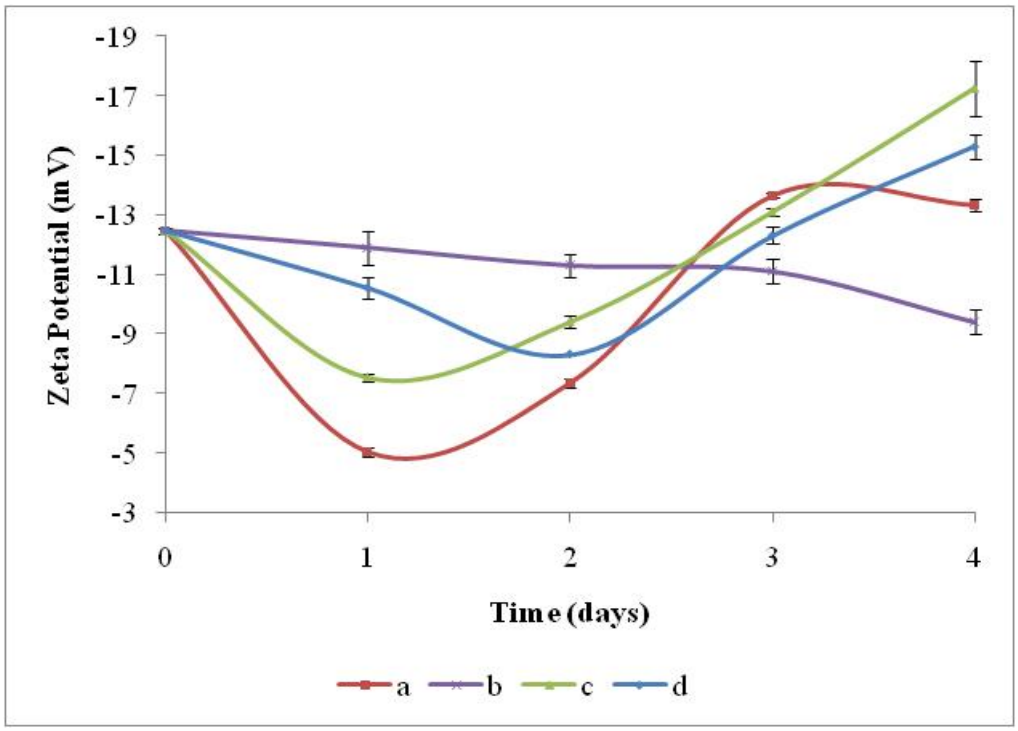

Figure 4.32: Change in zeta potential over time at 110 rpm, pH4.60 and 5.60, and [CNTs] of 54μg/ml. The standard deviations for the graphs were 3.92 for a, 1.16 for b, 3.73 for c and 2.58 for d.

The final zeta potential was outside the ±5 mV range (Table 2.2), but with well established flocculation. Experiments (a) and (b) had more negative zeta potential (a>b) than (c) and (d) (d>c) showing the effect of the presence of CNTs and differing in pH on zeta potential of yeast cells. The CNTs increased zeta potential from -12.47±0.10 to -9.70±0.40 mV and -13.33±0.21 mV for (b) and (a) respectively. Experiment (b) at pH 5.60 had a higher zeta potential than (a) at pH 4.60 showing the effect of pH on zeta potential. Zeta potential for (a) and (b) were in the threshold for flocculation range as opposed to (c) and (d) which were in the threshold of light dispersion. Experiment (c) had the least zeta potential and it had the least flocculation capability. This could be attributed to the low more acidic pH (4.60) and lack of CNTs. Experiment (b) showed a steady increase in zeta

potential up to day 4 and this may help to explain the highest floc weight observed. The graphs for (a) and ((b) were steadily becoming more negative moving towards the ±5 mV showing strong tendency towards flocculation. The other graphs (c) and (d) which did not have CNTs were moving away from the ±5 mV range. Statistical analysis was conducted to see if there was a significant difference between the zeta potential graphs for the study. The p value was 0.0409 which was considered significant as variation among the graphs was significantly greater than expected by chance.

(D) 150 rpm

The studies were repeated at an agitation speed of 150 rpm. The experiments were stopped after 3 days because there was no flocculation observed (Figure 4.33) and no flocs were recovered by the centrifuge.

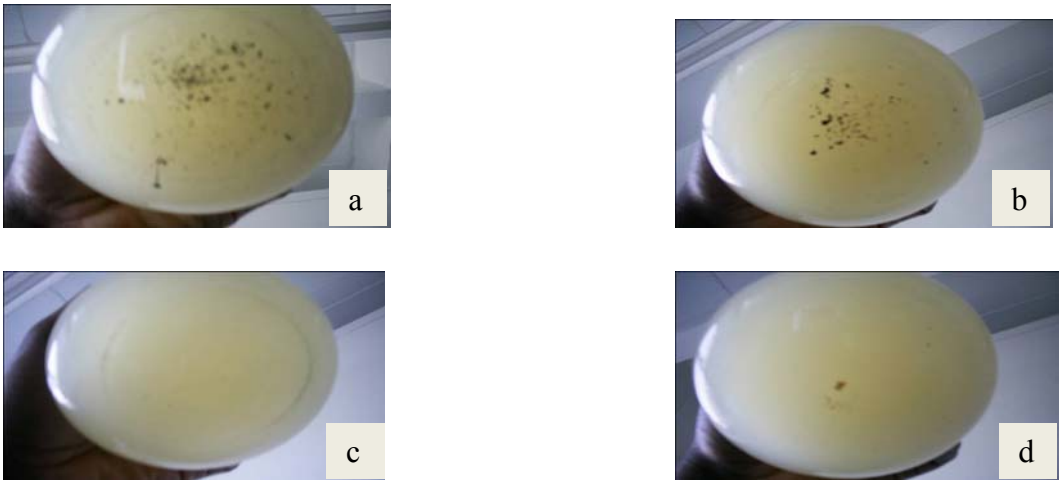

Figure 4.33: Digital photographs of yeast flocculation after 3 days at 150 rpm. (a) and (b) are main experiments while (c) and (d) are control experiments. (a) and (c) are at pH 4.60 while (b) and (d) are at pH 5.60.

Table 4.9: Analysis of flocculation at 150 rpm, 30°C, pH 4.60 and 5.60, and [CNTs] of 54µg/ml.

Experiment	a	b	c	d
Floc quality	-	-	-	-

The flocculation was ranked as (-) due to the absence of flocculation. Zeta potential was monitored to see its change with time for the 3 days (see Appendix VII, Table 4 for the average data with standard deviation).

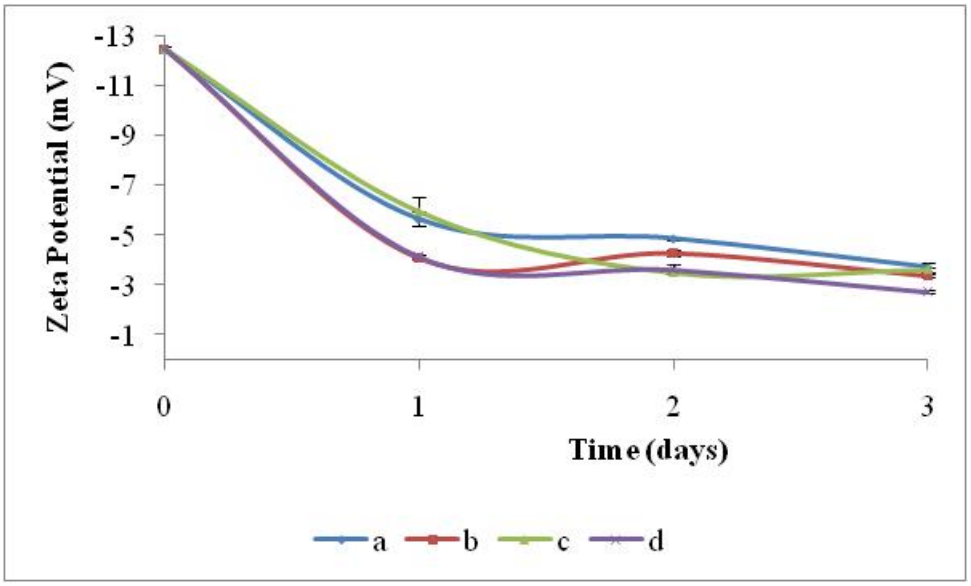

Figure 4.34: Change in zeta potential over time at 150 rpm, pH4.60 and 5.60, and [CNTs] of 54µg/ml. The standard deviations for the graphs were 3.95 for a, 4.30 for b, 4.22 for c and 4.53 for d.

The final zeta potential was within the ±5 mV range even though there was no flocculation observed. The zeta potential at pH 5.60 were more negative than those at pH 4.60 showing the same trend observed at 0, 50 and 110 rpm in the previous studies. The final zeta potential values were almost the same; -3.70±0.20,

-3.37±0.06, -3.59±0.07 and -2.72±0.08 for (a), (b), (c) and (d) respectively. Statistical analysis was conducted to see if there was a significant difference between the zeta potential graphs for the study. The p value was 0.1069 which was considered not significant as variation among the graphs was not significantly greater than expected by chance.

(E) 200 rpm

The studies were repeated at an agitation speed of 200 rpm and there was no flocculation observed under these conditions (Figure 4.35).

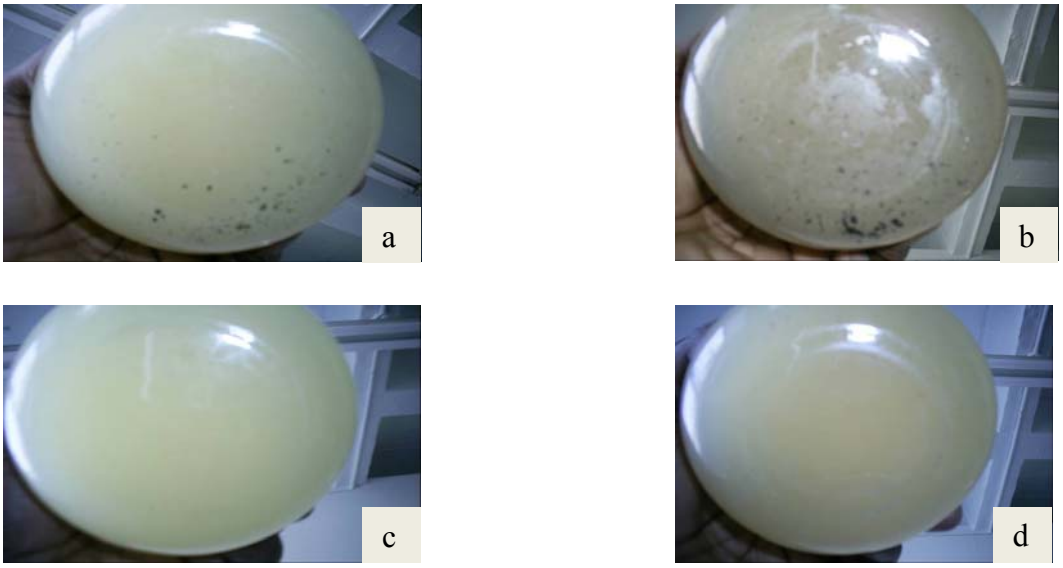

Figure 4.35: Digital photographs of yeast flocculation after 3 days at 200 rpm. (a) and (b) are main experiments while (c) and (d) are control experiments. (a) and (c) are at pH 4.60 while (b) and (d) are at pH 5.60.

Table 4.10: Analysis of flocculation at 200 rpm, 30^{o}C, pH 4.60 and 5.60, and [CNTs] of 54μg/ml.

Experiment	**a**	**b**	**c**	**d**

Floc quality	-	-	-	-

Flocculation was ranked as (-) as there were no flocs observed. The zeta potential was plotted to see how it will change against time (see Appendix VII, Table 5 for the average data with standard deviation).

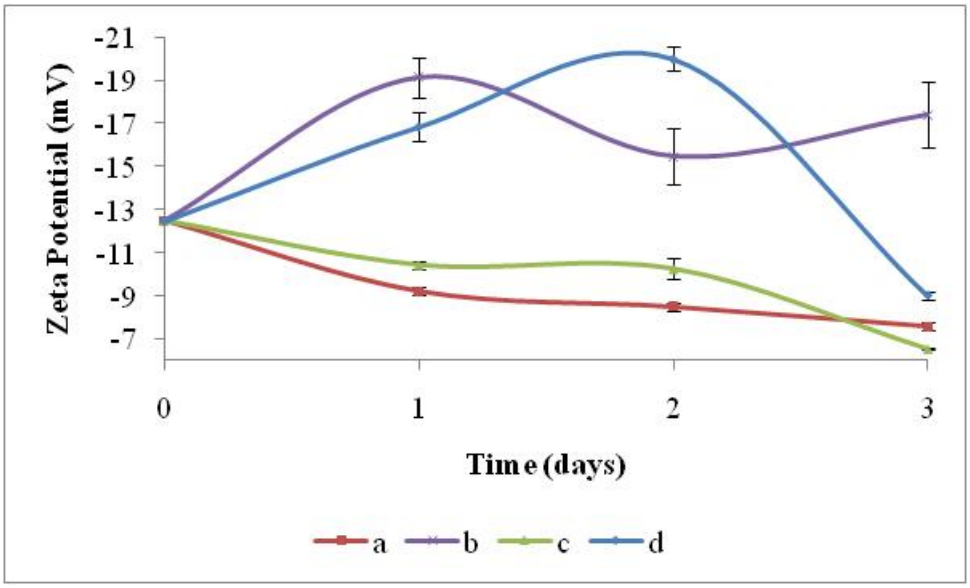

Figure 4.36: Change in zeta potential over time at 200 rpm, pH4.60 and 5.60, and [CNTs] of 54µg/ml. The standard deviations for the graphs were 1.90 for a, 3.65 for b, 2.21 for c and 4.44 for d.

The final zeta potential values were outside the ±5 mV range and that helped to explain the absence of flocculation during the study. The zeta potential for experiments at pH 4.60 [a (-7.59±0.17) and c (-6.55±0.01) were more negative than experiments at pH 5.60 [b (-17.40±1.55) and d (-9.03±0.18)] with (b) having the least negative potential. For (a), (c) and (d), the zeta potential was in the range of threshold of flocculation (Table 2.2) but for (b) it was in the threshold of light dispersion. The graphs for (a), (b) and (d) were steadily becoming more negative with time moving towards the ±5 mV showing strong tendency towards

flocculation. Only graph (c) was moving away from the ±5 mV range and that may also help to explain the absence of flocculation. Statistical analysis was conducted to see if there was a significant difference between the zeta potential graphs for the study. The p value was 0.0292 which was considered significant as variation among the graphs was significantly greater than expected by chance.

(F) Summary

The absence of flocculation at higher agitation speeds of 150 and 200 rpm maybe due to the disintegration of the flocs as they are formed and this is attributed to surface damage or disruption of individual cells. While an increase in collisions may help to grow the flocs there is a limiting agitation speed beyond which surface erosion or floc fracture sets in which limits the stable floc to a certain optimum size (Stratford and Wilson, 1990). Stratford and Wilson (1990) showed that the initial rate of flocculation was optimum at speeds between 110 and 115 rpm and it was negligible at low agitation speeds up to 60 rpm (Figure 4.37). The zeta potential was useful to predict flocculation onset at lower agitation speeds (0 and 50 rpm) but at higher speeds there was inconsistency in the relationship. The increase in agitation speed coupled with an increase in collisions seem to make zeta potential less reliable to predict flocculation of yeast cells.

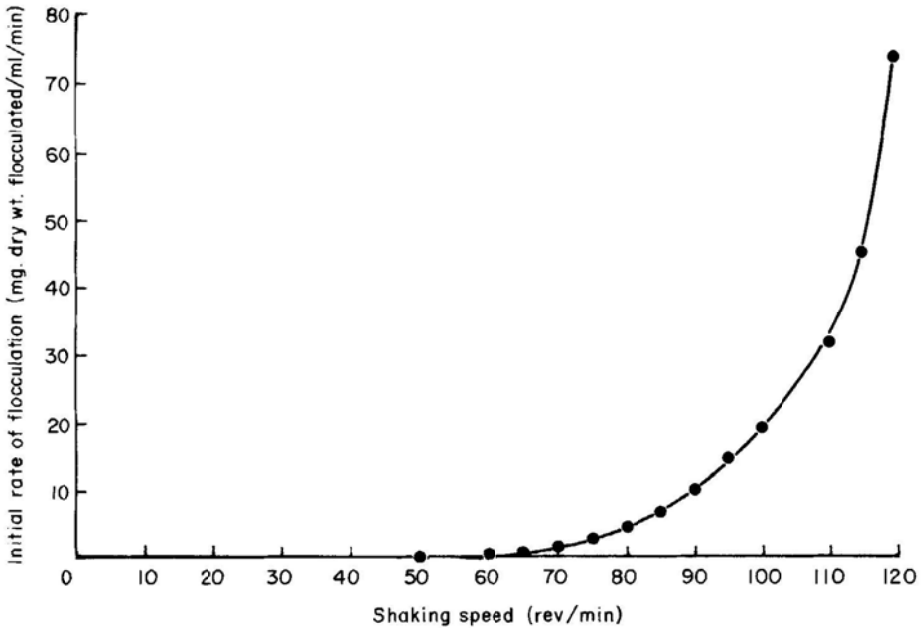

Figure 4.37: Effect of agitation speed on initial rate of flocculation of *Saccharomyces cerevisiae* S646-1B (from Stratford and Wilson, 1990).

An increase in agitation intensity should lead to a decrease in floc size with gentle agitation giving large flocs while vigorous agitation should give smaller, denser flocs that settle more slowly giving a more compact sediment (Domingues *et al*., 2000). However, this trend was not observed during the studies as there were no flocs observed at lower or higher agitation speeds. From Figure 4.37 it can be seen that flocculation is best observed between 65 and 115 rpm and this explains the absence of flocculation at agitation speeds of 50 rpm and below or 150 rpm and above.

4.2.2 pH

The second factor to investigate its effect on flocculation was pH. The pH for fermentation is in the range 3.80 – 5.60 (Ross and Harrison, 1970), but the study was conducted in the range of 1.30 – 6.50. The aim was to determine the optimum

pH which would give the best flocculation of brewers' yeast cells. The other conditions used during the study are in Table 4.11.

Table 4.11: Conditions used to investigate the effect of pH on the flocculation of brewers' yeast.

Parameter	**Agitation speed**	**pH**	**Temp**	**[CNTs]**	**[Ca^{2+}]**	**Presence of glucose**
Value	110 rpm	Variable	30 ^{o}C	54μg/ml	Nil	Nil

For the study on pH, there were two experiments conducted each time (a) the main experiment with 54μg/ml of CNTs added and (b) the control experiment without any CNTs.

(A) Acidic pH of 1.00 – 3.00

The study was conducted in the pH range 1.00 – 3.00. The pH was adjusted to 2.90 in (a) and 1.40 in (b). The experiments were stopped after 2 days as there was no flocculation observed. There were no flocs that were recovered using a centrifuge and the flocculation was ranked (-).

Table 4.12: Analysis of flocculation at pH 1.00 to 3.00, 110rpm, 30 ^{o}C and [CNTs] of 54μg/ml.

Experiment	**a**	**b**
Floc quality	-	-

At these low pH values the cells might have been denatured by the acidic environment and therefore no flocculation took place (Öztop *et al*., 2002). These

observations were in contradiction to some literature. Verstrepen *et al*., (2003) showed that flocculation can occur between pH 1.5 and 9.0, clearly indicating that pH is not the dominant factor causing flocculation but this does not mean that pH is not important.

(B) pH of 3.00 – 4.00

The studies were repeated at pH between 3.00 and 4.00. The pH for (a) was adjusted to 4.00 and for (b) it was adjusted to 3.70. The experiments were stopped after 2 days as there was no flocculation observed and no flocs were recovered by the centrifuge.

Table 4.13: Analysis of flocculation at pH 3.00 to 4.00, 110rpm, 30 ^{o}C and [CNTs] of 54μg/ml.

Experiment	**a**	**b**
Floc quality	-	-

The failure to observe flocculation in this pH range also contradicted literature which states that flocculation occurs in the range 3.50 – 5.80 (Jin and Speers, 2000; Jin *et al*., 2001; Mill, 1964; Soares *et al*., 1994; Stratford, 1992; Verstrepen *et al*., 2003).

(C) pH of 4.60

The studies were repeated at pH 4.60 for both (a) and (b). Flocculation was observed under these conditions (Figure 4.38) and the flocs were recovered and ranked according to procedures 1 and 2 in Section 3.2.12.

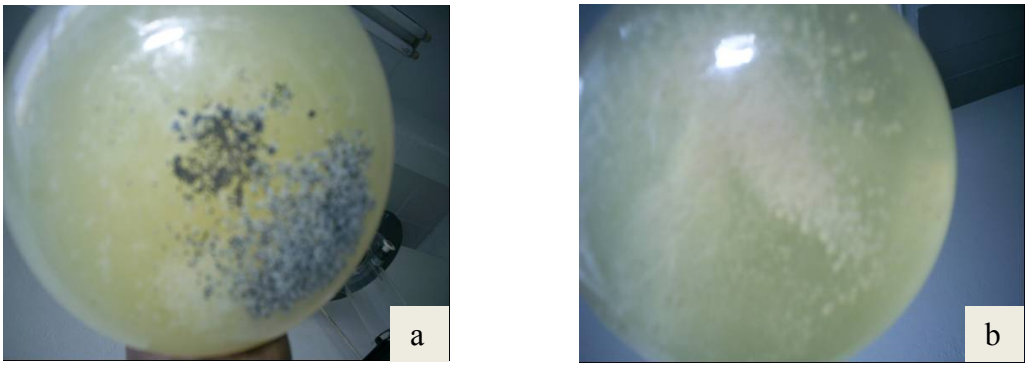

Figure 4.38: Digital photographs of yeast flocculation after 4 days at pH 4.60. (a) is the main experiment while (b) is the control experiment.

Table 4.14: Analysis of flocculation at pH 4.60, 110rpm, 30 ^{o}C and [CNTs] of 54μg/ml.

Experiment	**a**	**b**
Floc quality	+	+
Dry floc weight (g)	0.124±0.003	0.132±0.005

There was no significant difference in floc weight between the flocs in the presence of CNTs and in the absence of CNTs (0.007g). The flocculation quality was ranked (+). The zeta potential was observed during the 4 days and the data is presented in Figure 4.39 (see Appendix VII, Table 6 for the average data with standard deviation).

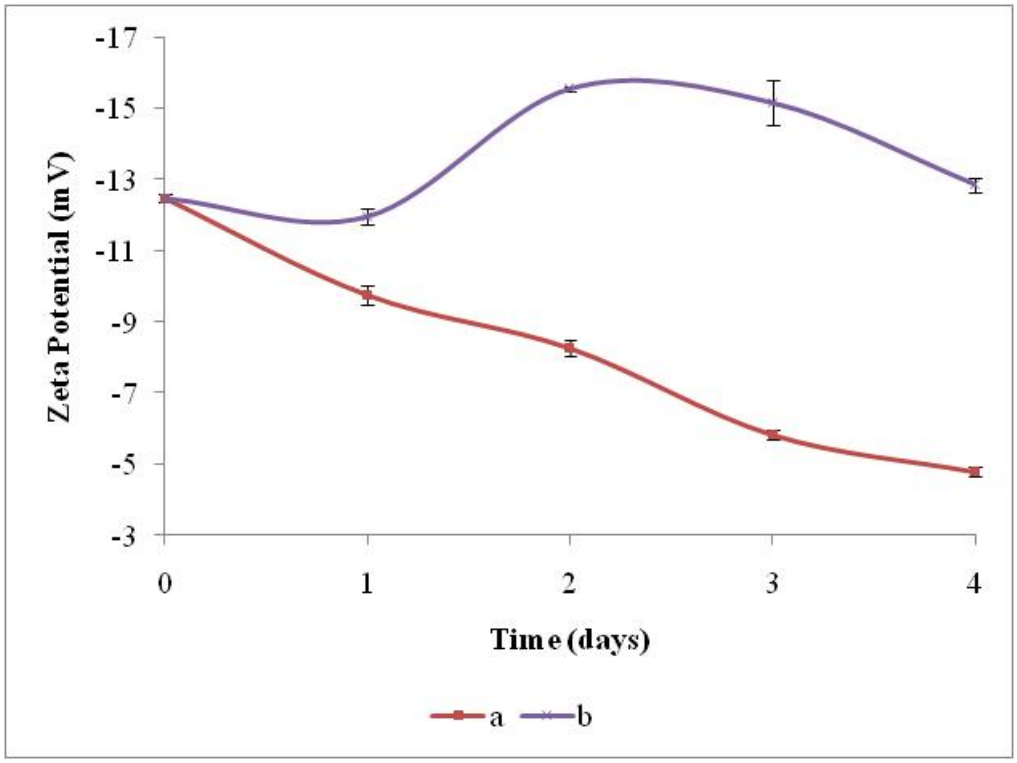

Figure 4.39: Change in zeta potential over time at pH 4.60, 110rpm, 30 ^{o}C and [CNTs] of 54μg/ml. The standard deviations for the graphs were 3.07 for a and 1.64 for b.

The final zeta potential for (a) was within the ±5 mV range while for (b) it was in the -15 to -10 mV range, the threshold of flocculation. There was flocculation observed in the two experiments but zeta potential for (b) was outside. Experiment (a) had a more negative zeta potential than experiment (b) and this may have been due to the presence of CNTs because all the other parameters were the same. This trend was opposite the one observed in the previous study for agitation speed at 110 rpm, pH 4.60, temperature of 30 ^{o}C and [CNTs] of 54μg/ml where the final zeta potential of the control experiment was more negative than that of the main experiment. The graphs for (a) and (b) were steadily becoming more negative with time moving towards the ±5 mV showing strong tendency towards flocculation especial (a). This may help to explain the observed

flocculation even though it was not the best. Statistical analysis was conducted to see if there was a significant difference between the zeta potential graphs for the study. The p value was 0.1253 which was considered not significant as variation among the graphs was not significantly greater than expected by chance.

(D) pH of 5.60

The studies were repeated at pH 5.60 for both (a) and (b). Better flocculation was observed at these conditions (Figure 4.40). Experiment (a) had higher floc weight than (b) showing the influence of CNTs. The flocs were recovered and ranked according to procedures 1 and 2 in Section 3.2.12.

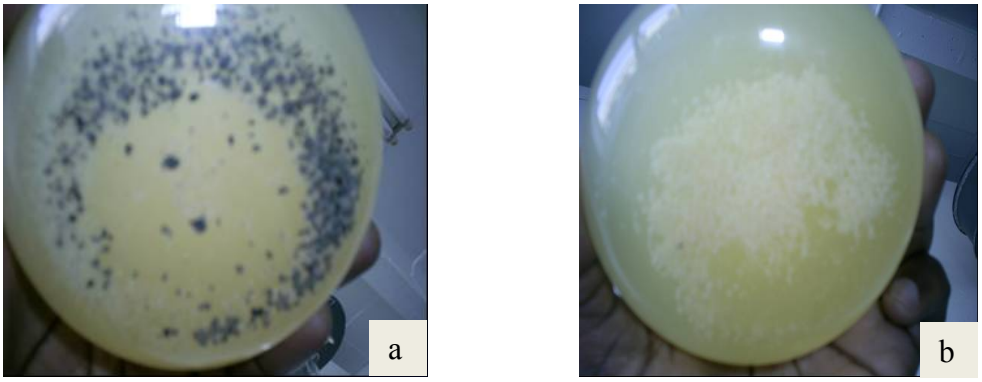

Figure 4.40: Digital photographs of yeast flocculation after 4 days at pH 5.60. (a) is the main experiment while (b) is the control experiment.

Table 4.15: Analysis of flocculation at pH 5.60, 110rpm, 30 ^{o}C and [CNTs] of 54μg/ml.

Experiment	**a**	**b**
Floc quality	+++	++
Dry floc weight (g)	0.143±0.007	0.123±0.005

The flocs observed were ranked as (++) for (b) and (+++) for (a). At pH 5.60, they were more flocs produced than at pH 4.60 a difference of +0.020 g for (a) and a difference of -0.007g for (b). These observations showed the significance of adding CNTs and increasing pH by one unit as these conditions increased the floc weight by +0.020g but there was a negligible change in floc weight from the control experiments. Zeta potential was measured for the 4 days and a plot is presented in Figure 4.41 (see Appendix VII, Table 7 for the average data with standard deviation).

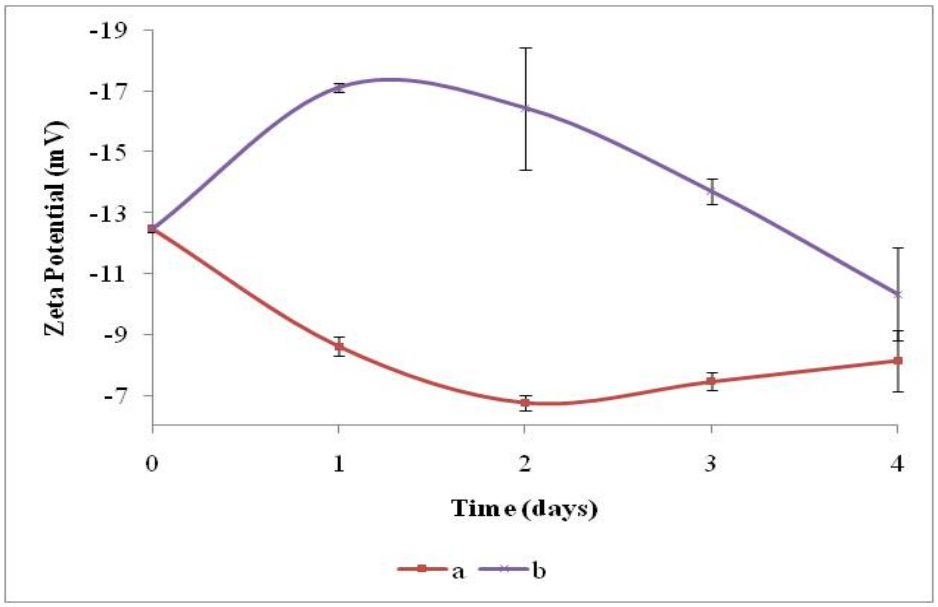

Figure 4.41: Change in zeta potential over time at pH 5.60, 110rpm, 30 ^{o}C and [CNTs] of 54µg/ml. The standard deviations for the graphs were 2.23 for a and 2.80 for b.

Figure 4.41 shows that the final zeta potential for (a) is more negative than that for (b) consistent with the results observed in the previous study for agitation speed at 110 rpm, pH 5.60, temperature of 30 ^{o}C and [CNTs] of 54µg/ml where the final zeta potential of the main experiment was more negative than that of the control experiment. The best flocculation was observed at the highest zeta potential of -

6.76±0.25 mV after 2 days in (a). This indicates the importance of the zeta potential in the analysis of flocculation onset. However, the final zeta potential for all experiments was outside the ±5 mV range but there was good flocculation showing the inconsistency observed at high agitation speeds. The graphs for (a) and (b) were steadily becoming more negative with time moving towards the ±5 mV showing strong tendency towards flocculation especial (b). Graph (b) took time to slope towards the ±5 mV region and this is shown by less flocculation weight observed. Statistical analysis was conducted to see if there was a significant difference between the zeta potential graphs for the study. The p value was 0.3338 which was considered not significant as variation among the graphs was not significantly greater than expected by chance.

(E) pH of 6.00

The studies were repeated at pH 6.00 for both (a) and (b). Flocculation quality was better at pH 6.00 than at pH 5.60 for experiments (a) and (b). The flocs were recovered and ranked (Figure 4.42).

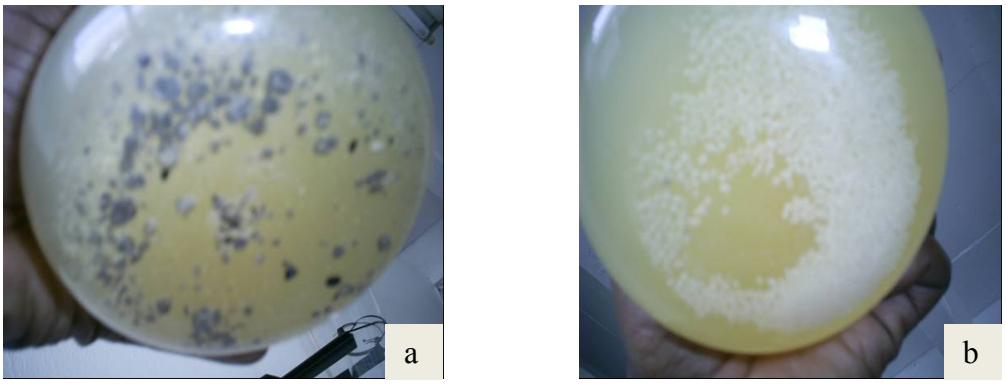

Figure 4.42: Digital photographs of yeast flocculation after 4 days at pH 6.00. (a) is the main experiment while (b) is the control experiment.

Table 4.16: Analysis of flocculation at pH 6.00, 110rpm, 30 ^{o}C and [CNTs] of 54μg/ml.

Experiment	**a**	**b**
Floc quality	++	+++
Dry floc weight (g)	0.136±0.001	0.146±0.004

The floc weight was higher for (b) than for (a), with a difference of 0.010g. There was a small change in the weight of flocs from 0.143±0.007 at pH 5.60 to 0.136±0.001 at pH 6.00, a difference of 0.007 g. However, the flocs produced were bigger at a pH of 6.00 than at 5.60. For the control experiments there was a big change in floc weight from 0.123±0.005 to 0.146±0.004 (a difference of -0.023 g) for pH of 5.60 and 6.00 respectively. The small change in floc weight for the main experiment showed the optimum pH required to get the best flocculation and this was consistent with the upper limit reported in literature of 5.80 (Jin and Speers, 2000; Jin *et al*., 2001; Mill, 1964; Soares *et al*., 1994; Stratford, 1992; Verstrepen *et al*., 2003).

Zeta potential was measured during the study and the plot is presented in Figure 4.43 below (see Appendix VII, Table 8 for the average data with standard deviation).

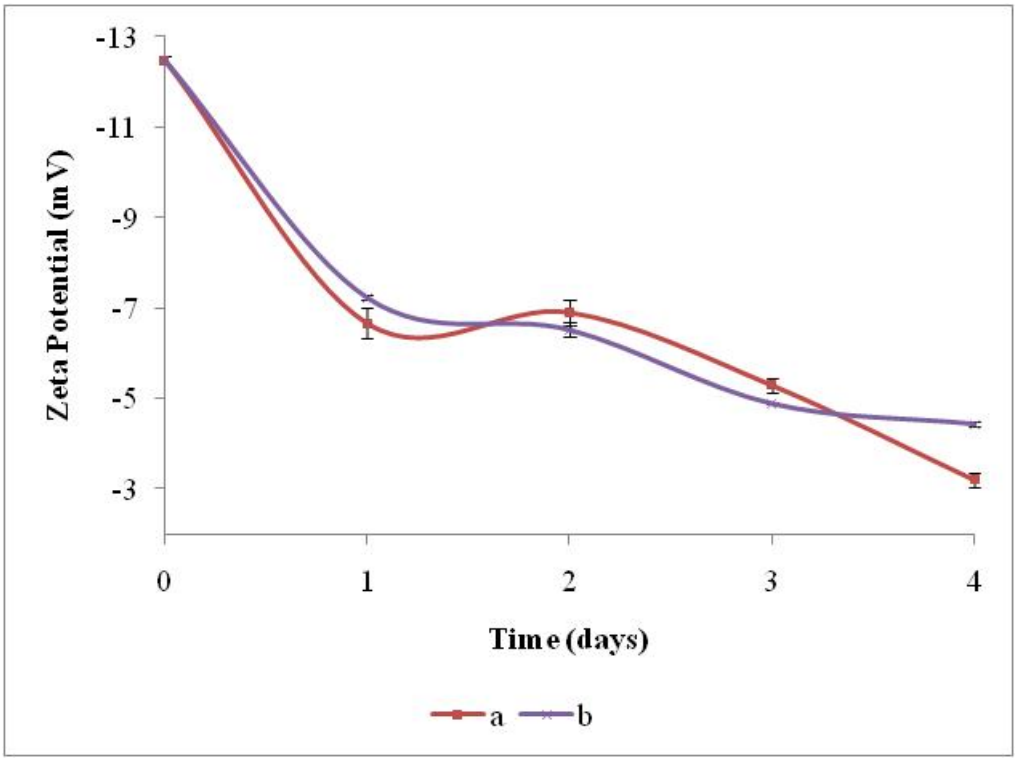

Figure 4.43: Change in zeta potential over time at pH 6.00, 110rpm, 30 ^{o}C and [CNTs] of 54μg/ml. The standard deviations for the graphs were 3.44 for a and 3.21 for b.

The zeta potential values were within the ±5 mV range showing strong tendency to flocculate. This was supported by the flocs observed which where biggest observed throughout the study so far. Figure 4.43 showed that the final zeta potential for (a) was more negative than that for (b) following the same trend observed in the previous study at pH 5.60. The zeta potential values for (a) and (b) at pH 6.00 were more negative than for (a) and (b) at pH 5.60 demonstrating the influence of pH increase on zeta potential. The graphs for (a) and (b) were becoming more negative with time moving towards the ±5 mV region showing strong tendency towards flocculation. This resulted in good flocculation observed especially for (b). Statistical analysis was conducted to see if there was a significant difference between the zeta potential graphs for the study. The p value

was 0.4484 which was considered not significant as variation among the graphs was not significantly greater than expected by chance.

(F) pH of 6.50

The studies were repeated at pH 6.50 for both (a) and (b) and there was a decrease in floc size and floc weight at these conditions. The flocs were recovered and ranked (Figure 4.44).

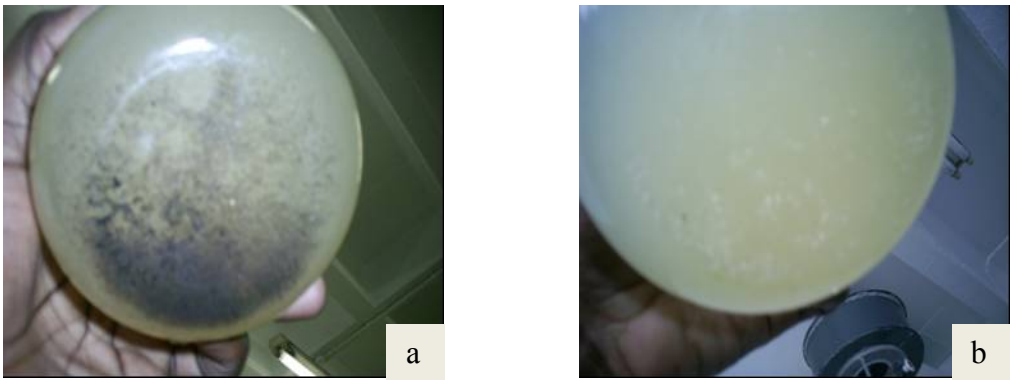

Figure 4.44: Digital photographs of yeast flocculation after 4 days at pH 6.50. (a) is the main experiment while (b) is the control experiment.

Table 4.17: Analysis of flocculation at pH 6.50, 110rpm, 30 ^{o}C and [CNTs] of 54μg/ml.

Experiment	**a**	**b**
Floc quality	+	+
Dry floc weight (g)	0.066±0.002	0.109±0.009

Better flocculation was observed in (b) than in (a), with a difference of 0.043 g. This showed the negative effect further increasing the pH on flocculation above 5.60. The floc weights were less than those observed at pH 6.00 and that helped to give the optimum pH required for flocculation. The zeta potential for the study

was followed up to day 4 and the data is presented below (Figure 4.45) (see Appendix VII, Table 9 for the average data with standard deviation).

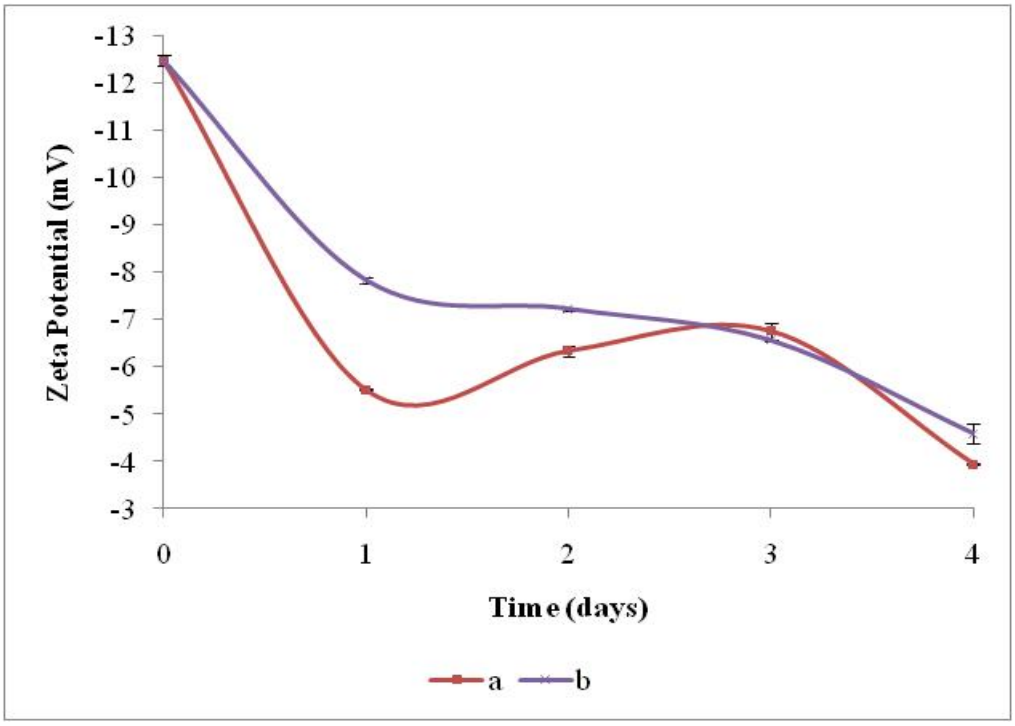

Figure 4.45: Change in zeta potential over time at pH 6.50, 110rpm, 30 ^{o}C and [CNTs] of 54µg/ml. The standard deviations for the graphs were 3.24 for a and 2.92 for b.

The final zeta potential was within the ±5 mV range showing a strong tendency to flocculate although poor flocculation was observed at the end of the study. The zeta potential for (a) was more negative than that for (b) but the floc weights were in reverse with (b) having the larger floc weight than (a). The graphs for (a) and (b) were becoming more negative with time moving towards the ±5 mV region showing strong tendency towards flocculation. The graphs slowed between 1 and 3 days and this may have led to the poor flocculation observed when compared to the results for pH 6.00. Statistical analysis was conducted to see if there was a significant difference between the zeta potential graphs for the study. The p value

was 0.4218 which was considered not significant as variation among the graphs was not significantly greater than expected by chance.

(G) Summary

All the data obtained was combined to see the relation unfolding as pH was increased whilst maintaining all other parameters. Two additional experiments at pH 6.25 and pH 6.65 were conducted, their floc weight measured and the results together with the previous data presented in Figure 4.46 (see Appendix VII, Table 10 for the average data with standard deviation).

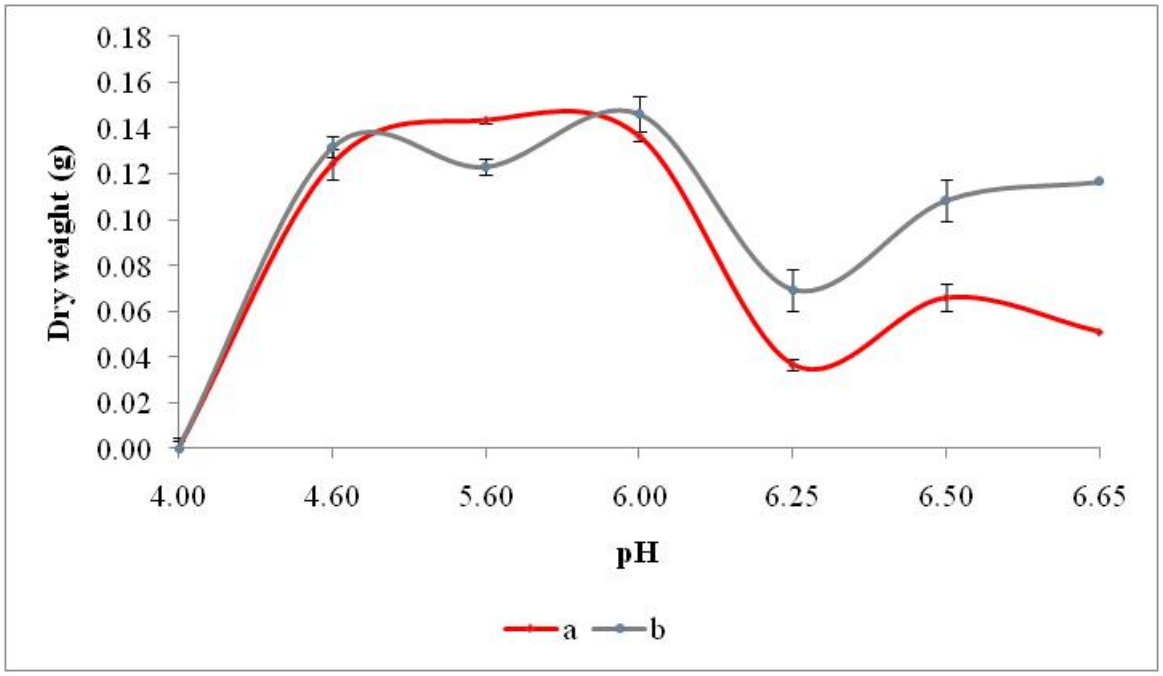

Figure 4.46: Effect of changing pH on flocculation at 110rpm, 30 ^{o}C and [CNTs] of 54µg/ml. The standard deviations for the graphs were 0.045 for a and 0.026 for b.

Statistical analysis was conducted to see if there was a significant difference between the immobilised and non-immobilised cells graphs as pH was increased. The p value was 0.1163 which was considered not significant as variation among

the graphs was not significantly greater than expected by chance. From Figure 4.46 it is observed that the optimum pH when using CNTs for yeast flocculation is between 5.00 and 5.80 as there is the highest floc weight as compared with the flocculation without using CNTs. The pH range obtained is within the brewing pH range of 3.80 – 5.60 as reported in literature (Jin and Speers, 1998; Jin and Speers, 2000; Jin *et al*., 2001; Ross and Harrison, 1970; Soares *et al*., 1994; Stratford, 1992). Yeast flocculation in the absence of CNTs was best in the pH range between 5.90 and 6.10. After pH 6.10 dry floc weight decreased rapidly up to pH 6.25 before increasing further again. The focus was mainly in the brewing pH as the application for the process was in the fermentation pH range.

Using CNTs to flocculate yeast cells had a negative effect beyond pH 5.80. This could be due to the fact that yeast cells reverse their charge above a pH of 5.60. In aqueous suspensions at the pH values of worts and beers (3.80–5.60), brewers' yeasts migrate to the anode in electrophoresis experiments, thus behaving as negatively charged colloids. At more acid pH values, reversal of the charge may take place (Ross and Harrison, 1970) and this may help to explain the decrease in flocculation weight below 4.60 and above 5.80 observed during the study. The fact that CNTs were able to flocculate yeast cells within the mentioned pH range showed that the CNTs are positively charged and these tends to repel the cells when the cells have a positive charge due to a change in pH. Yeast cells should flocculate anywhere between pH 2.00 and 8.00, depending on strains with optimum values between pH of 3.00 – 6.00. The study showed the same results with flocculation observed between 5.00 and 5.80. At low pH values (2.90 – 4.00) the cells might have been denatured and this resulted in poor flocculation of cells (Jin and Speers, 1998; Öztop *et al*., 2002).

4.2.3 Immobilisation Temperature

There is an apparent contradiction in the literature about the effect of temperature on flocculation, some authors noted deflocculation with increasing temperature while others noted an increase in flocculation with increasing temperature. This discrepancy maybe attributed to differences in the response of ale and lager strains (Speers *et al*., 1992). Jin *et al*. (Jin and Speers, 2000; Jin *et al*., 2001) found that flocculation of a lager yeast strain varied between 24.1 % at 5 ^{o}C to 66.8% at 25 ^{o}C showing an increase in flocculation as temperature was increased. However, there is little or no effect of temperature on flocculation of brewing yeast within the physiological temperature range of 15 – 32 ^{o}C (Jin and Speers, 1999).

Most brewing strains have an optimum temperature for growth between 30 and 34 ^{o}C (Briggs *et al*., 2004; Jin and Speers, 1999; Verstrepen *et al.*, 2003) with viability losses at 30 ^{o}C for 3 days during flocculation considered negligible (Zhao and Fleet, 2003). Yeast autolysis normally occurs at elevated temperatures of between 40 and 60 ^{o}C (Arnold, 1981; Hernawan and Fleet, 1995; Zhao and Fleet, 2003; Alexandre and Guilloux-Benatier, 2006). Studies were conducted at two different temperatures (25 and 30 ^{o}C) to investigate the effect of temperature on flocculation. The other conditions used during the study are in Table 4.18.

Table 4.18: Conditions used to investigate the effect of temperature on the flocculation of brewers' yeast.

Parameter	**Agitation speed**	**pH**	**Temp**	**[CNTs]**	**[Ca^{2+}]**	**Presence of glucose**
Value	110 rpm	5.60	Variable	54μg/ml	Nil	Nil

(A) 25 ^{o}C

The first temperature to be investigated was 25 ^{o}C. Flocs were recovered and ranked (Figure 4.47) after 4 days with the floc weight and floc quality are shown in Table 4.19.

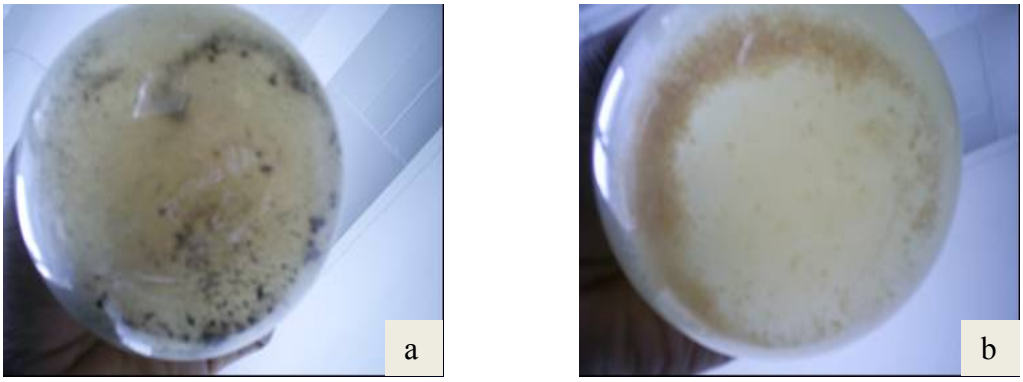

Figure 4.47: Digital photographs of yeast flocculation after 4 days at 25 ^{o}C. (a) is the main experiment while (b) is the control experiment.

Table 4.19: Analysis of flocculation at 25 ^{o}C, 110 rpm, pH 5.60 and [CNTs] of 54μg/ml.

Experiment	**a**	**b**
Floc quality	+	+
Dry floc weight (g)	0.043±0.013	0.124±0.010

The flocculation quality was ranked (+), but there was better flocculation from (b) than from (a) when considering the weight of the measured flocs. These observations means that CNTs have a negative effect on flocculation as the temperature is lowered. At lower temperatures there is less gain in using CNTs to increase flocculation as the natural process is faster. Zeta potential was measured as the study was being conducted and the data is presented below (Figure 4.48) (see Appendix VII, Table 11 for the average data with standard deviation).

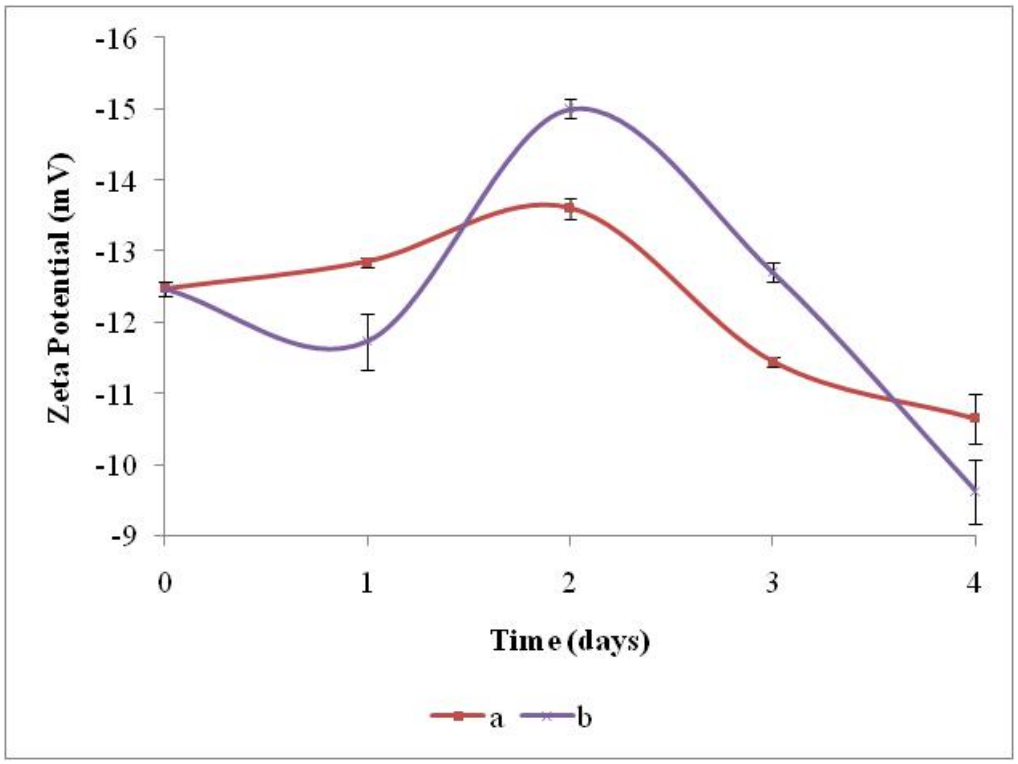

Figure 4.48: Change in zeta potential over time at 25 ^{o}C, 110 rpm, pH 5.60 and [CNTs] of 54μg/ml. The standard deviations for the graphs were 3.08 for a and 1.64 for b.

Figure 4.48 shows that the final zeta potential for the sample with CNTs was less negative than that without CNTs. Zeta potential values for the experiments were outside the ±5 mV range, but operating in the threshold of flocculation range. The graphs for (a) and (b) were steadily becoming more negative after 2 days moving towards the ±5 mV region showing strong tendency towards flocculation. This delay may have led to the reduced flocculation observed. Graph (b) sloped more and there was better flocculation weight observed. Statistical analysis was conducted to see if there was a significant difference between the zeta potential graphs for the study. The p value was 0.1742 which was considered not significant as variation among the graphs was not significantly greater than expected by chance.

(B) 30 ^{o}C

The study was conducted at an elevated temperature of 30 ^{o}C. An increase in flocculation and floc size were observed when compared with the results at 25 ^{o}C. The flocs were recovered and ranked (Figure 4.49) after 4 days.

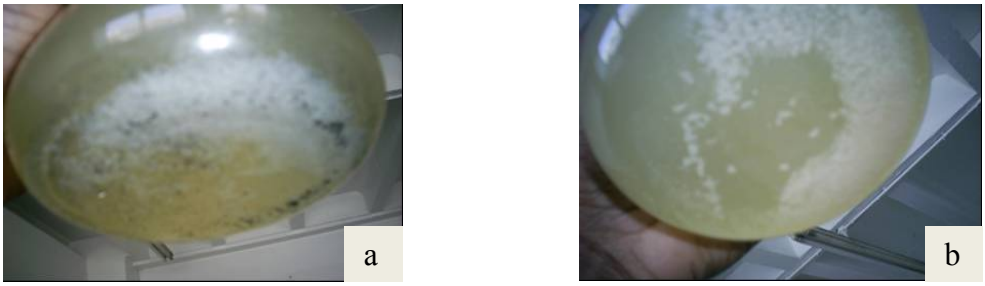

Figure 4.49: Digital photographs of yeast flocculation after 4 days at 30 ^{o}C. (a) is the main experiment while (b) is the control experiment.

Table 4.20: Analysis of flocculation at 30 ^{o}C, 110 rpm, pH 5.60 and [CNTs] of 54μg/ml.

Experiment	**a**	**b**
Floc quality	++	++
Dry floc weight (g)	0.143±0.007	0.123±0.005

Floc size at 30 ^{o}C was better than at 25 ^{o}C and ranked as (++). There was better flocculation from (a) than (b) with a weight difference of +0.013 g. These results were opposite those observed at 25 ^{o}C and this emphasised the effect of temperature change on the flocculation process with and without CNTs in the broth. Zeta potential was monitored and the data is presented in Figure 4.50 (see Appendix VII, Table 12 for the average data with standard deviation).

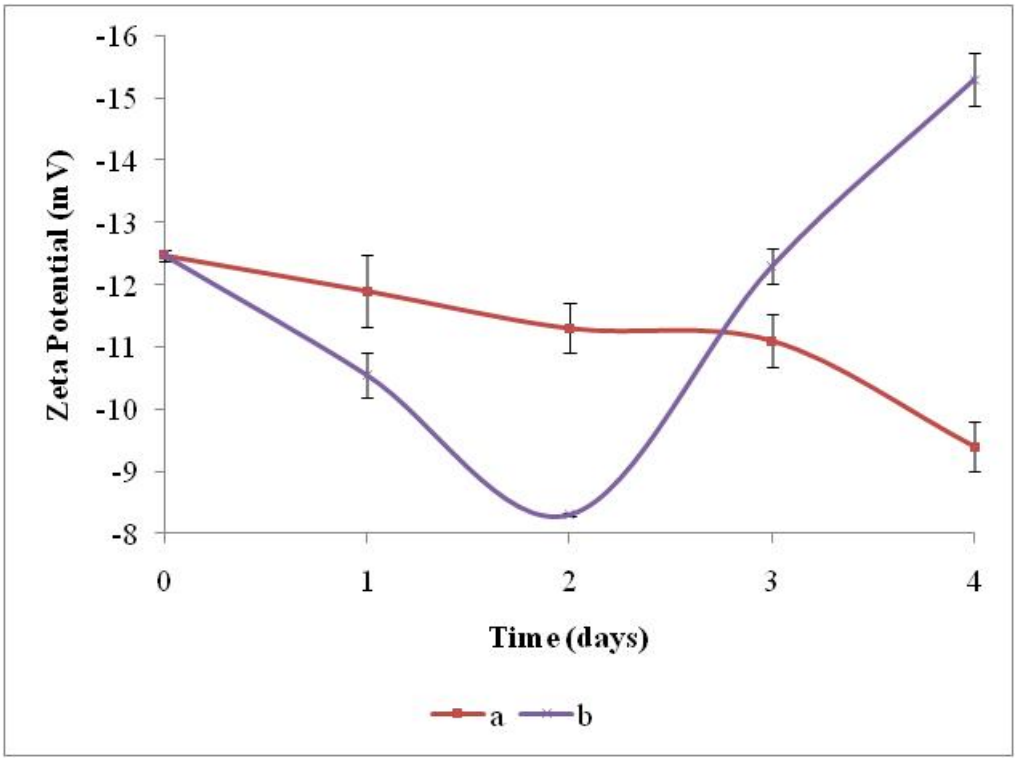

Figure 4.50: Change in zeta potential over time at 30 ^{o}C, 110 rpm, pH 5.60 and [CNTs] of 54μg/ml. The standard deviations for the graphs were 1.16 for a and 2.58 for b.

Figure 4.50 shows that the zeta potential for (a) was more negative (-9.40±0.40 mV) than for (b) which was -15.30±0.42 mV. Zeta potential values for the experiments were outside the ±5 mV range, but operating in the threshold of flocculation range for (a) and threshold of light dispersion for (b) even though there was good flocculation observed from the study. The graph for (a) was steadily becoming more negative moving towards the ±5 mV region showing strong tendency towards flocculation but (b) was moving away from the ±5 mV region. This may have led to the reduced flocculation observed for (b) and a higher floc weight for (a). Statistical analysis was conducted to see if there was a significant difference between the zeta potential graphs for the study. The p value

was 0.0745 which was considered not quite significant as variation among the graphs was not significantly greater than expected by chance.

(C) Summary

The change in temperature was analysed to determine its effect on flocculation and the data is presented in Table 4.21.

Table 4.21: Analysis of flocculation at 25 and 30 ^{o}C.

Temperature ^{o}C	**a (immobilised cells)**		**b (free cells)**	
	Floc quality	**Floc weight (g)**	**Floc quality**	**Floc weight (g)**
25	+	0.043±0.013	+	0.124±0.010
30	++	0.143±0.007	++	0.123±0.005

From the two temperatures investigated, the ideal temperature should be close to 30 ^{o}C to get the best results when using CNTs to aid in flocculation; 0.143±0.007g at 30 ^{o}C against 0.043±0.013 g at 25 ^{o}C with a difference of 0.100 g. In the absence of flocculation (b), flocculation rates are almost the same 0.124±0.010g at 25 ^{o}C against 0.123±0.005 g at 30 ^{o}C a difference of 0.001g. Öztop *et al*., (2002) found the optimum temperature for immobilisation to be 25 ^{o}C when they immobilised yeast cells on a chitosan film (Figure 4.51).

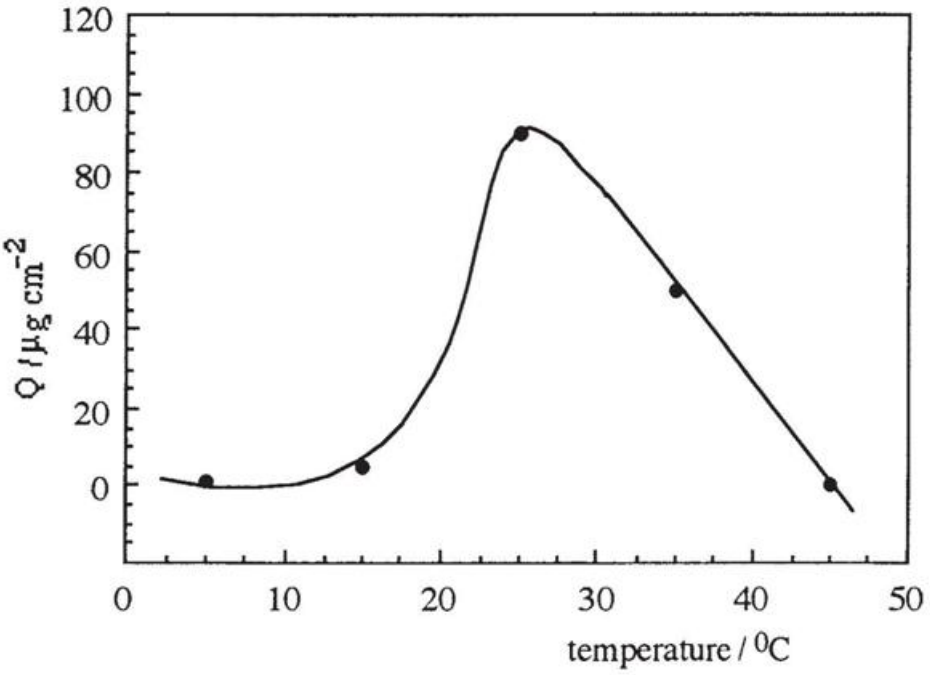

Figure 4.51: Effect of temperature on immobilisation (from Öztop *et al*., 2002).

Hsu *et al*. (2001) observed an increase in flocculation with an increase in temperature from 5 – 45 ^{o}C. This was in line with the observations in the study showing an increase in flocculation with an increase in temperature. Jin *et al*. (Jin and Speers, 2000; Jin *et al*., 2001) found that flocculation of a lager yeast strain varied between 24.1 % at 5 ^{o}C to 66.8% at 25 ^{o}C further supporting the observations of this study.

4.2.4 Effect of Concentration of Carbon Nanotubes on Flocculation

The fourth factor to analyse its effect on flocculation of brewers' yeast was concentration of CNTs. The concentration was varied from 0 – 72 µg/ml. Ghafari, *et al* (2008) investigated bacteria ciliated protozoa and used concentrations

between 0 – 17.2 μg/ml. The other conditions used during the study are presented in Table 4.22.

Table 4.22: Conditions used to investigate the effect of concentration of CNTs on the flocculation of brewers' yeast.

Parameter	**Agitation speed**	**pH**	**Temp**	**[CNTs]**	**[Ca^{2+}]**	**Presence of glucose**
Value	110 rpm	5.60	30 ^{o}C	Variable	Nil	Nil

Six different experiments were setup to assess their effect on flocculation. The flocs were recovered and ranked after 4 days (Figure 4.52). The data is presented below.

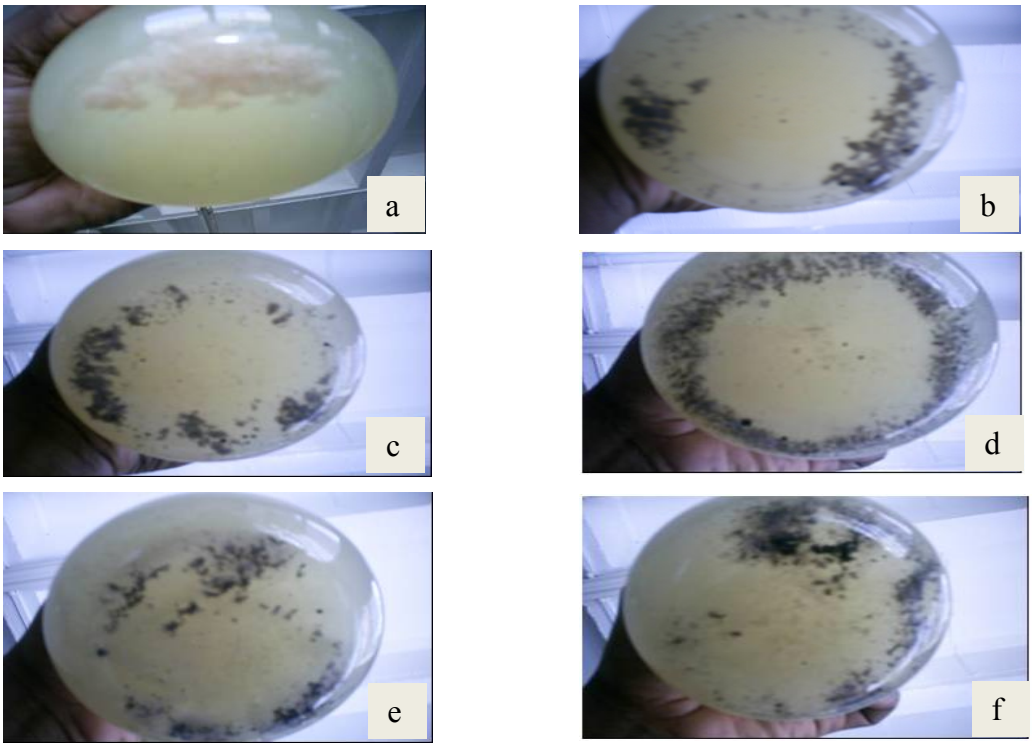

Figure 4.52: Digital photographs of yeast flocculation after 4 days at different CNT concentrations.

Table 4.23: Qualitative analysis of flocculation at different concentrations of CNTs, 110 rpm, pH 5.60 and 30 ^{o}C.

Experiment	**a**	**b**	**c**	**d**	**e**	**f**
CNT concentration (μg/ml)	0.00	17.86	26.79	35.71	44.64	53.57
Floc quality	+	++	++	++	+++	+++

Additional experiments were carried out at CNTs concentrations of 62.50 and 71.43 μg/ml to investigate the optimum CNTs flocculation and the data is presented in Table 4.24.

Table 4.24: Analysis of flocculation at 62.50 and 71.43 μg/ml, 110 rpm, pH 5.60 and 30 ^{o}C.

Experiment	**g**	**h**
CNT conc. (μg/ml)	62.50	71.83
Floc quality	+++	++

A table of floc weight observed was plotted against CNT concentration and it is presented below (Figure 4.53) (see Appendix VII, Table 13 for the average data with standard deviation).

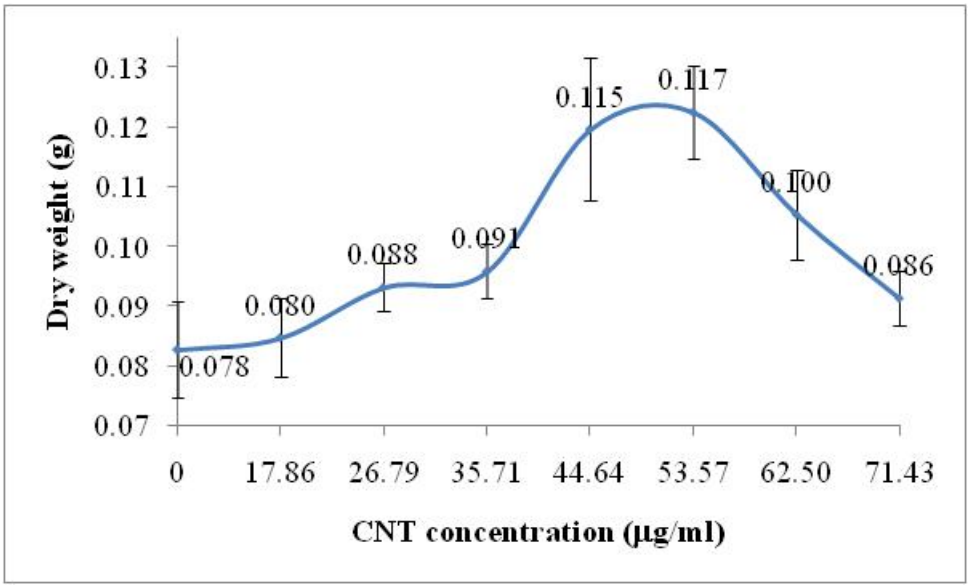

Figure 4.53: Effect of CNTs concentration on brewers' yeast flocculation (quantitative) at 110 rpm, pH 5.60 and 30 ^{o}C. The standard deviation for the graph was 0.015.

There was a general increase in floc weight with an increase in CNT concentration and the graph peaked at 53.57 µg/ml. Additional CNTs to increase their concentration above 53.57 µg/ml had negative effects on flocculation as the floc weight observed started to decrease. From 0 to 35.71 µg/ml there was a negligible gain in floc weight observed, +0.013g gained. Increasing the CNT concentration to 53.57 µg/ml gave a gain of +0.040 g as compared without using CNTs.

Zeta potential was monitored during the study and the data is presented in Figure 4.54 below (see Appendix VII, Table 14 for the average data with standard deviation).

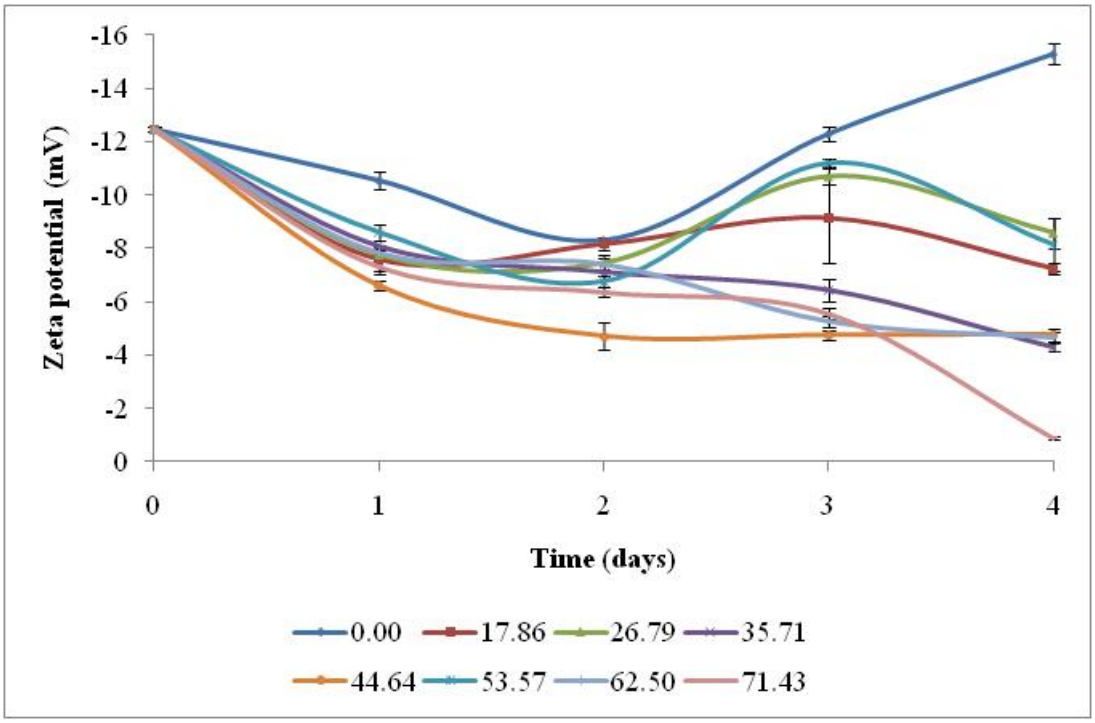

Figure 4.54: Change in zeta potential over time as a function of CNT concentrations, 110 rpm, pH 5.60 and 30 ^{o}C. The standard deviations for the graphs were 2.58 for a, 2.11 for b, 2.14 for c, 3.02 for d, 3.35 for e, 2.34 for f, 3.07 for g and 4.14 for h.

Most of the final zeta potential values were in the strong flocculation and threshold to flocculation range except zeta potential observed for the study at 0µg/ml which was in the threshold to light dispersion. The graph for 0 µg/ml was sloping away from the ±5 mV region and this may help to explain the reason there was the least flocculation observed.

Studies were also conducted with CNTs in the form of bulky paper or sheet-like form resulting in poor flocculation compared to CNTs in powder form. There were no flocs which were recovered. The photographs for studies at 4.60 and 5.60 with sheet-like CNTs are presented below. These results showed the importance

of surface area to volume ratio of CNTs when used for aiding flocculation of yeast cells (Figure 4.55).

Figure 4.55: Digital photographs of yeast flocculation after 4 days using sheet-like CNTs. (a) is at pH 4.60 and (b) is at pH 5.60.

4.2.5 Calcium Ion Concentration

The fifth factor that was analysed to see its effect on flocculation of brewers' yeast was concentration of calcium ions. Calcium ions are important in yeast cell flocculation (Section 2.3.4) and as such their effect on flocculation were studied (Jin and Speers, 1999; Mill, 1964; Taylor and Orton, 1973). Calcium ion concentration was varied from 0 – 9.55 mM and introduced into the broth as anhydrous calcium chloride ($CaCl_2 \bullet 2H_2O$). The flocs observed in the presence of calcium ions were powdery in nature. The other conditions used during the study are in Table 4.25.

Table 4.25: Conditions used to investigate the effect of concentration of calcium ions on the flocculation of brewers' yeast.

Parameter	**Agitation speed**	**pH**	**Temp**	**[CNTs]**	**[Ca^{2+}]**	**Presence of glucose**
Value	110rpm	5.60	30 ^{o}C	54 μg/ml	Variable	Nil

The calcium chloride weight was varied in steps of 0.05 grams to yield 7 experiments (a – h). Studies were done at these 7 conditions and the results are presented in Table 4.26 and Figure 4.56 (see Appendix VII, Table 15 for the average data with standard deviation).

Table 4.26: Effect of calcium ion concentration on flocculation at 110 rpm, pH 5.60, 30 ^{o}C and [CNTs] of 54 µg/ml.

Flask	**a**	**b**	**c**	**d**	**e**	**f**	**g**	**h**
Ca^{2+} ions conc. (mM)	0.00	1.62	2.93	4.11	5.49	6.85	8.25	9.55
Flocculation quality	+	+	+	++	+++	+	+	+++

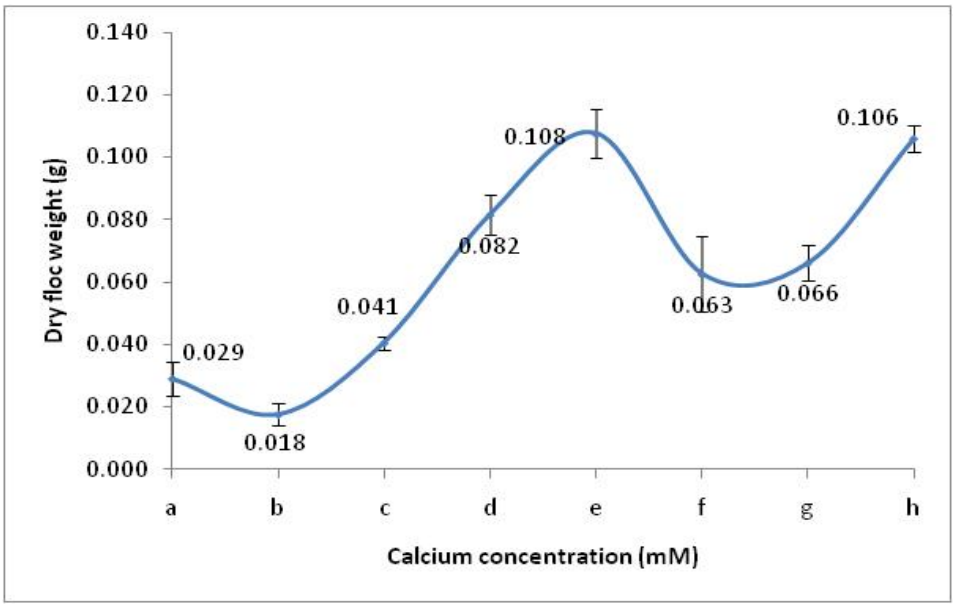

Figure 4.56: Effect of Ca^{2+} ions on brewers' yeast flocculation at 110 rpm, pH 5.60, 30 ^{o}C and [CNTs] of 54 µg/ml. The standard deviation for the graph was 0.033.

The best flocculation quality was observed in (d), (e) and (h) but when considering floc weight it was observed in (e) and (h). Figure 4.56 showed that 5.49 mM of Ca^{2+} ions (experiment e) gave the optimum conditions for flocculation when considering floc weight. Increasing the concentration to 9.55 mM yielded almost the same floc weight as at 5.49 mM. This data enables the optimisation of the concentration of calcium ions required. The presence of Ca^{2+} ions reduced flocculation than results obtained in the absence of the Ca^{2+} ions. Zeta potential data was measured during the study and the results are presented below (see Appendix VII, Table 16 for the average data with standard deviation).

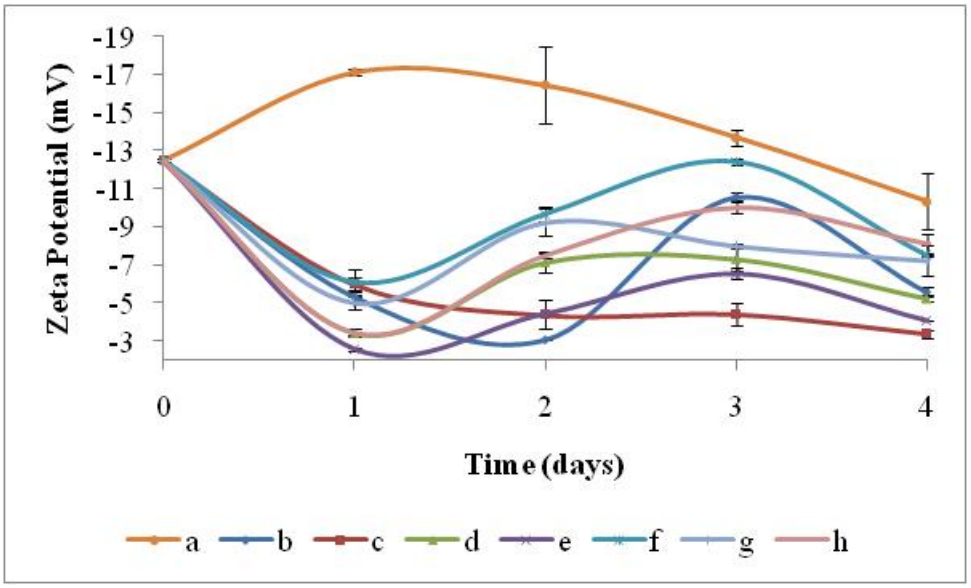

Figure 4.57: Change in zeta potential over time as a function of calcium ion concentration, 110 rpm, pH 5.60, 30 ^{o}C and [CNTs] of 54 µg/ml. The standard deviations for the graphs were 2.80 for a, 3.95 for b, 3.67 for c, 3.39 for d, 3.88 for e, 2.86 for f, 2.76 for g and 3.35 for h.

Final zeta potential for (b), (c), (d) and (e) were in the ±5 mV range for strong flocculation while those for (a), (f), (g) and (h) were in the threshold to flocculation range. Experiment (a) had the least final zeta potential after the 4

days and that may have resulted in the least floc weight observed. Experiment (e) had the second most negative potential followed by (d) with (h) having the least potential.

In the study it was observed that Ca^{2+} ions had a negative effect on flocculation in the presence of CNTs. This may be due to the repulsive forces between the Ca^{2+} ions and the positively charged CNTs existing in the same broth solution. Since flocculation was observed the results are in agreement with literature (Jin and Speers, 1999; Mill, 1964). Taylor and Orton (1973) concluded that the presence of calcium ions is required at a very low concentration in order to induce flocculation. For low salt concentrations (cations other than Ca^{2+} ions e.g. Mg^{2+}, Mn^{2+}), there was an observed flocculation enhancement, while at high concentrations inhibition of flocculation by the salt is observed (Domingues *et al*., 2000) which might have been the case during the study.

4.2.6 Presence of Glucose

The effect of glucose on flocculation of brewer's yeast cells was the last parameter to be investigated. Generally it was found that maltose and mannose were the most effective inhibitors of flocculation whereas sucrose and glucose were less effective (Jin and Speers, 1999). The study was aimed at observing the effect of the presence of glucose on the flocculation process. The other conditions used during the study are in Table 4.27.

Table 4.27: Conditions used to investigate the effect of glucose on the flocculation of brewers' yeast cells.

Parameter	Agitation speed	pH	Temp	[CNTs]	[Ca^{2+}]	Presence of glucose
Value	110 rpm	5.60	30 ^{o}C	54 µg/ml	5.49 mM	Variable

The presence of glucose promoted yeast cell growth and delayed the stationary phase for yeast cells thereby delaying the onset of flocculation. Ethanol was produced from the effect of yeast cells on glucose which decreases the pH of the broth resulting in the delay of flocculation. Studies were conducted to investigate the effect of glucose on flocculation using the optimised parameters. Glucose added is usually between 3 and 5 times the yeast extract weight according to literature (Dengis *et al*., 1995; Mallouchos *et al*., 2002; Nahvi *et al*., 2002; Öztop *et al*., 2003) and the glucose concentration used was 18 mg/ml. The results for the study were plotted as pH and zeta potential against time (Figure 4.58) (see Appendix VII, Table 17 for the average data with standard deviation).

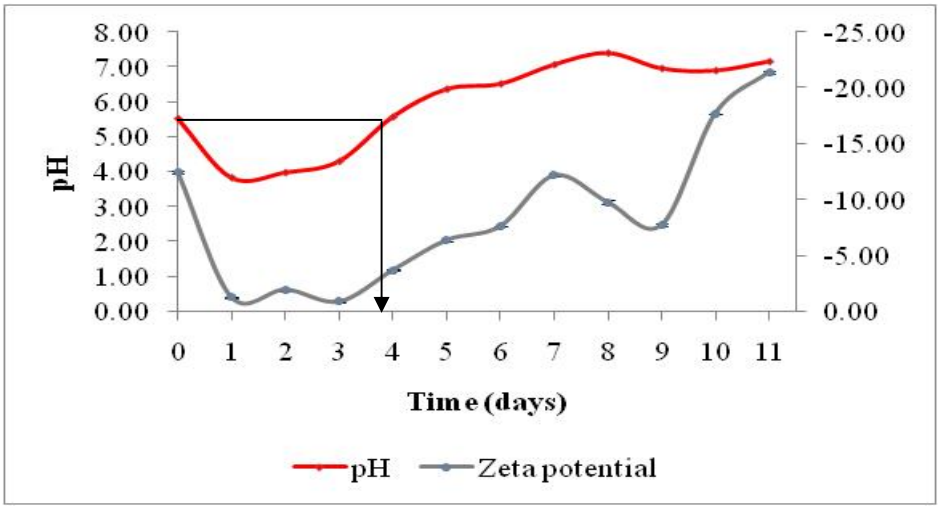

Figure 4.58: Effect of the presence of glucose on pH and zeta potential at 110 rpm, pH 5.60, 30 ^{o}C and [CNTs] of 54 µg/ml. The standard deviations for the graphs were 1.30 for pH and 6.50 for zeta potential.

The results showed a decrease in pH from 5.53 to 3.84 within a day and a progressive increase thereafter. pH 5.60 was reached after 3.95 days (~ 4 days) where flocculation onset was assumed to start and this showed a delay of 4 days for yeast cell flocculation to begin. Flocculation was observed after about 8 days.

The study was repeated with the inclusion of 5.49 mM calcium ion concentration to observe their effect on the zeta potential and the flocculation process (Figure 4.59) (see Appendix VII, Table 18 for the average data with standard deviation).

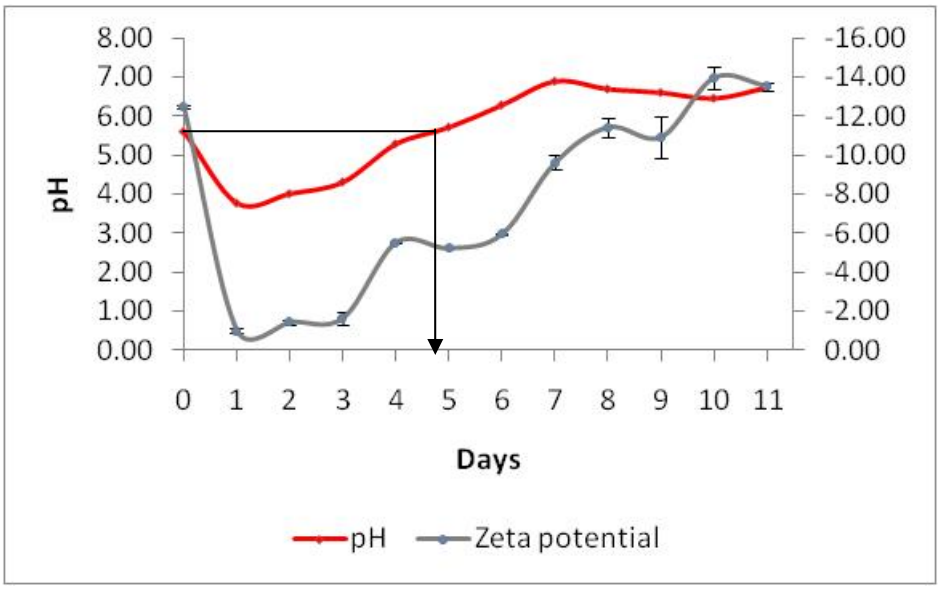

Figure 4.59: Effect of the presence of glucose and calcium ions on pH and zeta potential at 110 rpm, pH 5.60, 30 ^{o}C, [CNTs] of 54 µg/ml and [Ca^{2+}] of 5.49mM. The standard deviations for the graphs were 1.13 for pH and 4.86 for zeta potential.

Figure 4.59 showed that there was a decrease in pH from 5.59 to 3.76 within a day and a progressive increase. pH 5.60 was reached after 4.90 days (~ 5 days)

showing a delay of 5 days for flocculation to be observed. Flocculation was observed after about 5 days.

These results were in agreement with literature which states that glucose inhibits flocculation (Domingues *et al*., 2000; Jin and Speers, 1999; Verbelen *et al*., 2006). Several authors have indeed found that flocculation is triggered by carbon and/or nitrogen starvation and that addition of these compounds to the growth medium delays flocculation (Soares *et al.*, 1994; Soares and Mota, 1996; Stratford, 1992).

4.3 Theory of Yeast Cell Flocculation and Immobilisation on Carbon Nanotubes

Even though flocculation has been studied for many years; the complex interactions on how brewing yeast cells flocculate are still poorly understood and remain controversial. To date, three mechanisms have been suggested to explain yeast flocculation: the colloidal, Ca^{2+} bridge and zymolectin model theory. Currently, the zymolectin model theory is widely accepted to explain yeast flocculation (Strauss *et al*., 2007).

The observed results that CNTs increased the rate of flocculation of yeast cells could be explained by the Bridging Mechanism Theory (Section 2.3.8.1). Carbon nanotubes could be considered to be long chain particles which have large surface spikes and these would enable neutralisation of surface charge of brewers' yeast when there is contact made between the cells and the nanotubes. This would allow the cells to adsorb onto the tubes such that an individual chain can become attached to 2 or more cells thus "bridging" them together. Spike structures accumulate tip-charge, but the energy required to push a spike tip through a repulsion field would be considerably less than that for cell-cell wall contact. The

spike may contain a positive tip charge to most easily penetrate the negative charge repulsion of the yeast cells (Firon *et al*., 1982). This mechanism is depicted in Figure 4.60. Also the presence of CNTs seemed to have increased the water contact angle leading to an increase in CSH which in turn initiated flocculation. It was demonstrated that a relation existed between cell division arrest, the increase of Cell Surface Hydrophobicity (CSH) and initiation of flocculence during fermentation (Smit *et al*., 1992; Straver *et al*., 1993). A high level of CSH may facilitate cell-cell contact in an aqueous medium resulting in more specific lectin-carbohydrate interactions (Straver and Kijne, 1996).

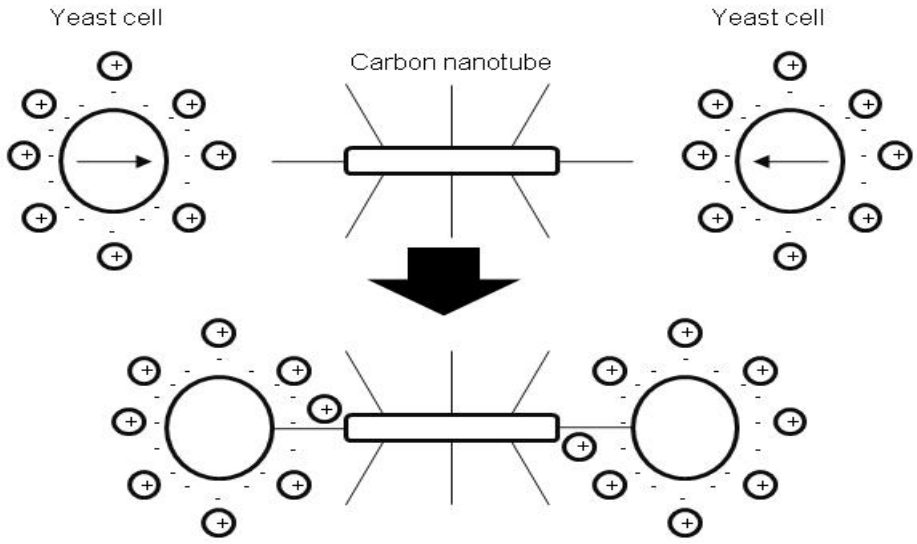

Figure 4.60: Theory of yeast cell immobilisation onto CNTs.

4.4 Fermentation Studies

The immobilised cells synthesised in the previous section were assessed for their fermentation capabilities. Two fermentation studies were conducted at 15 ^{o}C (Bekatorou *et al*., 2001b; Inconomopoulou *et al.,* 2000; Kopsahelis *et al*., 2006; Plessas *et al.*, 2005) and 30 ^{o}C (Batistote *et al*., 2006; Bekatorou *et al*., 2002; Bekers *et al*., 1999; Inconomopoulou *et al.,* 2000; Plessas *et al.*, 2005; Speers *et al*., 2006) with the ethanol content compared with those in literature. The

experiments were stopped after 9 days for the study at 15 ^{o}C and 3.5 days for the study conducted at 30 ^{o}C. The Original Gravity and Final Gravity were measured and reported in literature.

Bekatorou *et al*. (2001b) conducted their fermentation studies on hopped, filtered and sterilised wort at 15 ^{o}C for 5.7 days using a freeze dried *S. cerevisiae* strain immobilised on gluten pellets. Inconomopoulou *et al.* (2000) conducted their fermentation studies on glucose at 15 ^{o}C for 4.3 days using a freeze dried baker's yeast on DC material. Kopsahelis *et al*. (2006) conducted their fermentation studies on pausterised wort at 15 ^{o}C for at least 1 day using an *S. cerevisiae* strain immobilised on brewer's spent grains. Plessas *et al.* (2005) conducted their fermentation studies on glucose at 15 ^{o}C for at least 1 day using an *S. cerevisiae* strain immobilised in a starch-gluten-milk matrix usable for food.

Batistote *et al*. (2006) conducted their fermentation studies on maltose or glucose at 30 ^{o}C for 2.5 days using 4 yeast strains; brewers' ale strain LBCC A3 and lager strain LBCC L52 and wine strains VIN7 and VIN13 as free cells. Bekatorou *et al*. (2002) conducted their fermentation studies on glucose at 30 ^{o}C for at most 2.5 days using an *S. cerevisiae* strain immobilised on dried figs. Bekers *et al*. (1999) conducted their fermentation studies on a mentioned medium at 30 ^{o}C for 2 days using an *S. cerevisiae* strain immobilised on modified stainless steel wire. Inconomopoulou *et al.* (2000) conducted their fermentation studies on glucose at 30 ^{o}C for 3.5 days using a freeze dried baker's yeast on DC material. Plessas *et al.* (2005) conducted their fermentation studies on glucose at 30 ^{o}C for at most 2.5 days using an *S. cerevisiae* strain immobilised in a starch-gluten-milk matrix usable for food. Speers *et al*. (2006) conducted their fermentation studies on industrial wort at 30 ^{o}C between 72 and 120 hours using an ale brewing yeast strain.

For each study, 2 experiments were conducted; one with the immobilised cells and the other with free cells. Experiments were done at twice with the mean and standard deviation included in the results. Results for the pH, residual sugar and ethanol content were presented in tabular form as mean±standard deviation or as a graph showing standard deviation bars. The free amino nitrogen or the esters were not measured in these studies. The two sugars analysed during the study were maltose and glucose and these were both broken down to ethanol and carbon dioxide according to the following balanced stoichiometric equations.

Maltose

$$C_{12}H_{22}O_{11} + H_2O \rightarrow 4C_2H_5OH + 4CO_2 \qquad \text{Equation 4.1}$$

Glucose

$$C_6H_{12}O_6 \rightarrow 2C_2H_5OH + 2CO_2 \qquad \text{Equation 4.2}$$

Not all the parameters were analysed as they are during beer brewing, only three parameters considered key in the study were measured which were (a) pH of the broth (b) the sugar content (glucose and maltose), and (c) alcohol content. The studies were conducted for 9 days before being stopped and the final gravity was measured.

An increase in fermentation temperature reduces the time taken to attenuate the wort (Figure 2.13). Fermentation rates will increase with temperature by increasing the rate of yeast metabolism giving higher specific fermentation rates (Priest and Stewart, 2006). From this analysis the fermentation studies were conducted at the two different temperatures to see if there is an increase in ethanol

content as temperature is varied. The parameters which were analysed during the study are presented below in more detail.

4.4.1 Reversible Nature of Flocculation

When the immobilised cells and free cells were re-suspended in a nutrient-rich medium (malt extract), the cells deflocculated. This trend was observed both at 15 and 30 ^{o}C. Flocculation was observed at the end of fermentation with the observed flocs growing along the lengths of the CNTs. Flocs started to be observed after 6 days for the study conducted at 15 ^{o}C. For the study conducted at 30 ^{o}C, flocs were observed after 2.5 days but they were poorly formed as observed in the immobilisation studies. The fact that defloccation occurred when the cells were introduced in a nutrient-rich environment showed that the immobilisation process was reversible. Calleja, 1994 showed that flocculation had weak bonds and therefore deflocculation in a rich medium is possible as the bonds are weak. The presence of glucose in the wort rich environment has negative effects on the flocculation as well. Flocs are reversibly deflocculated by sugars especially mannose, suggesting a lectin-mediated mechanism (Calleja, 1994).

4.4.2 pH

The pH of lager brews changes from around 5.70 initially to about 4.40 after 10 days (Figure 4.61). The pH falls as organic acids are produced and buffering compounds (basic amino acids and primary phosphates) are consumed. The pH reaches a minimum of 3.8 – 4.4 before rising slightly toward the end of fermentation. The lowered pH inhibits bacterial spoilage during fermentation (Priest and Stewart, 2006).

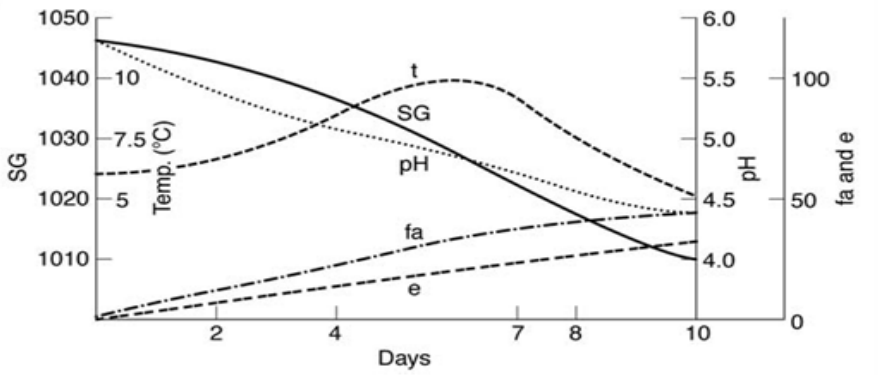

Figure 4.61: Time course of fermentation for lager beers (from Briggs *et al*., 2004).

Ross and Harrison (1970) highlighted that during fermentation pH will change within the range 3.80–5.60. The pH for the studies were monitored during the fermentation processes and analysed. The results are presented in Figures 4.62 and 4.63 (see Appendix VIII, Tables 1 and 2 for the average data with standard deviation).

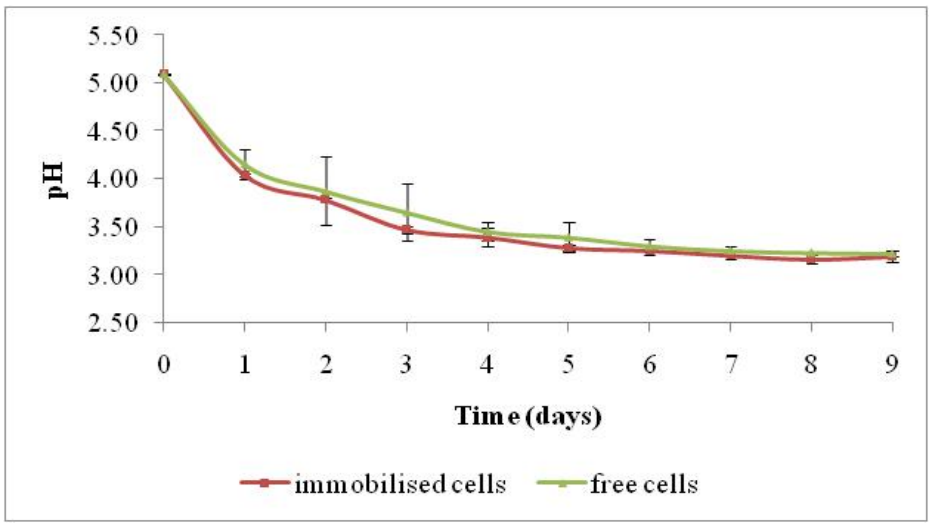

Figure 4.62: Change in pH over time during fermentation at 15 ^{o}C. The standard deviations for the graphs were 0.58 for immobilised cells and 0.60 for free cells.

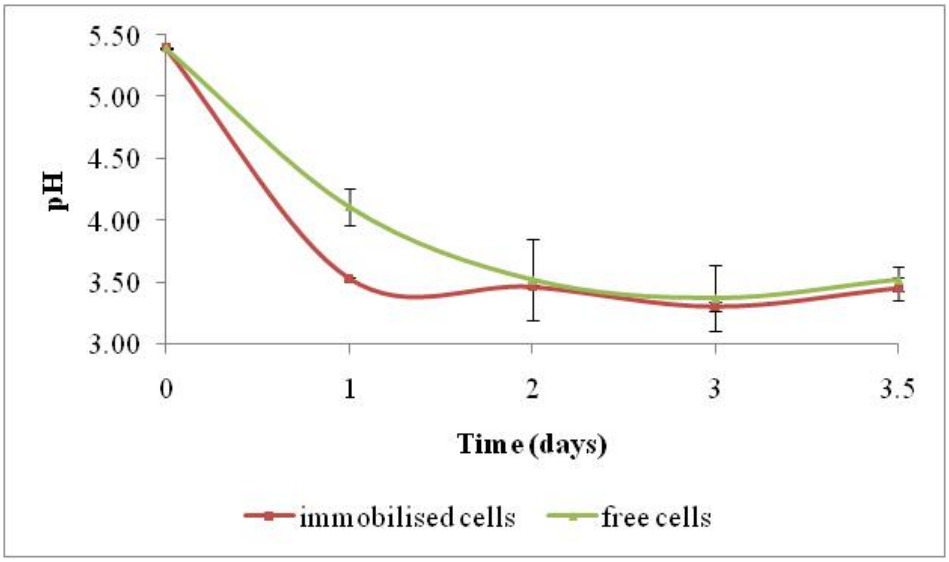

Figure 4.63: Change in pH over time during fermentation at 30 ^{o}C. The standard deviations for the graphs were 0.83 for immobilised cells and 0.74 for free cells.

The change in pH for the two studies was similar. The pH change for the study at 15 ^{o}C changed from 5.09±0.01 to 3.24±0.07 for the immobilised cells (a difference of 1.85) and 3.20±0.03 for the free cells (a difference of 1.89). The pH change for the study at 30 ^{o}C changed from 5.39±0.01 to 3.39±0.09 for the immobilised cells (a difference of 2.00) and 3.59±0.10 for the free cells (a difference of 1.80). The final pH values for all experiments were outside the fermentation range of 3.80 – 5.60. Generally the pH of the immobilised cells was below that of the free cells for both studies. Statistical analysis was conducted to see if there was a significant difference between the immobilised cells and non-immobilised cells graphs. The p value for Figure 4.62 was 0.4900 which was considered not significant as variation among the graphs was not significantly greater than expected by chance. The p value for Figure 4.63 was 0.4884 which was considered not significant as variation among the graphs was not significantly greater than expected by chance.

4.4.3 Sugar concentration

Hornsey (1999) highlighted that from the sugars present in the malt wort; some are taken up passively by the cells in an intact form (e.g. glucose and fructose), some are hydrolysed outside the cell and the breakdown products are absorbed (sucrose), whilst others are actively transported across the cell membrane and hydrolysed in the cytosol of the cells (maltose and maltotriose). Dextrins, comprising maltotetraose and larger starch breakdown products, are not metabolised. The general pattern of disappearance of fermentable sugars from wort during fermentation is sucrose→glucose→fructose→maltose→maltotriose, although there are differences between yeast strains (Batistote *et al*., 2006). The sugars analysed during the study were maltose and glucose.

(A) Maltose

The results for change in maltose during the studies are presented in Figures 4.64 and 4.65 (see Appendix VIII, Tables 3 and 4 for the average data with standard deviation).

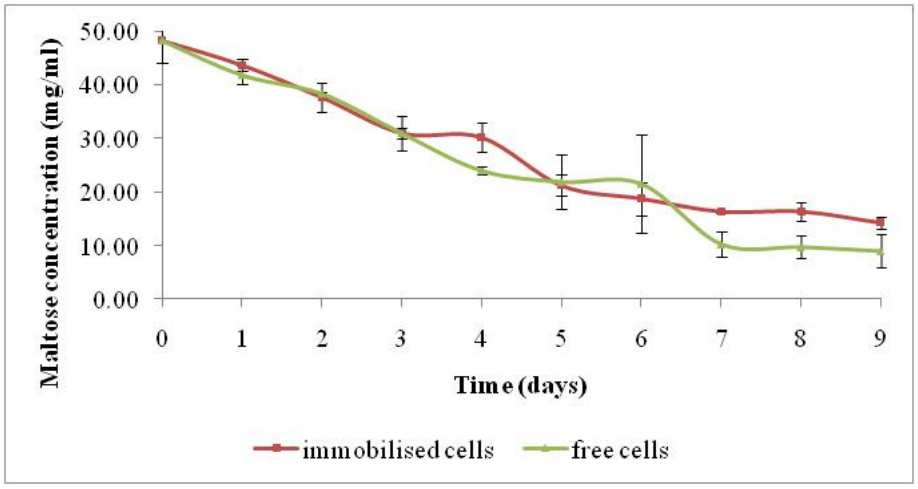

Figure 4.64: Change in maltose over time during fermentation at 15 ^{o}C. The standard deviations for the graphs were 12.07 for immobilised cells and 13.90 for free cells.

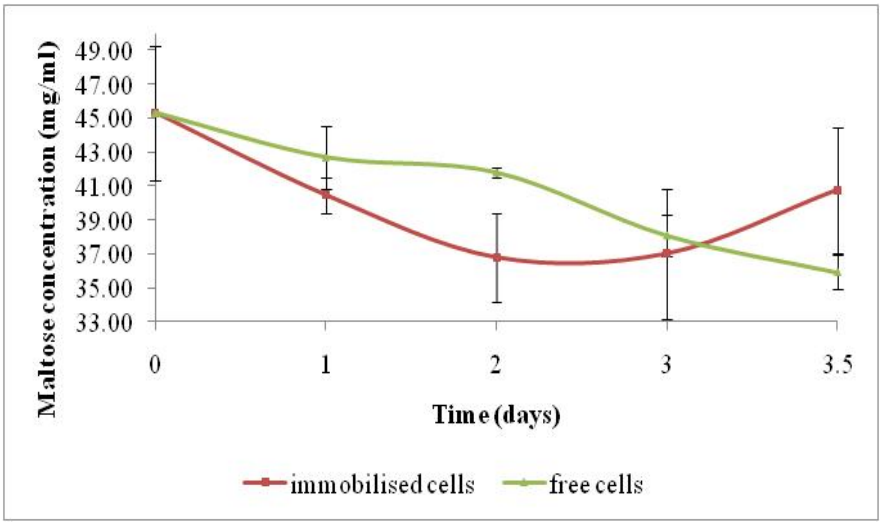

Figure 4.65: Change in maltose over time during fermentation at 30 ^{o}C.

At the end of the study, free cells utilised maltose more than the immobilised cells from both studies (Figures 4.64 and 4.65). There was a small difference in the residual maltose between the immobilised cells and free cells at the end of the experiment at 30 ^{o}C (4.84 mg/ml) than at 15 ^{o}C (5.25 mg/ml). The initial maltose concentrations were 48.23 mg/ml at 15 ^{o}C and 45.32 mg/ml for 30 ^{o}C. The final maltose concentrations are presented below (Table 4.28) with calculated utilisation in brackets. The immobilised cells and free cells did not utilise maltose at 30 ^{o}C as observed from the low utilisation in Table 4.28. There was no need to calculate the significance between the two graphs as the utilisation was very low. Statistical analysis was conducted to see if there was a significant difference between the immobilised cells and non-immobilised cells graphs. The p value for Figure 4.64 was 0.3511 which was considered not significant as variation among the graphs was not significantly greater than expected by chance.

Table 4.28: Final concentration of maltose during fermentation studies: utilisation is provided in brackets.

Final maltose concentration		
Temperature	Immobilised cells	Free cells
15 ^{o}C	14.24 mg/ml **(70.5 %)**	8.99 mg/ml **(81.4 %)**
30 ^{o}C	40.77 mg/ml **(10.0 %)**	35.93 mg/ml **(20.7 %)**

The highest utilisation of maltose was from the studies at 15 ^{o}C with free cells utilising 81% of maltose and immobilised cells utilising 71%. The cells at 30 ^{o}C had more residual maltose. This could mean that the experiment was still in progress. Only 10 % maltose was utilised by the immobilised cells and 20 % by the free cells, the free cells utilising twice of the maltose as the immobilised cells. The maltose utilisation for the study at 30 ^{o}C was very low than at 15 ^{o}C showing that the metabolism of the cells was being affected. The consumption rates of maltose were calculated and are presented in Table 4.29.

Table 4.29: Maltose consumption during fermentation studies.

	15 ^{o}C		**30 ^{o}C**	
	Immobilised cells	**Free cells**	**Immobilised cells**	**Free cells**
Consumption rate (mg/ml*d)	3.78	4.36	1.30	2.68

The rates showed that maltose metabolism was low at 30 ^{o}C than at 15 ^{o}C further signifying that the yeast growth was only from glucose and not maltose consumption.

(B) Glucose

The results for change in glucose during the studies are presented in Figures 4.66 and 4.67 (see Appendix VIII, Tables 5 and 6 for the average data with standard deviation).

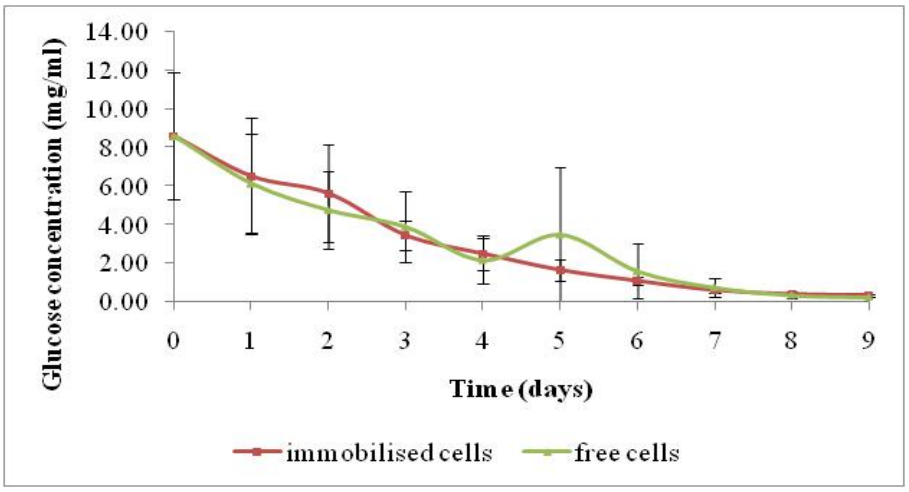

Figure 4.66: Change in glucose over time during fermentation at 15 ^{o}C. The standard deviations for the graphs were 3.04 for immobilised cells and 2.93 for free cells.

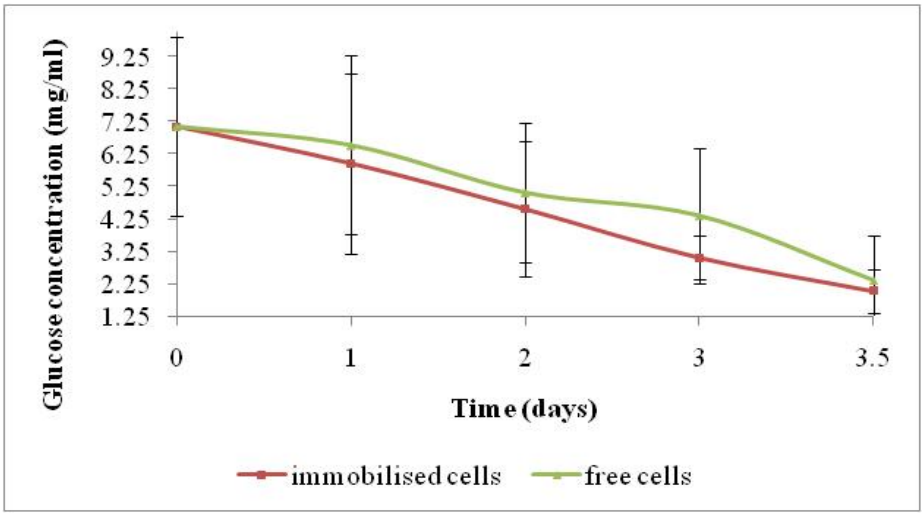

Figure 4.67: Change in glucose over time during fermentation at 30 ^{o}C. The standard deviations for the graphs were 2.61 for immobilised cells and 2.93 for free cells.

Utilisation of glucose was almost similar for all the studies showing that the rates of conversion of glucose were the same (Figures 4.66 and 4.67). The difference in the residual glucose between the free cells and immobilised cells at the end of the experiment at 15 ^{o}C was 0.07 mg/ml and at 30 ^{o}C it was 0.34 mg/ml. The initial glucose concentrations were 8.57 mg/ml at 15 ^{o}C and 7.08 mg/ml for 30 ^{o}C. The final glucose concentrations are presented below (Table 4.29) with calculated utilisation in brackets. Statistical analysis was conducted to see if there was a significant difference between the immobilised cells and non-immobilised cells graphs. The p value for Figure 4.66 was 0.4259 which was considered not significant as variation among the graphs was not significantly greater than expected by chance. The p value for Figure 4.67 was 0.3698 which was considered not significant as variation among the graphs was not significantly greater than expected by chance.

Table 4.30: Final concentration of glucose during fermentation studies: utilisation is provided in brackets.

Final glucose concentration		
Temperature	Immobilised cells	Free cells
15 ^{o}C	0.30 mg/ml **(96.5 %)**	0.22 mg/ml **(97.4 %)**
30 ^{o}C	2.02 mg/ml **(71.5 %)**	2.36 mg/ml **(66.7 %)**

Utilisation of glucose was above 95% for the study at 15 ^{o}C and between 66 and 72 % for the study at 30 ^{o}C. The results also showed that experiments at 30 ^{o}C were stopped before all the sugars were utilised resulting in the low utilisations observed. These results were expected because the glucose was utilised first before maltose by the yeast cells. The consumption rates of maltose were calculated and are presented in Table 4.29.

Table 4.31: Glucose consumption during fermentation studies.

	15 °C		30 °C	
	Immobilised cells	**Free cells**	**Immobilised cells**	**Free cells**
Consumption rate (mg/ml*d)	0.92	0.93	1.45	1.35

Table 4.31 showed that glucose metabolism was high at 30 °C than at 15 °C. From the rates of sugar metabolism (maltose and glucose), more glucose was utilised at 30 °C and more maltose was utilised at 15 °C. The trend highlighted the change in yeast metabolism as fermentation temperature was changed.

(C) Summary

The utilisation of the sugars was compared with literature. As mentioned earlier, glucose and fructose are consumed first (Figure 4.68) and as the glucose concentration diminishes, the enzyme systems required for assimilating maltose are synthesised and the yeast begins to utilise maltose and maltotriose. The production of ethanol and other fusel alcohols generally follows the consumption of carbohydrates (Priest and Stewart, 2006). The data from literature was compared with the results obtained in the studies (Figure 4.69).

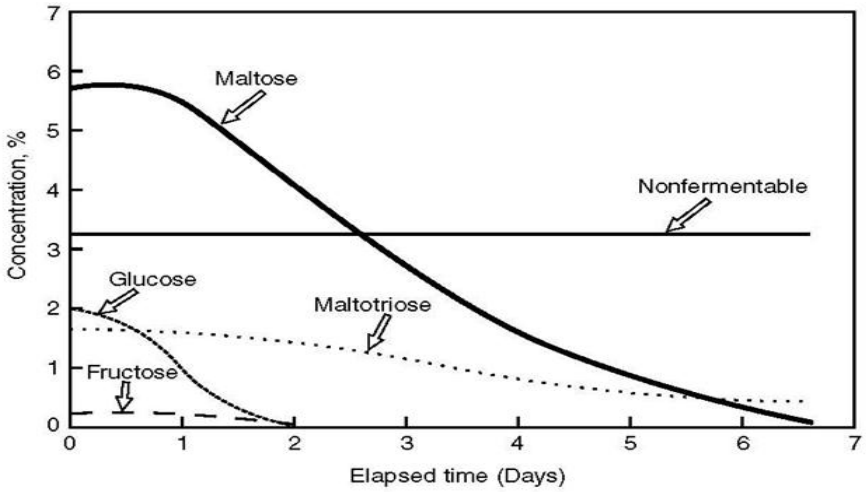

Figure 4.68: Carbohydrate assimilation profiles (from Priest and Stewart, 2006).

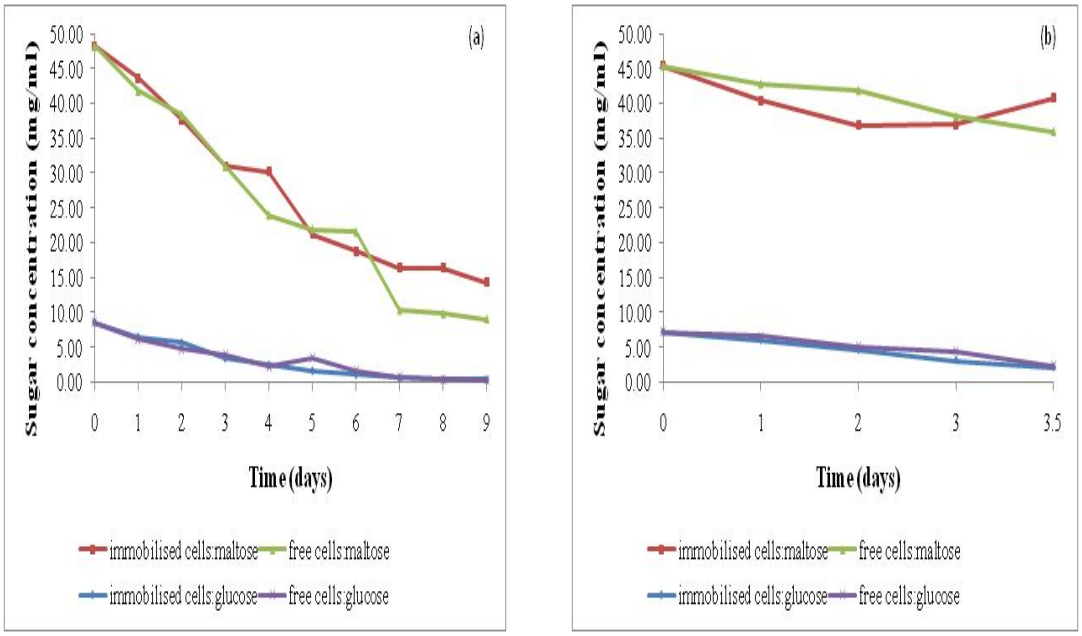

Figure 4.69: Carbohydrate assimilation profiles, (a) is at 15 ^{o}C and (b) is at 30 ^{o}C.

Figure 4.68 shows a graphical representation of fermentable carbohydrates during fermentation. Note that maltose and maltotriose generally are not assimilated in appreciable quantities until most of the glucose is assimilated. The profiles of the sugar assimilation from both studies look similar to the normal lager brew shown

in Figure 4.68. Glucose however, was utilised up to 7 days for the study at 15 ^{o}C and 3.5 days for the study at 30 ^{o}C as compared to 2 days from the general profile. Less maltose was utilised at 30 ^{o}C as shown in Figure 4.69 and the growth of yeast cells was from glucose utilisation only. The overall sugar utilisation was calculated and is presented in Table 4.32.

Table 4.32: Sugar consumption during fermentation studies.

	15 ^{o}C		**30 ^{o}C**	
	Immobilised cells	**Free cells**	**Immobilised cells**	**Free cells**
Consumption rate (mg/ml*d)	4.70	5.29	2.75	4.03

The highest consumption rate was observed from free cells at 15 ^{o}C, followed by the immobilised cells at 15 ^{o}C. At 30 ^{o}C, the highest consumption rate was from free cells followed by the immobilised cells. The low consumption rates observed for immobilised cells maybe attributed to the low cell concentrations observed when viability tests were conducted before fermentation studies ($5.22x10^3$ CFU/ml of free cells and $4.51x10^3$ CFU/ml of immobilised cells).

4.4.4 Alcohol Content

The alcohol concentration was monitored during the two studies. The original gravity and final gravity were measured and the fermentability percentage was calculated (see Section 2.6.8). The results for the alcohol content and fermentability percentage are presented in Table 4.33, Figures 4.70 and 4.71 (see Appendix VIII, Tables 7 and 8 for the average data with standard deviation).

Table 4.33: Gravities during fermentation studies at 15 and 30 ^{o}C

Temperature ^{o}C	Type of cells	Original Gravity	Final Gravity	Fermentability (%)
15	Immobilised cells	1038	1024	36.8
	Free cells	1038	1020	47.4
30	Immobilised cells	1041	1037	9.8
	Free cells	1041	1034	17.1

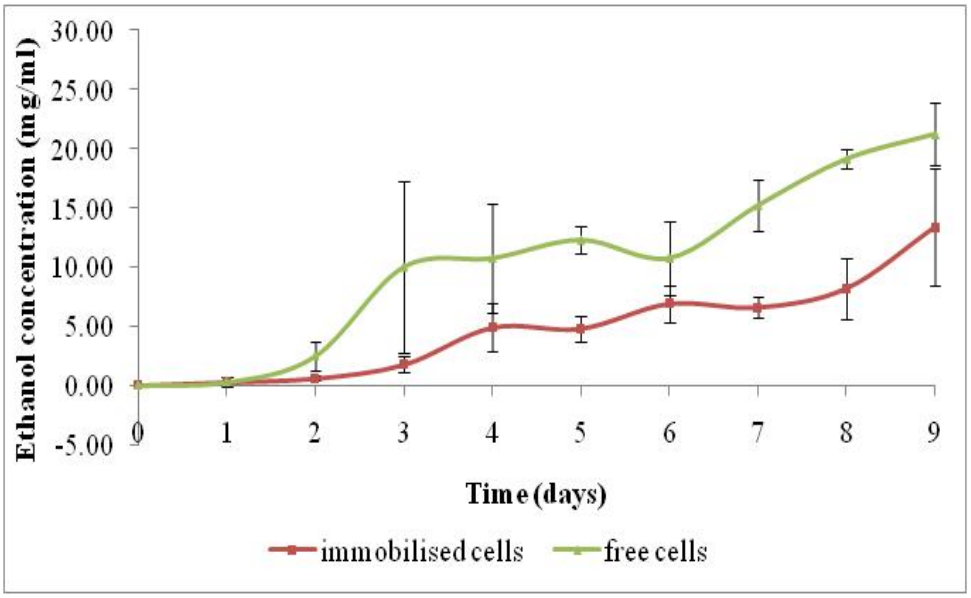

Figure 4.70: Change in ethanol content over time during fermentation at 15 ^{o}C. The standard deviations for the graphs were 4.39 for immobilised cells and 7.55 for free cells.

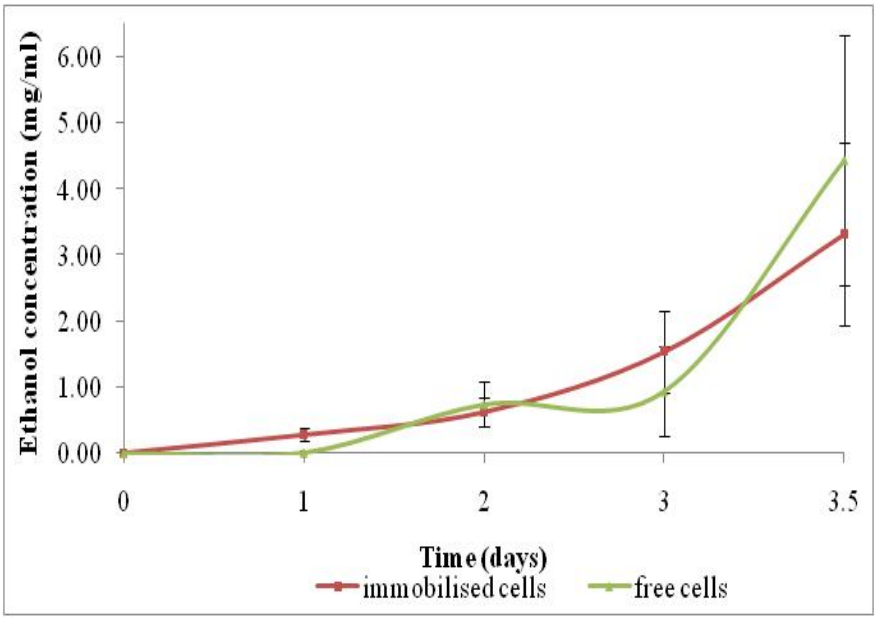

Figure 4.71: Change in ethanol content over time during fermentation at 30 ^{o}C. The standard deviations for the graphs were 1.36 for immobilised cells and 1.86 for free cells.

From Figures 4.70 and 4.71 it can be seen that the free cells produced more ethanol than the immobilised cells at the two temperatures investigated. The final ethanol concentrations for the study at 15 ^{o}C were 1.56 % (v/v) for immobilised cells and 2.49 % (v/v). For the study at 30 ^{o}C, the ethanol concentrations were 0.39 % (v/v) for immobilised cells and 0.52 % (v/v). The observed ethanol content was compared with literature at 15 and 30 ^{o}C. Statistical analysis was conducted to see if there was a significant difference between the immobilised cells and non-immobilised cells graphs. The p value for Figure 4.70 was 0.0474 which was considered significant as variation among the graphs was significantly greater than expected by chance. The p value for Figure 4.67 was 0.0030 which was considered significant as variation among the graphs was significantly greater than expected by chance.

Table 4.34: Comparison of fermentation rates with literature for freeze-dried cells at 15 ^{o}C.

		Ethanol (g/L)	**Ethanol (% v/v)**	**Residual sugar (g/L)**	**Sugar utilisation (%)**
This study at 15 ^{o}C	Free cells	21.2	2.49	3.24	83.7
	Immobilised cells	13.3	1.56	14.5	74.4
Gluten pellets at 15 ^{o}C (Bekatorou *et al*., 2001)	Free cells	44.4	5.50	0.90	
	Immobilised cells	41.1	5.20	0.70	
Delignified cellulosic material ta 15 ^{o}C (Inconomopoulou *et al.,* 2000)	Free cells	9.5		15.1	93.4
	Immobilised cells	8.9		20.1	91.2

From Table 4.34, free cells produced more ethanol than the immobilised cells. Bekatorou *et al*., (2001) observed an alcohol concentration of 5.50 % from free cells using gluten pellets and 5.20 % from immobilised cells. The ethanol concentration observed during the study was 2.27 % (almost $\frac{1}{2}$ than that observed by Bekatorou *et al*., (2001) when using free cells and 1.15 % (almost $\frac{1}{4}$ than that observed by Bekatorou *et al*., 2001) when using immobilised cells. Inconomopoulou *et al*. (2000) observed less alcohol content using a baker's yeast on delignified cellulosic material. The authors from the two papers observed less alcohol produced using the immobilised yeast cells than using the free cells, the same trend observed in the study. This shows that the immobilisation process tend to affect the metabolic process for the cells.

Table 4.35: Comparison of fermentation rates with literature for freeze-dried cells.

		Ethanol (g/L)	**Ethanol (% v/v)**	**Residual sugar (g/L)**	**Sugar utilisation (%)**
This study at 30 ^{o}C	Free cells	4.42	0.52	38.28	26.94
	Immobilised cells	3.31	0.39	42.79	18.34
Delignified cellulose at 30 ^{o}C (Iconomopoulou *et al.,* 2000)	Free cells	9.50		12.2	94.7
	Immobilised cells	9.60		18.3	92.0
Dried figs at 30 ^{o}C (Bekatorou *et al*., 2002)	Immobilised cells	40.6	5.1	2.3	
Starch-gluten-milk matrix at 30 ^{o}C (Plessas *et al.*, 2005)	Immobilised cells	50.4	6.4	25.2	81.7

From Table 4.35, free cells produced more ethanol than the immobilised cells. Bekatorou *et al*., (2002) observed an alcohol concentration of 6.20 % from immobilised cells immobilised on dried figs. The difference in the alcohol concentration was very huge. Iconomopoulou *et al.,* (2000) observed an alcohol concentration of 9.50 g/L from free cells using delignified cellulose and 9.60 g/L from immobilised cells. The ethanol concentration observed during the study was 0.39 % (almost $\frac{1}{10}$ than that observed by Bekatorou *et al*., (2002) when using immobilised cells cells. Iconomopoulou *et al.,* (2000) also observed more alcohol

content than the study for both the free cells and immobilised cells. Plessas *et al*., (2005) had the highest alcohol observed.

The low alcohol concentrations observed in both studies may be explained by the fact that the viability of the yeast cells reduced by a magnitude of 10^4 when they were recovered by a freeze dryer. The yeast cells concentrations were on average $65.75x10^6$ CFU/ml after growth and $62.63x10^6$ CFU/ml on average before flocculation studies. The cells were freeze dried for analysis and fermentation studies, and viability tests showed that there were; on average $5.22x10^3$ CFU/ml for free cells and $4.51x10^3$ CFU/ml for immobilised cells. This showed a decrease in magnitude of 10^4. The reduction in the viability of the cells and the residual maltose observed may help to explain the low alcohol content.

CHAPTER 5: CONCLUSIONS AND RECOMMENDATIONS

5.1 Conclusions

Commonly flocculation occurs only when the sources of fermentable sugars are exhausted. It has been suggested that under such starvation conditions the ability to form flocs may represent a stress response. Thus flocs provide a sheltered environment where the chance of survival of the population is enhanced. Disaggregation of flocs occurs if the cells are again exposed to a source of fermentable sugars. In this case, the re-adsorption of a single cell mode affords unimpeded opportunity to utilize the supply of sugar (Briggs *et al*., 2004).

In conclusion the results of this study demonstrated the potential use of CNTs to increase the flocculation process of brewers' yeast cells. The conditions for synthesising CNTs and their use in immobilising yeast cells were thoroughly investigated and documented. The immobilised cells deflocculated when added to a nutrient-rich medium with sugars and the process may be best applied for the removal of suspended yeast cells after the fermentation process during ethanol production or beer brewing. The toxicity of CNTs is no yet known and this limits its application in the brewing processes but for ethanol production it works best as the ethanol will be used as fuel in automobiles.

In summary, the required conditions for the production of CNTs are discussed below:

- As the temperature was changed from 750 to 1000 ^{o}C, there was a change in the quality and the type of CNTs synthesised. The optimum temperature was observed to be 800 ^{o}C. This temperature produced more and better quality MWCNTs than any other temperature.

- High quality carbon nanotubes (MWCNTs) were synthesised at a flowrate of 594 ml/min and this was found to be the optimum flowrate. Higher flowrates investigated had a tendency to form carbon nanoballs at the expense of CNTs.

- A change in reaction time resulted in a change in the quality and quantity of CNTs synthesised. The optimum time was adjudged to be 20 minutes using the calculated production rate (37.458 g_{CNTs}/g_{Fe}/min*1000) and the carbon yield (78.5 %).

- The optimum catalyst quantity required was 3 g as obtained from efficiency data (50.121 g_{CNTs}/g_{Fe}/min*1000) but from TEM analysis this resulted in poor CNTs formed. The carbon yield and production rate at 2 g (44.254 g_{CNTs}/g_{Fe}/min*1000 and 88.5% respectively) was the best than at any other rate or yield except for yield at 3 g, so the optimum catalyst quantity required was considered to be 2 g.

These conditions were summarised in literature (Iyuke, 2009).

Live yeast cells have an intracellular negative charge because of the presence of a transmembrane potential and they can be attracted to cations or positively charged substances. However, dead cells, which have leaky membranes and cannot build a membrane potential, cannot be attracted (Van Zandycke *et al*., 2003). This suggests that during flocculation using positively charged CNTs, dead yeast cells were not attracted to CNTs and could not be flocculated by the nanotubes. The

required conditions for the immobilisation of yeast cells onto CNTs using flocculation method are discussed below:

- From the experiments it is observed that flocculation intensity increases with an increase in agitation speed until an optimum speed was reached then agitation began to have a negative effect. Optimum agitation speed for good flocculation rate was observed to be 110 rpm and it was comparable with literature (Stratford and Wilson 1990).

- pH is generally considered as a minor factor under brewing conditions and yeast cells may flocculate anywhere between pH 2.00 and 8.00, varying with strains, with optimum values of pH 3.00 – 6.00. The best flocculation in terms of quality of flocs and the quantity was observed in the pH range between 5.00 and 5.80 at an average of 5.60. The optimum pH does lie in the range for brewing 3.80 - 5.60.

- Comparing the quality and quantity of flocs obtained at the two different temperatures, the optimum temperature was concluded to be 30 ^{o}C as observed in literature (Jin and Speers, 2000; Jin *et al*., 2001; Hsu *et al*., 2001).

- The optimum concentration of CNTs was found to be 53.57 μg/ml. At this concentration the flocs obtained were of the best quality and quantity. It was also observed that CNTs in sheet form resulted in less flocculation effects as compared to the CNTs in powder form.

- Calcium ions generally had a negative effect of flocculation by decreased the flocculation weight i.e. the quantity of flocs recovered by centrifuge. The optimum concentration for calcium ions required was 5.49 mM taking into consideration the quality aspect. This may be due to the repulsive forces between the Ca^{2+} ions and the positively charged CNTs existing in the same medium. Since flocculation was observed the results are in agreement with

literature (Jin and Speers, 1999; Mill, 1964). Taylor and Orton (1973) concluded that the presence of calcium ions is required at a very low concentration in order to induce flocculation.

- The presence of glucose in yeast extract delayed flocculation because it promotes cell growth and delay stationary phase. This will increase the time required to flocculate the yeast cells which was against the objectives of this study. These results were in agreement with literature which states that glucose inhibits flocculation (Domingues *et al*., 2000; Jin and Speers, 1999; Verbelen *et al*., 2006). Several authors have indeed found that flocculation is triggered by carbon and/or nitrogen starvation and that addition of these compounds to the growth medium delays flocculation (Soares *et al.*, 1994; Soares and Mota, 1996; Stratford, 1992).

- Zeta potential data was not entirely consistent to predict the flocculation process and there is need to do more investigations to conclude the range were flocculation will be best observed.

Analysis of the alcohol produced during the fermentation studies resulted in low alcohol content. Free cells produced higher alcohol content from fermentation than the immobilised cells for the two studies conducted but the alcohol content for both studies were below that reported in literature. The immobilised yeast cells deflocculated when introduced into a medium rich with wort sugars showing that flocculation was reversible (Calleja, 1994; Domingues *et al.,* 2000; Stewart and Russell, 1981; Priest and Stewart, 2006. The literature is on pages 20 and 21 of dissertation). Calleja, 1994 showed that flocculation had weak bonds and therefore deflocculation in a rich medium is possible as the bonds are weak. The presence of glucose in the wort rich environment has negative effects on the flocculation as well. Flocs are reversibly deflocculated by sugars especially mannose, suggesting a lectin-mediated mechanism (Calleja, 1994). The flocculation process can be applied in the ethanol production industry to remove

the suspended yeast cells after the fermentation process to reduce the turnaround time for the process. This is so because the flocculation process was higher with CNTs than with free cells within the fermentation pH range.

5.2 Recommendations

During the study there were some unanswered questions which give room for future work. The points to note are:

- Work is currently in progress to determine the toxicity of the CNTs on yeast cells and animal cells. If they are toxic, the immobilisation will be best suited to the production of ethanol.

- Further investigation of the parameters that lead to the production of HCNTs and HCNFs should be conducted since these were observed during the synthesis of CNTs.

- Investigating the parameters that affect fermentation to improve alcohol content during fermentation of malt extract using the immobilised cells from immobilisation of yeast cells on CNTs.

- Investigating the additional parameters such as aeration and effect of ethanol on immobilisation of yeast cells on CNTs.

- Optimisation of the freeze-drying process should also be conducted as any major flaws in interpretation will follow if freeze-drying affects viability and

vitality. For instance, when trying to understand potential toxicity of CNTs, if it is based on cells already compromised during the freeze-drying process, wrong conclusions will be reached.

- A model to predict the mechanism of yeast cell flocculation using CNTs should be provided. The model should fit the kinetics during the flocculation processes and this should be compared with other models for other flocculating agents.

CHAPTER 6: REFERENCES

Abdel-Azeem, H. H.M. (2009) Some factors affecting the accumulation of glycogen in *Saccharomyces cerevisiae* and *Saccharomyces carlsbergeneis*, *Australian Journal of Basic and Applied Sciences*, vol.3(3), pp2355-2359.

Alexandre, H. and Guilloux-Benatier, M (2006) Yeast autolysis in sparkling wine – a review, *Australian Journal of Grape and Wine Research*, vol.12, pp119–127.

Arnold, W.N (1981) Autolysis in yeast cell envelopes, (Edited by Arnold W.N), *Biochemistry, Biophysics and Ultrastructure*, New York, CRC Press, pp129–137.

Azamian, B.R., Davis, J.J., Coleman, K.S., Bagshaw, C.B. and Green, M.L.H. (2002) Bioelectrochemical single-walled carbon nanotubes, *Journal of the American Chemical Society*, vol.124, pp12664–12665.

Babushok, V I. and Miziolek, A W. (2004) Condensation flame of acetylene decomposition, *Combustion and Flame*, vol.136, pp.141–145.

Baddour, C E. and Briens, C. (2005) Carbon nanotube synthesis: a review, *International Journal of Chemical Reactor Engineering*, vol.3, R3.

Barker, M. G. and Smart, K. A. (1996) Morphological changes associated with the cellular aging of a brewing yeast strain, *Journal of the American Society of Brewing Chemists*, vol.54, pp121–126.

Batistote, M., da Cruz, S.H. and Ernandes, J.R. (2006) Altered patterns of maltose and glucose fermentation by brewing and wine yeasts influenced by the complexity of nitrogen source, *Journal of the Institute of Brewing*, vol.112(2), pp84–91.

Bekatorou, A., Koutinas, A. A., Kaliafas, A. and Kanellaki, M. (2001a) Freeze-dried *Saccharomyces cerevisiae* cells immobilised on gluten pellets for glucose fermentation, *Process Biochemistry*, vol.36, pp549–557.

Bekatorou, A., Koutinas, A. A., Psarianos, K. and Kanellaki, M. (2001b) Low temperature brewing by freeze-dried immobilised cells on gluten pellets, *Journal of Agricultural and Food Chemistry*, vol.49, pp373–377.

Bekatorou, A., Sarellas, A., Ternan, N G., Mallouchos, A., Komaitis, M.,

Koutinas, A A. and Kanellaki, M (2002) Low-temperature brewing using yeast immobilised on dried figs, *Journal of Agricultural and Food Chemistry*, vol.50, pp7249–7257.

Bekers, M., Ventina, E., Karsakevich, A., Vina, I., Rapoport, A., Upite, D.,

Kaminska, E. and Linde, R. (1999) Attachment of yeast to modified stainless steel wire spheres, growth of cells and ethanol production, *Process Biochemistry*, vol.35, pp523–530.

Berger, M. (2007) Ethanol production inside carbon nanotubes, Nanowerk LLC,

INTERNET. http://www.nanowerk.com/spotlight/spotid=2053.php. Cited 3 August 2009.

Berny, J.F and Hennebert, G.L. (1991) Viability and stability of yeast cells and

filamentous fungus spores during freeze-drying: effects of protectants and cooling rates, *Mycologia*, vol.83(6), pp805–815.

Bhattacharyya, S., Salvetat, J-P., Roy, D., Heresanu, V., Launois, P. and Saboung,

M-L. (2007) Self-assembled lamellar structures with functionalized single wall carbon nanotubes, *Chemical Communications*, pp4248–4250.

Boulton, C. and Quain, D. (2001) Brewing yeast and fermentation, Blackwell Science Ltd, Oxford.

Brányik, T., Vicente, A.A., Machado Cruz, J.M. and Teixeira, J.A. (2002) Continuous primary beer fermentation with brewing yeast immobilized on spent grains, *The Journal of the Institute of Brewing*, vol.108, pp410–415.

Brányik, T., Silva, D.P., Vicente, A.A., Lehnert, R., Almeida e Silva, J.B., Dostálek, P. and Teixeira, J.A. (2006) Continuous immobilized yeast reactor system for complete beer fermentation using spent grains and corncobs as carrier materials, *Journal of Industrial Microbiology and Biotechnology*, vol.33, pp1010–1018.

Briggs, D.E., Boulton, C.A., Brookes, P.A. and Stevens, R. (2004) Brewing: science and practice, Woodhead Publishing Ltd, Cambridge, England, pp.1–9.

Calleja, G. B. (1987) Cell aggregation. In The Yeast, (Ed. A. H. Rose and J. S. Harrison), Academic Press, London, vol. 2, 2nd ed., pp. 165–238.

Calleja, G.B. (1994) Hooks, loops, and the shallow minimum: mechanistic aspects of yeast flocculation, Colloids and Surfaces B Biointerfaces, vol.2, pp133–149.

Correa-Duarte, M.A., Wagner, N., Rojas-Chapana, J., Morsczeck, C., Thie, M. and Giersig, M (2004) Fabrication and biocompatibility of carbon nanotube-based 3D networks as scaffolds for cell seeding and growth, *Nano Letters*, vol.4(11), pp 2233–2236.

Coutts, M.W. (1966) The many facets of continuous fermentation, *Proceedings of the 9th Convention of the Institute of Brewing*, Australia & New Zealand Section, Auckland, pp 1–7.

Dengis, P B., Nelissen, L R. and Rouxhet, P G. (1995) Mechanisms of yeast flocculation: comparison of top- and bottom-fermenting strains, *Journal of Applied and Environmental Microbiology,* vol.61, pp.718–728.

Diniz-Mendes, L., Bernardes, E., de Araujo, P.S., Panek, A.D. and Paschoalin, V.M.F (1999) Preservation of frozen yeast cells by trehalose, *Biotechnology and Bioengineering*, vol.65(5), pp)572–578.

De Jong, K P. and Geus, J W. (2000) Carbon nanofibres: catalytic synthesis and applications, *Catalysis Reviews: Science and Engineering*, vol.42(4), pp481–510.

Di Ventra, M., Evoy, S. and Heflin, J. R. Jr. (2004) Introduction to Nanoscale Science and Technology, New York: Springer, pp153–157.

Dömény, Z., Šmogrovičová, D., Gemeiner, P., Šturdík, E., Pátková, J. And Malovíková, A. (1998) Continuous secondary fermentation using immobilized yeast, *Biotechnology Letters*, vol.20(11), pp1041–1045.

Domingues, L., Vincente, A A., Lima, N. and Teixeira, J A. (2000) Applications of yeast flocculation in biotechnological processes, *Journal of Biotechnological Bioprocess Engineering,* vol.5, pp288–305.

Dunbar, J., Campbell, S.I., Banks, D.J. and Warren, D.R. (1988) Metabolic aspects of a commercial continuous fermentation system, *Proceedings of the 20th Convention of the Institute of Brewing*, 8th–13th May, Brisbane, pp151–158.

EBC Microbiologica (1981) Method 2.5.2. Flocculation. *Journal of Institute of Brewing*, vol.87, pp319–320.

Elkin, T., Jiang, X., Taylor, S., Lin, Y., Gu, L., Yang, H., Brown, J., Collins, S. and Sun, Y-P. (2005) Immuno-carbon nanotubes and recognition of pathogens, *ChemBioChem*, vol.6(4), pp640–643.

Firon, N., Ofek, I. and Sharon, N. (1982) Interaction of mannose-containing oligosaccharides with the fimbrial lectin of *Escherichia coli, Biochemical and Biophysical Research Communications,* vol.105, pp1426-1432.

Ghafari, P., St-Denis, C H., Power, M E., Jin, X., Tsou, V., Mandal, H S., Bols, N C. and Tang, X S. (2008) Impact of carbon nanotubes on the ingestion and digestion of bacteria by ciliated protozoa, *Nature Nanotechnology Letters,* vol.3, pp347 – 351.

Gheith, M.K., Sinani, V.A., Wicksted, J.P., Matts, R.L. and Kotov, N.A. (2005) Single-walled carbon nanotube polyelectrolyte multilayers and freestanding films as a biocompatible platform for neuroprosthetic implants, *Advanced Materials*, vol.17, pp2663–2670.

Gutiérrez, M.C., García-Carvajal, Z.Y., Marı´a J. Hortigüela, M.J., Yuste, L., Rojo, F., Ferrer, M.L. and del Monte, F. (2007) Biocompatible MWCNT scaffolds for immobilization and proliferation of *E. coli*, *Journal of Materials Chemistry*, vol.17, pp2992–2995.

Hernawan, T. and Fleet, G. (1995) Chemical and cytological changes during the

autolysis of yeasts, *Journal of Industrial Microbiology*, vol.14, pp440-450.

Hornsey, I. S (1999) Brewing, RSC Paperbacks. Royal Society of Chemistry. Suffolk. pp 101–107.

Hsu, C M., Lin, C H., Lai, H J. and Kuo, C T. (2005) Root growth of multi-walled carbon nanotubes by MPCVD, *Thin Solid Films*, vol.471, pp140–144.

Hsu, J.W.C., Speers, R.A. and Paulson, A.T. (2001) Modeling of orthokinetic flocculation of *Saccharomyces cerevisiae*, *Biophysical Chemistry*, vol.94, pp47–58.

Huang, T.S., Tzeng, Y., Liu, Y.K., Chen, Y.C., Walker, K.R., Guntupalli, R. and Liu, C (2004) Immobilization of antibodies and bacterial binding on nanodiamond and carbon nanotubes for biosensor applications, *Diamond and Related Materials*, vol.13, pp.1098–1102.

Hunter, R.J. (1981) Zeta potential in colloid science – principle and applications, San Diego, CA, Academic Press.

Iconomopoulou, M., Kanellaki, M., Psarianos, K. and Koutinas, A A. (2000)

Delignified cellulosic material supported biocatalyst as freeze-dried product in alcoholic fermentation, *Journal of Agricultural and Food Chemistry*, vol.48, pp958–961.

Iyuke, S E. (2005) Swirled fluidised bed chemical vapour deposition reactor, University of the Witwatersrand, Johannesburg, South Africa provisional patent applied, No: 21 01 200503438.

Iyuke, S. E., Mamvura, T. A., Liu, K., Sibanda, V., Meyyappan, M., Varadan, V. K. (2009) Process synthesis and optimisation for the production of carbon nanostructures, *Nanotechnology*, vol.20, pp111–123.

Jin, Y-L. and Speers, R A. (1999) Flocculation of *Saccharomyces cerevisiae, Food Research International,* vol.31, pp421–440.

Jin, Y-L and Speers, A. (2000) Effect of environmental conditions on the flocculation of *Saccharomyces cerevisiae*, *Journal of the American Society of Brewing Chemists*, vol.58, pp108–116.

Jin, Y-L., Ritcey, L.L., Speers, R.A.R. and Dolphin, P.J. (2001) Effect of cell surface hydrophobicity, charge and zymolectin density on the flocculation of *Saccharomyces cerevisiae*, *Journal of the American Society of Brewing Chemists*, vol.59, pp1–9.

Jorio, A., Dresselhaus, G. and Dresselhaus, M S. (2008) Carbon nanotubes:

Advanced topics in the synthesis, structure, properties and applications, Berlin: Springer-Verlag, vol.1, chapter 3.

Kamada, K. and Murata, M. (1984) On the mechanism of brewer's yeast

flocculation, *Agric. Biol. Chem.*, vol.48(10), pp2423–2433.

Kihn, J C., Masy, C L. and Mestdagh, M M. (1988) Yeast flocculation:

competition between non-specific repulsion and specific bonding in cell adhesion, *Canada Journal of Microbiology*, vol.34, pp773–778.

Kock, J.L.F., Venter, P., Smith, D.P., Van Wyk, P.W.J., Coetzee, D.J., Pohl, C.H.,

Botha, A., Riedel, K.-H., and Nigam, S., (2000) A novel oxylipin-associated 'ghosting' phenomenon in yeast flocculation, *Antonie van Leeuwenhoek*, vol. 77, pp401–406.

Kourkoutas, Y., Bekatorou, A., Banat, I M., Marchant, R. and Koutinas, A A.

(2004) Immobilisation technologies and support materials suitable in alcohol beverages production: a review, *Food Microbiology*, vol.21, pp377–397.

Kopsahelis, N., Kanellaki, M. and Bekatorou, A. (2007) Low temperature brewing using cells immobilized on brewer's spent grains, *Food Chemistry*, vol.104, pp480–488.

Kunze, W., Wainwright, T. and Mieth, H O. (1999) Technology brewing and malting, Berlin: VLB, vol. 2.

Li, Y F., Hatakeyama, R., Kaneko, T., Izumida, T., Okada, T. and Kato, T. (2006) Synthesis and electronic properties of ferrocene-filled double-walled carbon nanotubes, *Nanotechnology*, vol.17, pp4143–4147.

Linko, M., Haikara, A., Ritala, A., Penttilä, M. (1998) Recent advances in the malting and brewing industry, *Journal of Biotechnology*, vol.65, pp85–98.

Lin, D.Q., Brixius, P.J., Hubbuch, J.J., Thommes, J. and Kula, M.R. (2003) Biomass/adsorbent electrostatic interactions in expanded bed adsorption: A zeta potential study, *Biotechnology and Bioengineering*, vol.83(2), pp149 – 157.

Mallouchos, A., Reppa, P., Aggelis, G., Kanellaki, M., Koutinas, A A. and

Komaitis, M. (2002) Grape skins as a natural support for yeast immobilisation, *Biotechnology Letters*, vol.24, pp1331–1335.

Mensour, N., Margaritis, A., Briens, C.L., Pilkington, H. and Russell, I. (1997) New developments in the brewing industry using immobilised yeast cell bioreactor systems, *The Journal of the Institute of Brewing*, vol.103, pp363–370.

Mill, P. J. (1964) The nature of the interactions between flocculent cells in the flocculation of *Saccharomyces Cerevisiae, Journal of General Microbiology*, vol.35, pp61–68.

Morancais, A., Caussat, B., Kihn, Y., Kalck, P., Plee, D., Gaillard, P., Bernard, D. and Serp, P. (2007) A parametric study of the large scale production of multi-walled carbon nanotubes by fluidised bed catalytic chemical vapour deposition, *Carbon*, vol.45, pp624–635.

Nahvi, I. Emtiazi, G. And Alkabi, L. (2002) Isolation of a flocculating *Saccharomyces cerevisiae* and investigation of its performance in the fermentation of beet molasses to ethanol, *Biomass and Bioenergy*, vol.23, pp481–486.

Narong, P. and James, A E. (2006) Effect of pH on the ζ-potential and turbidity of

yeast suspensions, *Colloids and Surfaces. A, Physicochemical and Engineering Aspects,* vol.274, pp130–137.

O'Connor, L. (2009) Innovation in the Lab: emerging material could provide the breakthrough that nanotech needs, *Innovations in new product development and marketing,* vol.2, issue 1.

Ouyang, Y., Cong, L M., Chen, L., Liu, Q X., Fang, Y (2008) Raman study on single-walled carbon nanotubes and multi-walled carbon nanotubes with different laser excitation energies, *Physica*, vol.E40, pp2386–2389.

Öztop, H N., Saraydin, D. and Cetinus, S. (2002) pH-sensitive chitosan films for baker's yeast immobilisation, *Applied Biochemistry and Biotechnology*, vol.101, pp239–249.

Öztop, H N., Öztop, A Y., Karadağ, E., Işikver, Y and Saraydin, D. (2003) Immobilisation of *Saccharomyces cerevisiae* on to acrylamide–sodium acrylate hydrogels for production of ethyl alcohol, *Enzyme and Microbial Technology*, vol.32, pp114–119.

Park, J K. and Chang, H N. (2000) Microencapsulation of microbial cells, *Biotechnology Advances*, vol.18, pp303–319.

Pan, X., Fan, Z., Chen, W., Ding, Y., Luo, H. and Bao, X (2007) Enhanced ethanol production inside carbon-nanotube reactors containing catalytic particles, *Nature Materials*, vol.6, pp507–511.

Peinado, R.A., Moreno, J.J., Maestre, O. and Mauricio, J.C. (2005) Use of a novel immobilization yeast system for winemaking, *Biotechnology Letters*, vol.27, pp1421–1424.

Plessas, S., Bekatorou, A., Kanellaki, M., Psarianos, C. and Koutinas, A. (2005) Cells immobilized in a starch–gluten–milk matrix usable for food production, *Food Chemistry*, vol.89, pp175–179.

Powell, C.D., Van Zandycke, S.M., Quain, D.E. and Smart, K.A. (2000) Replicative ageing and senescence in *Saccharomyces cerevisiae* and the impact on brewing fermentations, *Microbiology*, vol.146, pp1023–1034.

Prabhuram, J., Zhao, T.S., Tang, Z.K., Chen, R. and Liang, Z.X. (2006) Multiwalled carbon nanotube supported PtRu for the anode of direct methanol fuel cells, *The Journal of Physical Chemistry B*, vol.110, pp5245–5252.

Pilkington, P.H., Margaritis, A., Mensour, N.A. and Russel, I. (1998)

Fundamentals of immobilized yeast cells for continuous beer fermentation: a review, *The Journal of the Institute of Brewing*, vol.104, pp19–31.

Priest, F. G and Stewart, G. G (2006) Handbook of brewing, Boca Raton, CRC Press, 2nd ed., pp 511 – 513.

Riddick, T M. (1968) Control of colloidal stability through zeta potential, New York: Livingston, Published for Zeta-Meter, inc., vol.1, pp359–365.

Ross, A H. and Harrison, J S. (1970) The yeasts, London: Academic Press, vol.3, Chapter 4, pp148–156.

Sakurai, A., Nishida, Y., Saito, H. and Sakakibara, M. (2000) Ethanol production by repeated batch culture using yeast cells immobilized within porous cellulose carriers, Journal of Bioscience and Bioengineering, vol.90(5), pp526–529.

Shen, H-Y., Moonjai, N., Verstrepen, K.J. and Delvaux, F.R. (2003) Impact of attachment on yeast physiology and fermentation performance, Journal of the Amerixcan Society of Brewing Chemists, vol.61, pp79–87.

Singh, G P., Volpe, G., Creely, C M., Grötsch, H., Geli, I M. and Petrov, D.

(2006) The lag phase and G1 phase of a single yeast cell monitored by Raman, *Journal of Raman Spectroscopy,* vol.37, pp858–864.

Smit, G., Straver, M.H. and Lugtenberg, B.J.J. (1992) Flocculence of

Saccharomyces cerevisiae cells is induced by nutrient limitation, with cell surface hydrophobicity as a major determinant, *Applied and Environmental Microbiology*, vol.58(11), pp3709–3714.

Soares, E.V., Texeira, J.A. and Mota, M. (1994) Effect of cultural and nutritional

conditions on the control of flocculation expression in *Saccharomyces cerevisiae*, *Canadian Journal of Microbiology*, vol.40, pp851–857.

Soares, E.V. and Mota, M. (1996) Flocculation onset, growth phase and

genealogical age in *Saccharomyces cerevisiae*, *Canadian Journal of Microbiology*, vol.42, pp539–547.

Speers, R. A., Tung, M.A., Durances, T.D. and Stewart, G.G. (1992) Biochemical

aspects of yeast flocculation and its measurement: a review, *The Journal of the Institute of Brewing*, vol.98, pp293-300.

Speers, R.A., Wan, Y-Q., Jin, Y-L. and Stewart, R.J. (2006) Effects of fermentation parameters and cell wall properties on yeast flocculation, *Journal of the Institute of Brewing*, vol.112(3), pp246–254.

Srivastava, A., Srivastava, O.N., Talapatra, S., Vajtai, R. and Ajayan, P.M. (2004) Carbon nanotube filters, *Nature Materials*, vol.3, pp610–614.

Stewart, G G. and Russell, I. (1981) Yeast. In: Brewing Science, (Pollock J. R. A. Ed), London, UK, Academic Press, vol.2, Chapter 2.

Stratford, M. and Wilson, P D G. (1990) Agitation effects on microbial cell–cell interactions: a review, *Letters in Applied Microbiology,* vol.11, pp1–6.

Stratford, M. (1992) Yeast flocculation: a new perspective, *Advances in Microbial Physiology*, (Ed. A. H. Rose), Academic Press, New York, vol.33, pp1-71.

Stratford, M. (1996) Induction of flocculation in brewing yeasts by change in pH value, *FEMS Microbiology Letters*, vol.136, pp13–18.

Strauss, C.J., van Wyk, P.W.J., Lodolo, E.J., Botes, P.J., Pohl, C.H., Nigam, S. and Kock, J.L.F. (2007) Mitochondrial associated yeast flocculation – the effect of acetylsalicylic acid, *Journal of the Institute of Brewing*, vol.113(1), pp42–47.

Straver, M.H., Aar, P.C., van der Smit, G. and Kijne, J.W. (1993) Determinants of flocculence of brewer's yeast during fermentation in wort, *Yeast*, vol.9, pp527–532.

Straver, M. H. and Kijne, J. W. (1996) A rapid and selective assay for measuring cell surface hydrophobicity of brewer's yeast cells, *Yeast*, vol.12, pp207–213.

Takenaka, S., Iguchi, T., Tanabe, E., Matsune, H. and Kishida, M. (2009) Formation of carbon nanotubes through ethylene decomposition over supported Pt catalysts and silica-coated Pt catalysts, *Carbon*, vol.47, pp1251–1257.

Tata, M., Bower, P., Bromberg, S., Duncombe, D., Fehring, J., Lau, V., Ryder, D. and Stassi, P. (1999) Immobilized yeast bioreactor systems for continuous beer fermentation, *Biotechnology Progress*, vol.15, pp105–113.

Taylor, N W. and Orton, W L. (1973) Effect of alkaline earth metal salts on flocculence in *Saccharomyces cerevisiae, Journal of Institute of Brewing,* vol.79, pp294–297.

Tosch, W., Geiger, W., Stretz, D., Robson, G.D. and Drucker, D.B. (20005) Polar lipids of brewer's yeasts, *Journal of Institute of Brewing,* vol.111(2), pp197–202.

Tripathy, T. and De Ranjan, B. (2006) Flocculation: a new way to treat the waste water, *Journal of Physical Sciences*, vol.10, pp93 – 127.

Tsinontides, S C., Rajniak, P., Pham, D., Hunke, W A., Placek, J. and Reynolds, S D. (2004) Freeze drying—principles and practice for successful scale-up to manufacturing, *International Journal of Pharmaceutics*, vol.280, pp1–16.

Van Zandycke, S., Siddique, R. and Smart, K.A. (2003) The role of the membrane in predicting yeast quality, *Master Brewers Association of the Americas*, vol.40(3), pp169–173.

Verbelen, P J., De Schutter, D P., Delvaux, F., Verstrepen, K J. and Delvaux, F

R. (2006) Immobilized yeast cell systems for continuous fermentation applications, *Biotechnology Letters*, vol.28, pp1515–1525.

Verstrepen, K J., Derdelinckx, G., Verachtert, H. and Delvaux, F R. (2003) Yeast flocculation: what brewers should know, *Applied Microbiology and Biotechnology*, vol.61, pp197–205.

Upadhyayula, V.K.K., Ghoshroy, S., Nair, V.S., Smith, G.B., Mitchell, M.C. and Deng, S. (2008) Single-walled carbon nanotubes as fluorescence biosensors for pathogen recognition in water systems, *Research Letters in Nanotechnology*, vol.2008, pp1–5.

Zeta Potential: An Introduction in 30 Minutes, Malvern Instruments Zetasizer Nano series MRK654-01, Technical Notes.

Zhao, J. and Fleet, G. H. (2003) Degradation of DNA during the autolysis of *Saccharomyces cerevisiae*, *Journal of Industrial Microbiology and Biotechnology*, vol.30, pp175–182.

APPENDICES

Appendix I: Publications

Iyuke, S. E., Mamvura, T. A., Liu, K., Sibanda, V., Meyyappan, M., Varadan, V. K. (2009) Process synthesis and optimisation for the production of carbon nanostructures, *Nanotechnology*, vol.20, pp111–123.

Mamvura, T. A., Iyuke, S. E., Sibanda, V., Yah, C. S. (2009) Yeast cell immobilisation using carbon nanotubes as a biocatalyst for brewing purposes, Provisional patent.

Appendix II: Procedure for using TEM

Consumables Required

1. Filter papers
2. Eppendorf tubes
3. Pipettes
4. Copper grids
5. Methanol or ethanol

Procedure for preparing sample for TEM

1. Take a little of the CNTs (0.005±0.0001g) from the sample bottle with spatula and transfer into an eppendorf tube.
2. Add 3 mL alcohol (methanol or ethanol)
3. Put the eppendorf tube into the Branson ultrasonic bath for 10 minutes supported with a stand and clamp.
4. Using a tweezer, transfer a copper (Cu) grid onto a filter paper.
5. After 10 minutes the carbon nanotubes will be dissolved in the alcohol. Using a pipette take a small sample of the dissolved CNTs from the eppendorf tube and drop it onto the Cu grid.
6. Let the sample dry for about 2 minutes or use a normal light in the TEM to speed up the process.
7. The sample is now ready to be viewed on the TEM.
8. Take the sample to the TEM room.

Procedure in the TEM room

1. Switch on the warning light to warn people that the TEM is in use.
2. Using a tweezer, transfer the Cu grid from the filter paper onto the TEM sample holder (made from brass).

Loading sample into TEM sample holder

1. Check that all the 2 sides for adjusting the sample holder with copper grid in TEM are on 7.5mm on each side as measured by micrometer screw gauge.
2. Insert the TEM sample holder into the TEM. This will activate the microswitch.
3. Wait for 30 seconds to create enough vacuum and turn the sample holder 180^{o}C in the clockwise direction.
4. Push the sample holder inside the TEM until it reaches the end.
5. Press on the holder to release the sample with CNTs and pull it out in reverse to step 4.
6. Turn the sample holder 180^{o}C in anticlockwise direction.
7. Pull out the sample holder and put it on its stand.

The next step is to turn on the TEM

1. Turn on the voltage to 80kV slowly in successive steps (40, 60, 80kV).
2. Turn the filament on slowly in the clockwise direction until the knob reaches the end.
3. If you open the black lid to see, the beam should be at the central position. If not align the green light at the central position.
4. Adjust the contrast and/or brightness to view the sample. Adjust focus and magnification for better viewing.

Taking a Photograph

1. Position your sample in the inner box because that is the size of the micrograph

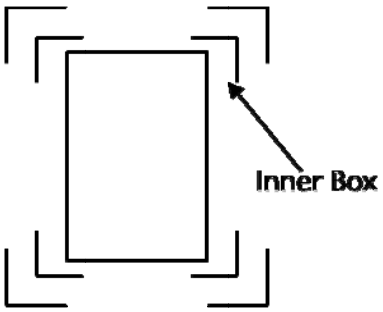

2. Close the black lid.
3. Adjust brightness until the two green lights are switched on simultaneously, you have adjusted the brightness required by the microscopy for a good image.
4. Pull the lever completely towards you, positioned at the left hand side of the fine focus knob. Wait until the red light in between the green lights switches on and then off.
5. Now push the lever back to its original position. Wait for there to be a clicking sound of a photo being taken and simultaneously the green light at the left side of fine focus will switch on and off.
6. Afterwards remove the lid and adjust brightness to the desired level and continue to view the sample.

Unloading sample from TEM

1. Check that all the 2 sides for TEM for adjusting viewing are on 7.5mm on each side
2. Turn the filament off slowly in the anticlockwise direction until the knob reaches the end
3. Turn off the voltage to OFF in successive steps (60, 40, OFF)
4. Insert the TEM sample holder into the TEM. This will activate the microswitch.
5. Wait for 30 seconds and turn the sample holder 180^{o}C in the clockwise direction.
6. Press on the sample holder and push it into the TEM until it reaches the end whilst pressing.

7. Release the button and it will clip on the sample.
8. Pull the sample holder out in reverse to step 4.
9. Turn the sample holder 180^{o}C in anticlockwise direction.
10. Pull out the sample holder and put it on its stand.

Appendix III: VirTis Freeze Dryer Cooling Rate Calculation

An experiment was done to monitor the decrease in temperature within a time range and the data was plotted to determine the cooling rate.

Table 1: Freeze dryer cooling time and temperature.

Time (minutes)	0	1	2	3	4	5	6	7	8
Temperature (^oC)	16.9	7.3	6.7	6.4	5.8	4.3	1.0	-2.1	-5.1
Time (minutes)	9	10	11	12	13	14	15	16	17
Temperature (^oC)	-7.7	-10.3	-12.8	-15.3	-17.5	-20.0	-22.5	-24.9	-27.3
Time (minutes)	18	19	20	22	24	25			
Temperature (^oC)	-29.6	-32.1	-34.7	-39.8	-45.2	-47.9			

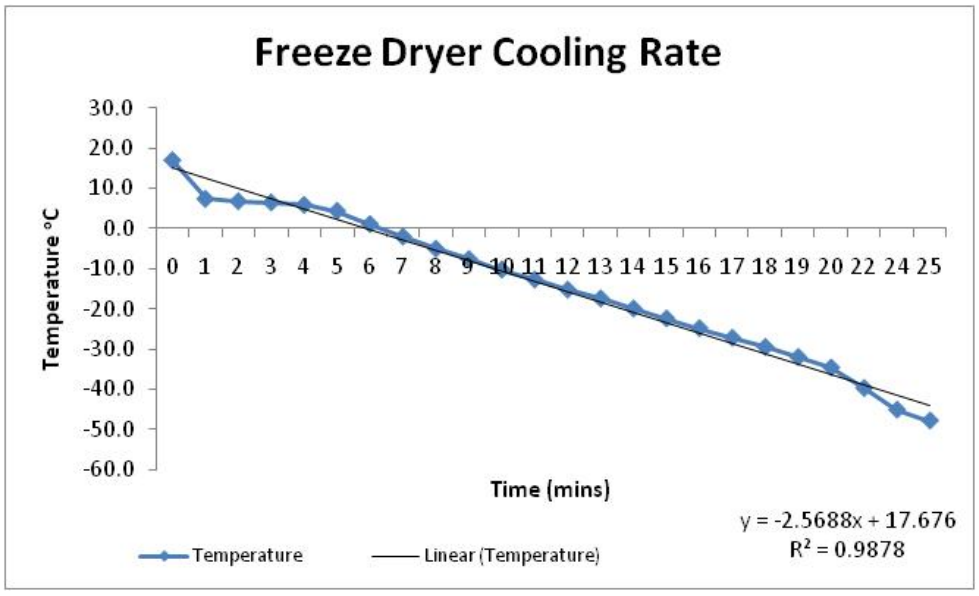

Figure 1: A curve fit of cooling temperature versus time taken for VirTis freeze dryer.

Appendix IV: Procedure for using SEM

Procedure for preparing sample for SEM

This procedure should be done at least 2 days before the day for using the SEM

1. Put graphite paste on the sample holder (silver in colour) or on carbon stickers if the sample absorbs the graphite.
2. Sprinkle the powdered sample onto the graphite paste or carbon sticker.
3. Mark each sample at the sides and at the bottom for identification.
4. Fill in form indicating the coating required to enhance conduction. Carbon treatment and gold palladium splutter treatment are required.

Procedure in the SEM room

1. Take the cylindrical sample holders (silver in colour) to SEM room.
2. Inserted it into another sample holder (brown in colour – brass) and tightened the screw at the side using a small screwdriver. The sample is ready to be inserted into the SEM for analysis.

Loading the Sample into Microscope Chamber

1. Ensure that X and Y translation are in mid-position. X =350mm, Y=250mm. The working distance should be at 39mm.
2. Using specimen exchange rod attach sample holder on the bottom hole by screwing it in until finger tight. Do not touch any part of the specimen exchange rod as it has vacuum grease to seal when inserted in the SEM.
3. Press the holder onto the chamber and press the perspex glass against the chamber whilst holding it.
4. Once again ensure that the working distance is at 39mm, X=350mm and Y=250mm
5. Press red button and wait until the red light switches off

6. Open isolation valve knob anticlockwise for a 90^{o} turn. Afterwards pull the knob slowly outside until it reaches the end, the valve is fully open.

7. Push the rod into the chamber slowly and locate the sample holder onto the specimen stage. If it is not located properly a blipping sound will be heard. This procedure should be done when the room lights are switched off to see easily into the chamber.

8. Unscrew the exchange rod from the sample holder counter clockwise slowly whilst looking through in the glass and pull it out until it reaches the Perspex glass.

9. Slowly close the isolation valve knob by pushing it back into the chamber.

10. Turn the knob clockwise for a 90^{o} turn back into a 12 o'clock position and wait after the micro switch sound is heard.

11. Turn the red light on.

12. Remove the exchange rod using two hands to balance and put it back on its position.

Procedure to switch on the Filament

1. Check that the current light is on first. If not wait a few seconds for it to switch on.

2. Flick the white switch to SEI (upward position).

3. Press down accelerating voltage button (red button).

4. Turn filament knob clockwise slowly until it reaches the end. There should be an image on the screen now.

5. Adjust brightness and/or contrast if there is no visual or image on the screen.

6. Adjust the working distance to 15mm, the magnification and focus for easy viewing.

Taking a Photography

1. Focus on the area you want to take the photograph

2. On Scan Mode press Line button (4^{th} from left)

3. Press WFM button, WFM – Wave Form Monitor
4. Using brightness control knob adjust the peaks to 2.5 line
5. Using contrast control button adjust the peaks to line 5.5 (0.5 from the top line). **NB:** Highest peaks should align to 5.5, the image is focussed now and the photography is ready to be taken.
6. On Scan Mode press PIC button.
7. Press NORM button.
8. Finally press PHOTO button on top left corner. The SEM will start to take the photograph.
9. Once finished, adjust the contrast first and then the brightness to the required level and continue to view the sample

Removing Sample from SEM

The filament is switched off first

Filament Switch Off Procedure

1. Turn filament knob counter clockwise slowly until you reach the end.
2. Press down accelerating voltage button (red button).
3. Flick the white switch to a downward position.

After this then perform the removal as follows:

1. Ensure that X and Y translation are in mid-position. X =350mm, Y=250mm. The working distance should be at 39mm
2. Press the holder onto chamber and press the perspex glass against the chamber and hold
3. Once again ensure that the working distance is at 39mm, X=350mm and Y=250mm
4. Press red button and wait until the red light switches off
5. Open isolation valve knob anticlockwise for a 90^{o} turn. Afterwards pull the knob slowly outside until it reaches the end, the valve is fully open.

6. Push the rod into the chamber slowly and locate the sample holder. Start to screw the exchange rod onto the sample holder in a clockwise direction cautiously.
7. Pull the exchange rod together with the sample holder out until it reaches the Perspex glass
8. Slowly close the isolation valve knob by pushing it back into the chamber.
9. Turn the knob clockwise for a 90^{o} turn into a 12 o' clock position and wait after the micro switch sound is heard.
10. Turn the red light on.
11. Remove the exchange rod and sample holder using two hands to balance.
12. Unscrew the sample holder from the exchange rod and either replace the rod on its position or put another sample for analysis.

Appendix V: Cole Parmer flowmeters calibration chart

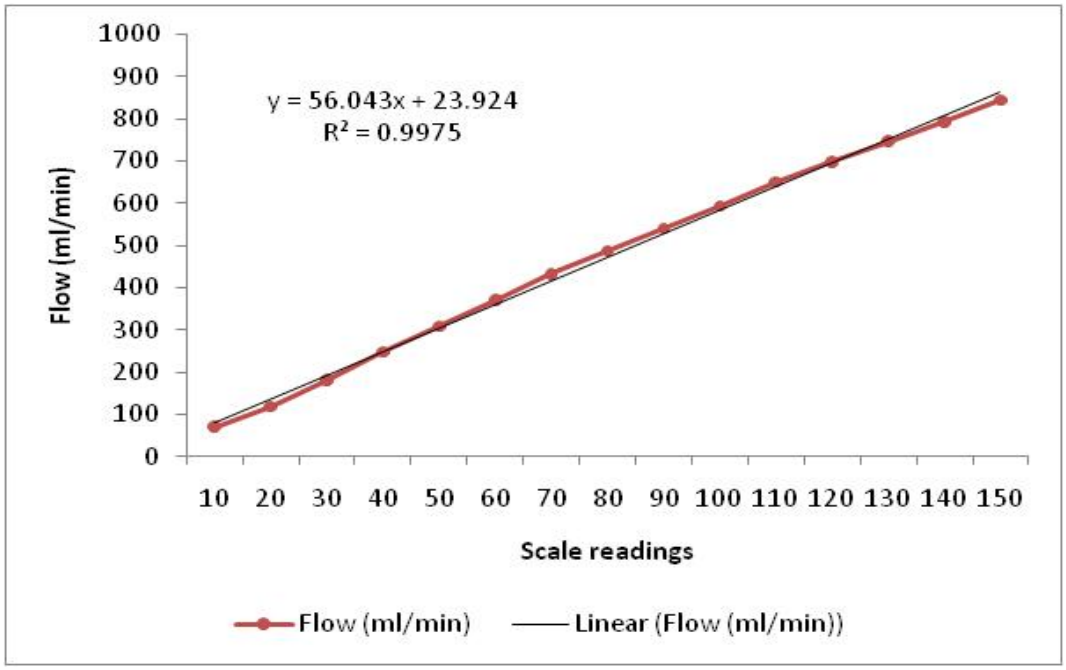

Figure 2: Calibration chart for Cole Parmer flowmeter used in the synthesis of carbon nanotubes.

Appendix VI: Statistical Results for CNTs Production

Table 1: Effect of Acetylene flowrate on production rate and yield. Results presented as mean±standard deviation.

Acetylene flowrate (ml/min)	**Production rate (g_{CNTs}/g_{Fe}*min)**	**Carbon Yield %**
308	21.6±0.51	40.5±3.3%
594	43.1±1.59	82.5±9.2%
844	63.3±2.35	118±7.1%

Table 2: Effect of reaction time on production rate and yield. Results presented as mean±standard deviation.

Reaction Time (minutes)	**Production rate (g_{CNTs}/g_{Fe}*min)**	**Carbon Yield %**
5	27.4±3.4	13.4±2.0%
10	19.4±1.9	20.4±0.5%
15	21.1±4.1	30.1±4.1%
20	40.2±3.9	78.5±5.0%
25	23.3±0.4	74.0±1.4%
30	25.5±3.5	75.7±3.2%
35	19.0±2.9	46.5±6.4%
50	6.4±2.2	28.7±6.1%

Table 3: Effect of catalyst quantity on production rate and yield. Results presented as mean±standard deviation.

Catalyst Quantity (grams)	**Production rate (g_{CNTs}/g_{Fe}*min)**	**Carbon Yield %**
2	43.1±1.6	82.5±9.2%
3	49.1±1.5	97.6±3.7%
4	26.8±1.8	54.5±4.9%
5	23.5±0.7	74.0±1.4%
10	6.4±2.2	28.7±6.1%

Appendix VII: Statistical Results for Yeast Immobilisation

Table 1: Change in zeta potential over time at 0 rpm, 30^{o}C, pH 4.60 and 5.60, and [CNTs] of 54μg/ml. Results presented as mean±standard deviation.

Time (days)	a	b	c	d
0	-12.47±0.10	-12.47±0.10	-12.47±0.10	-12.47±0.10
1	-7.40±0.32	-11.25±0.35	-10.85±0.21	-8.71±0.15
2	-7.61±0.44	-11.85±0.35	-8.96±0.16	-11.75±0.35
3	-7.19±0.32	-11.90±0.28	-6.89±0.20	-12.73±0.15
4	-7.59±0.06	-8.68±0.27	-7.42±0.14	-14.40±0.28

Table 2: Change in zeta potential over time at 50 rpm, 30^{o}C, pH 4.60 and 5.60, and [CNTs] of 54μg/ml. Results presented as mean±standard deviation.

Time (days)	a	b	c	d
0	-12.47±0.10	-12.47±0.10	-12.47±0.10	-12.47±0.10
1	-5.78±0.40	-9.78±0.10	-5.66±0.02	-11.10±0.17
2	-5.83±0.66	-16.80±0.14	-15.55±1.63	-15.27±0.38
3	-9.97±0.33	-16.90±0.42	-5.87±0.52	-16.80±0.71

Table 3: Change in zeta potential over time at 110 rpm, 30^{o}C, pH 4.60 and 5.60, and [CNTs] of 54μg/ml. Results presented as mean±standard deviation.

Time (days)	a	b	c	d
0	-12.47±0.10	-12.47±0.10	-12.47±0.10	-12.47±0.10
1	-5.03±0.14	-11.90±0.57	-7.54±0.12	-10.55±0.35
2	-7.36±0.15	-11.30±0.40	-9.41±0.21	-8.31±0.03
3	-13.65±0.07	-11.10±0.42	-13.10±0.14	-12.30±0.28
4	-13.33±0.21	-9.40±0.40	-17.25±0.92	-15.30±0.42

Table 4: Change in zeta potential over time at 150 rpm, 30^{o}C, pH 4.60 and 5.60, and [CNTs] of 54μg/ml. Results presented as mean±standard deviation.

Time (days)	a	b	c	d
0	-12.47±0.10	-12.47±0.10	-12.47±0.10	-12.47±0.10
1	-5.63±0.28	-4.08±0.10	-5.93±0.56	-4.13±0.06
2	-4.85±0.06	-4.28±0.12	-3.47±0.04	-3.61±0.18
3	-3.70±0.20	-3.37±0.06	-3.59±0.07	-2.72±0.08

Table 5: Change in zeta potential over time at 200 rpm, 30^{o}C, pH 4.60 and 5.60, and [CNTs] of 54μg/ml. Results presented as mean±standard deviation.

Time (days)	a	b	c	d
0	-12.47±0.10	-12.47±0.10	-12.47±0.10	-12.47±0.10
1	-9.21±0.20	-19.13±0.91	-10.43±0.21	-16.85±0.64
2	-8.49±0.16	-15.47±1.31	-10.25±0.50	-20.00±0.57
3	-7.59±0.17	-17.40±1.55	-6.55±0.01	-9.03±0.18

Table 6: Change in zeta potential over time at pH 4.60, 110rpm, 30 ^{o}C and [CNTs] of 54μg/ml. Results presented as mean±standard deviation.

Time (days)	a	b
0	-12.47±0.10	-12.47±0.10
1	-9.75±0.27	-11.95±0.21
2	-8.26±0.21	-15.55±0.07
3	-5.83±0.14	-15.15±0.64
4	-4.79±0.14	-12.85±0.21

Table 7: Change in zeta potential over time at pH 5.60, 110rpm, 30 ^{o}C and [CNTs] of 54μg/ml. Results presented as mean±standard deviation.

Time (days)	a	b
0	-12.47±0.10	-12.47±0.10
1	-8.61±0.30	-17.10±0.14
2	-6.76±0.25	-16.43±2.00
3	-7.45±0.29	-13.70±0.42
4	-8.14±1.00	-10.33±1.51

Table 8: Change in zeta potential over time at pH 6.00, 110rpm, 30 ^{o}C and [CNTs] of 54μg/ml. Results presented as mean±standard deviation.

Time (days)	a	b
0	-12.47±0.10	-12.47±0.10
1	-6.66±0.33	-7.22±0.05
2	-6.90±0.28	-6.51±0.16
3	-5.29±0.16	-4.88±0.02
4	-3.20±0.17	-4.43±0.06

Table 9: Change in zeta potential over time at pH 6.50, 110rpm, 30 ^{o}C and [CNTs] of 54μg/ml. Results presented as mean±standard deviation.

Time (days)	a	b
0	-12.47±0.10	-12.47±0.10
1	-5.51±0.02	-7.83±0.06
2	-6.33±0.11	-7.22±0.03
3	-6.75±0.17	-6.55±0.01
4	-3.94±0.02	-4.58±0.22

Table 10: Change in zeta potential over time at pH 6.50, 110rpm, 30 ^{o}C and [CNTs] of 54μg/ml. Results presented as mean floc weight±standard deviation.

pH	a	b
4.60	0.124±0.003	0.132±0.005
5.60	0.143±0.007	0.123±0.005
6.00	0.136±0.001	0.146±0.004
6.25	0.037±0.002	0.069±0.008
6.50	0.066±0.002	0.109±0.009
6.65	0.051±0.006	0.117±0.009

Table 11: Change in zeta potential over time at 25 ^{o}C, 110 rpm, pH 5.60 and [CNTs] of 54μg/ml. Results presented as mean±standard deviation.

Time (days)	a	b
0	-12.47±0.10	-12.47±0.10
1	-12.85±0.07	-11.73±0.40
2	-13.60±0.14	-15.00±0.14
3	-11.45±0.07	-12.70±0.14
4	-10.65±0.35	-9.62±0.45

Table 12: Change in zeta potential over time at 30 ^{o}C, 110 rpm, pH 5.60 and [CNTs] of 54μg/ml. Results presented as mean±standard deviation.

Time (days)	a	b
0	-12.47±0.10	-12.47±0.10
1	-11.90±0.57	-10.55±0.35
2	-11.30±0.40	-8.31±0.03
3	-11.10±0.42	-12.30±0.28
4	-9.40±0.40	-15.30±0.42

Table 13: Effect of CNTs concentration on brewers' yeast flocculation at 110 rpm, pH 5.60 and 30 ^{o}C. Results presented as mean±standard deviation.

CNTs concentration (μg/ml)	Mean floc weight
0.00	0.078±0.008
17.86	0.080±0.007
26.79	0.088±0.004
35.71	0.091±0.005
44.64	0.115±0.012
53.57	0.117±0.008
62.50	0.100±0.008
71.43	0.086±0.005

Table 14: Change in zeta potential over time as a function of CNT concentrations, 110 rpm, pH 5.60 and 30 ^{o}C. [CNTs] is CNTs concentration in μg/ml. Results presented as mean±standard deviation.

[CNTs]	0	1	2	3	4
0.00	-12.47±0.10	-7.58±0.40	-8.15±0.24	-9.13±1.66	-7.23±0.21
17.86	-12.47±0.10	-7.76±0.23	-7.45±0.29	-10.70±0.28	-8.58±0.58
26.79	-12.47±0.10	-8.09±0.05	-7.12±0.33	-6.44±0.43	-4.29±0.16
35.71	-12.47±0.10	-6.61±0.19	-4.71±0.51	-4.75±0.16	-4.77±0.24
44.64	-12.47±0.10	-8.61±0.30	-6.76±0.19	-11.20±0.14	-8.14±1.00
53.57	-12.47±0.10	-10.55±0.35	-8.31±0.03	-12.30±0.28	-15.50±0.42
62.50	-12.47±0.10	-7.85±0.08	-7.42±0.21	-5.28±0.21	-4.67±0.18
71.43	-12.47±0.10	-7.32±0.30	-6.36±0.18	-5.55±0.20	-0.89±0.05

Table 15: Effect of Ca^{2+} ions on brewers' yeast flocculation at 110 rpm, pH 5.60, 30 ^{o}C and [CNTs] of 54 μg/ml. Results presented as mean±standard deviation.

Ca^{2+} ion concentration (mM)	Floc weight (g)
0	0.029±0.006
1.62	0.018±0.004
2.93	0.041±0.002
4.11	0.082±0.006
5.49	0.108±0.008
6.85	0.063±0.012
8.25	0.066±0.006
9.55	0.106±0.004

Table 16: Change in zeta potential over time as a function of calcium ions concentration at 110 rpm, pH 5.60, 30 ^{o}C and [CNTs] of 54 μg/ml. [Ca^{2+}] is calcium ion concentration in mM. Results presented as mean±standard deviation.

[Ca^{2+}]	0	1	2	3	4
0.00	-12.47±0.10	-17.10±0.14	-16.43±2.00	-13.70±0.42	-10.33±1.51
1.62	-12.47±0.10	-5.32±0.32	-3.05±0.03	-10.55±0.21	-5.56±0.24
2.93	-12.47±0.10	-5.98±0.38	-4.36±0.04	-4.41±0.61	-3.38±0.21
4.11	-12.47±0.10	-3.42±0.22	-7.13±0.52	-7.30±0.62	-5.23±0.19
5.49	-12.47±0.10	-2.57±0.07	-4.42±0.77	-6.53±0.32	-4.06±0.02
6.85	-12.47±0.10	-6.10±0.69	-9.66±0.42	-12.40±0.14	-7.48±0.04
8.25	-12.47±0.10	-5.00±0.33	-9.22±0.72	-7.98±0.09	-7.21±0.83
9.55	-12.47±0.10	-3.41±0.08	-7.49±0.12	-10.01±0.28	-8.11±0.51

Table 17: Effect of glucose on pH and zeta potential at 110 rpm, pH 5.60, 30 ^{o}C and [CNTs] of 54 μg/ml. Results presented as mean±standard deviation.

Time (days)	Zeta potential	pH
0	-12.47±0.10	5.53
1	-1.26±0.08	3.84
2	-1.95±0.14	3.99
3	-0.87±0.01	4.31
4	-3.68±0.08	5.58
5	-6.37±0.11	6.37
6	-7.61±0.00	6.52
7	-12.15±0.07	7.07
8	-9.76±0.16	7.40
9	-7.73±0.14	6.96
10	-17.70±0.00	6.90
11	-21.40±0.14	7.16

Table 18: Effect of the presence of glucose and calcium ions on pH and zeta potential at 110 rpm, pH 5.60, 30 ^{o}C, [CNTs] of 54 μg/ml and [Ca^{2+}] of 5.49 mM. Results presented as mean±standard deviation.

Time (days)	Zeta potential	pH
0	-12.47±0.10	5.59
1	-1.01±0.13	3.76
2	-1.44±0.11	4.00
3	-1.65±0.31	4.30
4	-5.53±0.06	5.28
5	-5.23±0.01	5.71
6	-5.96±0.04	6.28
7	-9.64±0.40	6.89
8	-11.45±0.49	6.69
9	-10.95±1.06	6.60
10	-14.00±0.57	6.45
11	-13.55±0.21	6.73

Appendix VIII: Statistical Results for Fermentation Studies

Table 1: Change in pH over time during fermentation at 15 ^{o}C for immobilised cells (a) and free cells (b). Results presented as mean±standard deviation.

Time (days)	a	b
0	5.09±0.01	5.09±0.01
1	4.05±0.02	4.26±0.15
2	3.79±0.02	4.12±0.36
3	3.50±0.04	3.86±0.29
4	3.33±0.09	3.52±0.10
5	3.26±0.03	3.50±0.15
6	3.22±0.04	3.34±0.06
7	3.23±0.04	3.28±0.04
8	3.19±0.04	3.22±0.01
9	3.24±0.07	3.20±0.03

Table 2: Change in pH over time during fermentation at 30 ^{o}C for immobilised cells (a) and free cells (b). Results presented as mean±standard deviation.

Time (days)	a	b
0	5.39±0.01	5.39±0.01
1	3.54±0.01	4.22±0.15
2	3.47±0.01	3.75±0.33
3	3.33±0.04	3.56±0.27
4	3.39±0.09	3.59±0.10
5	3.32±0.03	3.47±0.15
6	3.30±0.04	3.37±0.06
7	3.12±0.04	3.12±0.04
8	3.09±0.04	3.14±0.01
9	3.17±0.06	3.23±0.03

Table 3: Change in maltose concentration over time during fermentation at 15 ^{o}C for immobilised cells (a) and free cells (b). Results presented as mean±standard deviation.

Time (days)	a	b
0	48.23±4.20	48.23±4.20
1	43.68±1.15	41.81±1.81
2	37.65±2.66	38.34±0.30
3	30.98±3.22	30.94±0.98
4	30.19±2.74	23.99±0.68
5	21.18±1.99	21.92±5.16
6	18.76±3.11	21.52±9.10
7	16.35±0.33	10.28±2.30
8	16.36±1.79	9.76±2.08
9	14.24±1.01	8.99±3.02

Table 4: Change in maltose concentration over time during fermentation at 30 ^{o}C for immobilised cells (a) and free cells (b). Results presented as mean±standard deviation.

Time (days)	a	b
0	45.32±3.95	45.32±3.95
1	40.46±1.06	42.71±1.85
2	36.79±2.60	41.81±0.32
3	37.01±3.84	38.10±1.21
4	40.77±3.71	35.93±1.03
5	29.96±2.81	18.02±4.24
6	21.01±3.49	3.58±1.52
7	27.02±0.54	3.82±0.85
8	26.00±2.84	3.28±0.70
9	20.41±1.45	4.32±1.45

Table 5: Change in glucose concentration over time during fermentation at 15 ^{o}C for immobilised cells (a) and free cells (b). Results presented as mean±standard deviation.

Time (days)	a	b
0	8.57±3.31	8.57±3.31
1	6.48±3.02	6.12±2.59
2	5.59±2.54	4.74±2.00
3	3.40±0.76	3.87±1.84
4	2.45±0.84	2.15±1.24
5	1.60±0.56	3.47±3.45
6	1.04±0.22	1.57±1.42
7	0.55±0.12	0.73±0.48
8	0.35±0.06	0.33±0.14
9	0.30±0.04	0.22±0.02

Table 6: Change in glucose concentration over time during fermentation at 30 ^{o}C for immobilised cells (a) and free cells (b). Results presented as mean±standard deviation.

Time (days)	a	b
0	7.08±2.74	7.08±2.74
1	5.95±2.77	6.51±2.75
2	4.55±2.07	5.05±2.13
3	3.05±0.68	4.34±2.07
4	2.02±0.69	2.36±1.37
5	1.55±0.55	0.71±0.71
6	0.49±0.10	0.46±0.42
7	0.63±0.14	0.37±0.25
8	0.50±0.08	0.25±0.11
9	0.40±0.06	0.29±0.03

Table 7: Change in ethanol concentration over time during fermentation at 15 ^{o}C for immobilised cells (a) and free cells (b). Results presented as mean±standard deviation.

Time (days)	a	b
0	0.00	0.00
1	0.27±0.09	0.29±0.38
2	0.60±0.21	2.50±1.18
3	1.76±0.71	10.03±7.26
4	4.89±2.05	10.76±4.62
5	4.79±1.12	12.29±1.18
6	6.89±1.60	10.77±3.10
7	6.58±0.88	15.21±2.19
8	8.19±2.61	19.13±0.78
9	13.36±4.95	21.21±2.62

Table 8: Change in ethanol concentration over time during fermentation at 30 ^{o}C for immobilised cells (a) and free cells (b). Results presented as mean±standard deviation.

Time (days)	a	b
0	0.00	0.00
1	0.27±0.08	0.01±0.02
2	0.62±0.21	0.74±0.35
3	1.53±0.61	0.93±0.68
4	3.31±1.39	4.42±1.90
5	2.89±0.67	12.86±1.24
6	5.81±1.34	12.93±3.72
7	4.63±0.62	15.75±2.27
8	6.45±2.05	16.33±0.67
9	7.43±2.76	16.64±2.05